Wearable exoskeletons to support ambulation in people with neuromuscular diseases, design rules and control

Thèse N° 9104

Présentée le 15 mars 2019

à la Faculté des sciences et techniques de l'ingénieur
Laboratoire de systèmes robotiques
Programme doctoral en robotique, contrôle et systèmes intelligents

pour l'obtention du grade de Docteur ès Sciences

par

Amalric Louis ORTLIEB

Acceptée sur proposition du jury

Dr R. Boulic, président du jury
Prof. H. Bleuler, Dr M. Bouri, directeurs de thèse
Prof. L. Marchal-Crespo, rapporteuse
Dr E. van Asseldonk, rapporteur
Prof. A. Ijspeert, rapporteur

2019

ÉCOLE POLYTECHNIQUE
FÉDÉRALE DE LAUSANNE

To my family,

To my friends,

And to those who hope

Acknowledgements

My first thanks go to my two supervisors that co-directed and allowed this work to flourish in a healthy and enjoyable environment, namely the Laboratory of Robotic Systems (LSRO) at EPFL. Head of the lab and director of the thesis, Prof. Hannes Bleuler, provided a complete and trustful support to the work while letting a full freedom of implementation. Through his serenity, broad knowledge in human sciences and openness, the laboratory largely benefited from his aura resulting in exchanges with eastern asia, winter retreats and sailing escapes. I am especially thankful to Dr. Mohamed Bouri that co-directed this thesis with a relentless commitment. From the management of resources and finances, through the close follow-up of the project, Dr. Bouri has been a real lead in this project. Open to the discussion and largely mindful of human values, he has been of great support in the carrying of the project.

I would like also to thank the members and the president of my jury committee: Laura Marchal-Crespo, Edwin van Asseldonk, Auke Ijspeert and Ronan Boulic. They, not only brought very interesting and challenging questions, but have also been a great source of inspiration in their respective field of interest from rehabilitation, bio-inspired locomotion and exoskeletons for SCI patients.

Je tiens particulièrement à remercier les délégués de l’ASRIMM et de la FSRMM, Yolande Joray et Jean-François Zürcher, rejoints en fin de thèse par Dominique Wunderle, pour leur disponibilité et le suivi périodique et bénévole du projet avec un regard orienté utilisateur. C’est notamment grâce à l’initiative et au soutien de Yolande Joray que le projet AUTONOMYO a été créé et a donné lieu à un financement conjoint de la part de l’Association Suisse Romande Intervenant contre les Maladies neuroMusculaires (ASRIMM) et de la Fondation Suisse de Recherche sur les Maladies Musculaires (FSRMM). J’adresse également un grand merci aux membres de ces associations que j’ai pu côtoyer pour les riches échanges que nous avons pu avoir, entre autre, Vincent, la famille Rognon, Lionel Capt, Thierry Bovay, les Fasola, etc. Je remercie également tous les volontaires de l’études sur la marche pour leur participation et leur bonne humeur. Finalement, je remercie chaleureusement David pour son rôle de pilote et testeur du prototype.

The collaboration with the CHUV (Centre Hospitalier Universitaire Vaudois) has been made possible thanks to the Prof. Thierry Kuntzer, Katrien van den Keybus-Deglon, Dr. Stefano Carda and Dr. François Ochsner. I also want to aknowledge the work of the team from Ortho-Reha Wallner: Florian Wallner, Dimitri Jolidon and Tim Baudin that supported the realization of orthopedic interfaces for the prototype. Finally, I want also to aknowledge the collaboration with the He-Arc and the design class of Nicolas Jeanson and Vassili Tikhomirov and all students that worked on the project.

Je remercie également les membres des trois ateliers de l’EPFL pour leur aimabilité et la qualité de leur travail : l’atelier de l’IGM dirigé successivement par Marc Salle et Maxime Ratton, l’atelier de l’IMT dirigé par Alfred Thomas et l’atelier de fabrication additive avec Roland Dupuis et Manuel Leitos. Un remerciement particulier s’adresse à Marc Jeanneret qui s’investit avec passion dans chaque projet, occasionnant de nombreux échanges sur des améliorations techniques.

I also want to thank Maria Del Rio Carral, Noémie, Vanlisa and Marie Santiago from the « Centre de recherche en psychologie de la santé, du vieillissement et du sport » from UNIL for conducting and collaborating on a research on the perception of the use of assistive exoskeletons by elderly people.

The work done in the context of the AUTONOMYO project was largely helped by several contributions from master students in semester project, namely, Jonas Graf, Anil Kodiyan, Salif Komi, Antoine Torcheboeuf and Vivien Streit; some internships, namely, Laure Delas-Escande, Hiroshi Matsuo, Seiffedine Ben Khelil and Mehrnaz Salehian; some master thesis, namely, Benoît Denkinger, Tommaso Tracchia and Peter Lichard; some civil services, namely, Dohan Schlichting, Lucien Troillet, Mehmet Kelbas and Quentin Herzig; and finally some senior contributions from Anaïc Cordoba, Stéphane Douget, Stéphanie Konik, Florin Dzeladini, Kelly McClary, Ricardo Araujo, Weiguang Huo and Romain Baud. A particular thanks goes to Romain, Dohan, Mehmet, Stéphanie, Anaïc, Florin, Stéphane and Kelly for their large and passionate implication in the project.

I would like to thank my labmates "noodles" that have made this experience more than enjoyable, first the graduated doctors, namely, Jeremy, Simon, David, Enrico, Elahe, Philipp, Ali, Solaiman, Qingwen, Yifan, Yuanping,… And the one still struggling (or not), namely, Romain, Jacob, Paul, Tobias, Tristan, Jemina, Julien, Luzius, Laurent, Jerry, Atena, Marek, Aurélie, François, Stéphane, Loïc, Evelyn,… Thank you for all the memorable time we have spent together and the epic atmosphere that spread around in the lab.

I would also like to thank my close friends Candice, Lorenz and Morgane, Anaïc, Gwenael and Marla, Emmanuel, Nadia, Sven, Sarah, Paul, Julia, Margaux,… for their huge support, the fun and the discussions we had. I had also the chance to meet and make international friends, namely, Heidi, Lucia, Simone, Harshal, Zoja, Taylor, Christoph, Marie, Mara, Caysha,… with whom we had great time, including linguistic and/or scientific exchanges.

Finalement, j'aimerais remercier tous les membres de ma famille et en particulier ; ma maman, Anouk, qui a été d'un grand soutien au-delà de tous les aspects que l'on peut imaginer ; ainsi que mes sœurs, mon père et sa femme, et ma grand-mère, Ava, Aelle, Aliocha, Jean-Louis, Danièle et Roswitha, pour leur soutien moral et leur amour.

Lausanne, December 8th 2018

Amalric Ortlieb

Abstract

Neuromuscular diseases are degenerative and, thus far, incurable disorders that lead to large muscle wasting. They result in constant deterioration of activities of daily living and in particular of ambulation. Some common types include Duchenne muscular dystrophy, Charcot-Marie-Tooth disease, polymyositis and amyotrophic lateral sclerosis. While these diseases individually have a low rate of occurrence and are mostly unknown to most people, collectively they affect a significant part of the population. About 1 person in 2000 suffer from neuromuscular diseases, which means an approximate total of 370'000 people over the European continent. Recent technology breakthroughs have made possible the realization of advanced powered orthotics, which are commonly called exoskeletons. The most advanced devices have successfully been able to support patients in walking despite a debilitating condition such as complete spinal cord injury. Such technology could be ideal for people with mid-stage neuromuscular diseases as it provides more mobility and independence.

This work investigates the definitions and requirements that would need to be fulfilled for any proposed orthotic device to assist people living with neuromuscular diseases. To define the needs of patients with neuromuscular disease, a large literature review is conducted on gait compensation patterns. The research also includes the data collection of experimental gait measurements from fourteen people with heterogeneous neuromuscular diseases. Conclusions show that orthotics for people with neuromuscular diseases require tunable assistance at each joint and a collaborative control strategy in order to let the user control motion. Eventually, most people may not be able to use crutches.

A full lower limb exoskeleton, AUTONOMYO, is designed, realized and evaluated. A particular attention is put on the optimization of the actuator and transmission units. In order to reduce the effects of inertia and weight of those units, a design is explored with actuation remotely located from the joints. The transmission is realized by custom cable wire and pulley systems, combined with standard planetary gears. The dynamics of different coupling between the hip and the knee flexion/extension joints are explored, and their benefits and tradeoffs analyzed.

A novel control strategy based on a finite-state active impedance model is designed and implemented on the AUTONOMYO device. The controller consists of three states of different active impedances mimicking a visco-elastic behavior. The switching condition between states is uniquely based on the hip flexion velocity to detect the user intent. The performance of the strategy regarding the detection of intention and the modulation of the assistance is evaluated on a test bench and in real conditions with healthy pilots and with a person with limb girdle muscular dystrophy. The preliminary results are promising since all pilots (including the one with muscular dystrophy) are able to initiate and terminate assisted walking on demand. They are all able both to walk with a good stride rate and to reach moderate velocities. Healthy pilots are able to ambulate alone with the exoskeleton, while the pilot with muscular dystrophy requires human assistance for the management of balance.

Keywords – Neuromuscular disease, muscular dystrophy, myopathy, lower extremity exoskeleton, powered orthosis, finite-state controller, active impedance, gait dynamics, compensating gait patterns, cable driven transmission

Résumé

Les maladies neuromusculaires sont dégénératives et, malheureusement, encore incurables à ce jour. Elles sont notamment marquées par une perte importante de la capacité musculaire, ce qui induit une détérioration des activités du quotidien dont la marche en particulier. Les principales formes de ces maladies sont, par exemple : la dystrophie musculaire de Duchenne, la maladie de Charcot-Marie-Tooth, les polymyosites ou encore la sclérose latérale amyotrophique. La somme de ces maladies dites rares touche d'une manière générale une part significative de la population, malgré cela, elles restent encore largement méconnues du grand public. Environ une personne sur 2000 souffre d'une maladie neuromusculaire, ce qui correspond à environ 370'000 cas en Europe uniquement. Le début du siècle a été marqué par l'avènement de technologies qui permettent la réalisation de systèmes orthopédiques motorisés, qui sont plus communément appelés exosquelettes. Les premiers développements de tels appareils ont réussi l'étonnant pari de permettre à des personnes paraplégiques de remarcher avec l'aide du dispositif. Une telle technologie pourrait également s'avérer très utile pour des personnes souffrant d'une maladie musculaire en stade modérément avancé, afin de leur offrir une meilleure mobilité et plus d'indépendance.

Le présent travail se concentre sur la définition des besoins nécessaires à l'assistance adaptée aux personnes souffrant d'une maladie neuromusculaire. La conception et l'implémentation d'un exosquelette complet pour les membres inférieurs, ainsi que d'une stratégie de contrôle, sont proposées et évaluées en termes de faisabilité et de performances. La compréhension et la définition des besoins relatifs aux maladies neuromusculaires sont explorées à travers une revue de la littérature des mouvements de compensation, ainsi qu'à travers des données expérimentales d'analyse de marche récoltées sur un groupe hétérogène de quatorze personnes souffrant de maladies neuromusculaires. La conception d'un exosquelette complet pour les membres inférieurs, AUTONOMYO, est réalisée. Une attention particulière est portée sur l'optimisation de la motorisation et des transmissions mécaniques. Afin de réduire les effets d'inertie et de masse de ces éléments, une conception avec des moteurs déportés des centres de rotation articulaires est évaluée. La transmission est réalisée par un système de câble et poulies combinés à un train d'engrenages planétaires en amont. La dynamique de différentes solutions couplant les articulations de flexion/extension de la hanche et du genou sont explorées.

Une stratégie de contrôle basée sur un modèle d'états-finis avec impédance active est conçue et implémentée sur le dispositif AUTONOMYO. Le contrôleur consiste en trois états avec une impédance active propre imitant un comportement visco-élastique. La condition de changement d'état est basée sur la vitesse de flexion de la hanche qui permet de détecter l'intention de l'utilisateur. Les performances de la stratégie, pour la détection d'intention et la modulation du niveau d'assistance, sont évaluées sur un banc d'essai et en conditions réelles avec des pilotes sains ainsi qu'un pilote atteint par une dystrophie musculaire des ceintures. Les résultats préliminaires sont encourageants alors que tous les pilotes (incluant le pilote souffrant de dystrophie musculaire) sont capables de marcher avec le dispositif.

Keywords – Maladie neuromusculaire, dystrophie musculaire, myopathie, exosquelette, orthèse motorisée, impédance active, dynamique de la marche, transmission à câble, motorisation de l'abduction de la hanche

Contents

List of Figures

List of Tables

List of Equations

List of Acronyms

2MWT	2 minutes walk test
6MWT	6 minutes walk test
10 Meter WT or 10MWT	10 meters walk test
ADL	Activities of daily living
AFO	Ankle-foot orthosis
ALS	Amyotrophic lateral sclerosis
ASRIMM	Association Suisse Romande Intervenant contre les Maladies neuroMuscu-laires
B	Billion
BMD	Becker muscular dystrophy
BLEEX	Berkeley lower extremity exoskeleton
CMD	Congenital muscular dystrophy
CMT	Charcot-Marie-Tooth muscular dystrophy
CHUV	Centre Hospitalier Universitaire Vaudois
DI	Disability insurance (of Switzerland)
DM	Myotonic dystrophy or Steinert muscular dystrophy
DM1	Myotonic dystrophy of type I

DeM	Dermatomyositis
DMD	Duchenne muscular dystrophy
EDMD	Emery-Dreifuss muscular dystrophy
EMG	Electromyogram
FSHD	Facioscapulohumeral muscular dystrophy
FSO	Federal statistical office (of Switzerland)
HR	Heart rate
IBM	Inclusion body myositis
LEE	Lower extremity exoskeleton
LGMD	Limb girdle muscular dystrophy
M	Million
MMT	Manual muscle test
MRC muscle test	Medical research council grading scale for manual muscle testing
MRI	Magnetic resonance imaging
MS	Multiple sclerosis
MVIC	Maximal voluntary isometric contraction
NMD	Neuromuscular diseases (note that it is used as a plural)
OASI	Old-age and survivor's insurance (Switzerland)
OMD	Oculopharyngeal muscular dystrophy
PM	Polymyositis
SCI	Spincal cord injury
SMA	Spinal muscular atrophy
STS	Sit-to-stand
RoM	Range of motion
RMS	Root mean square

Chapter 1 Introduction

1.1 Motivation

Ambulation is one of the fundamental freedoms that humans possess. Mobility plays a key role in the independence of people [1] and largely supports a good quality of life [2], [3]. A study by the National Health Interview Survey from 2012 [4] reported that about 7% of the adult population in the United States, about 17 million people, claimed not to be able to walk a quarter of a mile (about 400m), or to be able to do so with significant difficulty. The first representations of a “rolling chair” go back to the end of the 16^{th} century, when such a device was built for the King Philipp II of Spain [5]. While medical assistive technology has made important breakthroughs since then, the most common solution today against severe ambulation disorders is still the wheelchair. The only recent radical innovation in wheelchairs is the embedding of motors that allow the user to move without assistance of another person, and without the necessity of using arms to self propel. Nevertheless, wheelchairs still suffer from various limitations in standard non-adapted areas such as stairs, sidewalk edges, hinged doors, and so on. They are furthermore difficult to carry and transfer in standard cars.

Impairment of ambulation can arise from several medical causes, including but not limited to traumatic brain injury, spinal cord lesions, hip or knee replacements, arthritis, Parkinson’s disease, multiple sclerosis, cerebral palsy, and muscular dystrophy. This work focuses on neuromuscular disease that affect skeletal muscles; a definition which encompasses a large group of rare and hereditary diseases with which a genetic default or mutation leads to fiber deterioration and muscular atrophy. Approximately 1 person in 2’000 is affected by such diseases (see Chapter 2); this extends to about 370 thousand people over Europe. The targeted diseases include muscular dystrophies and atrophies, inflammatory myopathies and diseases of peripheral nerves. These disorders are reputed to be incurable and degenerative. They are also known for having a great variation in degenerating rate, primary muscles affected, age of onset and lifespan. People affected by such diseases usually begin to experience minor discomfort or abnormalities during sport activities, a diagnosis follows after a few visits to a specialized neurologist. As the degenerative mechanism progresses, muscles begin to atrophy and difficulties in daily activities grow. Climbing stairs, rising from a sitting position and managing balance can become difficult or even impossible. At the same time, gait compensating patterns become very apparent, often causing patients to feel uncomfortable in public. Any uneven terrain begins to pose a significant risk of falling and the person usually adopts a quite sedentary life or begins to use a wheelchair for safety. Using a wheelchair and reducing exercise then rapidly worsens the muscular condition of the person, who has lost much of its former independence by this point. In cases of rapid degeneration, as often seen with Duchenne muscular dystrophy, the disease can lead to death in patients aged in their twenties. In other cases, with slow degeneration, the person will be able to keep her/his walking ability until an advanced age.

Medical research is still a few decades away from developing viable cures. This heightens the importance of finding alternatives that can improve quality of life for patients. For example, helping patients to stabilize their standing position and promoting motion and physical activity could help sustain a certain muscular strength and slow down atrophy, although, to prevent overloading muscles and potentially irreversible injury, people with such diseases will require a varying level of intensity depending on their individual case [6]–[8].

Since the beginning of the century, as technologies such as embedded electronics and computing have progressed, powered orthopedics has emerged as a developing field. The ability to couple human limbs with actuated robotics has been realized with success in patients with spinal cord injury (SCI), hemiplegia and multiple sclerosis among others [9], [10]. The first exoskeleton devices were stationary, i.e. the robotic legs are supported by a static frame over a treadmill, such as the Lokomat® (Hocoma AG, Switzerland) [11] or the LOPES from Twente University [12]. More recently, wearable exoskeletons emerged with the primary goal of providing mobility for people with SCI. These included products from companies such as ReWalk™ (ReWalk bionics, USA), Ekso™ (Ekso bionics, USA) or REX (Rex Bionics, New Zealand) among others. These devices have demonstrated the feasibility of autonomous and safe ambulation for people with complete SCI [13]. After a few years of availability on the market, the devices have also demonstrated major medical benefits for users with SCI, such as better bowel and bladder function and a reduction in the level of spasticity [13]. Despite these tremendous accomplishments, the accessibility of the exoskeleton as a personal device is still very low. This is certainly due not only to the high costs (about 80’000 $ to 140’000 $ per unit), but also to the limited performances; crutches in both hands are necessary in order to ensure balance control, walking velocities are about only 2 km/h and, for safety reasons, stair climbing is not yet fully supported. Currently, some of these devices, plus newly developed ones, are undergoing several clinical trials to evaluate the benefits as rehabilitative devices, not only for people with SCI, but also for stroke victims. It is the hope of researchers that growing the market availability will make the prices drop and make the devices more accessible to more people.

Wearable exoskeletons have great potential to improve quality of life in people suffering from neuromuscular diseases (NMD). First, it could prevent early fatigue experienced by people with NMD, which leads to necessary resting and greater risk of falling. It can also stabilize weaker joints for a greater range of activity. Eventually, it can also provide gait compensation to the user, or as a training device for physical therapy. With such a large list of benefits provided by the potential of wearable exoskeletons to those afflicted by NMD, one might wonder why it is not a more popular option for investment and advertisement.

There are some complications in adapting exoskeletons to the needs of those suffering from NMD. The strategies of “mobilization” employed for enabling persons with SCI to walk cannot be directly applied to mobilizing those with NMD. Firstly, the use of crutches requires important strength in the upper limbs which is not compatible with symptoms of NMD. Secondly, the “mobilization” strategy implemented to assist persons with SCI is based on predefined trajectories performed by the exoskeleton independently from the contribution of the user. However, the complications of NMD require adaptive “assistive” strategies, where both the device and the user can contribute together to the motion. These adaptive strategies are important in allowing assistance of weak joints and promoting user mobility.

1.2 Objectives and Approach

The development and optimization of novel orthopedics integrating latest technologies to allow safe and efficient ambulation in people suffering from neuromuscular diseases is a tremendous project. The objectives and contributions to that work are partitioned in smaller tasks.

1. Determine the specific needs for mobility assistance in people with NMD.
2. Evaluate a specific orthopedic design to improve the quality of life in people with NMD.
3. Develop adaptive control strategies for people with weak muscle condition but residual walking capacity.

The first task is the understanding of the effect on mobility of neuromuscular diseases. It includes understanding symptoms and their implications in daily activities, particularly those involving ambulation. Data on these symptoms are gathered from multiple sources, such as interviews with physicians and physiotherapists specialized in neuromuscular diseases, interviews and experimental gait analyses of people with NMD, national statistics from Switzerland, interviews with orthopedists, and specialized scientific literature. A major contribution comes from gait analyses of 14 people with heterogeneous NMD. This information covers a wide range of the NMD problem space, from the diseases and their heterogeneity, through the difficulties encountered in daily activity, to the causes and consequences of compensating gait pattern.

The second task consists in proposing solutions based on the specifications taken from the previous task. Particular attention will be focused on the architecture of the exoskeleton and determining which joints need to be assisted to provide the seven degrees of freedom within one human leg. The design will then focus on the design of actuators that are able to fulfill these specifications, while keeping the weight and bulk of the device to a minimum. Solutions of joint coupling between the hip and the knee flexion/extension are explored through design and implementation with a cable driven system. Further solutions to optimize the constraints on the actuation and transmission are then proposed. A full lower limb exoskeleton called AUTONOMYO is built for assessments with people with NMD.

The last task considers the design of adaptable collaborative control strategies to assist people with NMD. A novel finite-state active impedance controller is implemented on the AUTONOMYO device. Preliminary tests on a test bench are conducted to evaluate the sensitivity of the gait initiation and termination. Tests with a few healthy pilots and a pilot with moderately severe limb girdle muscular dystrophy are conducted to tune the parameters of impedance of the assistance, and to evaluate the feasibility of the controller with regards to the condition of the pilot operator.

1.3 Thesis Outline

The structure of the present document follows the order of the aims discussed in Section 1.2. Chapter 2 introduces various types of neuromuscular diseases, key statistics and a literature review on the walking disorders and corresponding compensating patterns. Chapter 3 describes the methodology of collecting gait information from a small group of heterogeneous NMD patients, and discusses the specifications of the assistance required by these people. Exoskeletons are introduced in 1.1, which focuses on the mechanical design of a lower limb device adapted for people with NMD. It addresses in particular the optimization of the actuation and transmission units to augment performances while keeping a compact and lightweight design.

The general design of the AUTONOMYO exoskeleton is also described in this chapter, and the performances are evaluated on a test bench. Chapter 5 presents novel control strategies specifically adapted to people with NMD. The implementation and the first evaluations with healthy pilots and one pilot with limb girdle muscular dystrophy are also described. All the elements from the contribution of the thesis are summarized in the last chapter while perspectives of future work are disserted.

Chapter 2 Neuromuscular Diseases

Neuromuscular diseases (NMD) are characterized by a disorder at the muscle level or at the peripheral nervous system responsible for the control of voluntary muscles. Such diseases are degenerative as the symptoms deteriorate with time. A large part of NMD are inherited such as muscular dystrophies but can also be inflammatory or caused by metabolic disorders. The NMD term groups together a large number of diseases that are individually categorized as rare; i.e. each affects less than 5 in 10’000 people following the definition of the European commission[1]. This chapter introduces different forms of neuromuscular diseases and presents the characteristics of the most common forms. It then discusses the implication of impairments in daily life and the statistical data available in Switzerland.

2.1 Types and forms of Neuromuscular Diseases

More than one thousand varieties of NMD exist. These variants have been grouped in a limited number of diseases, such as Duchenne muscular dystrophy or amyotrophic lateral sclerosis. A variant is usually characterized by a relative homogeneity in affected parts of the body, the rate of degeneration and the age of onset. Because of the numerous varieties of NMD and their low individual prevalence, NMD are often grouped under a common name such as limb girdle muscular dystrophy or congenital muscular dystrophy. Thus, NMD can be quite heterogeneous and is usually unpredictable. For example, it is common that, within one family, two siblings can have large differences in the rate of degeneration of the disease. Those diseases can be very severe with rapid deterioration and poor longevity, or on the milder side, with a slow progression over a few decades and with muscle weakness limited to certain parts of the body. Table 2-1 summarizes the main groups of NMD with their principal characteristics.

The following common types of NMD will be looked at in more detail: Duchenne and Becker muscular dystrophy, myotonic dystrophy, facioscapulohumeral muscular dystrophy, limb girdle muscular dystrophy, inclusion body myositis and Charcot-Marie-Tooth disease.

[1] https://ec.europa.eu/health/non_communicable_diseases/rare_diseases_en

Table 2-1 List of the most common neuromuscular diseases with the main characteristics

Neuromuscular disease		Abbreviation	Age at onset	Longevity	Body parts affected	Prevalence per 100’000
Muscular Dystrophies	Duchenne	DMD	2-6	Young adult	Proximal and distal muscles, Cognition, Heart muscles	1.7 – 4.2 [14]
	Becker	BMD	14-20	Subnormal	Proximal and distal muscles	0.4 – 3.6 [14]
	Myotonic (Steinert)	DM	20-40	Subnormal	Distal muscles Eyes, Cognition, Heart	0.5-18.1 [14]
	Facioscapulohumeral	FSHD	5-20	(Sub)normal	Face, shoulder and tibialis anterior muscles	3.2-4.6 [14]
	Limb girdle	LGMD	12-40	(Sub)normal	Proximal muscles	0.9-2.3 [14]
	Emery-Dreifuss	EDMD	5-12	(Sub)normal	Shoulder and calf muscles Heart muscles	0.1-0.4 [14]
	Oculopharyngeal	OMD	40-70	Subnormal	Extraocular muscles Respiratory functions	0.1 [14]
	Congenital	CMD	0	Variable	Variable	0.6 [14]
	Distal (various forms)	-	40-60	(Sub)normal	Distal muscles	-
Inflammatory Myopathies	Inclusion Body Myositis	IBM	>40	(Sub)normal	Proximal muscles Heart and lungs	1.5 [15]
	Polymyositis	PM	5-60			8-13 [16], [17]
	Dermatomyositis	DeM	5-60			
Diseases of Peripheral Nerves	Charcot-Marie-Tooth	CMT	5-70	Normal	Distal muscles	16-36 [18], [19]
Spinal Muscular Atrophies	Spinal Muscular Atrophy	SMA	0-70	Childhood to normal	Proximal muscles Respiratory functions	1.9 [20]
	Amyotrophic Lateral Sclerosis (Charcot)	ALS	50-70	About 3 years after onset	Cognition Full body muscles	2-5 [21]

2.1.1 Duchenne and Becker muscular dystrophies

Duchenne and Becker muscular dystrophies affect similar groups of muscles. The diseases both first affect the proximal muscles about the pelvic and shoulder girdles. Distal areas around the hands and feet, as shown in Figure 2-1, are affected less or at a later point.

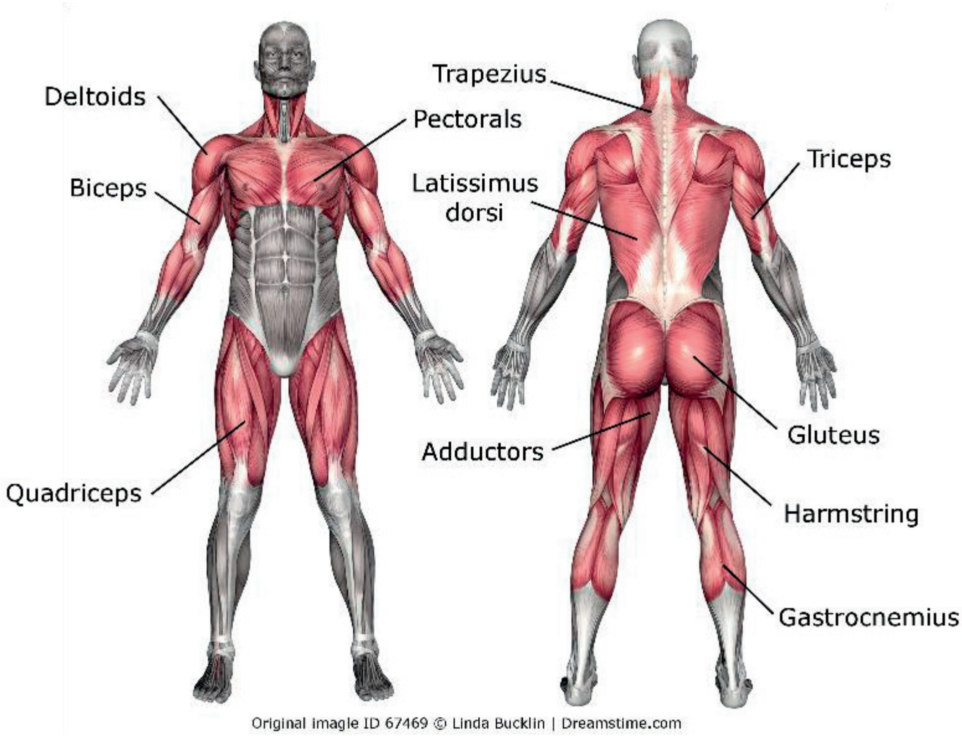

Figure 2-1 Muscles commonly affected in Duchenne and Becker muscular dystrophies (in red/dark)

Duchenne muscular dystrophy (DMD) is notorious for often occurring in children and teenagers and frequently decreasing life expectancy. Children affected by DMD are often bounded to wheelchairs by age 13; the disease leads to death by early adulthood due to vital organ dysfunction [22]. Moreover, DMD has the greatest rate of incidence among all muscular dystrophies. It is responsible for about fifty percent of the total incidence of all muscular dystrophies, combined. DMD primarily affects boys, as it is an X-linked disease; nevertheless, milder symptoms are also found in about 10% of female carriers [22]. Several studies report an incidence of 19-23.5 per 10^5 persons (~1/5'000) [23]–[25].

Becker Muscular Dystrophy (BMD) is a similar X-linked disease but takes a milder form than that of DMD. It progresses at a slower rate, with total loss of ambulation generally occurring in the thirties-forties. Persons with BMD have a near normal life expectancy and are, in most cases, diagnosed between the ages of 5 and 45 [26]. The prevalence of BMD is about 1.53 per 10^5 males as reported by Mah et al. [27] based on ten studies completed between 1991 and 2009.

2.1.2 Myotonic dystrophy

Myotonic Dystrophy (DM), also called Steinert's disease, is the most frequent muscular dystrophy that sets in during adulthood. There exist two forms of DM, caused by two different mutated genes: DM type 1 (DM1) and DM type 2 (DM2). DM appears usually in patients' twenties or thirties and reduces life expectancy due to cardiac conduction defects [28], [29]. Across Europe, between 3 and 15 cases per 10^5 are reported [14]. The muscles affected in DM1 are around the distal segments, such as hands, forearms, feet, calves, neck or face (see Figure 2-2). Muscles of the diaphragm are also often affected by DM1. DM1 also encompasses other disorders such as myotonia, which deteriorates the release of contracted muscles, cardiac conduction defects, cataracts, potential intellectual deficits, gastrointestinal disorders and more. DM1 is a slowly progressing muscular dystrophy where a loss of ambulation usually does not occur before the end of life [28]. People with DM1 suffer primarily from a lack of dexterity in the hands which prevents them from performing many simple activities of daily living (ADL) such as using a fork, a toothbrush and other tools. Foot drop is also common in people with DM1, and can be improved by the use of ankle foot orthosis (AFO).

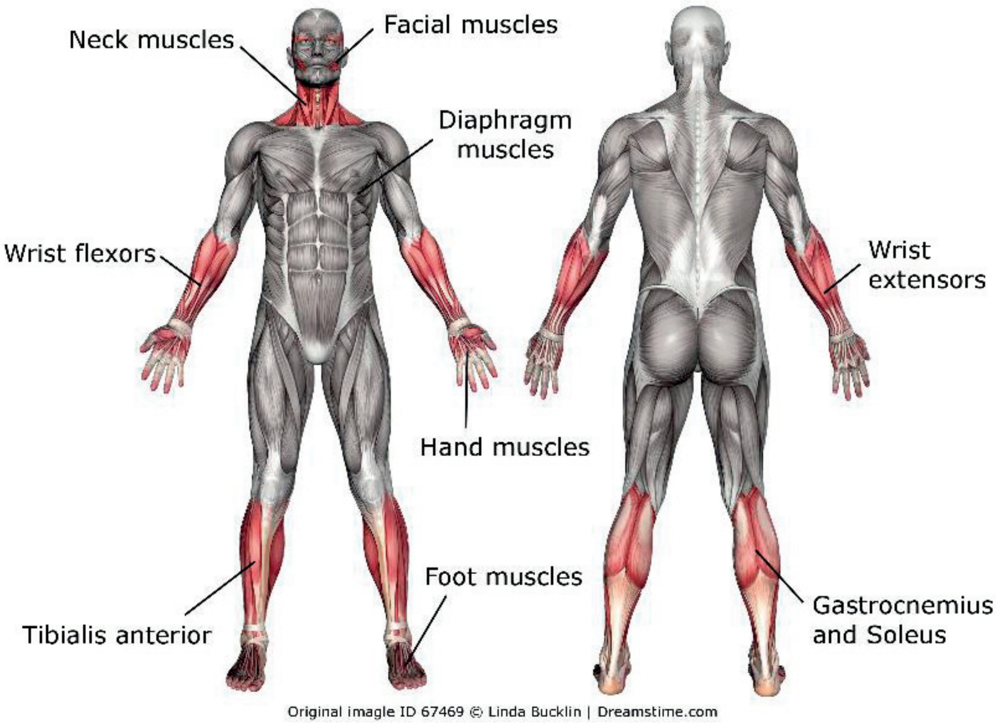

Figure 2-2 Muscles commonly affected in myotonic dystrophy type 1 (in red/dark)

DM2 is a milder form of DM1 which is less likely to reduce life span [28], [29]. While both DM1 and DM2's complications include myotonia and other disorders such as cataracts, there are several important differences. DM2 presents common proximal muscle weakness at the elbow extensors, the hip flexors and at the neck. It is also characterized by large muscle pain, muscle stiffness and muscle fatigue [30].

2.1.3 Facioscapulohumeral muscular dystrophy

Facioscapulohumeral Muscular Dystrophy (FSHD) is the third most common muscular dystrophy after DMD and DM [14]. It is named after the various muscle groups it affects i.e. the facial muscles, muscles about the shoulder (scapula) girdle and upper arm (humerus). It also frequently affects the muscles about the pelvic girdle and the foot dorsiflexors leading to foot drop syndrome, although the latter can usually be managed with ankle-foot orthosis [31], [32]. Muscle groups commonly involved in FSHD are highlighted on Figure 2-3. FSHD is a very slow degenerative disease, with a loss of strength of about 4,4% per decade [32]. Patients in the cohort of Kilmer et al. [32] were 36% to 68% weaker than controls in all weak muscle groups, which shows a relatively moderate weakness. Tawil et al. [33] also reported that about 20% of FSHD patients become wheelchair-bound, while the disease has poor incidence on the patient's longevity.

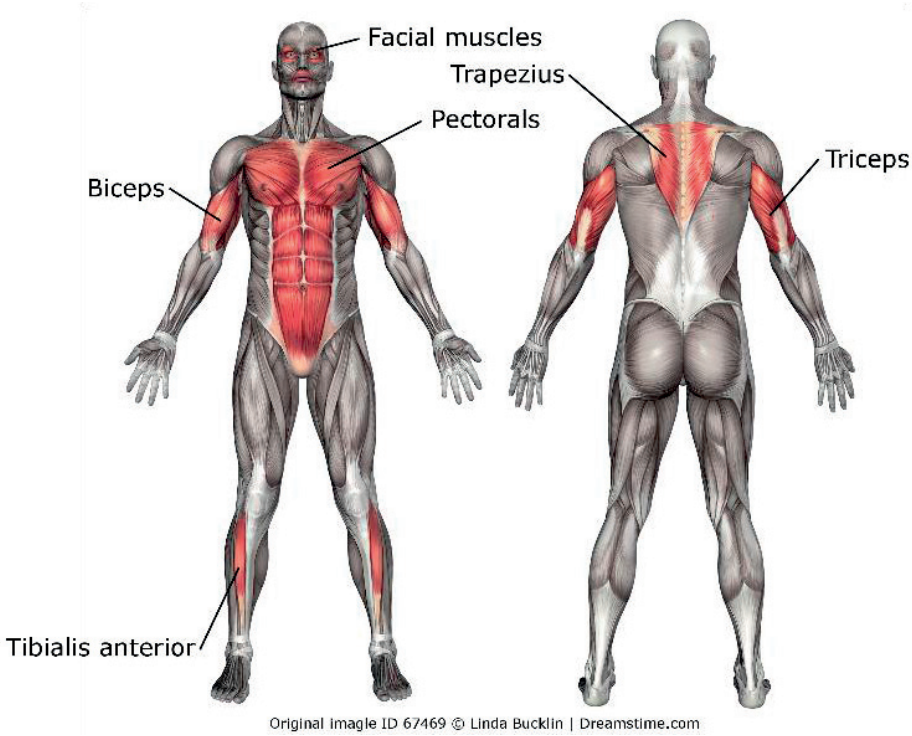

Figure 2-3 Muscles commonly affected in facioscapulohumeral muscular dystrophy (in red/dark)

2.1.4 Limb girdle muscular dystrophy

Limb Girdle Muscular Dystrophy (LGMD) currently encompasses about 30 forms, identified through the different genes involved in muscle atrophy. There are two types of LGMD; type 1 is autosomal dominant and type 2 is autosomal recessive [34]. As highlighted in Figure 2-4, proximal muscles, or muscles around the pelvic and shoulder girdles, are commonly affected by LGMD. As LGMD refers to a family of isolated forms of NMD, heterogeneity in muscle affection, age of onset, and rate of deterioration can be quite variable. It seems that the later the first symptoms appear, the slower the deterioration. As LGMD usually appears in adulthood, patients experience serious functional disabilities after a few decades, as the disease is mildly progressive [34], [35].

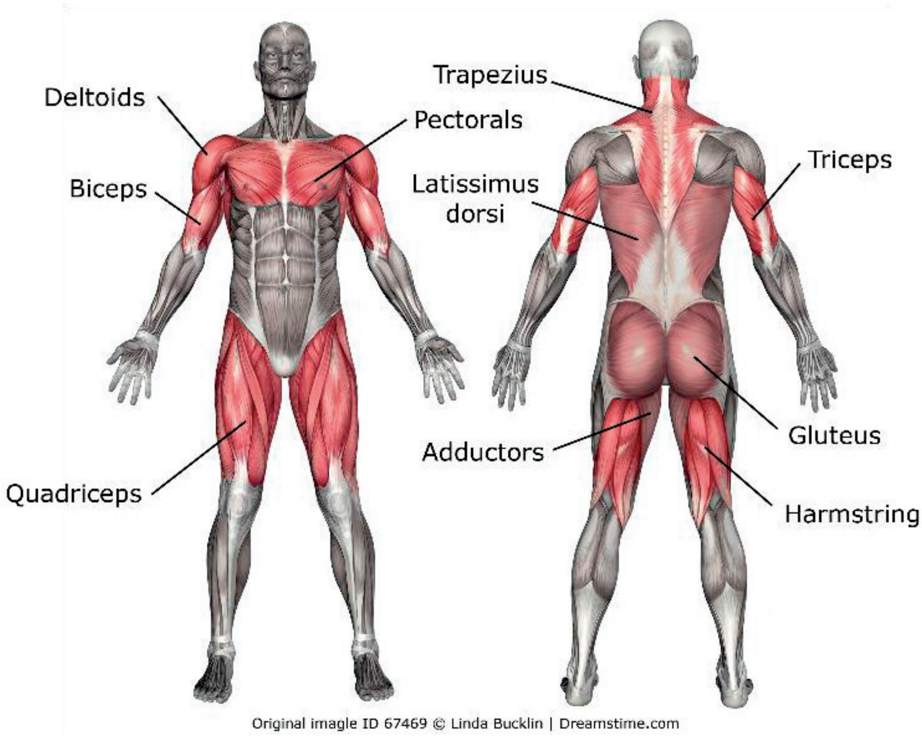

Figure 2-4 Muscles commonly affected in limb girdle muscular dystrophy (in red/dark), in lighter red/dark are additional muscles commonly affected in different forms of limb girdle muscular dystrophy

2.1.5 Inclusion body myositis

Inclusion Body Myositis (IBM) is a form of inflammatory myopathy which falls under the category of auto-immune diseases. Symptoms are very similar to those of muscular dystrophies and consist largely of muscle weakness and deterioration over time. IBM is characterized by late onset; most symptoms occur in patients around or over 50 years of age [36]. Another trait of IBM is a high homogeneity of affected muscles with very localized weakness. Quadriceps are primarily and most frequently affected, followed by elbow, wrist and finger flexors and extensors as illustrated in Figure 2-5 [36]. The disease also commonly affects pharyngeal muscles and leads to swallowing problems [36]. People with IBM experience moderate difficulty walking, but can suffer from frequent and abrupt falls due to weakness in the quadriceps. While most patients need an assistive device (e.g. 73% in the Badrising's cohort [36]) to ambulate, wheelchair use is much lower in this population (e.g. 14% [36]) and does not imply a total loss of ambulation (e.g. 78% of wheelchair users could still ambulate on their legs [36]). Badrising et al. [36] reported a mean time of 13 ± 8 years after onset before the necessity of wheelchair-assisted mobility.

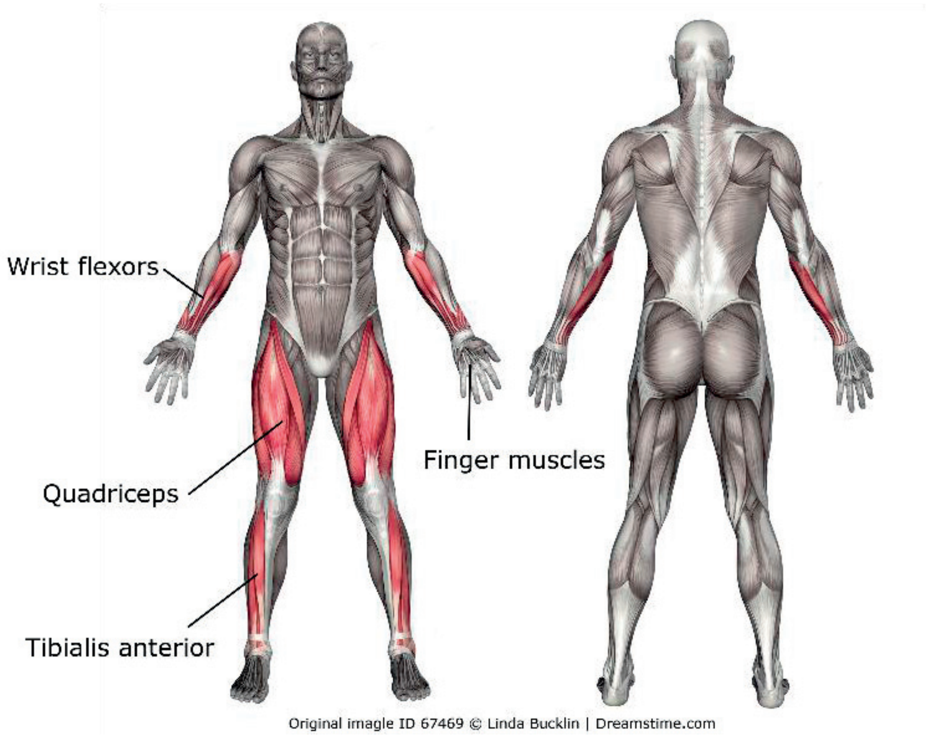

Figure 2-5 Muscles commonly affected in inclusion body myositis (in red/dark)

2.1.6 Charcot-Marie-Tooth disease

Charcot-Marie-Tooth disease (CMT) is a peripheral nerves disease and has the largest prevalence of the NMD described in Table 2-1. It affects about 1 in 2’500 persons [18], [19]. CMT, like LGMD, is a family of hereditary diseases that includes more than 50 genetic forms that can be dominant or recessive [19]. CMT is a neuropathy where the peripheral nerves, whether categorized as motor (efferent nerves) or sensory (afferent nerves), are subject to demyelination. Demyelination leads too poor conduction of signals by the nerves and thus a loss of sensation and motor control. Demyelination can also be found in major diseases such as multiple sclerosis. Muscle weakness, loss of sensation and general effects upon peripheral nerves are found mostly in the feet, calves, hands and forearms first, as seen in Figure 2-6 [37]. The age of onset of CMT varies largely due to its different forms [18], [37]. Symptoms are slow to increase in severity, and the disease rarely affects life expectancy.

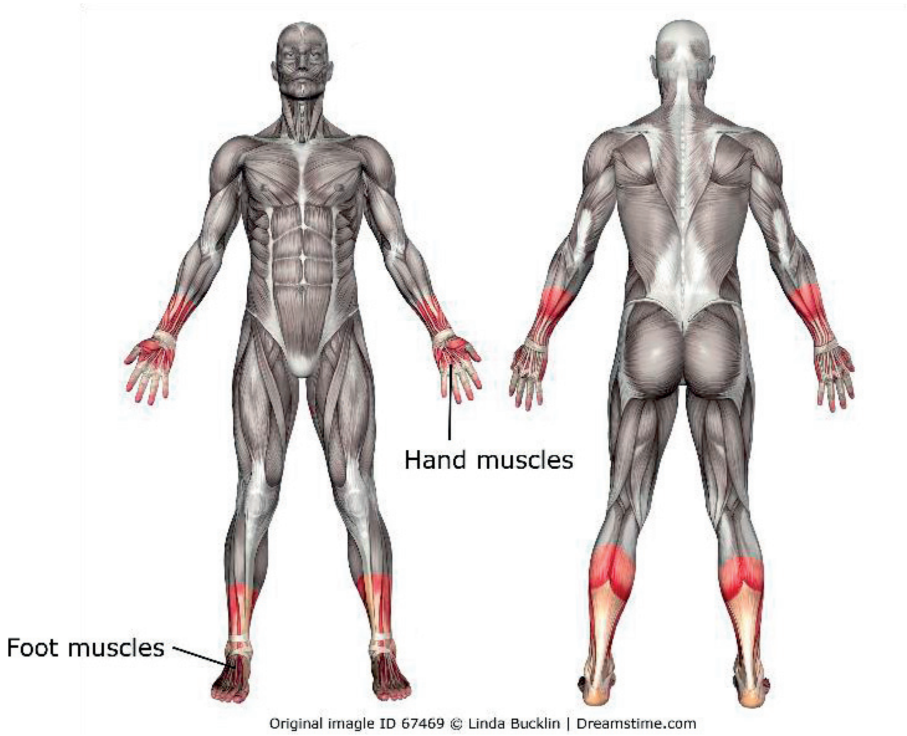

Figure 2-6 Muscles commonly affected in Charcot-Marie-Tooth disease (in red/dark)

2.2 Swiss Statistics about Neuromuscular Diseases

As previously discussed, more than a thousand of neuromuscular diseases exist, with very heterogeneous symptoms. It is thus difficult to gather statistical data from people suffering from neuromuscular diseases. Most complete data sets are kept by medical centers; however, no numerical database has been made that would allow a global statistical analysis. The Federal Statistical Office (FSO) in Switzerland collects data from the Disability Insurance (DI), which provides the largest available database on people suffering from neuromuscular diseases in Switzerland. In this section, data from the year 2012 is presented and discussed.

The available data sets from the DI have several flaws. First, the statistics reports only documented people that benefited from financial support from the DI during the given year, that includes people receiving a regular pension due to a reduced working capacity as well as patients with infrequent needs. These needs can be related to mobility solutions (car adaptations, home adaptations, wheelchair purchases, etc.). The data collected thus represents people with difficulties that impede their ability to work (thus they receive a pension). In addition, the report includes a fluctuating number of people without pensions that nevertheless benefit from regular financial support. People over 64 are no longer eligible to the DI, but belong to the Old-Age and Survivor's Insurance (OASI). Another bias comes from the processes of diagnosis, which requires extensive investigations and can be inconclusive. Statistics provided corresponds to the group defined by the disability code 184: Progressive muscular dystrophies and other congenital myopathies.

2.2.1 Demography of Neuromuscular diseases in Switzerland

In 2012, the Swiss population numbered over 8 million people [38]. 604 persons with muscular dystrophies or congenital myopathies are identified in the year 2012. In comparison to the projections made from the statistical rates of occurrence, this number represents about 56% of the total estimated persons with muscular dystrophies and congenital myopathies. Figure 2-7 shows the distribution across age of people with muscular dystrophies as compared to the total population of Switzerland.

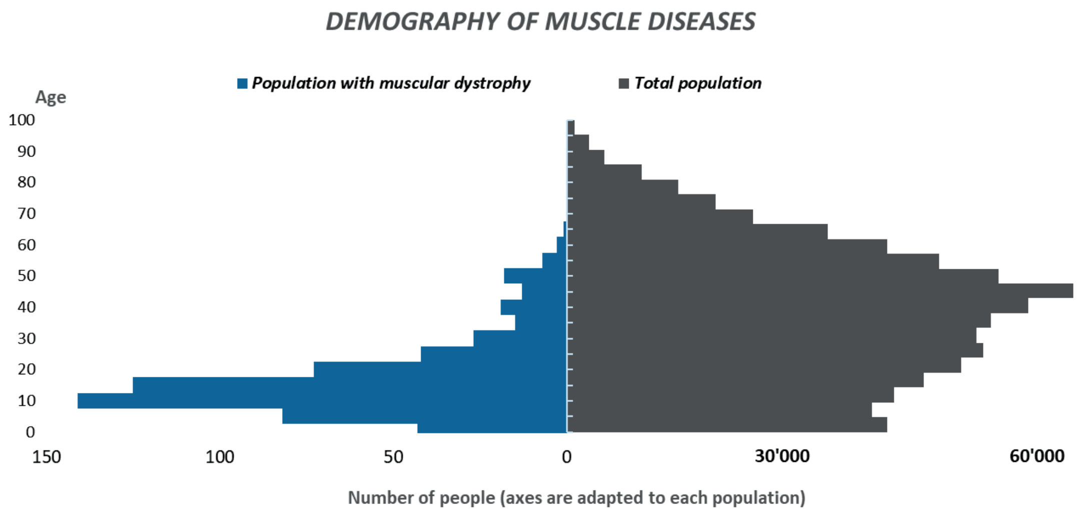

Figure 2-7 Demography of persons with a muscular dystrophy or congenital myopathy as reported by the Swiss Disability Insurance in 2012, on left. Demography in Switzerland, on right.

Based on the provided statistics, about two third of the persons affected by NMD are younger than 20 years old. One can also observe two trends. First, there is a high increase in cases from birth to pre-adolescence. Second, there is a constant decrease in cases from adolescence to the thirties. The first trend can be explained by the typical appearance of first symptoms during childhood, and therefore an increase in reported cases of NMD. The second trend could suggest that radical decrease in support by the DI are due to higher mortality rates. The hypothesis of a high mortality during the 20s and 30s is encouraged since the demography change is permanent. This idea is also supported by literature on Duchenne muscular dystrophy, as similar trends are found in the literature from 0 to 30 years old for Duchenne muscular dystrophy [23]. In conclusion, this demographic illustrates the high incidence rate of severe muscle diseases such as Duchenne muscular dystrophy with an onset at early childhood and a high mortality rate from adolescence to young adult ages.

While the absence of reported people with muscular dystrophies over 64 is related to the change insurance from DI to OASI as mentioned previously, the low number of instances between 40 and 64 is not totally understood. Indeed, a significant portion of NMD cases are detected and diagnosed after the forties and represent a considerable amount of people with muscular dystrophies. A possible explanation for the low count of people with late disease onset can be related to milder disabilities, where people are less prone to benefit from the disability insurance.

2.2.2 Impairments Related to Neuromuscular Diseases

NMD are characterized by progressive muscle atrophy. Not only does the atrophying of initially affected muscles become exacerbated, but the disease also spreads to other muscle groups with time. As illustrated in the figures above, most common NMD affect muscles in both lower and upper limbs. However, the level of impairment can vary depending on the level of weakness of the muscle group. The impairments reported to the DI are illustrated in Figure 2-8.

About 47% of the people with NMD and supported by the DI suffer from a full body impairment, while 24% suffer only from lower extremity impairment and 24% have other musculoskeletal impairments. People suffering only from upper extremity impairments represent less than 2%. In conclusion, most impairments are reported for the full body. A significant proportion of people with NMD are affected only at the lower extremities, while impairment of the upper extremities only is rare.

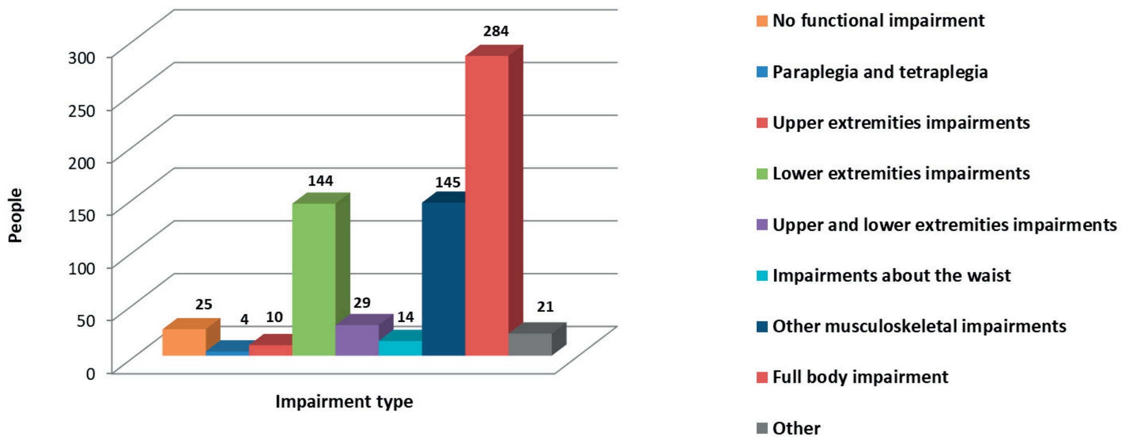

Figure 2-8 Types of impairment and distribution of people with muscular dystrophy or congenital myopathy, based on data from the Swiss Disability Insurance in 2012.

2.2.3 Nature of Services Provided to People with Neuromuscular Diseases

The type of services financed by the DI are reported below in Figure 2-9. Wheelchairs, leg orthoses and car modifications are the most common services provided, and motorized wheelchair make up the most frequently provided service due to full body impairment from NMD. While non-motorized wheelchair use is less common in NMD people, it offers better transportability, e.g. it can be easily carried in a car. Leg orthosis can be recommended to be worn at night with severe diseases such as Duchenne muscular dystrophy to prevent muscle shortening during childhood, although children often do not tolerate the orthoses well. Other leg orthoses are AFO (ankle-foot orthoses) which are effective in correcting foot drop disorders. Car modifications allow people with NMD to drive a car, as they cannot drive or enter a standard car. Another service is house modification; for example, improving access to the bathroom.

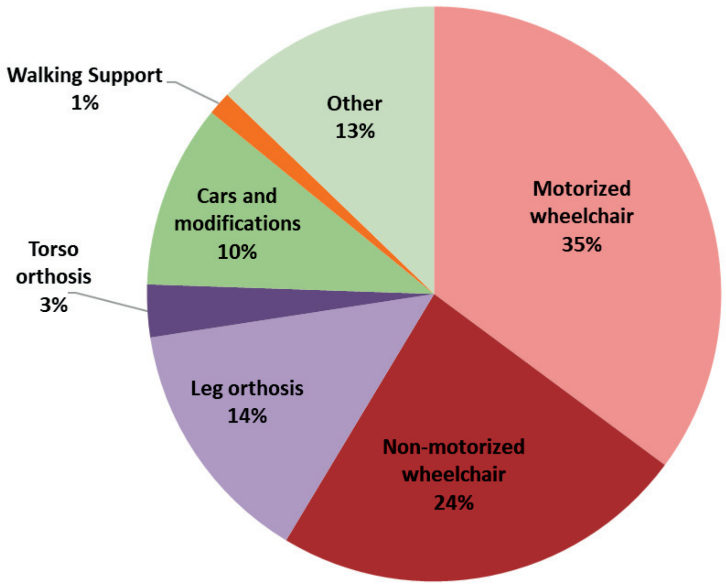

Figure 2-9 Proportion of services provided by the Swiss Disability Insurance by type for people with muscular dystrophies or congenital myopathies in 2012.

2.3 Research and Treatment for Neuromuscular Diseases

Neuromuscular diseases are the subject of large interest around the world from medical research facilities. It is a growing field where new types of diseases are constantly being discovered. A search of the Web of Science database (including MEDLINE®) shows that the number of publications per year covering the topic “muscular dystrophy” (see Figure 2-10) is constantly growing. The threshold of 300-500 publications per year was reached about the 60’s – 70’s.

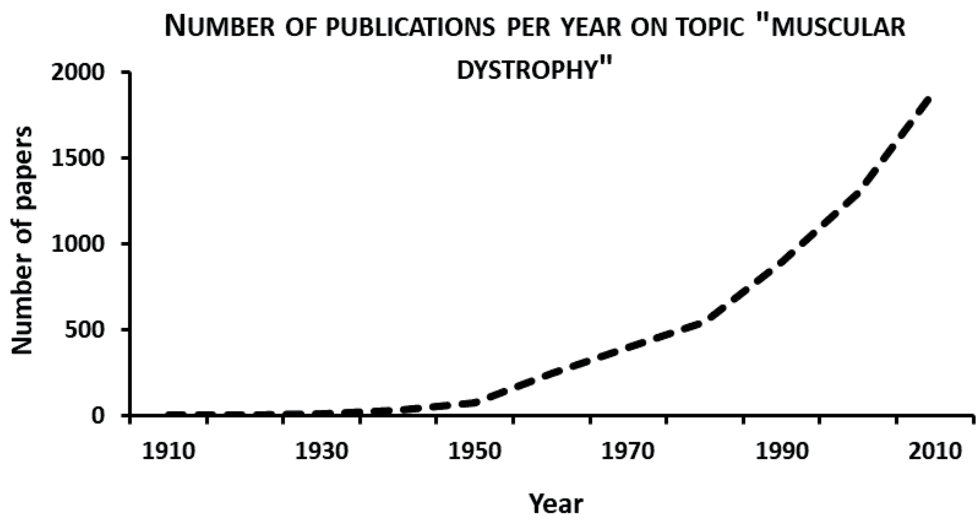

Figure 2-10 Number of publications per year on the topic “muscular dystrophy” reported by the *Web Of Science* research engine including *Web of Science core collection* and *MEDLINE®* databases

2.3.1 Genetics and Medications

The primary and greater research on NMD is genetic, as there currently exists no cure for NMD. Much effort has been made towards identifying the mutations in the genome that cause symptoms [39]. Currently, research is oriented towards developing biological mechanisms that could decrease or counter the effects induced by the defective genes [39]. Another promising topic in treatment of neuromuscular diseases is gene therapy [40] [41]. Gene therapy consists of injecting subjects with vectors (modified viruses that are meant to be innocuous) that carry a selected gene. Those vectors then transmit the gene into the human cells nucleus [42]. Two genetic therapies for NMD have been already granted FDA approval: eteplirsen for Duchenne muscular dystrophy and nusinersen for spinal muscular atrophy [41]. However, these therapeutical therapies are not completely developed, and trials show that patients respond in very different manners. Gene therapies are also currently very expensive, costing from several hundreds of thousands of dollars to a few million for a single therapy [43]. Another issue of gene therapy in rare diseases lies within the very small population included in clinical trials; this leads to a lack of evidence for efficacy [43].

Other than the recent entry of gene therapy, corticosteroids have typically been used and tested in Duchenne muscular dystrophy. Corticosteroids are reported to improve muscle strength over a period of six months to two years [44]. Adverse effects of corticosteroids include the apparition of Cushing Syndrome (e.g. weight gain, facial puffiness, etc), excessive hair growth and others [44]. Other medications, not specific to NMD help to preserve vital organs affected by NMD, such as the heart or the lungs. One example is angiotensin-converting enzyme inhibitors that reduce the rate of death of people with vascular disease [45].

2.3.2 Physical Treatments

Physical treatment refers to physiotherapy-like sessions that consist of stretching exercises, physical exercise, respiratory endurance exercises and so on. Muscles and muscle fibers are composed of cells that are constantly subject to atrophy (decrease in cell's size), hypertrophy (increase in cell's size) and hyperplasia (increase in cell number). Immobilization or the lack of exercise leads naturally to muscle atrophy, following a simple rule of "use it or lose it" [46]. A non-NMD example of this can be seen in astronauts, who live in zero-gravity conditions in low Earth orbit for significant periods of time. Kawakami et al. [47] highlighted that the loss of strength after a bedridden period is not only due to muscle atrophy. They noticed that after being bedridden for 20 days, the neural activation levels dropped significantly and better expressed the low forces measured than the muscle change in volume (atrophy). It is thus important, in order to loss of strength, for NMD-afflicted to maintain a minimal level of exercise for the entire body. While this statement is true for any person, people with NMD are more prone to a sedentary lifestyle due to the increased risk of fall, the level of fatigue, etc.

Hypertrophy is caused by mechano-biological stimulus, commonly called resistance exercise, that results in an increased muscle volume and strength [48]. The skeletal muscles' adaptation to some stimulus can take three forms: it can expand radially or longitudinally, by the addition of sarcomeres in series or in parallel, or it can produce more mitochondrial oxidative enzymes and augment the resistance to fatigue [49]. It seems that resistance exercise, typically exercises including muscle overloading, increases muscle atrophy in cases of NMD. It has been reported that some exercises induce muscle damage, repair and adaptation [50]. To the awareness of the author, no study details the mechanisms of damage and repair, nor the involvement of these mechanisms in neuromuscular diseases. However, it is believed that typically, in people with muscular dystrophy, the process of repairment is hindered by the disease and leads only to an irreversible damage of the muscle fibers.

NMD prevents the strengthening of muscle through intensive exercises, meaning that muscular atrophy can only be avoided by exercising or maintaining a certain level of physical activity. Recommendations for physical exercises can be found in the literature. For example, Cup et al. [43] reviewed a total of 58 studies on exercise therapy differentiating between motor neuron disorders, motor nerve root disorders and peripheral nerve disorders, neuromuscular transmission disorders, muscle disorders and heterogeneous groups. Children (<18 yo) were excluded from the review. Significantly effective studies are reported in Table 2-2.

Table 2-2 Significantly effective studies considering physical treatments in NMD (N=number of subjects, sn=session, wk=week)

Reference	N	NMD type	Body parts	Type of exercise	Sessions plan
Alexanderson et al. 2000 [51]	11	Poly-/dermatomyositis	Shoulder, hand, hip, knee	• Exercise for strengthening, 15min walking, stretching	15min 5 sn/wk X 12 wk
Aldehag et al. 2005 [52]	5	Myotonic dystrophy	Hand	• Exercise with silicone putty	4min 3 sn/wk X 12 wk
Taivassalo et al. 1999 [53]	24	Mitochondrial/Non-metabolic myopaties	Legs and trunk	• Treadmill exercise 70-85% of heart rate reserve	20-30 min 3-4 sn/wk X 8 wk
Taivassalo et al. 1998 [54]	10	Mitochondrial myopathies	Legs and trunk	• Treadmill exercise 60-80% of heart rate reserve	20-30 min 3-4 sn/wk X 8 wk
Taivassalo et al. 2001 [55]	10	Mitochondrial myopathies	Legs	• Cycling 70-80% of maximal heart rate	30-40 min 3-4 sn/wk X 14 wk
Trenell et al. 2006 [56]	10	Mitochondrial myopathies	Legs	• Cycling 70-80% of maximal heart rate	30 min 3 sn/wk X 12 wk
Haller et al. 2006 [57]	8	McArdle's disease	Legs	• Cycling 70-80% of maximal heart rate	30-40 min 4 sn/wk X 14 wk
Olsen et al. 2005 [58]	8	Facioscapulohumeral MD	Legs	• Cycling 65% of VO2 max	35min 5 sn/wk X 12 wk
Cejudo et al. 2005 [59]	20	Mitochondrial myopathies	Full body	• Cycling 30min at 70% of peak work rate • 10-15 repetitions of different arm exercises	60 min 3 sn/wk X 12 wk
Wiesinger et al. 1998 [60]	14	Poly-/dermatomyositis	Legs and trunk	• Cycling 60% of maximal HR • Step aerobics at different intensities • Stretching	60 min 2-3 sn/wk X 6 wk
Wiesinger et al. 1998 [61]	8	Poly-/dermatomyositis	Legs and trunk	• Cycling 60% of maximal HR • Step aerobics at different intensities • Stretching	60 min 1-3 sn/wk X 6 months
Aitkens et al. 1993 [62]	27	Various dystrophies (DM, LGMD, FSHD), neuropathies and SMA	Arm, hand, legs	• 3x4 repetitions with load at 10%-30% for knee, elbow and hand grip • Increase of resistance and repetitions with therapy	15-20min 3 sn/wk X 12 wk
Florence and Hagberg 1984 [63]	12	Various dystrophies (CMD, LGMD, FSHD), myopathies, CMT and SMA	legs	• Cycling series of 5min with 2min rest intervals at 70% of VO2 max	3 sn/wk X 12 wk
Dawes et al. 2006 [64]	18	Various dystrophies (BMD, DM, LGMD, FSHD), myositis and myopathies	legs	• Walking at light intensity for 20min then with moderate intensity	8 wk

In summary of Table 2-2, it is shown that some exercises can improve the quality of life of certain type of NMD. Cycling, referred to as an aerobic exercise, shows efficacy in addressing symptoms of: mitochondrial myopathies, McArdle's disease, facioscapulohumeral muscular dystrophy, polymyositis, dermatomyositis and to some extent to congenital myopathies, limb girdle muscular dystrophy and spinal muscular atrophy. However, persons with Charcot-Marie-Tooth disease were insensitive to the therapy [63]. Treadmill exercise has proven effective in cases of mitochondrial myopathies, and to a lesser degree with non-metabolic myopathies [53], [54]. Hand exercises also proved effective in myotonic dystrophy, polymyositis and dermatomyositis [51], [52]. Pure strength training seems to be less beneficial unless done with few repetitions and low resistance in poly-/ dermato- myositis and various NMD [51], [64].

Other studies do not demonstrate significant effectiveness of the physical therapy, however constraints make it difficult to address such as large heterogeneity in people with NMD and the low number of participants recruitable per region. Studies found in the literature primarily address cases of slowly progressive diseases and retaining significant muscle capacity (as demonstrated by the more mobile and strenuous types of activities proposed during these therapies) [43]. Y. P. Demir [65] investigated the different elements provided in the literature and reported major points – mainly, that exercise programs need to be tailored regarding the disease parameters such as progression, severity, onset, and the patient's characteristics such as age and sex [59]. Exercise programs for strengthening are recommended only at mild to moderate levels and at the early stages of the disease while muscle capacity is only mildly affected by the disease [66].

2.4 Ambulation in Neuromuscular Diseases

2.4.1 Introduction

Ambulation in neuromuscular diseases can be very singular and easily recognizable. With the effects of NMD often very localized to a particular body part or area, persons with NMD develop unique compensation patterns for frequent movement patterns such as walking and shifting from a sitting to a standing position. In order to discuss solutions for improving mobility, exercising and quality of life in persons with NMD, it is important to thoroughly investigate the causes and consequences related to muscle atrophy. The next section presents a literature review on compensatory motions related to NMD. The following section presents the results from a study conducted for this thesis on gait pattern in a heterogeneous group of NMD patients. Lastly, these are combined to define the problem space in terms of kinematics and kinetics for improving ambulation.

2.4.2 Literature Search

In order to understand the compensatory motions while walking with NMD, a literature review is summarized in this section. Both Web of Science "All databases" (Clarivate Analytics) and SciVerse Scopus® (Elsevier) were searched for literature. Details on terms of search and results are described in Table 2-3. The search was first performed in Web of Science, then it was sorted based on titles and abstract and finally it was sorted through the content. As the first search was very broad, the second search using the Scopus database was refined from the search terms to dismiss studies on animals (mostly dogs and mice). Inclusion criteria for the acceptance of paper were: study on the kinematics of people with NMD, study on the kinetics of people with NMD, study on compensatory motions in people with NMD. Exclusion criteria were: case studies on one or two persons with NMD, disorders not related to NMD, studies not available (at least the abstract) in English.

Table 2-3 Parameters and results of the literature review on gait patterns in neuromuscular diseases

Database	Advanced search terms	Period	Results raw	Results after first sorting through titles	Results after sorting by content
Web of Science	TS = ((duchenne OR becker OR ((myotonic OR steinert) AND dystrophy) OR facioscapulohumeral OR "limb girdle" OR "emery dreifuss" OR oculopharyngeal OR "congenital dystrophy" OR "inclusion body myositis" OR polymyositis OR dermatomyositis OR "charcot marie tooth" OR "spinal muscular atrophy" OR "amyotrophic lateral sclerosis" OR "charcot disease" OR dystrophy OR myopathy OR atrophy) AND (gait OR walk OR walking) AND (pattern OR motion OR kinematics))	Up to 19.05.2018	751	133	53
Scopus	TITLE-ABS-KEY (((duchenne OR becker OR ((myotonic OR steinert) AND dystrophy) OR facioscapulohumeral OR "limb girdle" OR "emery dreifuss" OR oculopharyngeal OR "congenital dystrophy" OR "inclusion body myositis" OR polymyositis OR dermatomyositis OR "charcot marie tooth" OR myopathy OR myopathies) AND (gait OR walk OR walking) AND (pattern OR motion OR kinematics)) **AND NOT (dog OR dogs OR mouse OR mice OR animal OR animals))**	Up to 19.05.2018	327	+14 new (compared to web of science list)	

2.4.3 Diseases Investigated and Sizes of the Studies

From the fifty-three studies found in the literature and respecting the inclusion and exclusion criteria, ten types of NMD have been studied with a leading interest in Duchenne muscular dystrophy, Charcot-Marie-Tooth disease and myotonic dystrophy. Table 2-4 summarizes the number of studies per type of NMD, the average number of participants per study and whether children or adults or a mix were examined. Most studies investigated a single disease, while a few observed a mixed type of disease [67]–[70]. The size of the studies is largely limited in NMD, large one with DMD at a national scale can reach up to 60 [71], 70 [72] or even 145 [73] participants. While studies are commonly made of 10 participants or less, the average size of the studies is about 30 participants. Most studies investigated participants over 18 years old, except for studies on DMD and SMA type II as these diseases have early onset and shorter lifespan. Studies on CMT cases have mixed test sets of both children and adults. The number of studies is correlated with the prevalence (or incidence) of the diseases.

Table 2-4 Summary of number of studies found in the literature assessing gait patterns in NMD per disorder

Neuromuscular disease	Number of studies	Studies on children/ adults/mixed	Number of NMD participants (mean ±std)
Duchenne muscular dystrophy **DMD**	16 (+1 review)	15 / 1 / 0	26 ±35
Charcot-Marie-Tooth disease **CMT**	11 (+1 review)	2 / 2 / 7	21 ±16
Myotonic dystrophy **DM**	8	0 / 8 / 0	18 ±14
Facioscapulohumeral muscular dystrophy **FSHD**	5	0 / 5 / 0	10 ±4
Inclusion body myositis **IBM**	3	0 / 3 / 0	35 ±24
Limb girdle muscular dystrophy **LGMD**	2	0 / 2 / 0	17 ±4
Becker muscular dystrophy **BMD**	2	0 / 1 / 1	27 ±35
Spinal muscular atrophy **SMA**	2	1 / 1 / 0	5 ±4
Amyotrophic lateral sclerosis **ALS**	2	?	26 ±2
Poly- / dermato- myositis **PM/DeM**	1	0 / 0 / 1	3

2.4.4 Topics of the Studies

Studies tackling gait in NMD cases focus on different aspects, and can be categorized into the following broad labels: muscle strength vs performance, compensatory kinematics, gait parameters, and decline prediction. « Strength vs performance » investigates the correlation between muscle strength and walking performances. The muscle strength is usually evaluated by a simple manual muscle test or through magnetic resonance imaging (MRI), which reveals the level of residual muscle fibers. Walking performances are usually evaluated using a validated test such as the 2-minute walk test (2MWT) or 6 MWT. The second category « kinematics compensation » studies the compensatory motions by comparing the kinematics and kinetics between two groups, usually between one group with NMD and one control group. Such an experiment requires a motion tracking system and force plates to record the kinematics and kinetics of gait. The third category « gait parameters » investigates basic gait parameters, typically compared to a control group. Usual gait parameters are parameters such as stride length, stride rate, duration of double stance, walking velocity, etc. A fourth category « decline prediction » investigates correlations between degeneration and effects upon lifestyle to predict events; for example, a certain amount of muscle strength is required for ambulation. Other isolated studies investigated other factors such as the modifications of the ground reaction forces during gait in comparison to a control group. The different studies and topics are summarized in Table 2-5.

Table 2-5 Studies related to gait analysis in NMD people by topics treated

Category of study	Number of studies	Diseases Investigated	References
Muscle strength vs performance	9	DMD, IBM, FSHD, DM, BMD, ALS, SMA	[72], [74]–[81]
Compensatory kinematics	30	DMD, CMT, IBM, FSHD, DM, SMA, LGMD, PM, DeM	[67], [68], [70], [71], [82]–[107]
Gait parameters	6	DMD, CMT, DM, ALS	[108]–[113]
Decline prediction	2	DMD	[73], [114]
Other	4	DMD, BMD, CMT, DM, IBM, LGMD	[69], [115]–[117]

2.4.4.1 Muscle Strength versus Performance

Nine studies, covering the correlation between some muscle strength and the functional performances such as walking, are presented in Table 2-6. All studies seem to follow a recent interest as they were all published over the last six years. All examinations were focused on a single disease each, including inclusion body myositis and dystrophies such as facioscapulohumeral, myotonic, Duchenne and Becker. Three different muscle strength tests are reported in the conduction of the studies: maximum voluntary isometric contraction (MVIC), manual muscle test (MMT) and magnetic resonance imaging (MRI). Performances in ambulation are mostly examined using a 6-minute walk test (6MWT) or 10 meter walk test (10 meter WT).

The maximum voluntary isometric contraction (MVIC) is a test that allows to quantitatively assess the strength of a group of muscles, such as knee flexors or hip extensors. It measures the torque capacity at the joint using a dynamometer apparatus. Strength is measured only in a specific position, usually with both hip and knee flexed at 90° (sitting position). The manual muscle test (MMT), is a test that does not need a specific device. The person being evaluated is asked to perform motions under different constraints such as limb gravity, counter-force resistance of varying strength, or no constraint at all. A score is given depending on the highest resistance the subject can overcome. While this test is not very precise and is best suited for weak muscles, it is very simple and quick to perform. Magnetic resonance imagery (MRI) is commonly used in muscular atrophy and dystrophy, as it allows evaluation of how much fat has infiltrated muscles, and gives direct access to measuring individual muscle capacity. This approach requires more equipment and resources, but offers more precise results.

The 6-minute walk test (6MWT) evaluates the distance a person can travel in 6 minutes. This test evaluates the walking ability of the person and her/his endurance. It is usually conducted with people without severe gait condition as it requires a significant amount of effort. The 10 meter walk test (10 meter WT) assesses gait condition without relying as much on endurance, which induces fatigue. This test often records walking kinematics and kinetics, and is recommended for people with severely impaired walking abilities who cannot cover long distances.

Table 2-6 Summary of studies examinating the relation between muscle strength and walking performances

Reference	Country	Diseases/ Participants	Muscle test	Performance test
Alfano 2017 [74]	USA	(s)IBM / 55	MVIC	2MWT, 6MWT, timed stairs
Davenport 2014 [77]	USA	(s)IBM / 42	MVIC	10 Meter WT (comfor-table+fast)
Aprile 2012 [81]	Italy	FSHD / 16	MMT	10 meter WT, 2MWT
Rijken 2015 [80]	Netherlands	FSHD / 10	MRI (trunk+legs)	10 meter WT (comfor-table+fast)
Bachasson 2016 [75]	France/ Canada	DM(1) / 22	MVIC (neck+legs flexions)	6MWT
Park 2017 [78]	Korea	DM(1) / 19	MRI (trunk to neck)	6MWT
Park 2018 [79]	Korea	DM(1) / 19	MRI (legs)	6MWT
Bozgeyik 2017 [72]	Turkey	DMD / 70	MMT	6MWT
Barp 2017 [76]	Italy	BMD / 51	MRI (legs)	6MWT

Alfano et al. [74] reported that the strength of hip extensors, knee extensors and plantar flexors, and body-weight, best described performances in 2MWT in sporadic IBM participants. However, only knee extensors and plantar flexors expressed performances in 6MWT. The performances for climbing stairs were also evaluated and were correlated with the strength of the knee extensors. Davenport et al. [77] studied sporadic IBM participants over 10 meters at comfortable and fast walking speed. They reported that the strength of the knee flexors and ankle plantar flexors significantly and positively impacted comfortable walking, while the strength of the knee extensors alone significantly increases fast walking.

In people with FSHD, Aprile et al. [81] found that hip flexors, knee extensors and ankle dorsiflexors strength better expressed walking speed, but also greater step length and smaller lateral step width. Although step width in anterior studies was mostly correlated with hip abductors [118], [119]. Rijken et al. [80] observed both MRI of most leg muscles and some of the trunk, but also recorded the gait kinematics and kinetics over a 10 meter WT. Results show that performances at comfortable speed is correlated with the ankle push off power and muscle tissue proportion in calf (ankle plantar flexors) and gluteus maximus (hip extensor). The same correlations are observed for performances at fast walking speed, while an additional correlation is found with the hip power generated at push off.

Studies with people with myotonic dystrophy type 1 show a correlation between walking performances in 6MWT with ankle plantar flexors and neck muscles strength [75], [78], [79]. Bachasson et al. [75] also found some positive correlation between walking speed and knee extensors or ankle dorsi flexors.

Bozgeyik et al. [72] studied walking performances in children with Duchenne muscular dystrophy. They reported a correlation between neck strength and walking velocity. Barp et al. [76] largely investigated the muscle tissue proportion in people with Becker muscular dystrophy. They reported a correlation between the 6MWT performance and most lower limb muscles (gluteus maximus, vastus lateralis, adductors, biceps femoris, semitendinosus, semimembranosus, tibialis anterior, soleus, and gastrocnemius medialis), where the biggest correlation is found with the semitendinosus from the hamstrings group (hip extensor and knee flexor).

From the few studies presented here that investigate the muscle strength correlation with walking performances, the results are quite varied. Although each NMD affects different muscle group, gait is frequently affected. It seems that the muscles which are needed for walking motion are also those most affected by NMD. One possible conclusion is that all muscles contribute largely to the walking performances, however, the weakest muscles reflect more significantly the decrease in walking velocity. Another interesting and non-intuitive observation made in this section is that walking performances are reported to be largely influenced by the neck muscles in myotonic dystrophy and Duchenne muscular dystrophy. In conclusion, studies on correlations between muscles and performances do not clearly outline the overall scheme, as studies were biased by the homogeneity of the muscle weakness in the individual groups.

2.4.5 Compensation Kinematics

A large group of studies investigated the adaptation of NMD patients to the disease through the motion pattern during gait. Studies about compensation kinematics (angle at joints) often also measured the kinetics (moments at joints) and EMG (muscle activity). The moments at joint are calculated based on the ground reaction forces measured usually over two or three steps by force platforms, plus the kinematics and anthropometrics of the participant. The muscular activity can be measured by EMG sensors placed on the skin and are able to provide the timing of the muscle activation and a rate of activation relatively to maximal intensity; however, no force or absolute level of contraction can be measured or extracted to directly assess the human implication.

2.4.5.1 Duchenne Muscular Dystrophy

Duchenne muscular dystrophy is the most frequently seen NMD. The disease evolves largely during childhood or adolescent years with severe complications and death usually during early adulthood. The studies with DMD participants are resumed in Table 2-7. Trias et al. [106] defines three classes of the evolution of symptoms : early, intermediate and final. As the disease evolves rapidly, muscles are globally affected, which differs from slower diseases where very distinct groups of muscles are affected. The first observations reported in children with DMD, compared to controls, are a shorter step length ([85]–[87], [92], [106]), a larger step width ([85], [86]) and a similar ([86]) or increased cadence ([87], [92]) and a decreased walking velocity with a higher metabolic cost ([106]).

One of the main characteristics of DMD gait is toe walk, where the person walk mostly on the frontal part of the foot while the heel is less loaded [67], [85], [106]. To make it simple, toe walk resembles the gait of someone wearing with high heeled shoes. This complication comes at an advanced stage of the disease. Linked to that toe walk comes also a foot drop symptom which is due to the poor dorsiflexion capacity at the ankle [86], [87]. The foot drop symptom is marked by a larger plantar flexion of the ankle during the swing phase compared to controls. In order to allow a good foot clearance and avoid tripping, people adopt a steppage gait, where compensations are a circumduction motion of the full leg [70] accompanied by an abnormally large hip and knee flexions during swing phase [70], [85], [86], [94]. Hyperlordosis is reported in DMD by [86], [87] with a large range of motion of the pelvic frontal tilt [87]. In the frontal plane, large pelvic tilts and large hip abduction during swing are measured following waddling gait patterns [86], [87]. Both strategies are adopted to compensate for proximal muscle weakness about the trunk and the thighs. A tendency to muscle hyperactivity in all main muscles and proportional to the severity of symptoms has been observed in [103], [106]. It seems that hyperactivity helps co-contracting and thus stiffening the joints to diminish the effect of unpredicted perturbations and reduces the risk of falling.

Table 2-7 Summary of studies examinating compensation patterns in gait in DMD people

Reference	Country	Diseases/Participants	Participants age	Measurement
Armand 2005 [70]	France	DMD / 2 – SMA II / 2	Children	Kinematics / kinetics
Armand 2006 [67]	France	DMD / 1736	Children	Kinematics / kinetics
Boccardi 1997 [84]	Italy	DMD / 10	Children	Kinematics / kinetics / EMG
Chen 2013 [85]	China	DMD / 10	Children	Kinematics
D'Angelo 2009 [86]	Italy	DMD / 21	Children	Kinematics
Doglio 2011 [87]	Italy	DMD / 15	Children	Kinematics / kinetics
Gaudrealt 2009 [91]	Canada	DMD / 11	Children	Kinematics / kinetics / EMG
Gaudreault 2010 [92]	Canada	DMD / 11	Children	Kinematics / kinetics
Goudriaan 2018 [93]	Belgium	DMD / review paper	Children	-
Goudriaan 2018 [94]	Belgium	DMD / 15	Children	Kinematics / kinetics
Ropars 2016 [103]	France	DMD / 16	Children	Kinematics / kinetics / EMG
Trias 1994 [106]	France	DMD / 12	Children	Kinematics / EMG / Metabolic cost

2.4.5.1 Charcot-Marie-Tooth Disease

Ten studies focused on the gait pattern of people with CMT. Main characteristics of the studies can be found in Table 2-8. CMT includes several types of diseases; however, all CMT are quite homogeneous and affect mainly the flexors of the ankle. The age at onset may still vary, which is why studies include people with a large range of age from children to elderly.

The main gait parameters observed are similar to those seen in DMD: a slower walking velocity, shorter step length, slower cadence with a lower swing velocity and a larger step width [88].

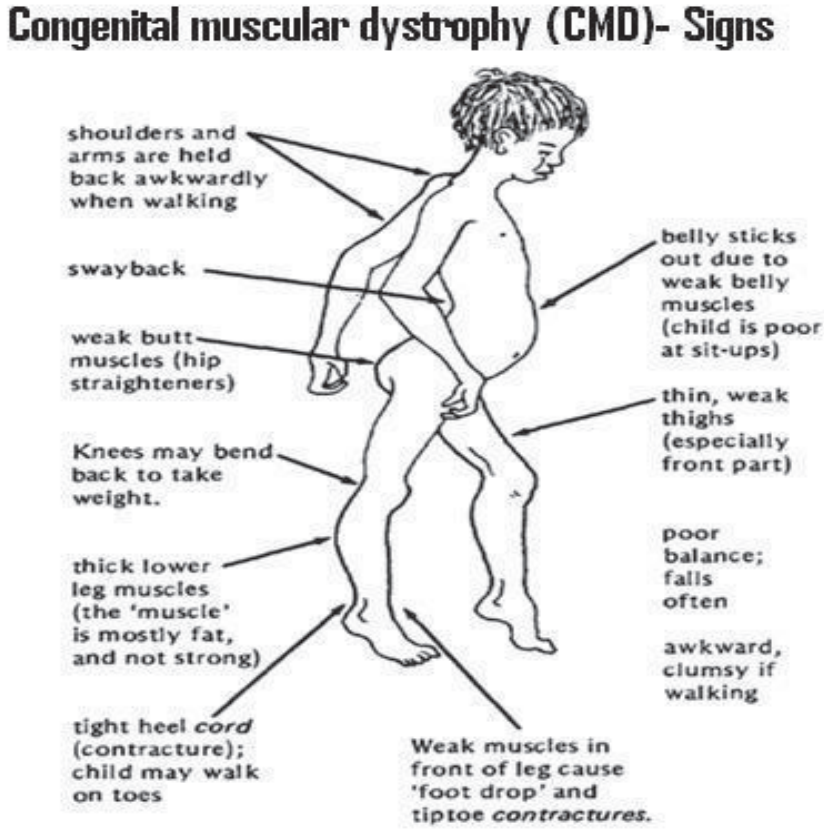

Figure 2-11 Illustration of the posture of a children with Duchenne muscular dystrophy during walking. Credits. Werner 1987[2].

Characteristic gait patterns will differ depending on the residual strength capacity in ankle dorsiflexors and plantarflexors muscles. Three groups have been extracted from studies of several diseases [71], [88], [89], [95]: a group presenting good dorsi- and plantar-flexors, a group with poor dorsiflexors but good plantarflexors and a group with both poor dorsi- and plantar-flexors. While the first group with low muscle weakness does not present highly noticeable deviations from the kinematics of healthy people, the two other groups can present quite different patterns. Since both groups have poor dorsiflexors strength, footdrop is a frequent first symptom [71], [88], [89], [95] that appears during the swing phase and requires the rest of the body to compensate for it, in order to mitigate the risk of tripping. Footdrop is marked by an abnormal plantar flexion during the swing phase, followed by a first contact with the ground with the toes, compared to a heel strike in healthy people, and lands in a stance phase with the foot flat on the ground. Depending on the types of ankle weaknesses, different compensating patterns are reported.

[2] https://cellbiology.med.unsw.edu.au/cellbiology/index.php?title=File:Congential_Muscular_Dystrophy.jpg

Table 2-8 Summary of studies examinating compensation patterns in gait in CMT people

Reference	Country	Diseases/Participants	Participants age	Measurement
Don 2007 [88]	Italy	CMT / 21	Adults	Kinematics / kinetics / EMG
Ferrarin 2012 [89]	Italy	CMT / 21	Children	Kinematics / kinetics
Guillebastre 2013 [95]	France	CMT / 26	Adults	Kinematics / kinetics
Kennedy 2016 [97]	Australia	CMT / review	Children	-
Kuruvilla 2000 [98]	USA	CMT / 5	Adults	Kinematics / kinetics
Lencioni 2018 [99]	Italy	CMT / 21	Mixed	Kinematics / kinetics / EMG
Marchesi 2011 [100]	Italy	CMT / 30	Adults	Kinematics / kinetics
Newman 2007 [101]	Ireland	CMT / 16	Mixed	Kinematics / kinetics
Ounpuu 2013 [120]	USA	CMT / 33	Children	Kinematics / EMG
Wojciechowski 2017 [71]	Australia	CMT / 60	Children	Kinematics / kinetics

Don et al. [88] observed steppage gait in a group of people with good plantar flexor strength but poor dorsi-flexors. It compensates the footdrop by augmenting the hip and knee flexion angles to allow a good clearance of the foot despite the footdrop. In this case, the metabolic expenditure is increased compared to healthy gait [88]. The push-off phase is also impacted, by increasing hip extension and delaying push until higher dorsiflexion is reached (the foot stays longer flat on the ground) [88], [120]. The good residual strength in the plantar flexor allows a push phase that is a direct factor of the walking velocity.

In case of both dorsi- and plantar-flexors weakness, the postural stability is largely hindered. Two studies observed a compensating pattern in the form of a stiff knee gait. The hip and knee flexions are limited, but there is a larger pelvic tilt (hyperlordosis) and a large hip abduction that provides foot clearance [88], [89]. The motion is mainly provided by the hip with a greater hip extension moment and power [89]. Wojciechowski et al. [71] reported that both dorsi- and plantar-flexors strength is highly related to the walking performances. People being affected at both sides of the group muscles around the ankle, and thus ambulate slowly. The walking performances and postural stability in CMT can however be greatly improved by wearing ankle-foot orthosis (AFO) than can contribute to correct the footdrop impairment [88].

2.4.5.1 Other diseases

Few studies investigated the compensation kinematics in cases of diseases other than Duchenne muscular dystrophy and Charcot-Marie-Tooth disease. Three studies examined myotonic dystrophy (DM), while no more than one study were found that tackle facioscapulohumeral dystrophy (FSHD), inclusion body myositis (IBM), limb girdle muscular dystrophy (LGMD), dermatomyiositis and polymyositis (DeM and PM) and spinal muscular atrophy of type II and III (SMA). These studies are described in Table 2-9.

Table 2-9 Summary of studies examinating compensation patterns in gait in non-DMD or non-CMT neuromuscular diseases

Reference	Country	Diseases/Participants	Participants age	Measurement
Galli 2012 [90]	Italy	DM / 10	Adults	Kinematics / kinetics / EMG
Tiffreau 2012 [105]	France/Bel-gium	DM / 15	Adults	Kinematics / kinetics / EMG
Wright 1995 [107]	USA	DM / 5	Adults	Kinematics / kinetics
Iosa 2007 [118]	Italy	FSHD / 12	Adults	Kinematics / kinetics
Moreno Izco 2005 [68]	Spain	DM / 40 – FSHD / 9 – LGMD / 14	Adults	Kinematics
Bernhardt 2011 [83]	USA	IBM / 9	Adults	Kinematics / kinetics
Siegel 2007 [104]	USA	PM / 2 – DeM / 1	Mixed	Kinematics / kinetics
Armand 2005 [70]	France	SMA II / 2 – DMD / 2	Children	Kinematics / kinetics / EMG
Matjacic 2008 [82]	Slovenia	SMA III / 7	Adults	Kinematics / kinetics / EMG

Myotonic dystrophy primarily affects the distal muscles. DM cases present a low walking velocity due to both a low cadence and step length, while the stride width is large [90]. Hyperextension at the knee during stance is reported in about 60% of cases and is combined with a high pelvic tilt and a small hip extension at push off [90]. Most effort is reported around the hip to minimize the power needed from the knee and ankle [90]. Hyper activation of the gastrocnemius (plantar flexor) is reported with a very small range of motion (RoM) about the ankle dorsi-/plantar-flexion during swing [105]. Oscillatory motions about the hip during stance in flexion/extension were noticed [107] and highlights impairment at nerve level.

Facioscapulohumeral muscular dystrophy affects first distal muscles and then spreads to proximal limbs. Hence, the weakness about the ankle is more severe than about the hip and knee. The main kinematics abnormalities reported are a large reduction of the maximal knee flexion (about 50%), combined with knee hyperextension during stance [118]. The hip and ankle pattern differs more moderately than the knee in the sagittal plane, where lower dorsiflexion can be observed at the ankle and the hip maximal extension before push off is also reduced [118]. The gait pattern is close to a stiff knee compensatory behavior.

Inclusion body myositis affects mostly the quadriceps muscles (knee extensor and hip flexor). The main kinematic compensation to lower the knee loading in extension is the knee hyperextension during the stance phase [83]. Foot drop symptoms can also appear later with the progression of the disease [83]. In other inflammatory myositis such as polymyositis and dermatomyositis, hip and knee muscles are mostly affected and leads to low knee flexion and low hip extension during stance in order to reduce torque [104].

Type II spinal muscular atrophy in children generally affects muscles. Hyperlordosis (large pelvic tilt), hyperextension of the knee during stance, small flexion of the hip and knee during swing and absence of plantarflexion have been recorded [70]. The combination of all compensations seems particularly effective as torques were largely decreased at every joints. Step length was increased by pelvic motions [70]. In type III SMA in adults, large pelvic tilt, knee hyperextension during stance and larger hip adduction are observed [82]. A higher hip adduction torque allows an increase in foot clearance while reducing torque on hip and knee flexion/extension[82]. The plantar flexion at the ankle is only slightly impaired as demonstrated by torque amplitudes similar to the one measured in the control group [82].

2.5 Conclusions

2.5.1 Specificities of Neuromuscular Diseases

Neuromuscular diseases include heterogeneous group of disease marked by progressive muscle wasting on variable locations. The research in this field is recent and no cure have been discovered yet. Exercising can help maintain a moderate strength of the muscle, but persons with NMD need to be cautious not to overload their muscle as it can lead to the destruction of remaining fibers. The full body, including some parts of the lower and the upper body, is usually affected. Ambulation disorders are one of the main consequences of neuromuscular diseases. However, there is a lack of solutions to support these disorders, canes are rarely used and ankle-foot orthosis significantly improve gait, but it is limited to person with mostly ankle weakness. The most reimbursed solutions in Switzerland are motorized and non-motorized wheelchairs. There is thus a great need for new type of assistive systems for the mobility and promotion of exercising in neuromuscular diseases. The biggest challenge of neuromuscular diseases is the large variability in the symptoms that would either require a multitude of solutions or only a few solutions that would be modular and adaptable.

2.5.2 Ambulation and Compensating Patterns

Over a literature review of 53 papers that reported observations on ambulation in neuromuscular diseases, 31 studies focused on the kinematics of compensating pattern. Duchenne and Charcot-Marie-Tooth muscular dystrophies account both for about one third of the studies. The rest consist mostly of isolated studies on one neuromuscular disease or heterogeneous studies. The following gait patterns have been reported in the studies:

- Toe walk, where the “heel strike” event that occurs at the beginning of the stance phase is replaced by a first contact with the ground with the toes. The gait is denoted by large plantarflexion during the full gait cycle due to a constant tension on Achilles tendon.
- Foot drop or steppage, where the dorsiflexors are very weak and the foot tends to plantarflex during the swing phase under the effect of the gravity.
- Hyperlordosis, which is denoted by an abnormal anterior tilt of the pelvis and a large curving of the lower back.
- Hyperextension of the knee, where the knee is slightly bended inwards during stance in order to avoid to load the quadriceps group.
- Waddling gait, where the upper body swings largely laterally during double stance in an inverted pendulum-like manner. This motion allows to help and compensate for hip drop in persons with hip abduction weakness.

- Co-contration or stiff gait, which is a common tendency in people with neuromuscular diseases in order to increase their stability.

Each of these compensating patterns are caused by a dysfunction from the musculoskeletal system. Their study allows to address the specific need for people with neuromuscular diseases. In a general manner, all the studies that observed the gait parameters denoted a lower walking velocity, a shorter stride length and a larger stride width in people with neuromuscular diseases compared to the control groups. The large majority of studies were performed on a small group of people, usually between 5 and 15 people. Moreover, apart from Duchenne and Charcot-Marie-Tooth muscular dystrophies, there exist very few studies on the other types of neuromuscular diseases. While the existing studies are non-representative as the number of participants are very limited.

Chapter 3 Ambulation in Neuromuscular Diseases – Experimental Observations and Projection of Needs for Assistance

3.1 Introduction

Following the literature review on gait compensations presented in section 2.4, an investigation was performed on a heterogeneous group of people with neuromuscular diseases. This study provided better understanding of different symptoms of NMD and its various paths of development, while also illustrating the implication of NMD-related impairments on various aspects of subjects' daily lives. In order to investigate the ambulation in a varied population of people with NMD, a group of NMD-impaired people were collected. These subjects all had a residual capacity to walk, whether it be with or without some type of assistive aid. Due to the severe symptoms and complex conditions that arise when a child with NMD is growing, only adults were included in the study. Subjects were found through advertisements in the neuromuscular disease unit of the CHUV (Centre Hospitalier Universitaire Vaudois) and through the ASRIMM (Association Suisse Romande Intervenant contre les Maladies neuroMusculaires).

The study consisted of two parts: an interview and a measurement of muscular strength and gait kinematics. The interview section addressed subjects' history of symptoms and collected information on how these symptoms impacted activities of daily living (ADL). Then, measurements of muscular strength and recordings of the gait kinematics were taken. The primary goal of the study was to observe the different compensation patterns in NMD, to understand what kind of needs each joint level had that an assistive device would need to provide, and to build up the full specifications for an assistive ambulation device. The work presented here is partially based on the publication "From gait measurements to design of assistive orthoses for people with neuromuscular diseases" by A. Ortlieb, J. Olivier, M. Bouri, H. Bleuler and T. Kuntzer [69]. The experiment was approved by the local Ethics Committee (CER-VD 174/14).

3.2 Method

3.2.1 Participants

Two groups of participants took part in the study: a group of people with NMD with a residual ability to walk at least 100m and a control group composed of healthy people without any walking disorder. Fourteen adult subjects with a genetically or histologically confirmed NMD condition volunteered in the study (8 males and

6 females, aged 48.7 ± 15.8 years) with the following distribution of conditions: 5 with facioscapulohumeral muscular dystrophy (FSHD), 3 with Charcot-Marie-Tooth neuropathies (CMT), 2 with Becker muscular dystrophy (BMD), 2 with myotonic dystrophy type 1 (DM1) and 2 with inclusion body myositis (IBM). All participants satisfied the main criterion of being able to walk at least 100 meters without any support other than ankle foot orthoses (AFO), if needed. Seven of the participants required their AFOs to be able to perform the gait measurements (see Table 3-1). The control group consisted of five participants (2 males and 3 females, aged 32.4 ± 15.5 years) who did not present any walking disorder.

3.2.2 Intervention

A short questionnaire was provided to participants that collected information on the participants' daily amount of ambulation, the limitations encountered when walking for long distances or durations, over uneven ground or while climbing stairs. The questionnaire also gathered history of symptoms and the progression of the NMD (e.g. age at onset, loss of the capacity to do a certain activity, etc.).

Following the questionnaire, a manual muscle test was performed on the participant following the medical research council (MRC) grading scale. The hip abduction, adduction, flexion, extension and the knee flexion, extension and the ankle plantarflexion and dorsiflexion were manually tested and a mark from 0 to 5 based on the MRC scale. Both legs of each participant were evaluated; the mean muscle strength over all the joints was documented. The MRC scale is as follows:

- 0 – indicates no contractility felt
- 1 – small motions are perceived
- 2 – the participant can largely move while the effect of gravity on the limbs is compensated
- 3 – the participant can largely move while the limbs are subject to the gravity
- 4 – the participant can hold against some resistance (manually exerted by the tester)
- 5 – the participant can hold against full resistance [121].

Finally, the main interview consists of recording the kinematics of the participants while walking. All participants with NMD were asked to walk at a comfortable velocity. The control group was asked to match the pace of the NMD participants. The walking path was more than 8 m long, with a handrail to secure participants; participants were asked to use it only in case of emergency. A custom made mobile tracking system recorded the motion of the heels, shanks, thighs and the pelvis of the user [122]. The system is presented in Figure 3-1. It is composed of a mobile cart (1) with two independent driving wheels in front (2) that are controlled by an embedded computer (7). Two draw-wire displacement sensors (6) mounted on the cart can be attached to the participant so that the distance and orientation of the cart can be regulated [123]. The tracking system Accutrack 250® (Atracsys LLC, Puidoux, Switzerland) includes a master optical sensor unit working in the infrared range and seven (customizable) active markers with 4 LEDs. The tracking sensor (3) is mounted on the cart while the markers (4) are placed on the lower limbs of the participant. The aim of the cart is to keep the markers within the working range of the tracking sensor (about 1.5m to 3m). The advantage of using a mobile tracking system is that it is not spatially dependent and permits fewer cameras to be used (only one, in this case) [123]. The tracking unit is able to record the 6-D positions (3-D position and 3-D orientation) of each markers with a sampling rate above 80 Hz [122].

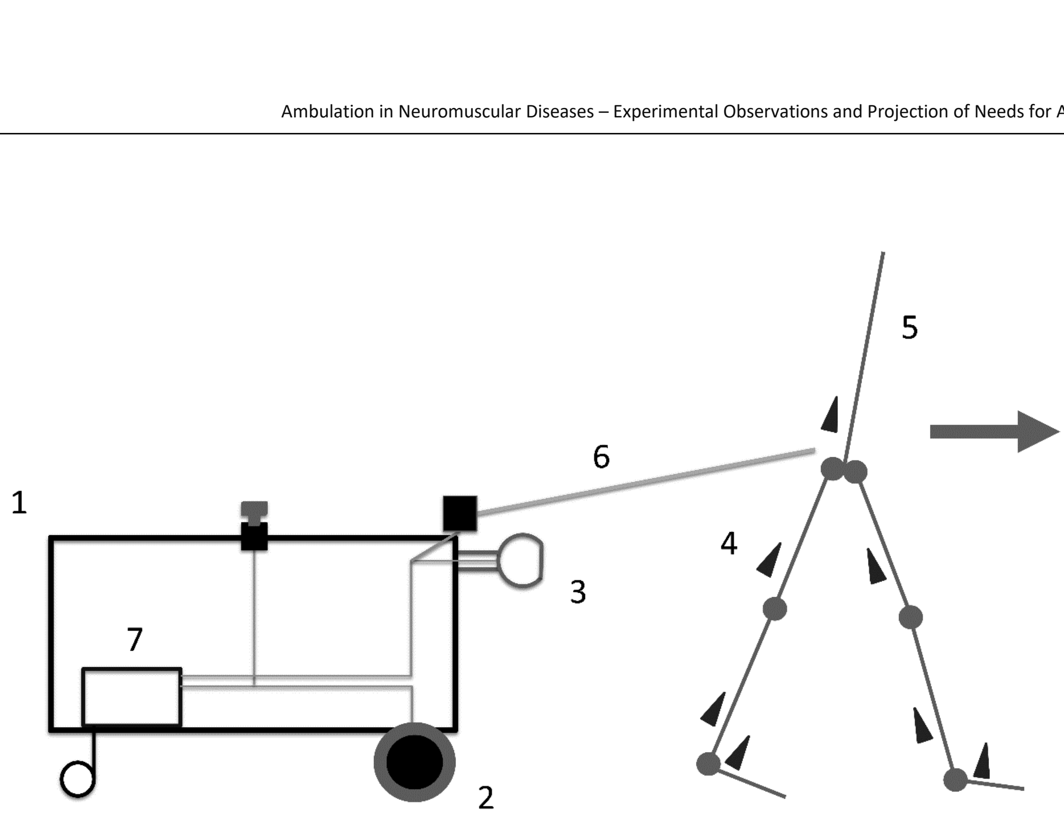

Figure 3-1 Representation of the optical tracking setup with: 1. Mobile platform, 2. Motorized front wheels, 3. Tracking camera unit, 4. Infrared active markers, 5. Subject, 6. Cable sensor of distance and 7. Embedded computer collecting data and controlling the cart motion. Copyright © 2015, IEEE

The Euler angles about the hip, knee and ankle joints are calculated based on the difference of orientation in the three planes of the two adjacent markers of each joint. In order to measure the gait cycle, the heel strike events are detected as the heel markers reach their lower vertical position. The collected data are then normalized over the gait cycle and superposed to obtain the mean and standard deviation of each data set.

3.3 Results

3.3.1 Walking aid and daily activities

Participants' ability to walk unaided or with a cane varied greatly, ranging from ten minutes up to two hours. None used rollators. Most participants reported that handrails were necessary for most of them to walk uphill or to climb stairs. Ankle-foot orthoses were common among the participants; most who used them were unable to walk without them. A few participants (2) preferred to use a wheelchair or scooter instead of walking. Those who used wheelchairs said that balance disorders and the risk of falling were primary reasons that they transitioned to regular use of a wheelchair.

3.3.2 Walking velocity and joint kinematics

The walking condition in the group with NMD is first analyzed based on what we will term "comfortable velocity criteria." Table 3-1 present the subjects and their main characteristics sorted from the low to the high comfortable walking velocity. The measured comfortable walking velocity of the group with NMD is, on average, 2.1 ±STD 0.6 km/h and ranging from 1.4 km/h to 3.2 km/h. The comfortable walking speed of a healthy person, by comparison, are about 4.9 km/h as reported by Bohannon et al. [124]. The average score of the group with NMD on the manual muscle test is 2.9 ±STD 0.4, where 3 represents a condition in which large motions can be performed if the limbs are only subject to gravity – however, if there is some resistance present, the limbs cannot hold these positions. The estimated mean strength loss is roughly about 40% compared to somebody healthy with a minimum muscle capacity. It was of interest to see if correlations existed between some characteristics of the participants and their respective comfortable walking velocities. None of the parameters, such as disease, age, sex, affection score and use of orthoses, showed any statistically relevant correlation with the walking performances. Figure 3-2 illustrates the poor correlation between the comfortable walking velocity and the muscle strength.

Table 3-1 Subjects characteristics and measured velocities

Subject	***Characteristics***				
	Disease	***Age***	***Sex***	***Affection score (MRC scale 0 – 5)***	***Comfortable walking velocity [km/h] ([cm/s])***
S1*	CMT	70	M	2,88	1,44 (40)
S2*	CMT	58	F	3,13	1,46 (41)
S3	FSHD	67	F	3,25	1,53 (43)
S4	BMD	40	M	2,38	1,71 (47)
S5*	CMT	34	F	3,31	1,71 (48)
S6	FSHD	29	F	2,19	1,77 (49)
S7	BMD	30	M	3,06	1,89 (53)
S8*	FSHD	54	F	2,88	1,95 (54)
S9	FSHD	66	M	3,00	2,48 (69)
S10*	DM1	44	M	3,06	2,5 (69)
S11*	FSHD	44	M	2,75	2,58 (72)
S12	DM1	42	M	3,31	2,63 (73)
S13*	IBM	31	F	2,13	2,9 (81)
S14	IBM	73	M	3,56	3,17 (88)

* Were wearing an ankle-foot orthosis during the test

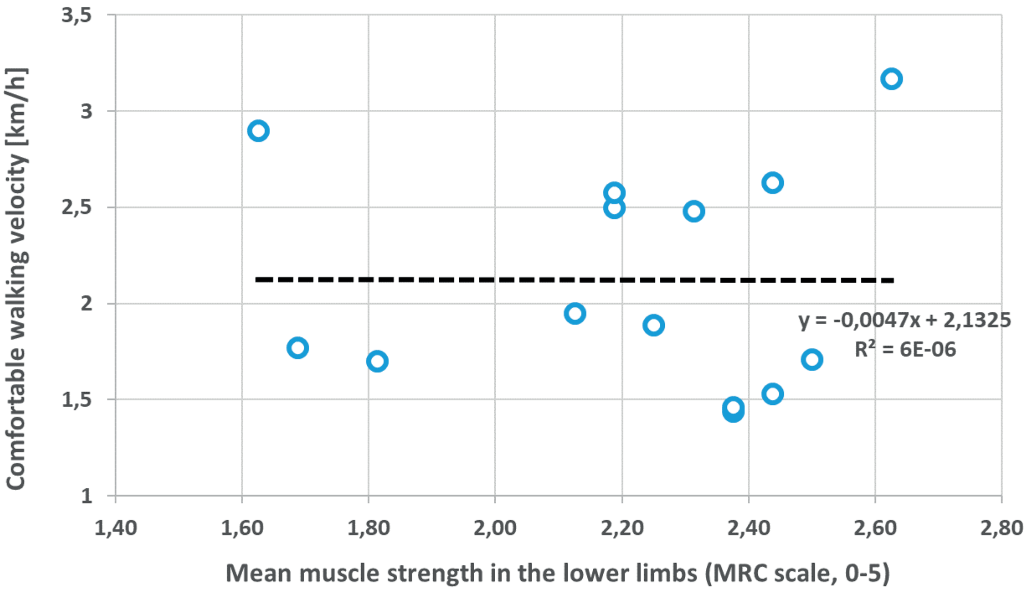

Figure 3-2 Regression of comfortable walking velocity versus muscle strength. The blue dots represent the raw data, while the black dashed line is a linear fit of the walking velocity by the muscle strength.

The three Euler angles about the hip, the knee and the ankle during level walking are presented in Figure 3-3. The kinematics are normalized over one gait cycle, starting at heel strike. The first 60%-70% of the cycle correspond to the stance phase, while the remaining 30%-40% correspond to the swing phase. Among the group with NMD, two main gait patterns were identified and results were split into two groups: NMD group 1 and NMD group 2. No correlations are found between the groups and other parameters such as muscle strength, age, sex, use of orthoses or walking velocity. The kinematics of the control group follows the schemes of typical gait pattern at low velocity as recorded by Stoquart et al. [125] previously.

The group 1 with NMD has a quite similar gait pattern than the control group. The hip and knee range of motion (RoM) in flexion and extension have the same amplitude in group 1 and in the control group. The main dissimilarities appear around the ankle. During the swing phase at the end of the cycle, subjects in group 1 do not present dorsiflexion of the ankle after push-off during the swing phase. The dorsiflexion happens while the foot is in contact with the ground, which modifies both ankle and knee flexion during heel strike. Those in group 1 also present a large variation of the foot orientation during swing in the form of large ankle rotations and inversion at early swing. Finally, those in group 1 have more pronounced knee extensions during mid-stance than subjects in the control group.

Subjects in group 2 demonstrate a more evident compensation pattern. Hip and knee flexions are more pronounced during the swing phase, and stance is marked by a greater hip extension while the knee is fully, or even hyper, extended during the full stance phase. At the ankle level, the stance phase is similar to the control group, but subjects in group 2 do not present any plantar flexion at toe-off (early swing) or during the swing phase. Compared to those in group 1, subjects in group 2 have a high variation of ankle internal rotation and inversion during the swing phase. Eventually, the control group has larger amplitude of internal/external rotations at the hip and knee joints compared to group 1 and group 2.

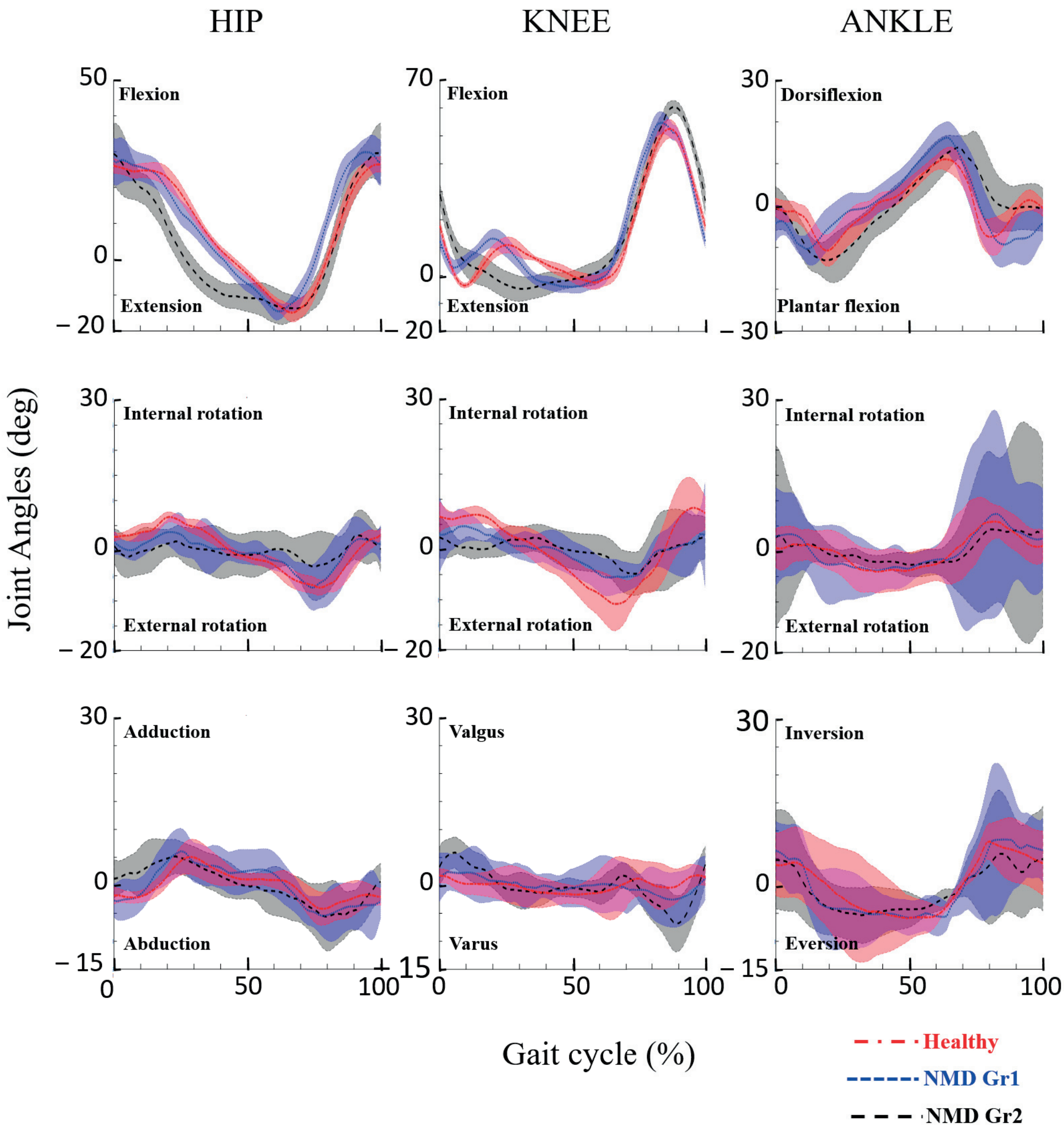

Figure 3-3 Hip, knee and ankle angles in function of percentage of gait cycle are presented for healthy subjects at a low walking velocity and for the neuromuscular patients at their comfortable walking velocity. Patients are split into homogenous group in function of gait pattern. NMD group 1 is composed of patients {5, 6, 8, 10, 11, 12, 14} and NMD group 2 of {1, 2, 3, 4, 7, 9, 13} relatively to Table I. Copyright © 2015, IEEE

In summary, three modified kinematics are observed in the groups with NMD. Knee hyperextension combined with larger hip extension (or pelvic tilt) patterns are observed in subjects in group 2. An absence of ankle dorsiflexion during swing is observed in subjects in group 1, while an absence of plantarflexion during swing is observed in subjects in group 2. The next section addresses how the previously discussed data, gathered from literature, and findings from this study together illuminate the needs that assistive devices must be able to provide for people with NMD.

3.4 Projections of the Need for Assistance in Person with Neuromuscular Diseases

Neuromuscular diseases are degenerative diseases that initially affect a small region of musculature and spreads, with varying speed, to eventually extend to the full body. Two key characteristics of NMD are thus the extent to which each muscle atrophies, and with that atrophying the decrease in functional capacity of corresponding joints, and the progression of loss of strength over time. Assisting persons with NMD requires a support than can be tailored to individual user needs, and which can adapt over time to accommodate progressing symptoms. Three main activities are prioritized as representative of important daily movements: walking on level ground, sit-to-stand transitioning and stair climbing. The three activities are discussed separately in the following sections. The needs are first examined in terms of the symptoms and gait patterns observed in people with NMD, after which the data from the literature on healthy people are taken to evaluate the targeted performances and the support needed to achieve them.

As symptoms in people with NMD can vary in severity, it is important to define the target demographic for an assistive mobility device. There are two primary conditions that must be considered. First, the impairment of the subject's ability to walk should be severe enough; this implies that the burden of being supported will not outweigh the benefits provided by the support. Second, the level of impairment cannot be too drastic; the user must still be in charge of the motion of the device while receiving a certain level of assistance while ambulating and thus the patient's musculoskeletal system must still be strong enough to ambulate. Quantitatively, the two criteria are expressed as follows: first, at least one joint should be affected with a minimal residual strength about 30% (equivalent to a score of 2 on the MRC scale), and second, the mean residual strength over all the lower joints (hip, knee and ankle) should be at least 50% (equivalent to a score of 3 on the MRC scale). These two criteria express the conditions under which the use of an exoskeleton is recommended to support mobility. These criteria serve also as references as they better define the condition and, hence, the need of the end-users.

3.4.1 Projections made from observed compensation kinematics

The first aim of the assistance provided is the compensation of deteriorated or lost functions such as walking, climbing stairs or rising from a seated position. The observed nature of the impairments in NMD include the following:

- muscles weakening, which leads to strength limitations and early fatigue
- altered sensations, which leads to difficulty managing limbs and balance
- deterioration of reflex and coordination, creating late response time or abnormal movement control

There are two distinct issues related to the movement of walking while afflicted by NMD. The first issue is propulsion; a subject must have the capacity to perform each necessary limb motion to push the upper body forward. The second issue is the management of balance, which is highly critical for one's safety.

Predicting users' assistive needs can be initially assessed by exploring the primary questions "what are the critical joints that most need support?" and "what is the nature of the support needed?" Observing compensation patterns in people with NMD while walking yields interesting possible answers to these questions.

One remarkable compensation pattern is the compensated Trendelenburg gait, also called waddling gait. It is a recurring gait pattern in people with proximal muscle weakness around the trunk and hips. The characteristics of this gait pattern is illustrated in Figure 3-4. Due to weak hip abductors, the swinging leg is subject to hip drop as the leg weight cannot be supported. In order to compensate and avoid hip drop (pelvic obliquity), people with NMD compensate by moving the upper body laterally on the side of the supporting leg. The weight of the upper body counter-balances the weight of the leg and allow adjustment of the pelvis. Waddling gait is also often characterized by very small flexions about the hip and the knee, which are compensated by a larger rotation of the pelvis in the transverse plane. Hip flexors and extensors weakness seem to originate these compensations. Waddling gait can potentially be rectified by providing additional force to support the weakened muscles, i.e. the hip abductors, flexors and extensors. The type and amount of support will be investigated in the next section, which analyzes the kinetics about the joints during different activities.

Another common compensation pattern is “foot drop”. It is caused by weak dorsiflexors (distal weakness) at the ankle and impairs mostly the swing phase from push-off to heel strike. As both push-off and heel strike cannot be performed with large extension or flexion of the hip, foot drop gait results in a small step length. The main issue with foot drop is the poor toe clearance and, as a result, a high risk of tripping. Two patterns can be adopted to increase toe clearance. The first one is a higher flexion of both hip and knee during swing as illustrated in Figure 3-5. The second uses a circumduction motion that is created by a large abduction of the hip on the swinging side. A common solution for people with NMD and others suffering from foot drop is an ankle foot orthosis (AFO) brace. An AFO brace is composed of a light structure that is slightly flexible and constrains the foot about a small flexion angle of the ankle. It is a passive, non-bulky and very lightweight solution to symptoms of foot drop disorder. It does not allow a complete physiological gait as it limits the amplitude of plantarflexion (necessary for a strong push-off) and does not adapt to slopes, resulting in balance issues. However, AFOs have radically improved ambulation in most of the person with weak dorsiflexors.

AFO braces can also improve discomfort from weak plantar flexors, which often cause poor push-off and difficulties in managing balance. A walking study where the ankle flexions of healthy participants were constrained using ski boots has been performed and showed that despite some larger flexions of both hip and knee, slow walking velocities (3.5 km/h) were achievable [126].

Another gait compensation pattern is denoted by knee hyperextension, which is usually combined with hyperlordosis of the spine. This is often observed in people who have weak knee extensors. Figure 3-6 illustrates the difference in patterns between a physiological gait and a gait affected by knee hyperextension and spine hyperlordosis. The compensation pattern exploits the singularity of the knee at 0° of flexion, plus the stability of the cruciate ligaments that prevent the knee from bending upwards. In this configuration, with an extension of a few degrees, the ligaments passively support the high forces directed along the line passing through the hip and ankle joints. Without this compensating posture, high extending torques are required and thus people with weak quadriceps experience frequent knee buckling and falls. Spine hyperlordosis comes from an anterior pelvic tilt which naturally stabilizes the knee hyperextension. Spine hyperlordosis is not caused by some muscle weakness about the hip, but rather, it is a result of the orientation of the pelvis which encourages the knee to hyperextend. In conclusion, this gait pattern is caused only by weak knee extensors. In order to rectify both knee hyperextension during stance and spine hyperlordosis, a support at the knee extension should be provided. Again, the type and amount of assistance will be addressed in next section based on the kinetics observed in physiological gait for different activities.

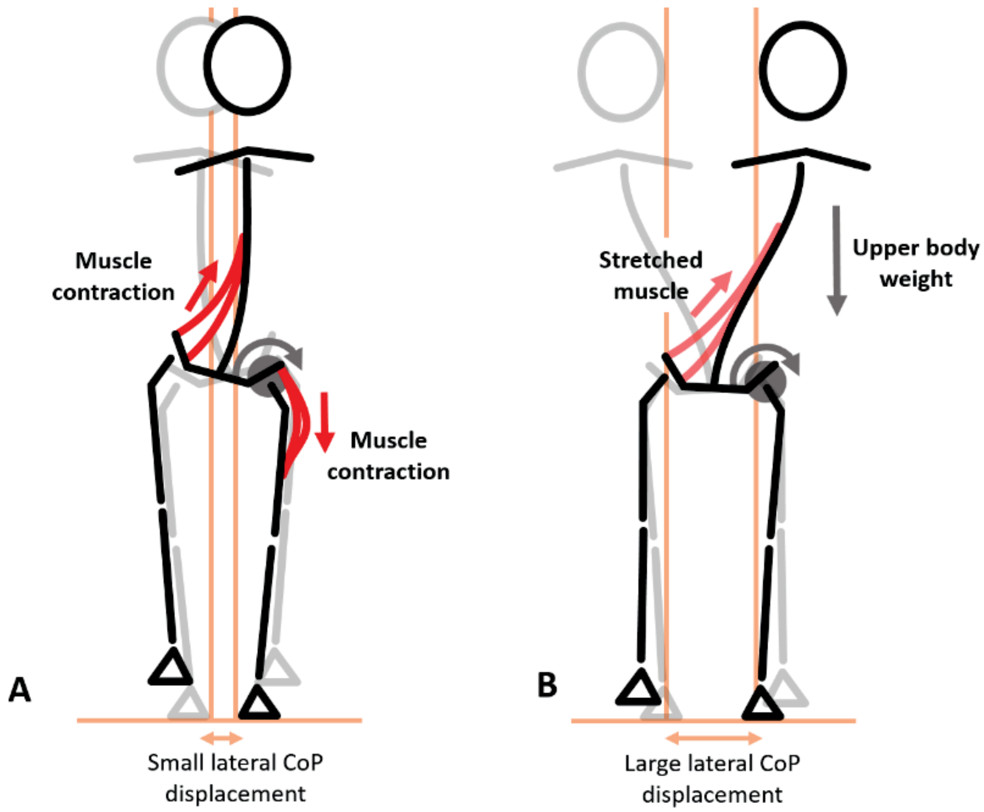

Figure 3-4 Schematic illustration of the difference between the physiological (A) and so-called waddling (B) gait patterns captured at mid-stance. *CoP: Center of pressure

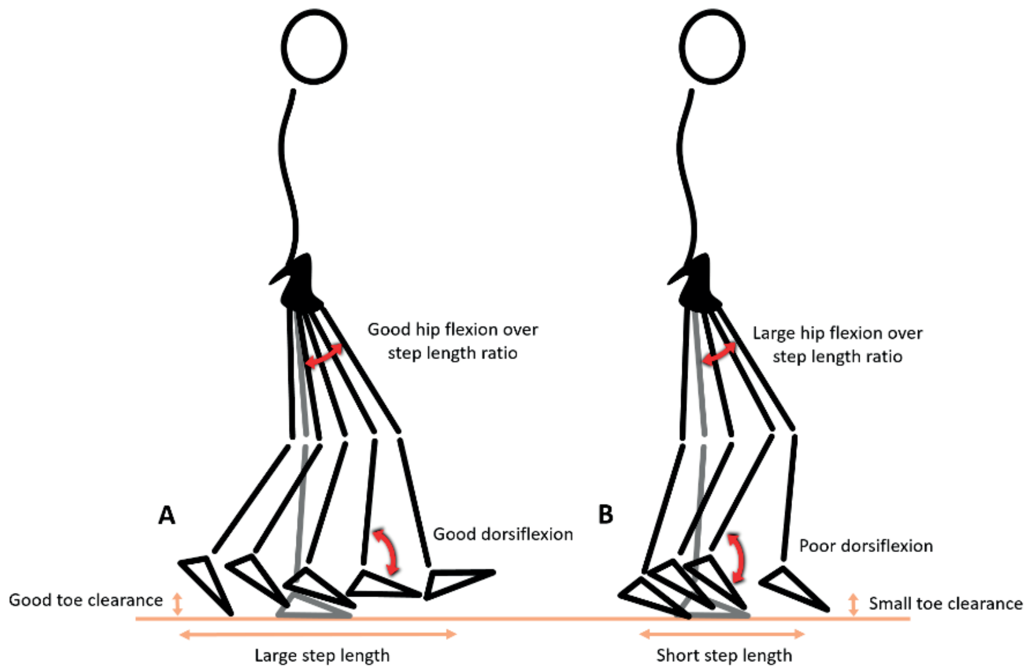

Figure 3-5 Difference of kinematics during swing in a physiological (A) and in foot drop (B) gaits.

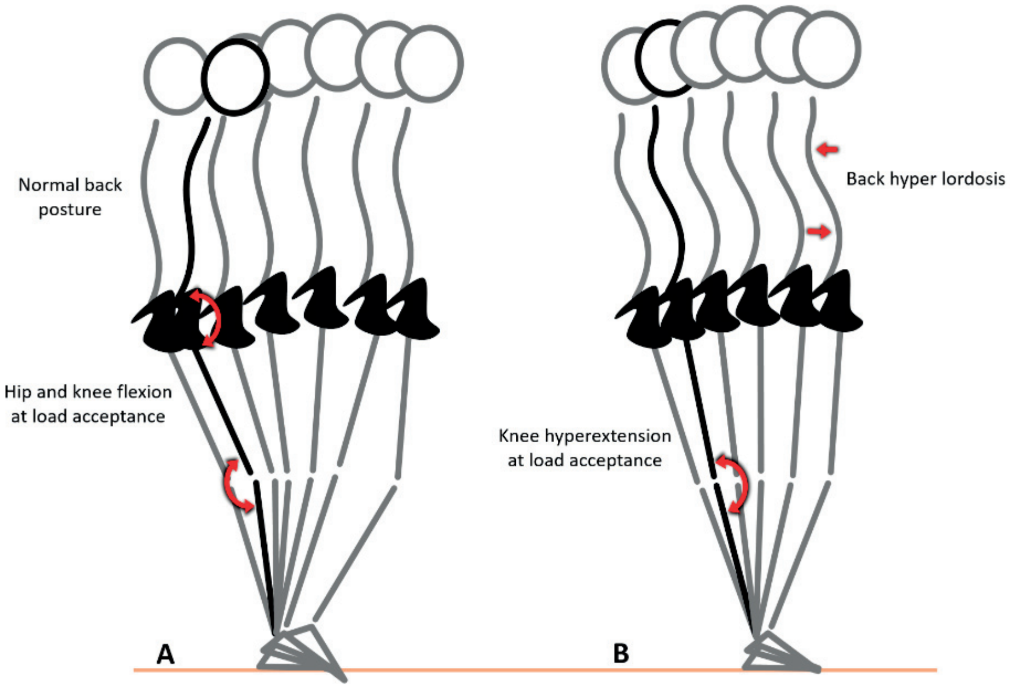

Figure 3-6 Difference of kinematics during stance in a physiological (A) and in knee hyperextension (B) gaits. Only the supporting leg is presented

3.4.1 Quantification based on physiological kinetics

This work uses three activities involving ambulation to qualitatively describe the needs of a "normal" daily autonomous lifestyle. These activities are walking, standing up from a seated position and climbing stairs. The kinetics related to these different activities have been thoroughfully reported in current literature. This section will quantify the amount of support needed to perform a task based on the literature, and then discuss whether this support should be active, semi-active or passive. The quantification made in this section focuses on the propulsion function; the implications of balance and rejection of perturbations will be taken into account in a later section.

3.4.1.1 Level walking

As demonstrated by Stoquart et al. [125], the torques and powers on joints involved in bipedal locomotion are highly dependent on walking velocity. Velocity is determined by the combination of the step length and the step rate (walking frequency). Body height and weight are also factors of walking kinetics. Data are usually presented normalized over the body weight, as body height is not a significant factor in walking kinetics. Walking speed and energy cost are nonlinearly related and plot as a quadratic function with a global minimum [127]. The energetic expenditure at different walking velocities investigated by Stoquart et al. [125] and Ralston [128] are illustrated in Figure 3-7. This figure shows that the most energy-saving walking velocity ranges are between 3.5 and 4.5 km/h. Walking slowly (under 3 km/h) has a higher metabolic cost. This is twice as disadvantageous for people with muscle weakness, as they are simultaneously subject to early fatigue while using a less energetically efficient gait.

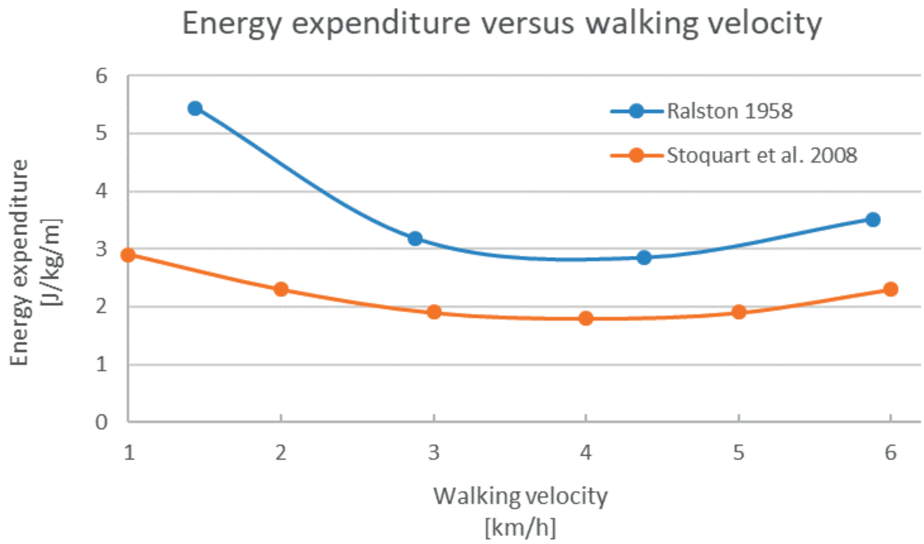

Figure 3-7 Evolution of the energy expenditure in function of walking velocity as measured by Ralston [128] and Stoquart et al. [125].

As demonstrated by previous studies, the exertion and kinetics of walking vary significantly depending on the gait velocity. In order to define the amount of support at the various joints, one must also specify the target walking velocity. The key knowledge about the walking velocity are the following. First, the mean comfortable velocity in healthy people is approximately 4.9 km/h [124]. Second, the most efficient walking velocity is between 3.5 km/h and 4.5 km/h. Third, the peak joint torques and power increase significantly with gait velocity [125]. With these factors in mind, two target velocities are selected for two levels of muscle weakness. For people with a global residual muscle capacity about 50%, the targeted velocity is 3,5 km/h, while for people with about 30% of residual muscle capacity, the velocity targeted is 2,5 km/h.

Stoquart et al. [125] investigated the joint kinematics and kinetics for walking speed from 1 km/h to 6 km/h. Based on these data, the joint angular velocities were extracted from the angular position curves and data for 2.5 km/h and 3.5 km/h were extrapolated by averaging the two available closest data (which were measured at 2, 3 and 4 km/h). The measurements, presented in Figure 3-8 for the walking speeds of 2.5, 3.5 and 5 km/h, highlight how subjects modify their gait to increase or decrease their walking speed. Globally, one can observe that higher walking speeds are reached by amplifying both peak angles and torques, while keeping timing relatively unchanged. Angular velocities are similarly amplified as both step length and cycle rate are increased to perform higher walking speed [125]. As both peak angular velocities and torques are increased, the effect on the peak power generated is tremendous, as it is a product of those two terms. Measurements presented show that there is a rise about 180 % in peak power generated for a 140% increase in walking speed. Thus, the peak power observed for each ankle, knee and hip joint is more than doubled when comparing a walking speed of 5 km/h to one of 2,5 km/h.

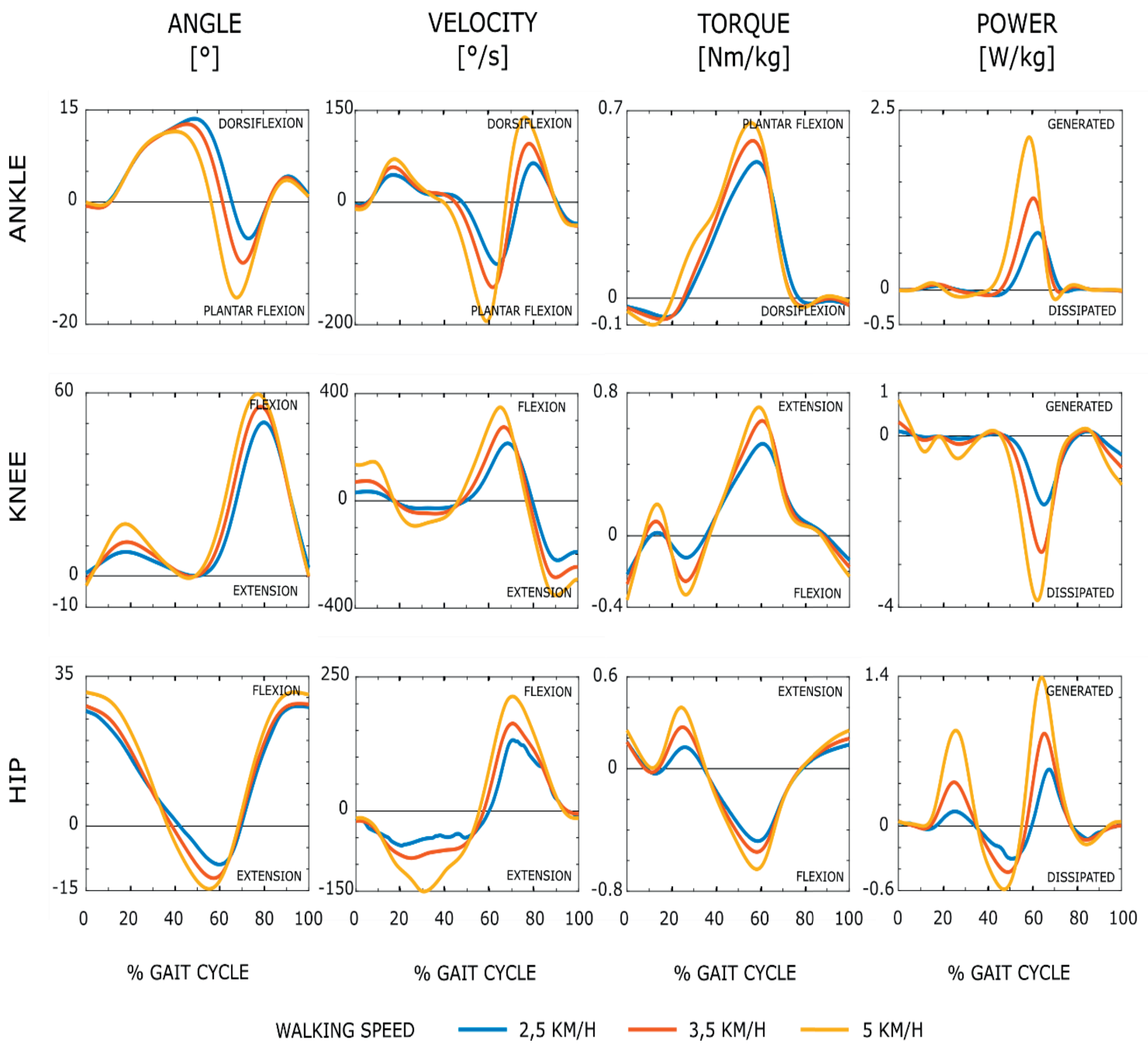

Figure 3-8 Illustration of the hip, knee and ankle joint angle, velocity, torque and power during walking at different speed on a treadmill. Data are extracted from the measurements reported by Stoquart et al. 2008 [125]. Torque and power are normalized over the bodyweight.

Measurements from Stoquart et al. [125] address the relation between walking speed and gait characteristics such as joint angular trajectory, velocity, torque and power. However, the measurements were performed over a treadmill, which differs from ground-walking conditions in several significant ways. For example, the torque pattern about the knee joint differs largely from measurements of Winter [129] or Ounpuu [130]. Table 3-2 documents the main properties in level walking as measured by Ounpuu [130], where the mean cycle duration is 0.9 s (cycle rate of 1.11 Hz) for a mean walking speed of 4.2 km/h. This is higher than the targeted efficient velocities of 2,5 and 3,5 km/h.

Table 3-2 Dynamic Specifications for Level Walking based on Ounpuu [130] and Schache and Baker [131]

Joints	Specifications in Level Walking (4.2 km/h – 1.11 Hz)				
	Angle min/max [°] (RoM [°])	***Peak Velocity [°/s]***	***RMS Torque [Nm/kg][a]***	***Peak Torque [Nm/kg][a]***	***Peak Power generation [W/kg][a]***
Hip Abduction/Adduction	– 5.4 / + 7.5 (12.9)	55.7	0.36 (18 - 36 Nm)[b]	0.66 (33 - 66 Nm)[b]	-
Hip Flexion/Extension	– 10 / + 35 (45)	178.5	0.3 (15 - 30 Nm)[b]	0.72 (36 - 72 Nm)[b]	0.78 (39 - 78 W)[b]
Hip Rotation	– 3.2 / + 8.6 (11.8)	-	-	0.088 (4.4 – 8.8 Nm)[b]	-
Knee Flexion/Extension	+ 5 / + 65 (60)	360	0.18 (9 - 18 Nm)[b]	0.53 (26.5 - 53 Nm)[b]	0.59 (29.5 -59 W)[b]
Ankle Inversion/Eversion	– 7.5 / + 2.1 (9.6)	-	-	0.085 (4.25 – 8.5 Nm)[b]	-
Ankle Dorsi-/Plantarflexion	– 15 / + 13 (28)	201.6	0.5 (24 - 50 Nm)[b]	1.26 (63 - 126 Nm)[b]	3.49 (175.5 - 349 W)[b]
Ankle Rotation	0 / + 7.5 (7.5)	-	-	0.12 (6 – 12 Nm)[b]	-

a. Torques are normalized over bodyweight, b. Torque values for a bodyweight range of 50kg - 100kg

Each human leg has seven degrees of freedom (DoFs), plus several DoFs about the foot and toes. As demonstrated by Table 3-2, locomotion is mainly achieved in the sagittal plane, where the flexions and extensions are generated by large amplitudes of torque and power (several dozen of Newton-meter or Watts). The hip abduction also provides an important contribution in terms of torque, although it performs only small displacements (RoM about 10° to 20° [131]). Bohannon et al. [124] reported that abductor strength was the factor best correlated to the walking speed, demonstrating the key importance of lateral motion in addition to forward motion. The other degrees of freedom about the hip and the ankle, however, seems not to generate much torque during walking, i.e. less than 10 Nm are reported for each of the hip rotation, ankle rotation and ankle inversion/eversion [131]. During walking cycles, the knee mostly dissipates energy as a damper, while the ankle almost only generates energy. The amplitudes of torque generated about the ankle while walking are twice as large as the hip and knee flexions, while the power provided is four times larger.

3.4.1.2 Rising from a chair

Another activity that is required in daily living is the sit-to-stand transition (STS). Mak et al. 2003 [132] measured the kinematics and kinetics of healthy, elderly subjects rising up from a chair to a vertical standing position. The obtained data are reported in Table 3-3. The torques that have to be generated depend largely on both the bodyweight and height of the person; both tend to increase the strength required, as longer legs induce longer distances between the CoM and the joints. The torques are the product of force and the distance to the point of application. The height of the sitting position also affects the strength required to rise up from a chair. The hip range of motion over the flexion/extension is particularly great during the rising phase, because, in order to ensure balance, the CoM needs to be situated over the feet, which are the base of support. In order to reach that stability without using the arms for help, one needs to lean forward while seated, about 30° [132], before one can start lifting the body to stand up. Once again, the range of flexion of hip, knee and ankle depends largely on the initial sitting position, which is determined by the height of the seat. The torque required at the knee joint for rising from a chair is much stronger than that required for level walking. The amplitudes of torque at the hip joint are similar, and reduced in the ankle joints compared to the amplitude found for level walking. The main difference between level walking and rising from a chair is that the latter is a single action lasting between one to five seconds; thus, it does not require as much continuous torque, as the peak torque is of more interest for the short time in which it is applied.

Table 3-3 Main kinematic and kinetic characteristics of rising from a chair in healthy elderly people based on [132]

Joints	Specifications in Sit-to-Stand (STS) Transition			
	STS duration [s]	*Angle min/max [°] (RoM [°])*	*70% of Peak Torque per Leg [Nm/kg/m][a]*	*Total Peak Torque per Leg [Nm/kg/m][a]*
Hip Flexion/Extension	1.4 in healthy elderly persons (2.3 in persons with Parkinson)	+ 0 / + 119 (119)	0.31 (25/61 Nm)[b]	0.45 (35/87 Nm)[b]
Knee Flexion/Extension		+ 5 / + 89 (83)	0.41 (32/78 Nm)[b]	0.58 (45/111 Nm)[b]
Ankle Dorsi-/Plantarflexion		+ 0 / + 12 (12)	0.22 (18/43 Nm)[b]	0.32 (25/61 Nm)[b]

a. Torques are normalized over bodyweight and body height and assumed symmetrical in both legs, b. Torque values for a bodyweight and height of 50kg and 1m55/100kg and 1m90 respectively

3.4.1.3 Climbing stairs

Protopapadaki et al. 2007 [133] measured the torque and duration on joints while ascending and descending stairs in a population of young adults. The results for the stair ascent (more strenuous than the descent) are reported in Table 3-4. Stair climbing is comparable to level walking; the cycle rate and step length are largely reduced compared to level walking, but the exertion required is increased as the joints must lift the body weight up each step. All ranges of motion for the hips, knees and ankles in the sagittal plane cover a larger range than that of level walking, and RMS and peak torques are also greater in the case of stair climbing.

Table 3-4 Main kinematic and kinetic characteristics of climbing stairs based on [133]

Joints	Specifications in Ascending Stairs			
	Cycle duration [s]	*Angle min/max [°] (RoM [°])*	*RMS Torque [Nm/kg/m][a]*	*Peak Torque [Nm/kg/m][a]*
Hip Flexion/Extension	1.45	+ 8 / + 65 (57)	0.29 (22/55 Nm)[b]	0.67 (50/127 Nm)[b]
Knee Flexion/Extension		+ 1 / + 92 (91)	0.26 (20/49 Nm)[b]	0.54 (40/102 Nm)[b]
Ankle Dorsi-/Plantarflexion		– 24 / + 17 (41)	0.6 (45/114 Nm)[b]	1.3 (98/247 Nm)[b]

a. Torques are normalized over bodyweight and body height, b. Torque values for a bodyweight and height of 50kg and 1m55/100kg and 1m90 respectively

3.5 Discussion

The current chapter presented a study of the gait kinematics in a heterogeneous group of 14 persons with neuromuscular diseases. Aside from confirming some observations already made in the literature, this study allowed to get information about the preoccupation and daily activities of the participants. One key information, for example, is that the transition to a wheelchair is usually made when the risk of fall becomes an issue to the person. Thus, most people are still able to ambulate as they start using a wheelchair. Another interesting aspect is the burden that can represent STS transitions, that can take up to more than a minute to be performed. The compensatory patterns observed in this study are mostly the knee hyperextension, the back hyperlordosis, foot drop and the waddling gait. Some participants would adopt four compensating patterns in their gait as they have generalized muscle weaknesses. The experiment also allowed to observe the performances of ankle foot orthoses with patients with ankle muscle weaknesses. The AFO proved to be very efficient as participants demonstrated to be able to walk at a moderate velocity while wearing them. However, the stability, in particular in slopes or uneven terrain can be difficult to manage.

A better understanding of the different compensating pattern following the experiment is presented. The implication of poor abductor strength at the hip in the waddling compensating pattern is explained and reveals the large need for assistance at that joint. The knee hyperextension that allow to avoid knee buckling because of weak knee extensors is also highlighted. It expresses the significant need for the support of the knee extension to avoid falls and provide more safety to the user.

In the second part, the specifications of dynamics required in level-walking, stairs climbing and STS transition are studied based on the literature. The study of level walking first shows that a slow gait is energetically more demanding than a gait between 3 km/h and 4 km/h which is optimum. Stoquart et al. [125] also demonstrated that the range of motion and the torques at the joints increase with the walking speed. Hence, the level of assistance can be designed in function of the targeted walking speed. The study of stairs climbing and sit-to-stand transition revealed that the torque requirements to perform such activities are much greater than the peak torques generated during level walking. These data will be further used in the design of the actuation units of the assistive design.

Chapter 4 Assistive Lower Extremity Exoskeletons – Application to Neuromuscular Diseases

4.1 What are exoskeletons?

An exoskeleton, also referred to as powered orthoses, is an apparatus composed of a structure external to the body which is attached to different points of the body and actuated. The role of exoskeletons is to transport the user wearing the device or exert force on behalf of the user. Exoskeletons have several application domains, including but not limited to:

- military sectors, where exoskeletons empower the soldiers to augment their capacities or to extend their endurance (carry heavy loads, walk faster, etc.) while also offering protection on the battle field.
- industrial sectors, where exoskeletons allow manipulation of heavier loads or tools by re-distributing or alleviating loads on worker's musculoskeletal system in order to prevent injuries.
- space missions, where the device can be used as a fitness machine to prevent muscle loss in zero gravity.
- medical sectors, where exoskeletons can be used for rehabilitation by supporting neurological patients and assisting them in maintaining a vertical position (lower extremity exoskeleton), or in training motor difficulties.
- private sectors, where exoskeletons can improve ease in daily tasks by assisting locomotion, dexterity, etc. for those with spinal cord injuries or other afflictions.

4.1.1 Lower extremity exoskeletons

The concept of lower extremity exoskeletons (LEEs) was first found in a patent from the late 19th century [134]. Yagn's invention, presented in Figure 4-1 A, is a passive exoskeleton described as an "exercising apparatus specially adapted for conditioning the cardio-vascular system, for training agility or co-ordination of movements" [134]. The first claimed active exoskeleton, which opened the recent era of bipedal robots, was developed in 1969 [135], [136] at the Mihailo Pupin Institute in Belgrade, Serbia, under the supervision of Miomir Vukobratović, the father of the Zero Moment Point theorem (also published in 1969 [137]). The first version of the exoskeleton was pneumatically actuated and electronically programmed, Figure 4-1 B.

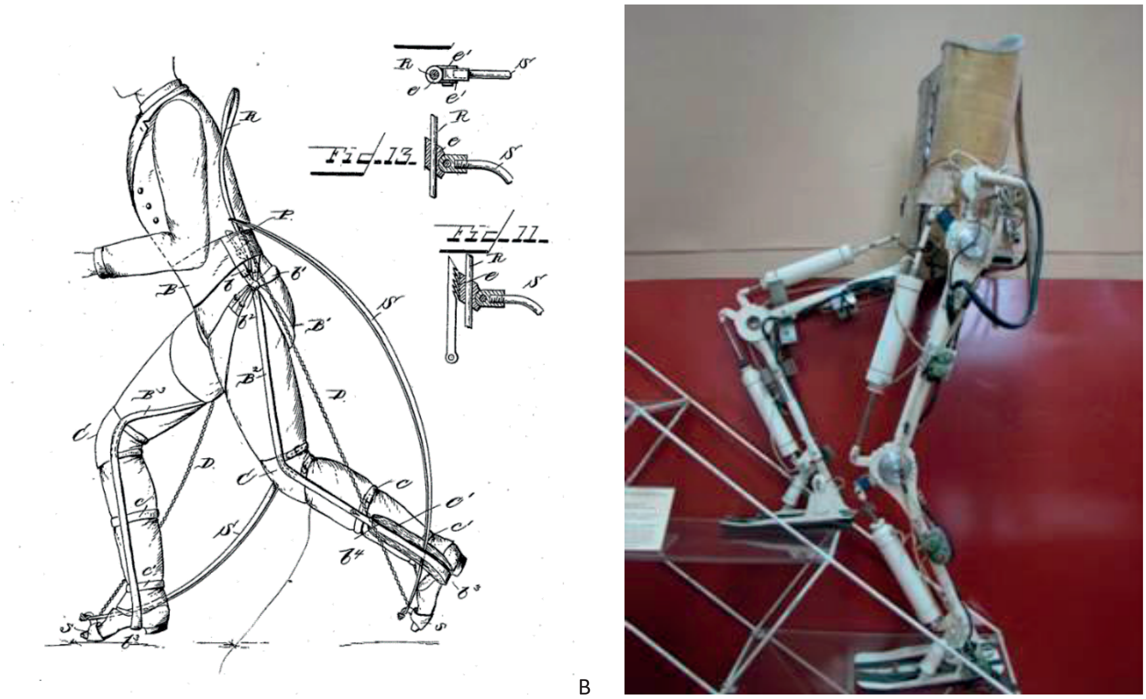

A B

Figure 4-1 A) Illustration taken from the US patent of Nicholas Yagn from 1890, "Apparatus for facilitating walking, running, and jumping" [134] B) Picture of one of the first active exoskeletons, developed at Mihailo Pupin Institute

The group from Mihailo Pupin Institute achieved the first mobilization of a paraplegic patient with an active LEE in 1972 [135]. However, the technologies available at the time, particularly in terms of computational capacity, were very constraining. The next achievement was realized by the Berkeley lower extremity exoskeleton (BLEEX), that is claimed to be the first energetically autonomous exoskeleton (2006) [138] with the HAL (Hybrid Assistive Limbs) exoskeleton from Tsukuba university (2002) [139]. Since the beginning of the millennium, interest in exoskeletons has exploded. Most advanced developments have reached the market, first with stationary LEE such as the rehabilitation product Lokomat® from Hocoma (Volketswil, Switzerland) [11] (see Figure 4-2)). The Lokomat® was successful, with 500 devices sold within its first 10 years of commercialization[3]. It, however, did not succeed in proving a significant improvement in therapy results compared to intensive/standard therapy (non-robotized) [10], [140], [141]. Approximately a decade after the emergence of stationary LEE, wearable exoskeletons entered the stage. The first commercial products include:

- ReWalk™ (ReWalk Robotics, Marlborough, USA): CE marked in 2010 and FDA cleared in 2014 (home and public use)
- REX (REX bionics LTD, Auckland, New Zealand): CE marked in 2010 and FDA cleared in 2016
- EksoGT™ (Ekso bionics, Richmond, USA): FDA cleared in 2012 and CE marked in 2012 and 2016 (medical)
- Hybrid Assistive Limb HAL® (Cyberdyne Inc., Tsukuba, Japan): CE marked in 2013 (medical), FDA cleared in 2017 (medical)

[3] Ref. https://www.hocoma.com/news/hocoma-celebrates-the-sale-of-the-500th-neurorehabilitation-robot-lokomat/

- Indego® (Parker Hannifin Corp, Macedonia, USA): CE marked in 2015 and FDA cleared in 2016 (personal and medical)

(Pictures courtesy of, Hocoma, ReWalk bionics, REX bionics, Eksobionics, Tsukuba university and Parker Hannifin, respectively).

Figure 4-2 From left to right: Lokomat® from Hocoma, ReWalk™ from ReWalk bionics, REX from REX bionics, EksoGT™ from Eksobionics, HAL® from Cyberdyne and Indego® from Parker Hannifin.

These devices are shown in Figure 4-2. The first commercialized LEE belongs to the medical sector and is the first commercial development targeted towards people suffering from spinal cord injury (SCI) for private home use. With a high selling cost between sixty thousand to a few hundred thousand dollars, plus additional mobility constraints, i.e. slow walking speed, ease of use, bulky appearance, safety, etc., the number of sales to date is very low. Most devices are now redirected toward rehabilitation applications and larger populations, such as stroke victims. A review of the past and current clinical trials with wearable LEE has been performed using the “ClinicalTrials.com” database and the trials documented by the exoskeletons’ companies. Results are illustrated in Figure 4-3. Out of a total of 110 trials found in the cited database, SCI is the most studied disorder (72%), followed by stroke (22%), with a few studies on multiple sclerosis cases and the elderly. On the device side, Ekso accounts for half of the studies reported (57), followed by ReWalk and Indego, with 17 and 16 studies respectively. Cyberdyne’s HAL accounts for 8 cases, and the remaining account for less than 5 studies.

Miller et al. 2016 [13] performed a systematic review on the effectiveness and safety of LEE assisted gait in people with SCI. Fourteen studies (8 ReWalk, 3 EksoGT, 2 Indego, 1 other) with a total of 111 people with SCI were included. The success ambulation rate is 76%, with an average walking velocity of 1 km/h and a level of effort of 3.3 MET (metabolic equivalent of task, 3 = limit between light ant moderate intensity activity). Improvement of the bowel function was seen in 61 % of participants and spasticity diminution in 38% of participants. In terms of safety, a fall incidence of 4.4% is reported, while the bone fracture incidence reached 3.4%. In conclusion, the use of wearable LEE by people with SCI is reasonably safe and brings the user significant health benefits. There are, however, still limitations in walking speed and mobility. The benefits of wearable LEE for people suffering from strokes and other disorders are still unclear, more in-depth studies are needed to be able to draw conclusions.

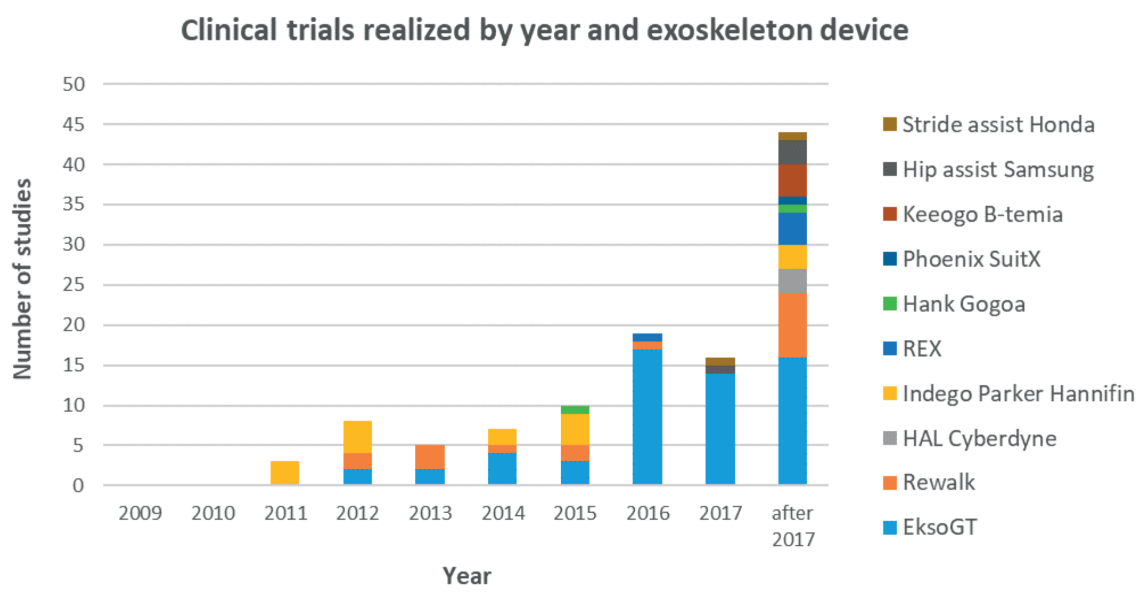

Figure 4-3 Number of studies realized per year and per device (wearable exoskeleoton)

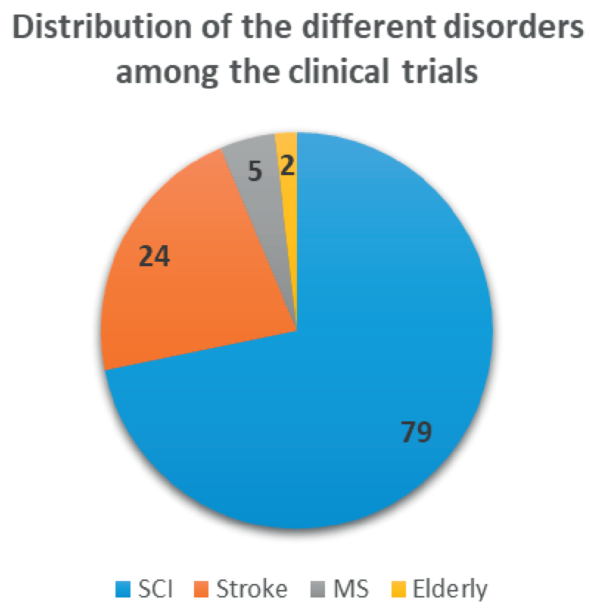

Figure 4-4 Number of studies on wearable exoskeleton use per type of disorder

Although the medical sector launched the first commercializalized exoskeletons for personal use and rehabilitation, the military sector, primarily in northern America, played a key role in the development of the technology in the early aughts ([142], [143]). Examples include the Berkeley Lower Extremity Exoskeleton, BLEEX [138], the Sarcos exoskeleton, and the MIT exoskeleton [144].

Currently, the industry sector is investing in exoskeleton research. Minimally actuated exoskeletons are designed to lower the level of exertion and the constraints on the musculoskeletal system in different activities such as squatting and lifting up large objects, holding heavy tools in different positions, and repetitively picking up objects necessitating forward bending of the trunk.

4.1.2 Architecture of Powered Wearable Exoskeletons

This section describes several common subsystems that comprise powered wearable exoskeletons. The different components, illustrated in Figure 4-5, are described in **Erreur ! Référence non valide pour un signet.**, with a description of their functions and some examples of realization.

Table 4-1 Subsystems of wearable powered exoskeletons and their function

#	Powered exoskeleton subsystem	Function(s)	Example(s) of realization
1	Human-robot interface	Allow the user(s) to interact with the control unit • Turn on/off the device • Select a working mode (e.g. select activity) • Tune parameters (e.g. walking speed) • Provide a visual feedback to the user	• Remote control with buttons • Emergency stop • Tactile and visual tablet-like interface • Remote computer
2	Power supply	Store energy for actuation and powering of joints and electronic components	• Electrical batteries • Tank of fuel or other propellant • Tank of compressed air

3 and 6	Mechanical structure and joints	Manage interaction between actuators, inertia, user limbs and body, and ground	Ball bearing or spherical joint, with 3D printed, machined aluminium, or molded carbon fiber structure
4	Physical interface	Integrate forces generated between the limbs of the body and the structure of the exoskeleton; distributing physical stresses prevents user pain and skin abrasion and damage	• Molded thermoplastic thigh interface with straps • Textile brace with Velcro fastening
5	Central control unit and drives	Run the controller of the actuators and other feedback mechanisms using signals received from the human-robot interfaces and the sensors	• Embedded computer with linux processor (motherboard), connected to multiple microcontroller-based drivers which control the actuators
7	Sensors	Collect information from the environment to provide control inputs for actuators and generate feedback for users	• Potentiometers or encoders as position sensors • Load cells as force sensors • Gyroscopes and accelerometers as motion sensors
8 and 9	Actuators and transmission unit	Generate a force/motion to be provided to the user for movement	• Pneumatic or hydraulic cylinder • Electric motor with ballscrew, planetary gears or harmonic drive • Hybrid electric motor with hydraulic transmission • Series elastic actuator

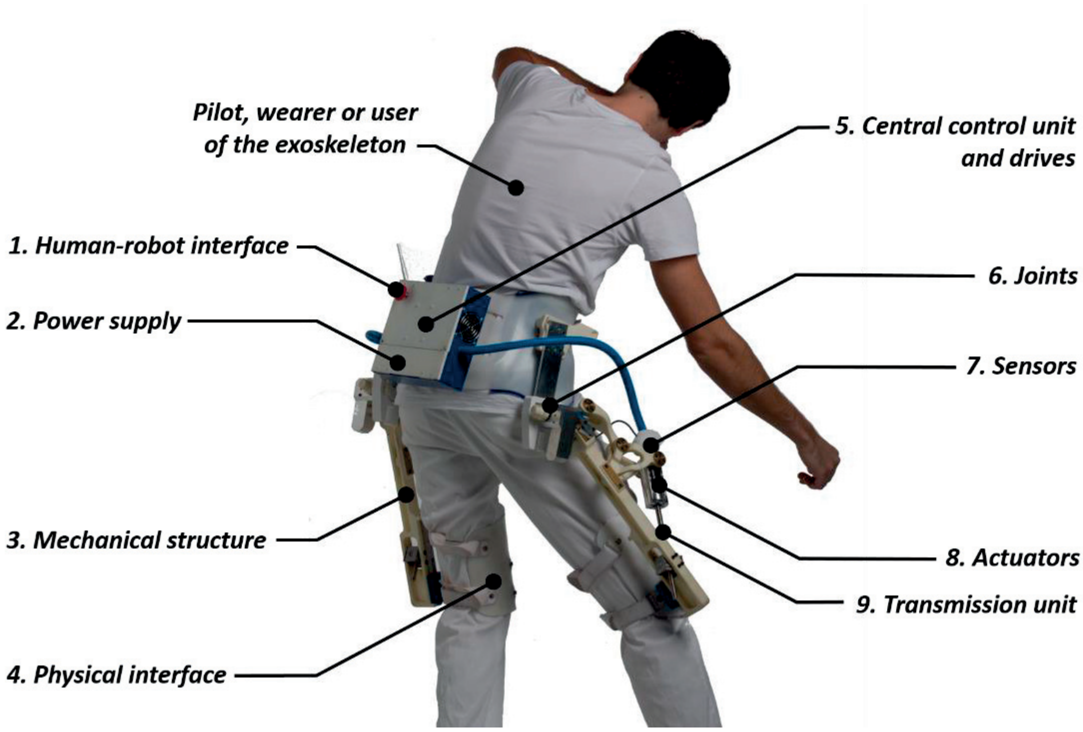

Figure 4-5 Illustration of the common subsystems of any powered wearable exoskeletons. Depicted is the HiBSO: a powered ball-screw hip orthosis

4.1.3 Design Specifications and Challenging Aspects Towards Neuromuscular Diseases

As highlighted in This section describes several common subsystems that comprise powered wearable exoskeletons. The different components, illustrated in Figure 4-5, are described in **Erreur ! Référence non valide pour un signet.**, with a description of their functions and some examples of realization.

Table 4-1, a wearable exoskeleton is composed of several sub-systems with large degrees of complexity. Designing a full exoskeleton requires advanced techniques encompassing biomechanics, medicine, structure mechanics, dynamics, electronics, programmation, control, mechatronics, and orthopedics, at the least. Depending on the type of actuators chosen, it could also include electromechanics, fluid mechanics or chemistry. The performance of the exoskeleton is inherently linked to the available market options for needed joints, sensors, actuators, transmission units, electronic drives and embedded computers.

The specifications regarding a wearable LEE for walking assistance with people with NMD are sorted in three categories: practicality and safety, performance, and collaboration. The specifications and challenges for design are described by categories in the following sections and discussed in terms of the State of the art.

4.1.4 Practicality and safety

After the validation of main functional performance of an exoskeleton, practicality is usually considered next to give a realistic assessment of implementation likelihood. Practicality is defined using the following scenario as a test case. The primary use of the exoskeleton would be either in a home or a clinical setting, with an auxiliary person available for monitoring and assistance if needed. This also implies that the device will first need to be moved out of a storage location by an able-bodied person. The device is then turned on for operation; the power supply needs to be able to provide steady operation for as long as the person needs. If the device is used by multiple people, it will need to be adjusted to size. The user must be able to put the device on, meaning they must transfer themselves or be transferred into the device and fasten any and all physical interfaces. She/he should be able to turn it on, configure the device for desired activities and start ambulating with it. Ambulating includes the three activities of walking, climbing/descending stairs, and standing up from/sitting down in a chair. Moving in outdoor environments and public places, including public transportation should be considered, as well as car transportation while wearing the device. Eventually, the device must be turned off and removed from around the user. The critical points are discussed in the following.

Adjustment of the device to the user size is very important in two aspects: first, the alignment of the joints of both the user and the exoskeleton is an important issue, since a poor alignment could have dramatic consequences such as high discomfort or, in the worst case, fracture. Second, a poor fit of the physical interfaces to the limbs of the user can lead to skin damage or displacement of the interface during use, which increases the risk of falling. Three types of adjustment can be found in the literature/commercialized products:

1. Mechanical adjustment of each segments based on prismatic joints and a locking system (most frequently found e.g. EksoGT™)
2. Interchangeable segments of different sizes (e.g. Indego®)
3. Tailor made exoskeleton (e.g. TWIICE's startup concept[4])

[4] http://twiice.ch/

Options 1 and 2 allow rapid adjustment of the device for patients of varying size; thus, several users can share the same device. This is the best scenario in a rehabilitation center. Option 1 involves adjustable segments, which usually weaken the structure and thus require use of slightly heavier and bulkier segments. Interchangeable segments as in option 2 do not provide as fine an adjustment unless a large set of such segments is assumed. It is further complicated by the need for the connection between the control signals and the structure to be re-made after each adjustment. Option 3 provides potential, if there is a significant benefit in having a perfect adjustment to the user morphology.

Option 1 is considered first for its ability to accommodate several users with fine adjustment. Considering a target population with body height between 150cm and 188cm (corresponding respectively to the 5th percentile of female adults and 95th percentile of male adults in the United States over 2007-2010 [145]), the segments sizes are derived from available anthropometric data found in the literature. If no documentation covers the span of dimensions needed, sources such as size charts from clothes are applied. The dimensions of interest are illustrated in Figure 4-6, and the span of dimensions are reported in Table 4-2.

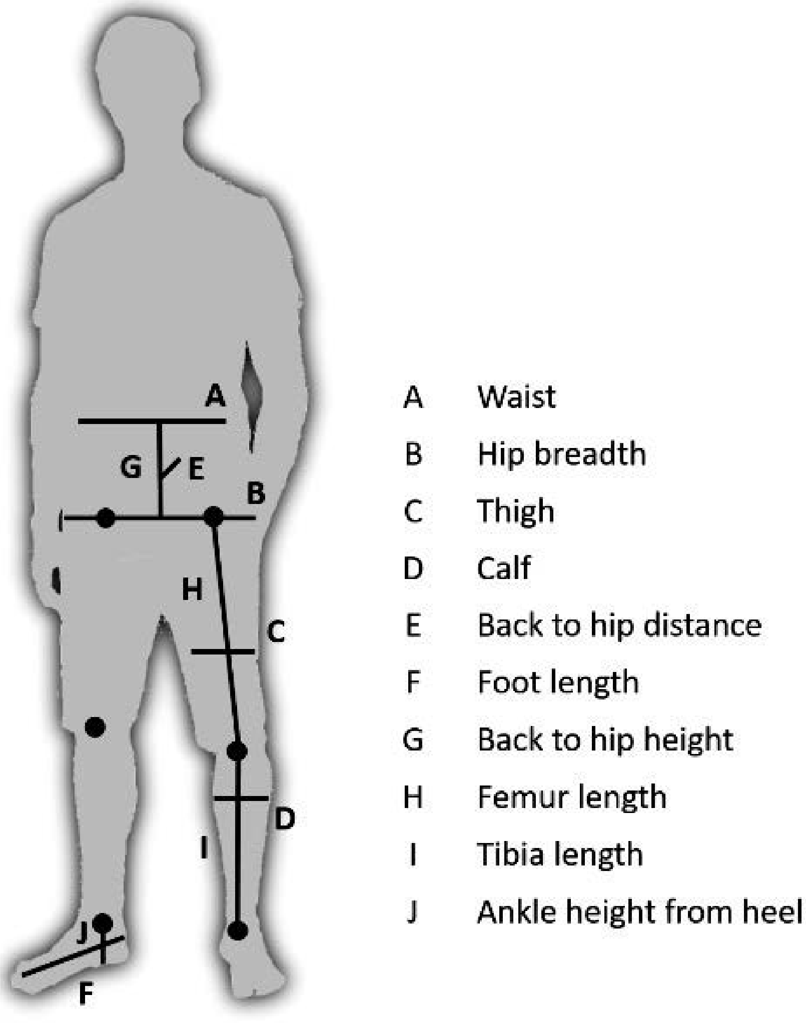

Figure 4-6 Illustration of the relevant dimensions considered for the adjustment of the lower limb exoskeleton

Table 4-2 Range of sizes for different body parts in order to set the span of adjustment of the device's segments

#	Body part	Reference	Notes	Range of sizes
A	Waist	[146]	Circumference	60 – 126 cm
B	Hip breadth	[147]	for fit people, should be increased for higher BMI	30 – 42 cm
C	Thigh	Ref[5]	Circumference size S – XL	41 – 67 cm
D	Calf	Ref[5]	Circumference size S – XL	31 – 45 cm
E	Back to hip distance	-	No documentation found	-
F	Foot length	UK chart	Size UK 0-13	18 – 30.4 cm
G	Back to hip height	-	No documentation found	-
H	Femur length	[148]	0.237-0.245 x Body height (150x0.237 – 188x0.245)	35 – 46 cm
I	Tibia length	[148]	0.22-0.237 x Body height (150x0.22 – 188x0.237)	33 – 45 cm
J	Ankle height from heel	[148]	0.043-0.048 x Body height (150x0.043 – 188x0.048)	6.5 – 9.0 cm

4.1.5 Performance

The performance of a device relates to its capacity to assist a certain activity with high precision and speed. The performances are thus expressed with two metrics: the level of assistance, and speed. The level of assistance is commonly expressed by how much force is provided to the user compared to how much force the user would need to exert to perform the task at hand without assistance. Speed is measured through walking velocity, the time to climb a few stairs, the time to rise from a chair, or another such action. The ideal performances would be to be able to walk, stand up from a chair, and climb stairs with the ability of a healthy athlete, for several hours. Unfortunately, there are limiting technological and physical constraints such as the density of the power supply, the actuator efficiency and inertia, the torque density of the actuator and transmission unit, etc. As with any other self powered and mobile object, a trade-off in LEE must be made between the performance of the system and its weight.

High performance in LEE is challenging because, as power supplies and actuators are mounted on the device to provide more power capacity, device bulk and weight also increase drastically. Actual performance of LEEs for assistance in cases of SCI is hard to assess for the following reasons:

1. The use of crutches, or other supports, largely impacts the distribution of the power exerted by the user and by the device during any activities.
2. Any performance observed is related not only to the device, but also to the management of balance and of the crutches by the user. The only device that can be operated without crutch assistance is

[5] Sigvaris compression socks dimensions : https://www.compressionstockings.co.uk/sigvaris-traditional-500-half-thigh-class-3-ral-beige-compression-stockings-with-open-toe.html

the REX exoskeleton, which provides too low of a walking velocity with an average of 0.2 km/h [149], mainly due to the static management of balance.

Hence, it is hard to evaluate the limitations of LEE and, subsequently, to define specifications regarding the level of assistance, walking velocity, etc. However, it is still of interest to discuss the challenges in function of the different targeted activities and look at achievements previously made in the field.

4.1.5.1 Level walking

Out of the three activities used to measure exoskeleton performance, level walking is the least demanding in terms of torques; however, it can be very dynamic, with high angular velocities at hip, knee and ankle joints. In terms of balance, the mass of the body while walking needs to be transferred from one leg to the other at each step. All joints must be well coordinated. As mentioned in section 3.4, the level of assistance is a function of the users's residual muscle capacity. The target walking speed is 3.5 km/h for moderately affected people requiring about 50% of assistance, and 2.5 km/h for people requiring about 70% of assistance. Where the percentage of assistance is scaled based on the physiological torques, that vary with the walking speed and a person bodyweight. The performance aspects of interest are:

1. The range of motion of each joint

Following specifications reported in section 3.4.1, the range of motion can be a challenge if a translational type of transmission is selected such as a pneumatic cylinder or a driven screw solution. However, if a rotational transmission such as a gear train is selected, the range of motion would be infinite. The range of motion should also be considered in the design of the structure of the exoskeleton. The range of motion is a more of a critical factor in STS movement than it is with level walking.

2. The maximum velocities

Torques and velocities are critical regarding the design and selection of the actuation unit. Both torque and velocity are in opposition since the maximum power of the actuation is usually limited. A compromise has to be made between torque and velocity maxima, which is defined by the transmission ratio. Technical solutions can also be investigated to increase velocity limits.

3. The peak and RMS torques

Torque capacity is certainly the most critical aspect of the design. Augmenting the target torque limit increases the bulkiness of several components quadratically. For example, if a pneumatic solution is used with cylinders, doubling the torque capacity can be obtained in two ways. One may augment the cylinder diameter, which leads to a heavier cylinder, and acquire a tank or compressor that has twice the original capacity to produce the volume of air that has also doubled. The other option is to double the pressure source, which needs a reinforced tank or a high pressure compressor. In both cases, the weight of the solution is usually more than doubled. In a more conventional case such as current robotics, electric motors would be used. By doubling the length of the rotor, the torque capacity is doubled. This means doubling the inertia, the mass of the motor, and the battery capacity. Gears and other components of transmission mechanics will also increase in size to support the torques required. Eventually, the increase of inertia of the motor will also need more torque and power to be compensated, such as the mass of actuators located on moving parts. The design of the actuators is thus a very critical aspect and it will be largely discussed in this work.

4. The peak and RMS power

Power is an important metric, as it includes both torque and velocity specifications. The documentation of actuation units is usually reported in terms of power, and the power supply can also be directly designed based on the power specifications. Systems usually have two specifications: the peak power, torque or velocity, which can be maintained for a short period of time, and the nominal power, torque, velocity, which indicates the limit of the continuous working mode. Typically, an electric motor is mostly limited in torque due to the mechanical temperature limit of the rotor. The heat induced is proportional to the square of the current as stated by Joule's first law, and the current is directly proportional to the torque. An electric motor has, thus, a continuous working torque (nominal torque) and a peak torque, typically about 2 or 3 times the nominal.

The RMS and peak torques based on Ounpuu [130] and Schache and Backer [131] (gait at 4.2 km/h) are illustrated on Figure 4-7 for the seven joints of the leg. Based on Stoquart et al. [125], reducing the walking velocity to the targeted velocity (2.5-3.5 km/h) decreases the peak torques of approximately 10-30% (see Figure 3-8). At the same time, the exoskeleton assists persons with residual strength. It is assumed that in the worst case, the user would still be able to provide about 20% of the peak torques. In the end, the peak torque specifications will be based on 70% of what is reported by the literature. The RMS and peak power calculated, based on walking cycle frequency of 0.84 Hz (100.8 steps/min) with the trajectory and torque curves reported by Ounpuu [130] and Schache and Backer [131], are shown in Figure 4-8. The torques and powers involved follow similar patterns for each joint. The ankle plantar-/dorsi- flexion needs large peak torque and power. The hip flexion/extension and abduction/adduction, plus the knee flexion/extension require slightly smaller RMS torques and powers, but largely less peak torques and powers than the ankle flexion/extension. Hip and ankle rotation (internal/external) and the ankle inversion/eversion require less torque and power than others.

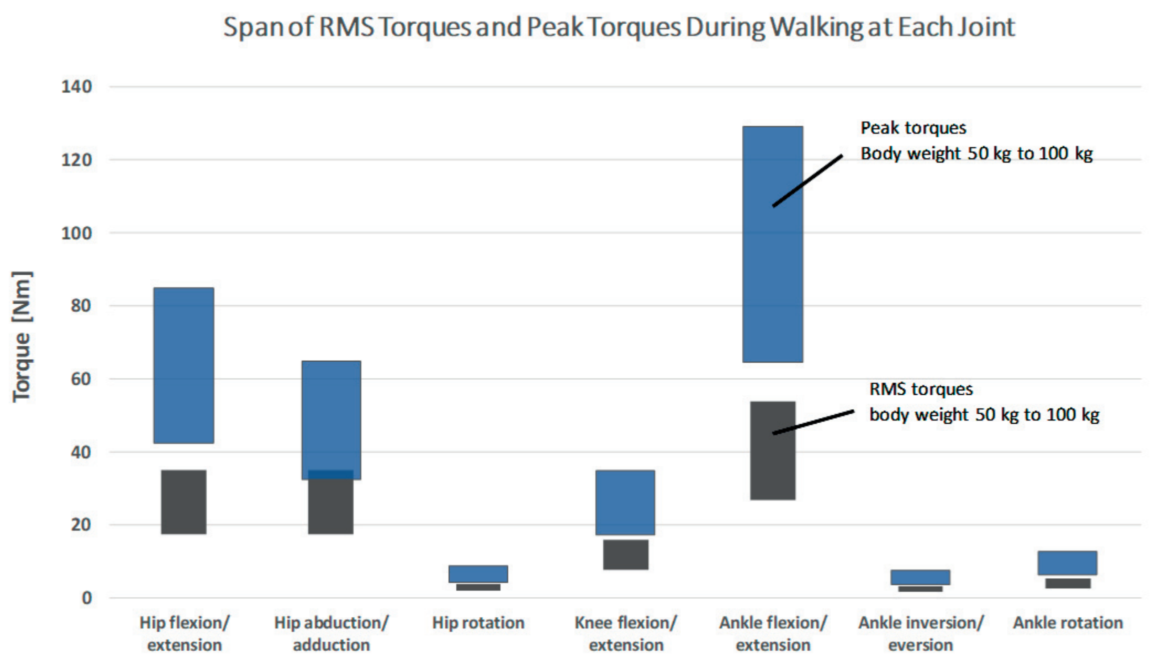

Figure 4-7 RMS torques and peak torques for each joint during walking based on Schache and Baker [131]. The span covers the torque needed for a human body weight range of 50 kg to 100 kg.

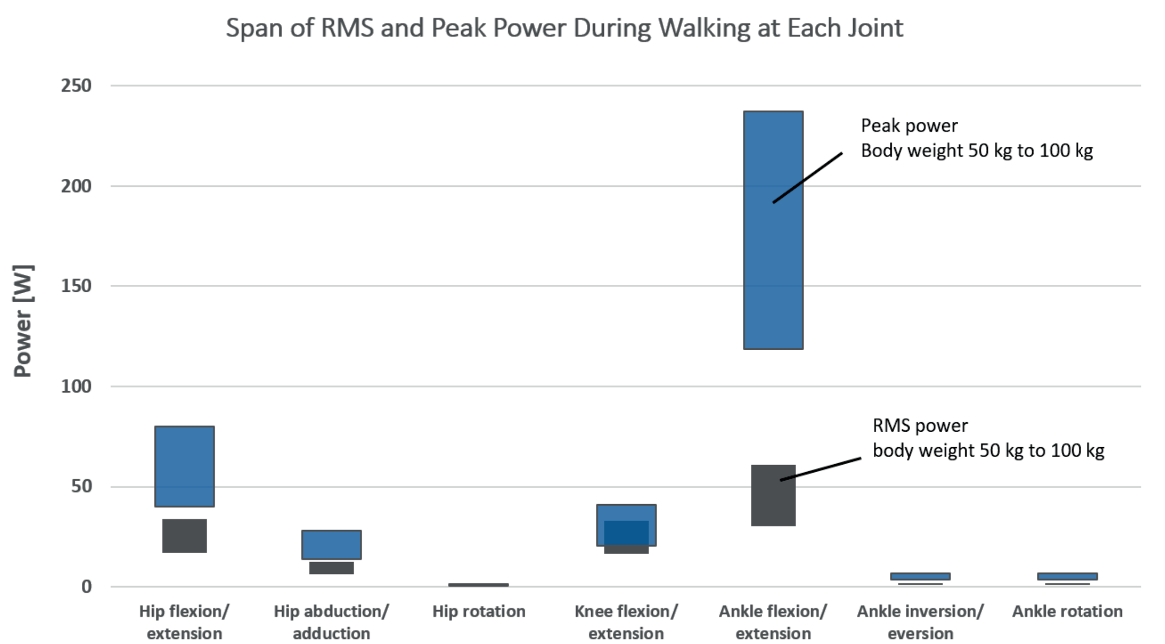

Figure 4-8 RMS and peak power for each joint during walking based on Schache and Baker [131]. The span covers the power needed for human body weight range of 50 kg to 100 kg.

4.1.5.2 Rising from a chair

The action of rising from a chair, termed the sit-to-stand (STS) transition, is a demanding task in terms of power generation. It largely depends on the weight of the body, as the center of mass is risen against the gravity, but also on the height of the body because the torques augment proportionally with the length of the limbs. The RMS and peak torques are illustrated in Figure 4-9, while the RMS and peak power for the joints in the sagittal plane are given in Figure 4-10. Data are extracted from the measurements of Mak et al. [132]. The participants in this study were healthy elderly people with weight between 43 and 75 kg and with heights from 1.47m to 1.69m. Hence, the data for body weight and height outside of those two ranges have been linearly extrapolated from gathered data.

The hip and knee torques during STS are similar in amplitude with RMS torques ranging from 20 Nm to 50 Nm and peak torques between 40 and 100 Nm. The ankle torques are slightly greater than the half of those of the hip and the knee. The hip peak and RMS powers are high, about 30% higher than those of the knee, with maxima about 110 W RMS and 260 W peak. The ankle power is very small, less than 20 W, because the torque exerted is for stabilization, and is necessary only once the body is standing still.

The notion of RMS values does not make a lot of sense here since the motion of standing is not cyclic and take only about 2.1 s as reported in [132]. However, it is interesting to know the mean values over the total duration. Compared to level walking, and regarding only peak values, there is a slight increase in hip torque, a large increase of 200-300% in knee torque and a decrease of 50% in ankle torque. Power compared to level walking show an increase of 300% and 500% for the hip and the knee respectively, while there is a 90% reduction at the ankle.

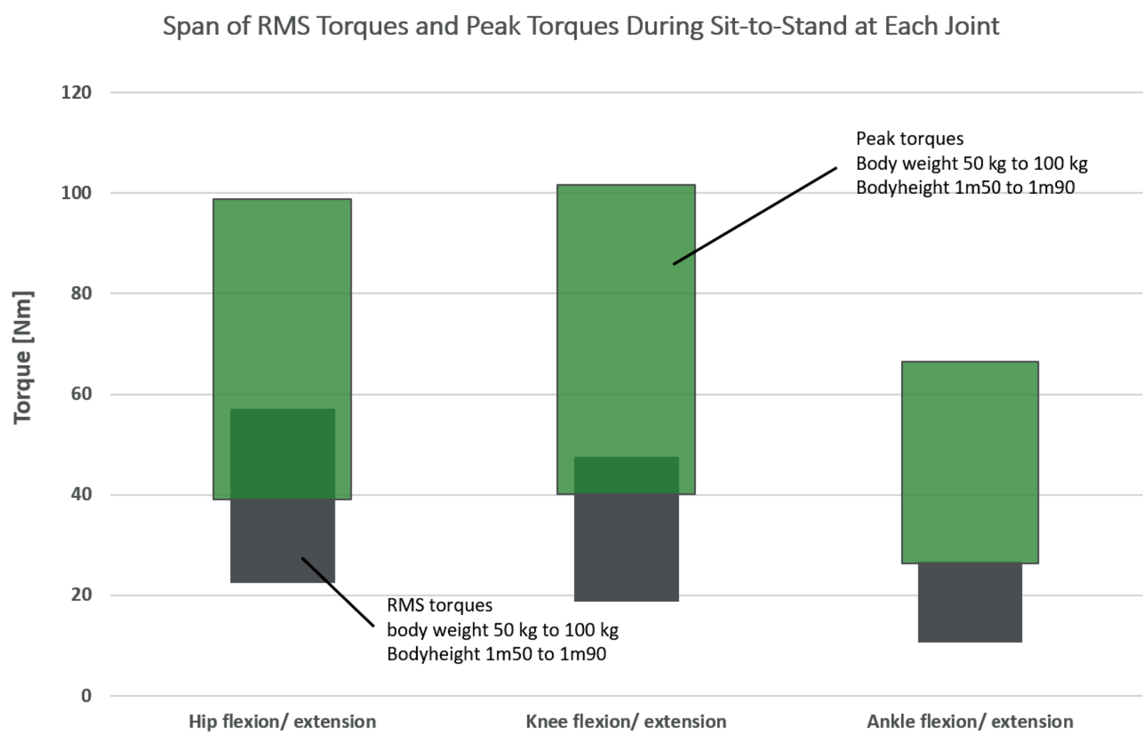

Figure 4-9 RMS torques and peak torques for each joint during STSbased on Mak et al. [132]. The span covers torque for humans ranging in height from 1m50 to 1m90 and weighing from 50 kg to 100 kg.

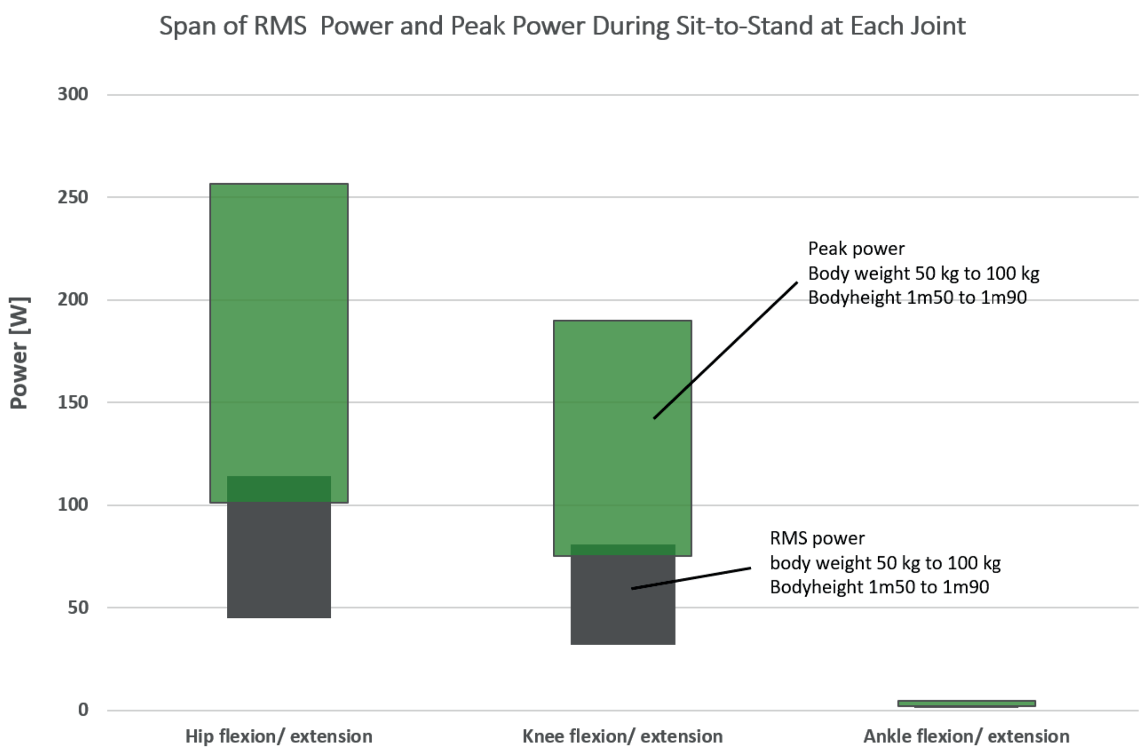

Figure 4-10 RMS power and peak power for each joint during STS based on Mak et al. [132]. The span covers torque for humans ranging in height from 1m50 to 1m90 and weighing from 50 kg to 100 kg.

It is also interesting to compare the performances of healthy people with those of people who have health conditions and yet are able to fully achieve the STS transition without external aid. Mak et al. [132] studied the kinematics and kinetics of STS in people with Parkinson's disease. The results show a longer transition time in patients with an increase of about 150%. The hip peak torque is reduced of 20% while the knee peak torque is increased of 10%. These measurements demonstrate that for the STS transition, no large torque reduction is gained from adapting the trajectories. However, using armrests and arm support has diminishes the hip and knee extension peak torques by 40% and 25%, respectively [150], [151]. It could be relevant to consider a small contribution from the arms in case of design limitations on the hip and knee peak torques.

4.1.5.3 Climbing stairs

Measurements from healthy people (Protopapadaki et al. [133]) are reported in the following in Figure 4-11 and in Figure 4-12 for the target population weighing between 50 kg and 100 kg, and ranging in height between 1.50 m and 1.90 m. Stair climbing as an action is normalized to be two steps climbed per cycle (one step each with the left and right foot), as healthy people tend to do. However, people with difficulties in ambulation such as some elderly people, tend to climb the steps one by one. The torques illustrated in Figure 4-11 shows, compared to STS, slightly greater torques at the hip, similar torques at the knee and enormous torques at the ankle. The same trends are shown in Figure 4-12 for the power.

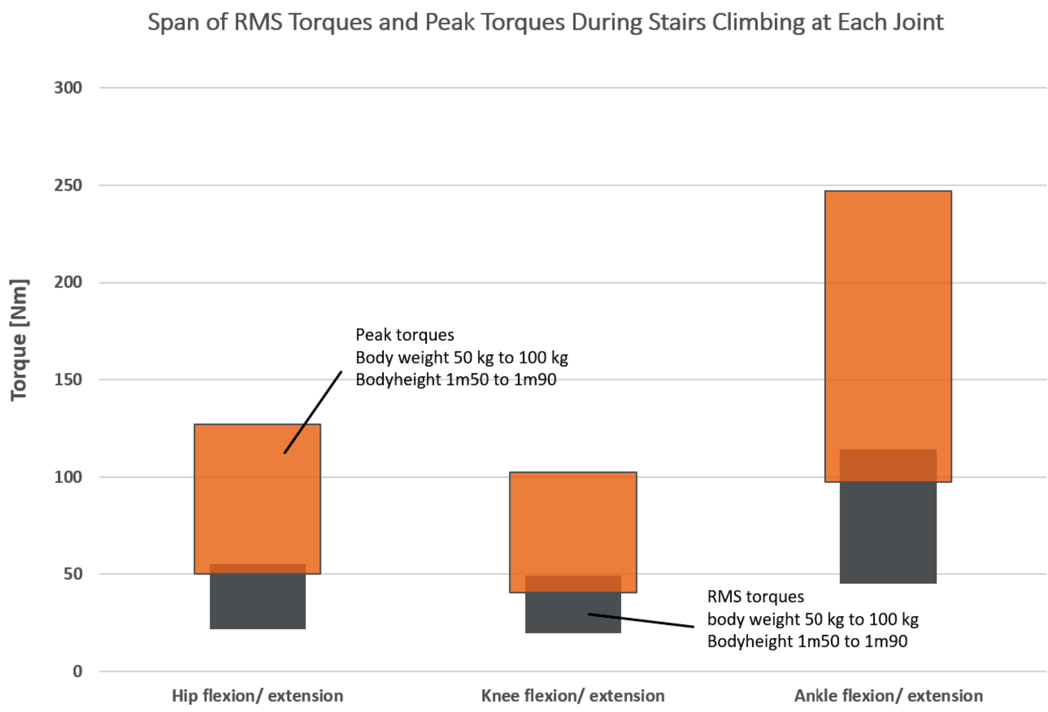

Figure 4-11 RMS torques and peak torques for each joint during stairs climbing based on Protopapadaki et al. [133]. The span covers torque for human heights from 1m50 to 1m90, and weights from 50 kg to 100 kg.

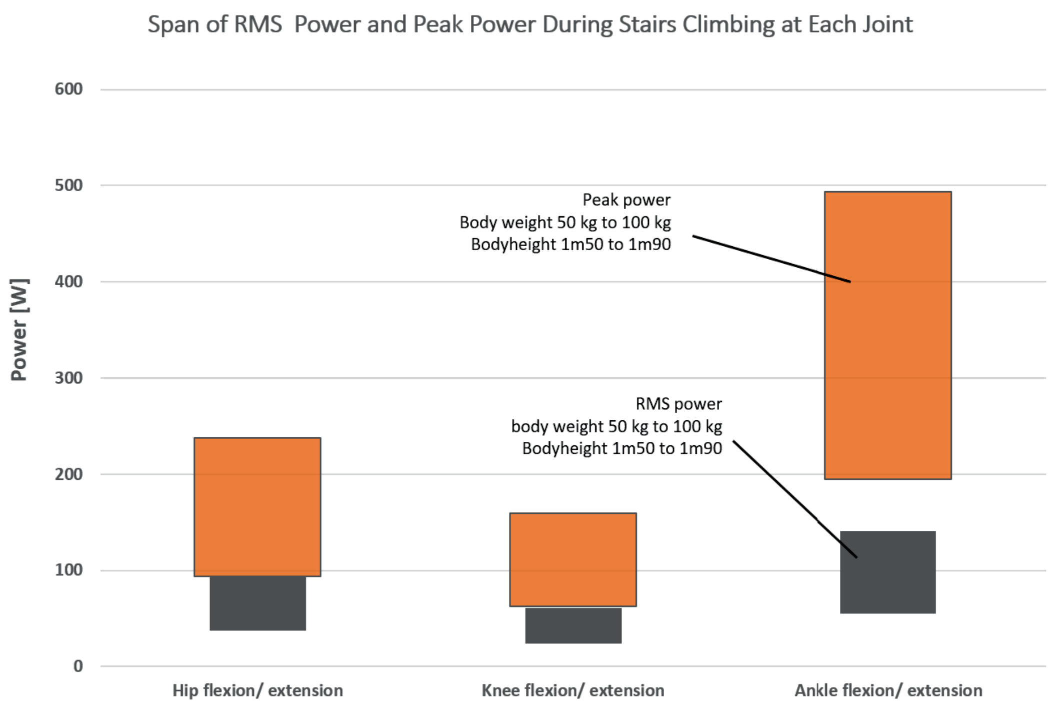

Figure 4-12 RMS power and peak power for each joint during stairs climbing based on Protopapadaki et al. [133]. The span covers torque for human heights from 1m50 to 1m90, and weights from 50 kg to 100 kg.

Radtka et al. [152] compared stair locomotion in healthy adults both with and without solid ankle-foot-orthosis (AFO) . While subjects were wearing the AFO, a decrease of the climbing velocity of 12 %, a decrease in knee extension peak torque of 20%, and an increase of knee flexion peak torque of 5 % was observed. It is not clear how much torque was generated at the ankle, since the AFO is supposed to entirely support the joint but the participants were all healthy people and thus did not need the support. Hence, it is assumed that the contribution from the participants at the ankle was largely decreased by the use of the solid AFO. In conclusion, the use of an AFO dramatically reduces the ankle torques, the knee extension peak torque by 20% while also decreasing stair-climbing velocity by 12 %.

4.1.5.4 Discussion

The specifications for each joint are evaluated following the different elements provided above and the elements already reported in 3.4.1 such as the range of motion and the maximum velocity. These specifications are reported in Table 4-3.

Table 4-3 Specifications of the maximal values considering a pilot of 1.90 m and 100 kg at an assistance level of 70%

Joints	**Specifications based on the maxima among the three activities (with 70% of assistance) (Level walking – rising from a sitting position – climbing stairs)**					
	Angle (min/max [°]) RoM [°]	***Peak Velocity [°/s]***	***RMS Torque [Nm]***	***Peak Torque [Nm]***	***RMS Power [W]***	***Peak Power generated [W]***
Hip Abduction/Adduction	(– 7.5 / + 5) 12.5	47	25	46	13	28
Hip Flexion/Extension	(– 10 / + 110) 120	160	40	89	80	180
Knee Flexion/Extension	(+ 5 / + 90) 95	330	34	56	56	133
Ankle Dorsi-/Plantarflexion	(– 23 / + 17) 40	197	80	173	98	346

A simulation based on actual technologies will be addressed in the next section that will evaluate, optimize and implement a mechanical architecture.

4.2 AUTONOMYO Design and Implementation

This section describes the design process of a lower limb exoskeleton named AUTONOMYO. The description is primarily oriented towards the design and technological choices for the actuation units, and will also include a discussion on aspects such as sensors and segment adjustment.

4.2.1 General Architecture

Weight, bulkiness and cost are key challenges for the adoption of exoskeleton apparatus as practical solutions for people with ambulation impairments. The best way to keep these constraints as low as possible is to keep the number of actuators and the power capacity as low as possible. The following guidelines were adhered to during the design process:

- Assist as few joints as necessary
- Prefer non-actuated compliant and/or lockable systems over actuated systems
- Optimize (lower) the required energy and peak torques by coupling active systems with compliant and/or lockable solutions

4.2.1.1 Selection of joints for assistance

The first questions, in order to define the architecture of the exoskeleton, are the following:

1. Which joints need assistance?
2. What is the nature of the assistance needed (active, passive and compliant or passive and stiff)?
3. What technology can best perform the specifications required?

In order to answer the first question, the contribution of the seven joints per leg are analyzed based on the elements provided in sections 3.4 and 4.1.5, which specify the dynamic motions targeted at each joint for which the exoskeleton is to provide assistance.

Hip Flexion/Extension

Hip flexion/extension is one of the main actor in all three targeted activities (level walking, stair climbing and rising from a sitting position). The work generated by the hip flexion/extension is majoritarily positive, as shown on Figure 4-13, supporting the need for an actuated assistance. The role of the hip flexion/extension is essential in the control of the anterior-posterior balance as it affects the swaying movement of the upper body. In both stairs climbing and STS transition, for example, the phases are initiated by a large forward bending of the upper body in order to place the center of mass over the polygon of sustentation. The motion of the hip is very important for that change of support from one foot to the other, or from the chair to the feet.

Hip Adduction/Abduction

The second hip motion is the adduction/abduction. Contrary to the case of flexion, it is not agreed upon if this motion needs actuated assistance. This is partially because it is not systematically measured and analyzed in the literature of gait dynamics and other stairs climbing, etc. Secondly, most exoskeletons for the mobility of people with SCI have a rigid segment in place of the hip adduction/abduction joint; users with the exoskeleton are still able to walk at acceptable velocities (2-3km/h) with the aid of devices such as crutches or rollators. Third, the range of motion at the hip adduction/abduction is small, about 15° in healthy people [131].

The author believes that hip adduction/abduction is an important motion for actuated assistance to take into account. The lack of abduction strength has been reported as to lead to waddling gait (see section 3.4) with large torso lateral displacement, slow gait and hip drop at swing. Other studies have demonstrated that abductor strength is highly correlated not only with walking speed [124] but also with balance and functionality in older adults [153]. In conclusion, hip abduction needs to be supported. What type of assistance would be sufficient then? Could it be feasible to use a non-actuated or minimally actuated joint?

A passive compliant constraint seems impractical, as the abduction energy generated is much greater than the energy dissipated during gait (see Figure 4-13). A rigid segment, however, could be a potential candidate as demonstrated by the existing exoskeletons using crutches. As experienced by people with complete SCI, a locked joint restriction prevents hip drop; however, the weight transferal from one leg to the other can only be managed with the assistance of crutches or similar support. The REX exoskeleton has proved that the lateral motion of hip abduction/adduction and the ankle inversion/eversion are keys in unlocking static lateral balance control. However, the gait achieved by the REX exoskeleton is very slow and largely exaggerates the physiological abduction pattern.

Abduction at the hip is essential for weight transfers during level walking, which provides lateral balance control. An actuated moving mass system could also provide a balance assistance with a much predictable behavior. Another benefit of not locking this joint is that it allows the user to perform exercises that can strengthen relative abductors. For example, a simple exercise would be to perform a lateral walk while adjusting the level of resistance/assistance to the user strength.

Hip Rotation

Although the torques (and power) generated during level walking are about ten times smaller than those of the hip flexion/extension, the contribution of hip internal/external rotation to walking movement is worth investigation and discussion [131]. The hip rotation is often used by people with other hip and/or knee flexion/extension weakness. No specific disorders have been observed in people with neuromuscular diseases that could be related to poor hip rotation conditions. The range of motion of this joint is quite small, approximately 10° while walking [131]. In conclusion, it is proposed to keep the hip rotation free for users that do not experience any trouble with it, and to have the possibility to lock the motion in the device in the case of undesired effects.

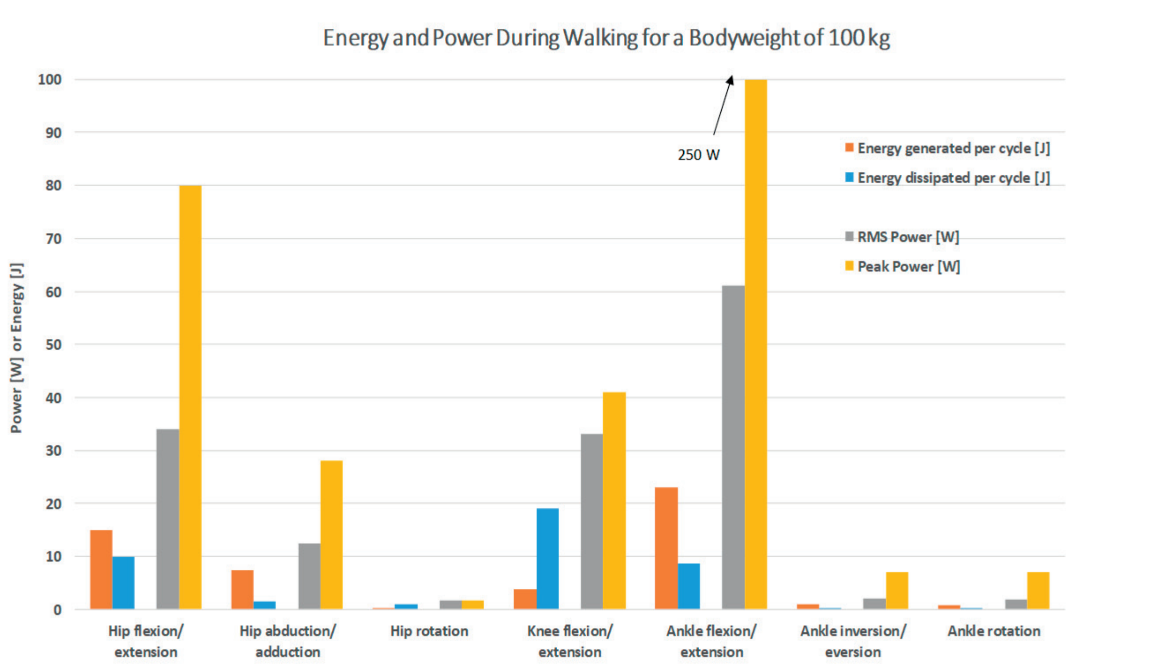

Figure 4-13 Energies and power transmitted to/from each joint while walking, taken from Schache and Baker [131]. The data shown are the maximum values with a bodyweight of 100 kg. Note that all values can be divided by a factor two for the minimal bodyweight of 50 kg.

Knee Flexion/Extension

The knee flexion/extension contributes greatly to the three different movements of discussion. While the body walks, the knee is mainly dissipating energy (see Figure 4-13). Exoskeletons (Phoenix, SuitX, USA), orthoses [154], and prostheses (Total Knee®, Össur, Iceland or C-Leg, Ottobock, Germany) using only a controllable damper or brake to manage knee motion during level walking are examples of implementation of this motion. However, the knee needs to generate large amount of torque and power during stair climbing or STS transition (see Figure 4-9 to Figure 4-12). Hence, while a passive solution would be able to account for level walking, it would not be able to supply the torque and power to support the other activities. Thus, an actuated joint is proposed for the knee joint.

Ankle Dorsi-/Plantar Flexion

As demonstrated by the very large torques and power shown in Figures 4-7 to 4-12, ankle flexion contributes greatly to walking and stair-climbing. The torques and power engaged for these two activities are about two times larger than the contributions from hip and knee flexion/extension. As described in the next section, placing a weight at the location of the ankle, i.e. at the extremity of the leg, has a dramatic impact on the performances due to the addition of inertia created by the weight. While the ankle is frequently used for walking and stair-climbing, experiments have also demonstrated that comfortable walking (at least 3km/h) can be achieved with a locked ankle [126]. Radtka et al. [152], as cited in section 0, observed that the use of ankle-foot-orthosis (AFO) to perform stairs climbing was possible, at the cost of a small climbing reduction in velocity. The AFO significantly decreases the power that the user's ankle must develop without creating more loading at the hip or knee as compensation [152]. The ankle torques involved in the STS transition rise only at the end of the phase to stabilize the vertical position [132]. It is thus compatible with the contributions provided by an AFO support. Despite the limitations in terms of performances that are inherent to the use of an AFO, this solution allows to significantly decrease the weight and inertia that would be generated by the use of an actuated design.

Ankle Inversion/Eversion and Rotation

The two other DoFs of the ankle, i.e. the inversion/eversion and the internal/external rotation, do not play a large role in the three activities based on the small kinematics observed. Inversion/eversion DoF is important to stability as it allows compensation for inclination relative to the ground; this is particularly useful in case of sloping terrain.

4.2.2 Challenges in the Actuation

4.2.2.1 Technology

There exist three main types of technologies frequently considered for the actuation of exoskeletons. The first one is electrical power, using batteries as power supply, electric motors as energy converters, and gears or other transmission components as torque amplifier (e.g. belt and pulley system, planetary gears, epicycloidal gears, ballscrew, etc.). The second and third are pneumatic and hydraulic power, with a tank or electric pump with batteries as power supply, and cylinder or pneumatic muscle as energy converter and transmitter. Because hydraulic energy is not compressible and thus difficult to store, hydraulic technology can best be used as a transmission system in combination with electric actuators. It would then be a hybrid system based primarily on electrical technology. Pneumatic energy can be stored in a tank under the form of compressed air. A lightweight carbon fiber tank of 6.8 liters can hold a pressure of 30 MPa, which is equal to about 1.2 MJ of energy in a 3.9-kg bottle. In comparison, 1 liter of lithium-polymer (LiPo) battery weights 2.2 kg and can store about 1.4 MJ. Hence, for a similar capacity, a battery is more than 2 times lighter and 6 times less bulky than a tank. The alternative to the tank for the pneumatic technology would be a pump that generates a stock of compressed air; however, this will include additional mass, batteries, and compressors for operation, which at low pressure levels (4-7 bar) often adds vibration. Another drawback of pneumatic actuation is the noise from air exhaust when emptying the cylinders. One potential benefit of pneumatic cylinder is that it functions as a variable stiffness actuator. Indeed, in adiabatic conditions, the pressure change is proportional to the volume change. Since only the piston position varies, the force is proportional to the position of the piston (see Figure 4-14). The elastic properties of a pneumatic cylinder have been observed in a previous work from the author [155]. It demonstrates the elastic behavior and the possibilities to change the attractive position and the stiffness by modulating the pressure in the two chambers of the cylinder.

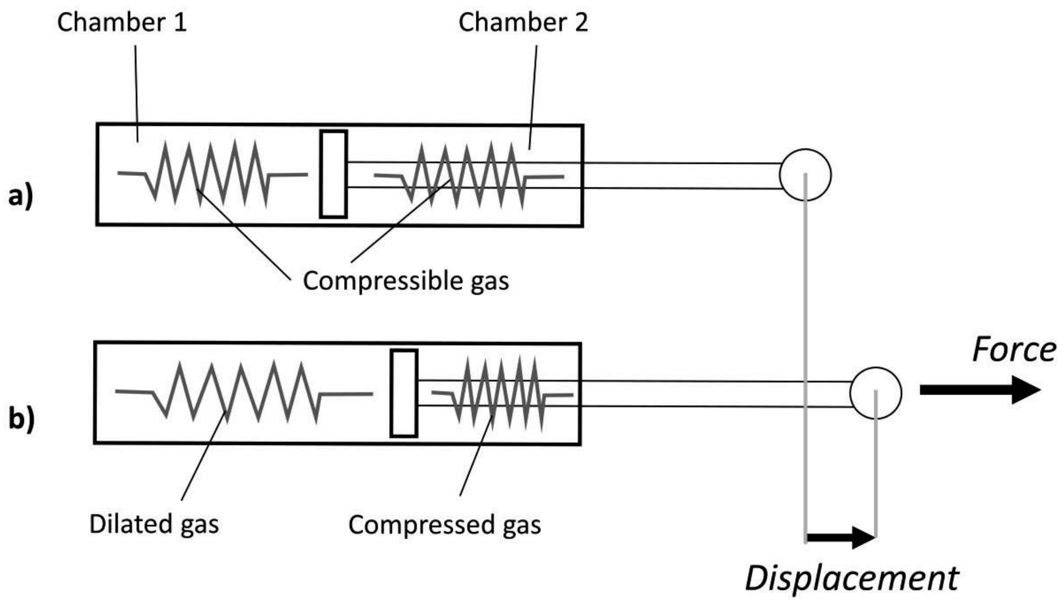

Figure 4-14 Illustration of a pneumatic cylinder acting as a parallel elastic mechanism a) at rest, and, b) under a force that creates a displacement of the piston. Copyright © 2016, Springer

Hydraulic technology enables more compact solutions, as the force density can be very high due to the incompressible properties of the fluid. Conversely, it is not compliant as gas would be, and thus, cannot be directly used as a variable stiffness actuator. The two main difficulties with hydraulic systems are: the realization of a fully closed hydraulic system and the design of the supply source. For these reasons, hydraulic systems are mostly used as transmission mechanisms with motorized pistons, remotely located from the joints, used for the actuation.

Electric technologies and systems are the most developed elements for compact and embedded systems, mostly used in robotics. Batteries have a high density of energy for a compact and lightweight ratio. Motors are quite efficient (about 80-90%), compact, low-cost and lightweight, and benefit from a large diversity of manufacturers with a large range of dimensions and power. The main drawbacks of electric motors are their low torque and the comparatively high inertia. Due to the high velocity–low torque properties, transmission mechanisms including a reduction are necessary for transmission of higher torques at lower velocities. Typical reductors are spur gears, planetary gears, cable or belt and pulley, leadscrew and ballscrew, worm drive, bevel gear, cycloidal gears, etc. These elements have usually an efficiency, size and weight that increase with the reduction ratio and the maximal torque supported.

4.2.2.2 Simulation of simple architecture

In this section, a simple architecture is simulated to evaluate the key aspects for the design of the actuation and the additional power required. A simple architecture would be to use the same motorization for the 4 joints of the hip abduction/adduction and the three flexions/extensions of the hip, knee and ankle. Particular attention is paid to the hip and knee flexion/extension as the accelerations are quite large in magnitude at these joints, while only small motions are transmitted through the ankle flexions and hip abduction/adduction. The simulation is a tool for indicating key limitations that can narrow down the potential selection of technology and architecture of the first actuation units. The simulation is simplified to a two dimensional study in the sagittal plane of the hip and knee joints during a walking cycle. The goal is to evaluate the importance of the additional efforts the motors must provide in order to reach the performances specified. Indeed, the motors do not only need to provide a torque to the user of the exoskeleton, but they do need to propel themselves and the rest of the exoskeleton. In order to evaluate this contribution, a single leg model of the exoskeleton is used and suspended in the air. This model is simplified since, neither the forward motion of the trunk nor the forces generated by maintaining an upright stance are taken into account. However, the forces related to the support phase can be approximated by adding the mass of the exoskeleton to the weight of the user; this provides a reference for calculating physiological torques during walking. The model is illustrated in Figure 4-15 and the dynamic equations for the hip and the knee joints in the sagittal plane are presented in Equation 4-1. The model used is similar to a double pendulum, where the two upper joints are actuated and the inner inertia of these joints are considered. The mass and inertia of the segments of the exoskeleton are not taken into account; however, their effect can be inferred from observation of the mass of the knee and ankle actuators. Note that the dynamic model depends neither on the mass of the actuator at the hip nor on the inertia of the motor at the ankle, as they are not considered.

$$\tau = M(\theta)\ddot{\theta} + C\big(\theta,\dot{\theta}\big)\dot{\theta} + g(\theta) \quad \text{(a)}$$

$$M(\theta) = \begin{bmatrix} m_K \cdot l_{HK}{}^2 + m_A \cdot \left(l_{HK}{}^2 + l_{KA}{}^2 + 2 \cdot l_{HK} \cdot l_{KA} \cdot cos(\theta_K)\right) + J_H & m_A \cdot \left(l_{KA}{}^2 + l_{HK} \cdot l_{KA} \cdot cos(\theta_K)\right) + J_K \\ m_A \cdot \left(l_{KA}{}^2 + l_{HK} \cdot l_{KA} \cdot cos(\theta_K)\right) + J_K & m_A \cdot l_{KA}{}^2 + J_K \end{bmatrix} \quad \text{(b)}$$

$$C\big(\theta,\dot{\theta}\big) = -m_A \cdot l_{HK} \cdot l_{KA} \cdot sin(\theta_K) \cdot \begin{bmatrix} \dot{\theta}_K & (\dot{\theta}_H + \dot{\theta}_K) \\ -\dot{\theta}_H & 0 \end{bmatrix} \quad \text{(c)}$$

$$h(\theta\,) = \begin{bmatrix} g \cdot (m_K \cdot l_{HK} + m_A \cdot l_{KA}) \cdot \sin\theta_H + g \cdot m_K \cdot l_{HK} \cdot \sin(\theta_H + \theta_K) \\ g \cdot m_K \cdot l_{HK} \cdot \sin(\theta_H + \theta_K) \end{bmatrix} \quad \text{(d)}$$

Equation 4-1 (a) General expression of dynamic model based on the inertia matrix expressed in (b), the Coriolis and centrifugal elements (c) and the gravity elements (d), based on the model and notations from Figure 4-15.

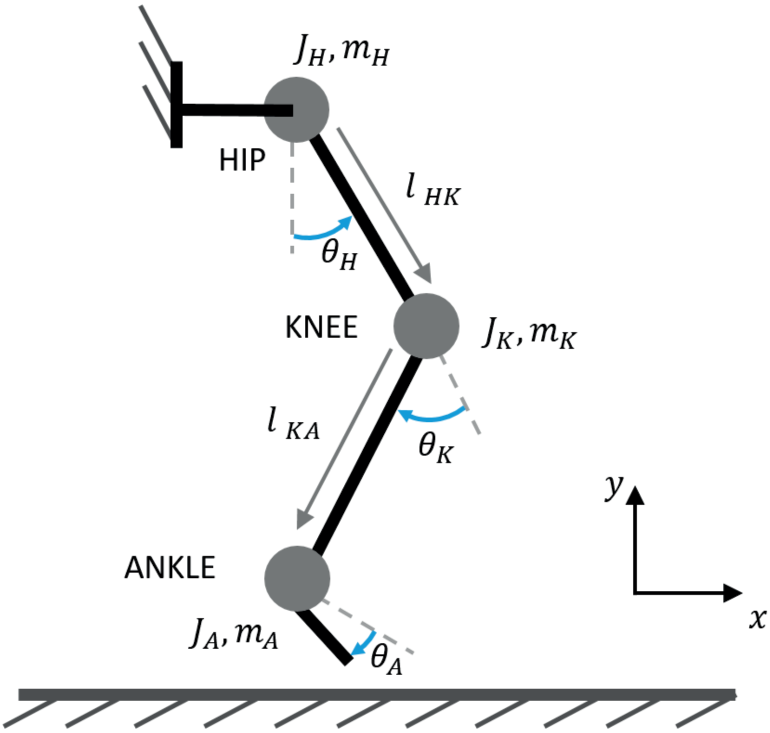

Figure 4-15 Model of one leg of the exoskeleton, which isolates the effects of the actuators mass and inertia on the amount of the torques required. "*J*" and "*m*" denotes the motor inertia and mass respectively, "*l*" the distance inter joints and "θ" the angular position of the joints. "*H*", "*K*" and "*A*" indicates the joints to which it belongs, respectively, the hip, knee and ankle.

Both hip, knee and ankle joints are realized with the same actuating unit that suits the specifications previously described. A compact solution located directly on the joints is selected. It is composed of a flat brushless electric motor EC 90 flat (Maxon motor AG, Sachseln, Switzerland) with 260 W of nominal power and nominal torque of 1 Nm. The motor weights 980 g and has an inertia of 5060 gcm^2. In order to reach a nominal torque at the joint about 40 Nm, the selected reductor is the compact CSD-32-50-2UH from Harmonic Drive® (Tokyo, Japan). The reductor has a transmission ratio of 1:50 and can support the torques required (150 Nm in repeated peaks). It weighs 2.4 kg and its inertia is neglectable compared to that of the motor. The unit inertia is then the motor inertia multiplied by the square of the transmission ratio, which is equal to 1.25 kgm^2 at the joint. The actuation unit mass is about 3.4 kg. A final mass of 4.5 kg is modeled to take into account the structure necessary to hold the actuator.

The results of the simulation for the hip and the knee are presented in Figure 4-16 and Figure 4-17. The upper graphs show the torques required to move the exoskeleton, the physiological torques that correspond to the torques required by the person to walk, and the approximate final torque required by the actuators. The approximate final torque is the sum of the former two torque quantities. In the lower graphs, the torques required only to move the actuators are split into the different constituents, which are the effects from the different inertias and masses. Results highlight a considerable effect of the inertia and masses of the actuators. It follows peak torques about three times more important than in physiological gait. For the knee actuation, the additional torques appear only in the swing phase and is related to the mass of the ankle actuator located at the ankle joint and to the knee motor inertia. The latter introduces peak extension torque about 50 Nm and peak flexion torque about 80 Nm, while the additional weight on the ankle is a bit lower with only

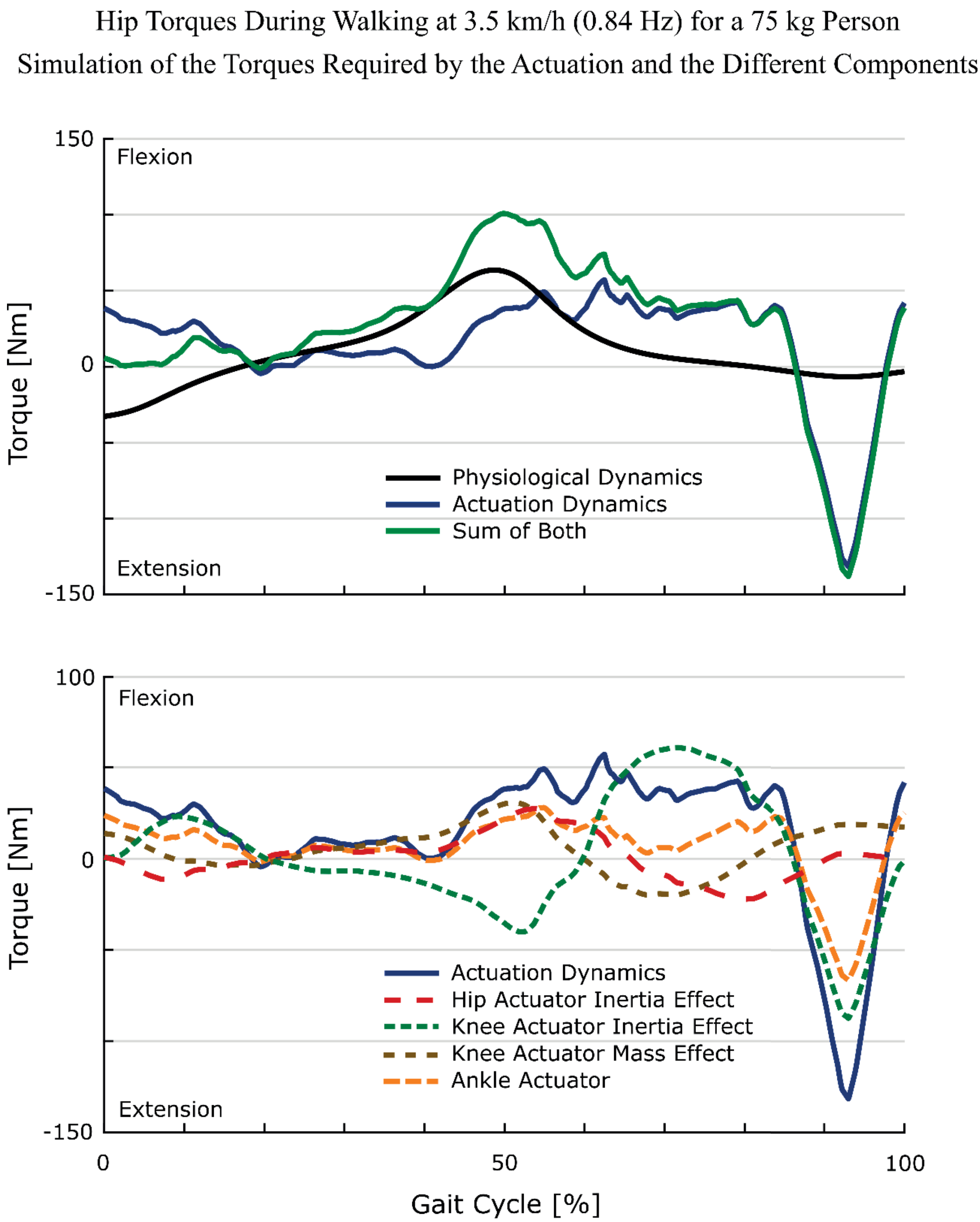

Figure 4-16 Simulation of the actuator mass and inertia effects on the total torque at the hip for a person walking at 3.5 km/h based on the kinematics from Schache and Backer [131]. 'Physiological dynamics' is defined as the natural torque exerted by a person while walking freely.

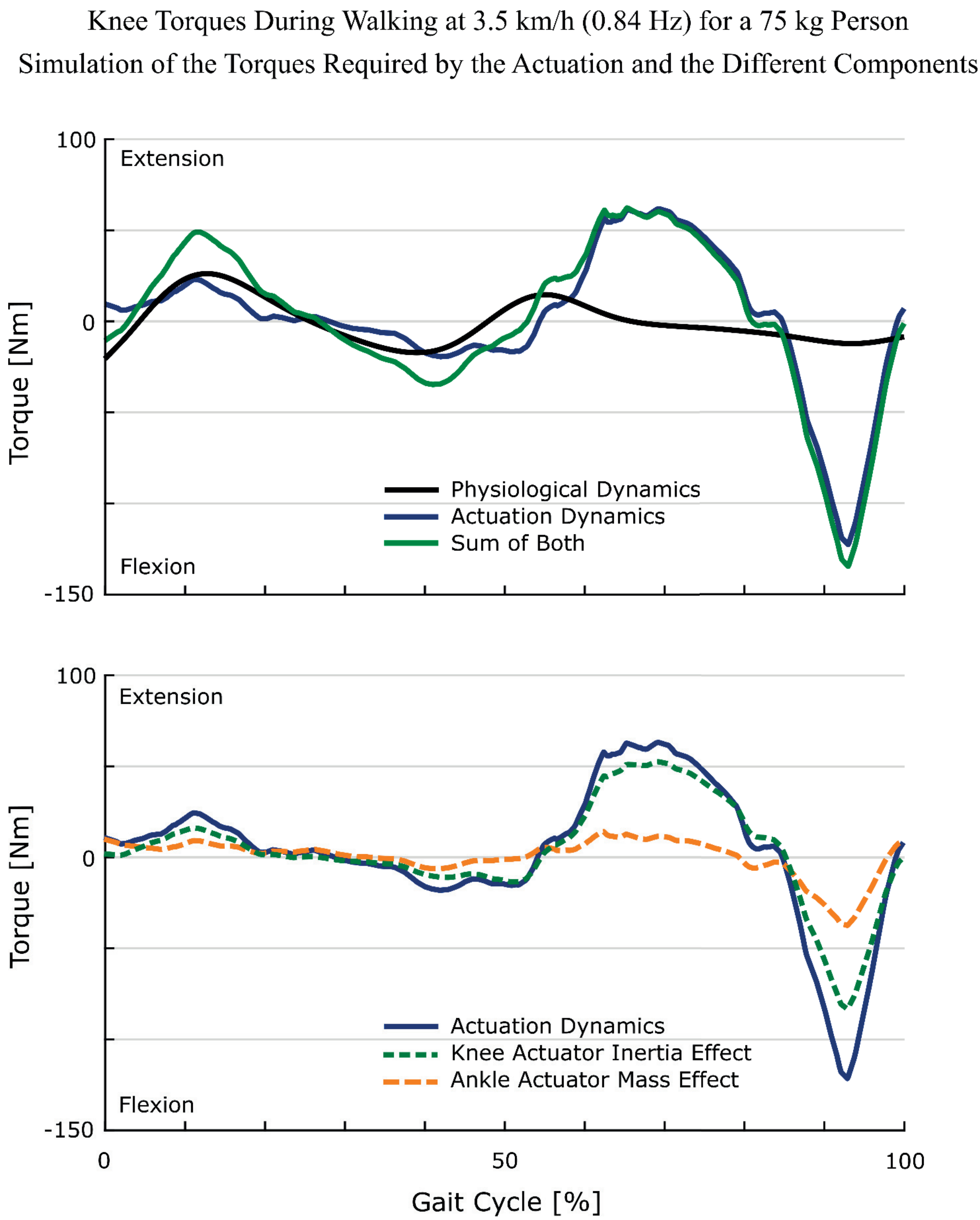

Figure 4-17 Simulation of the actuator mass and inertia effects on the total torque at the knee for a person walking at 3.5 km/h based on the kinematics from Schache and Backer [131]. 'Physiological dynamics' is defined as the natural torque exerted by a person while walking freely.

about 15 Nm and 35 Nm in peak extension and flexion respectively. These peak torques are large in magnitude and highlight the limitations of such actuators due to their inertia and mass. The same peaks are replicated at the hip. The mass at the ankle even has a worse effect as the two joints are further from one another. A large peak is denoted at the end of the swing phase due to the motion of the actuation. The negative effects (amplification of torque) are felt at the hip from mid-cycle to end of the cycle. However, the actuation has a positive effect (reduction of torque) at heel strike and load acceptance as shown in Figure 4-16. Surprisingly, the effects of inertia of the actuator at the knee are alleviated by the effects of the mass of the same actuator; this is because the hip and knee accelerations are mostly in opposition during gait.

The knee actuator inertia produces the worst impact on both the knee and the hip torques, followed by the effect of the mass of an actuator located at the knee. The effects of the mass of an actuator at the knee and of the inertia of the hip actuator require high peak torques of about 25 Nm each, which should be reduced in order to reach the targeted performances. Possible ways to reduce these effects are to avoid actuating one joint by replacing it with a passive system, to find a more appropriate technology with lower inertia, to locate the actuators more proximally to the trunk of the user, or to modify the kinematics so that the accelerations are lowered.

4.2.3 Design of the Actuation in the Sagittal plane

The design in the sagittal plane is based upon the three flexions/(extensions) of the hip, knee and ankle. As highlighted in the previous section, the mass and inertia of the actuators play a key role in determining the amount of power required. The challenge of actuator inertia in different motorized hip orthosis, including HiBSO (Hip Ball Screw Orthosis), is shown in Figure 4-5 [156]. In [157], J. Olivier ultimately proposes a double clutch system in order to use the motor as a power source while also selecting the direction of rotation of the joint and modulating the velocity or torque through a variable clutch, based on disk brakes. While necessitating some development, the solution of a double clutch system is bulky and also difficult to control, as the modulation of torque is based on the variation of dry friction.

The challenges are to reduce the effects of the ankle and knee actuators' collective mass, as well as that of the actuator inertia for all the joints.

Mass and inertia of the ankle actuator

As discussed in section 4.2.1, and observed in people with large deficits of strength about the ankle, the use of a rigid ankle-foot-orthosis offers a large support over the joint. However, it also diminishes performance and worsens balance over different terrain in comparison to a fully actuated joint. This configuration allows a weight increase of at least 3 kg located at the ankle, which represents an inertia of about 1.92 kgm^2 at the hip level (estimation assuming a hip-ankle distance of 0.8m). The benefit of using a passive support for the ankle is the creation of a large power saving; this significantly reduces the amount of energy required and, thus, the volume and weight of the battery system needed.

Inertia of the actuators

The inertia of all actuators can be improved by selecting the appropriate technologies. For example, brushless electric motors have lower rotor inertia than brushed motors for similar nominal torque and volume specifications. Some manufacturers can also have some advantages with patented technologies. In order to optimize the inertia at the joint, one should take into account not only the inertia of the motor, but also the transmission ratio, which is defined based on the nominal torque of the motor and the required nominal torque at the joint. The derivation of the "reported inertia" criteria for defining the lower motor inertia effect at the joint is shown in Equation 4-2.

$$J'_{motor} = J_{motor} \cdot \eta^2 \quad \text{(a)}$$

$$\eta = \frac{\tau_{\ joint\_nominal}}{\tau_{\ motor\_nominal}} \quad \text{(b)}$$

$$J'_{motor} = J_{motor} \cdot \frac{\tau^2_{joint\_nominal}}{\tau^2_{motor\_nominal}} \quad \text{(c)}$$

$$\min J'_{motor} \propto \min \frac{J'_{motor}}{\tau^2_{joint_{nominal}}} = \boxed{\min \frac{J_{motor}}{\tau^2_{motor\_nominal}}} \quad \text{(d)}$$

Equation 4-2 (a) Motor inertia reported to the joint, (b) Definition of the transmission ratio, (c) Replacement of (b) in (a), and, (d) Criteria for the minimization of inertia at the joint. With "*J* " the inertia, "*J'* " the inertia reported at the joint "*η* " the transmission ratio and "*τ* " the nominal torque from the motor or required at the joint.

After some research and comparison of different motors based on the « reported inertia » criteria, the selected motor is a brushless EC-i 40, 100 W (Maxon motor AG, Sachseln, Switzerland) with a rotor inertia of 44 gcm^2 and a nominal torque of 207 mNm. If this motor of 40 mm of diameter is compared to the flat motor (EC 90 flat) used for the simulation in section 0 with an identical target joint nominal torque of 40 Nm, the transmission ratios, based on the motor nominal torques, are respectively of 1:200 and 1:40. Applying Equation 4-2 (a) to these two solutions gives the projected inertias on the joint that are equal to 0.176 kgm^2 for the 40mm diameter motor and 0.810 kgm^2 for the flat 90 mm diameter motor. Hence the inertia has been reduced to 22% of its initial value by optimizing the motor based on the "reported inertia" criteria.

Mass of the knee actuator

One possible approach to reduce the effect of the mass of the knee actuator on the hip joint is to remotely locate the knee actuator away from the joint. This can be done by using a belt or cable and pulley transmission which transmits the torque from a certain distance. Relocating the actuators also allows optimization of the volume and the location occupied by these elements.

By locating the knee actuator ahead of the hip joint, a coupling between the hip and the knee joints can be introduced. The impact of such a coupling is explored in the next section.

4.2.3.1 Coupling of the hip and knee flexion/extension

This section explores the effects of coupling the hip and knee flexion/extension. The design, as presented in Figure 4-18, is composed of two actuators located behind the hip joint. Motor B is coupled to the hip joint through a cable and pulley transmission, while Motor A is coupled to the knee joint with the same system, but passes through the hip joint. Two configurations of coupling can be set with this architecture: a positive coupling, where a hip flexion induces a knee flexion, or, a negative coupling, where a hip flexion generates a knee extension. Mechanically, the two configurations can be obtained by either crossing or not crossing the cables linking the pulley at the hip to the pulley at the knee.

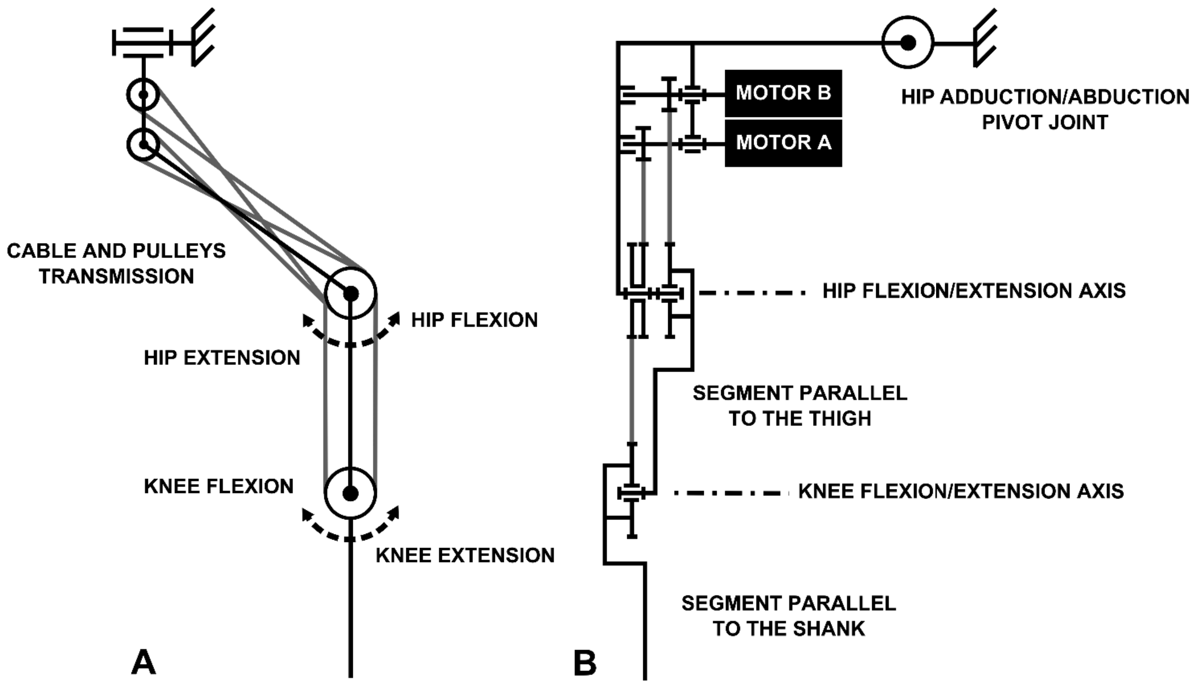

Figure 4-18 Hip and knee flexion/extension architecture with remotely located actuators from the hip and knee joints, and executed through cable and pulley transmission. A. View in the sagittal plane, B. View in the frontal plane. Copyright © 2017, IEEE

The current section is comparing the three following configurations:

1. Hip and knee joints are independent
2. Hip and knee joints are positively coupled, a hip flexion leads to a knee flexion
3. Hip and knee joints are negatively coupled, a hip flexion leads to a knee extension

The inverse kinematics for the three configurations can be obtained by inverting the Jacobian which expresses the relationship between the joint velocities and the motor velocities. In order to simplify the calculations, a transmission ratio of 1:1 is assumed between the motor and the joints. The inverse kinematics of the different configurations are calculated by inverting and transposing the Jacobian of the forward kinematics as presented in Equation 4-3. The value of the Jacobians are reported in Table 4-4. Note that the hip flexion is positive and the knee flexion is negative if the two joints share the same referential system.

$$\begin{pmatrix} \dot{\theta}_{Hip} \\ \dot{\theta}_{Knee} \end{pmatrix} = J \cdot \begin{pmatrix} \dot{q}_B \\ \dot{q}_A \end{pmatrix} \quad \text{(a)}$$

$$\begin{pmatrix} \tau_{Hip} \\ \tau_{Knee} \end{pmatrix} = J^{-T} \cdot \begin{pmatrix} \tau_B \\ \tau_A \end{pmatrix} \quad \text{(b)}$$

Equation 4-3 Expression of direct (a) and inverse (b) kinematics. With “*J* ” the jacobian, “θ” the joint position, “q” the motor position and “τ” the torques, while “A” and “B” refers to the different motors.

Table 4-4 The Jacobians of the different configurations from the expression of Equation 4-3

No coupling	Positive coupling	Negative coupling
$J_{ind} = \begin{pmatrix} 1 & 0 \\ 0 & 1 \end{pmatrix}$	$J_{pos} = \begin{pmatrix} 1 & 0 \\ -1 & 1 \end{pmatrix}$	$J_{neg} = \begin{pmatrix} 1 & 0 \\ 1 & 1 \end{pmatrix}$
$J_{ind}^{-T} = \begin{pmatrix} 1 & 0 \\ 0 & 1 \end{pmatrix}$	$J_{pos}^{-T} = \begin{pmatrix} 1 & 1 \\ 0 & 1 \end{pmatrix}$	$J_{neg}^{-T} = \begin{pmatrix} 1 & -1 \\ 0 & 1 \end{pmatrix}$

In positive coupling, motor B generates both hip and knee flexions or extensions simultaneously. Because motor A can also contribute, these combined motions be made faster. However, negative coupling increases the hip torque while causing synchronous hip and knee flexions or extensions. The effects of the three configurations are evaluated based on simulated activities such as of level walking, STS transition, and climbing stairs.

Level Walking

Level walking is denoted by a cyclic motion where high accelerations can occur, typically during the swing phase. The amplitude of the torques are, however, moderate in comparison to the two other activities. Figure 4-19 shows the effect of coupling or uncoupling the hip and the knee flexion/extension and its impact on the velocities, the reference torque to be assisted (physiological torque), and the actuator inertia based on the optimized technology. The coupling has affects neither on the kinematics of the motor B, which is always equal to the hip motion, nor the torque at motor A, which is identical to the torque applied at the knee. Figure 4-19 highlights, however, the large effect the coupling has on the velocity motor A must be able to achieve. A positive coupling significantly decreases two peaks of velocity on motor A by a factor of 2; however, the coupling has no effect on the last peak of velocity, which has a magnitude close to that of the maximum velocity achieved. Hence, a positive coupling can reduce two of the peak velocities but does not affect the specifications on the maximal velocity. The different configurations do not have a significant impact on the torque amplitudes. For the torque resulting from the inertia of the actuator, the maximal amplitude is about 12 Nm. The positive coupling decreases this effect of about 30%; however, the gain is quite low in this application. The main contribution of positively coupling the hip and the knee flexions is primarily found in the velocity changes.

Rising from a Chair

The STS transition is marked by moderate velocities and high torques at the hip and knee joints as shown in Figure 4-20. The positive coupling and the no coupling configurations have lower velocities at motor A, but since the STS is not a very dynamic motion, the velocities are acceptable even with the negative coupling configuration. For the physiological torques, the negative coupling drastically reduces the peak torques down to a value of 40 Nm, while the uncoupled configuration is more moderate, with a peak of about 60 Nm. The positive coupling requires about 130 Nm. The third graph in Figure 4-20 shows that the effect of the inertia of the actuator is negligible in all configurations. In conclusion, it is seen that there is a large benefit in using a negative coupling configuration to perform STS transitions.

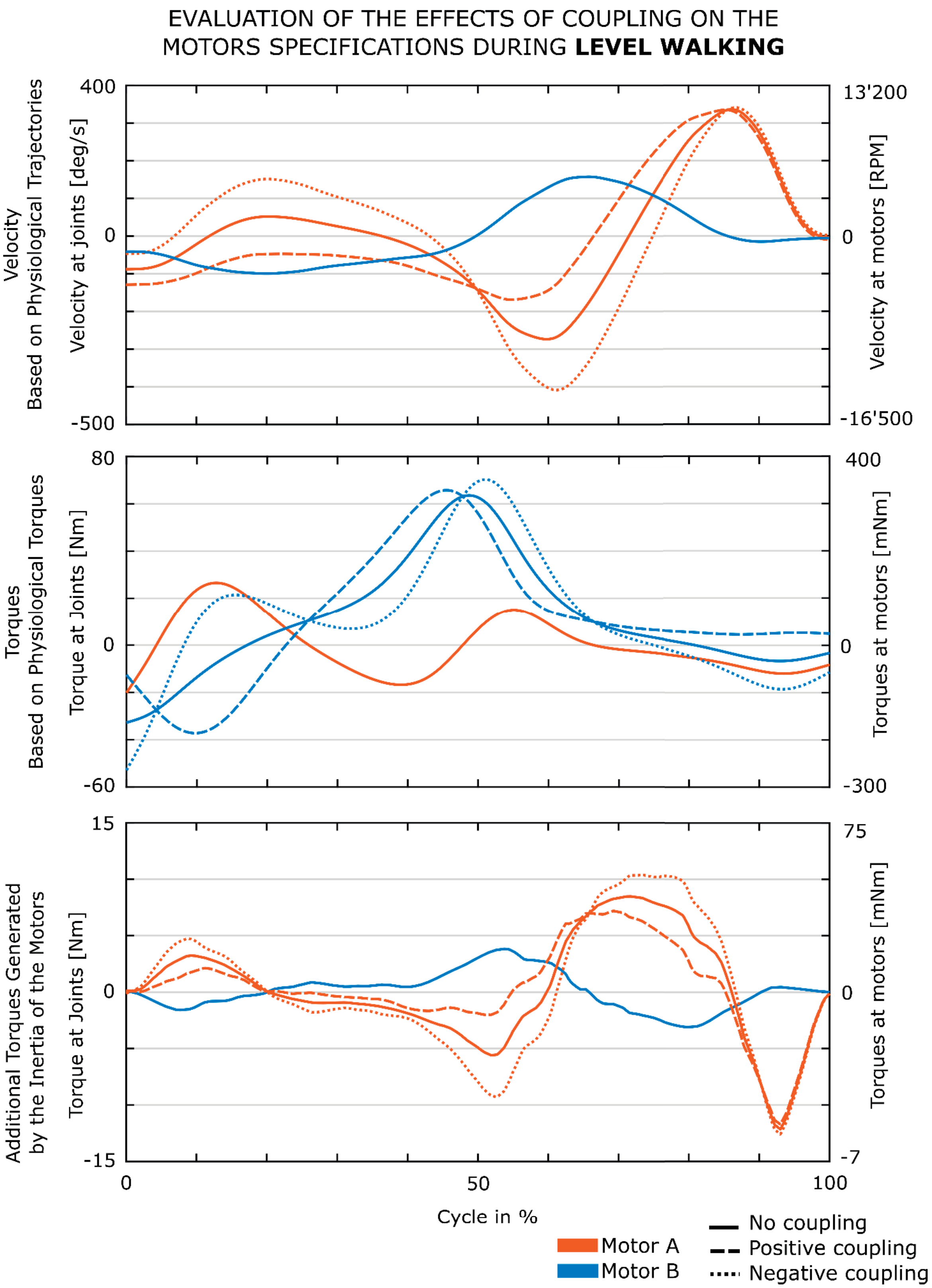

Figure 4-19 Effect of the different coupling configurations on the required velocities and torques at the motors during level walking. The physiological torque is based on the mechanical properties of a human with median body weight of 75kg.

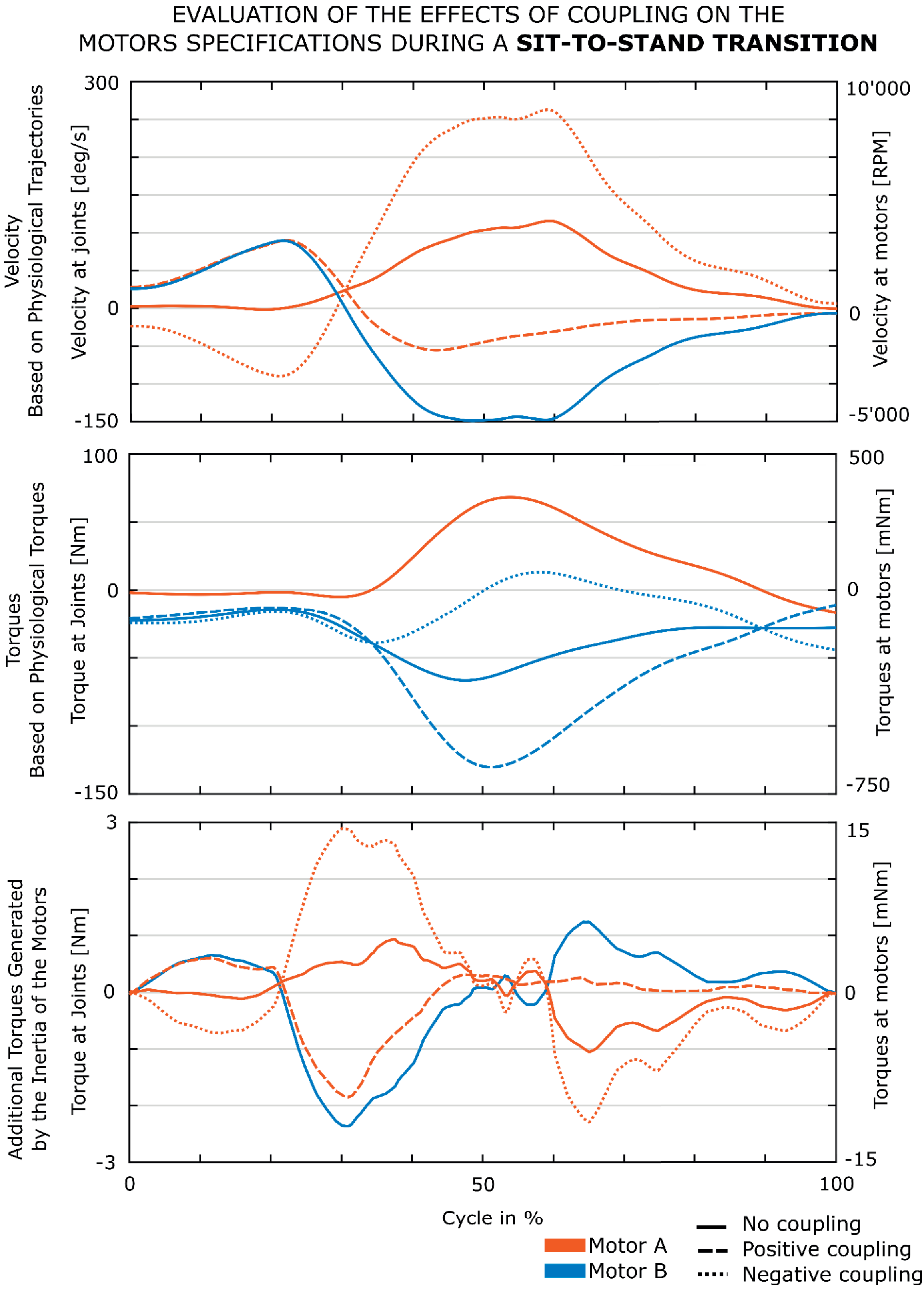

Figure 4-20 Effect of the different coupling configurations on the required velocities and torques at the motors during a sit-to-stand transition. The physiological torque is based on the mechanical properties of a human with a median body weight of 75kg and body height of 1.70m.

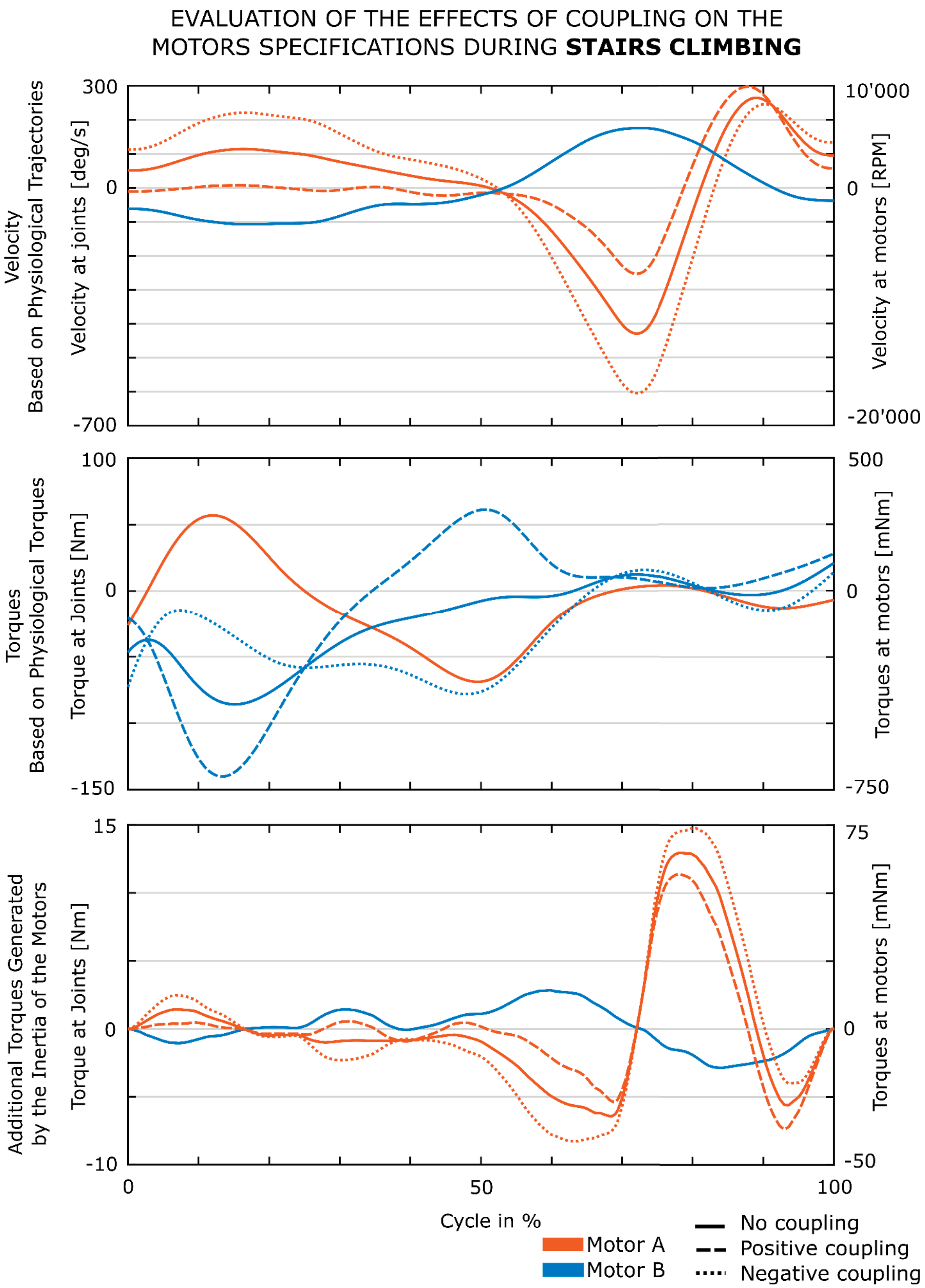

Figure 4-21 Effect of the different coupling configurations on the required velocities and torques at the motors during stairs climbing. The physiological torque is based on the mechanical properties of a human with median body weight of 75kg and body height of 1.70m.

Stairs Climbing

The effect of the different configurations of coupling upon stair climbing performance are reported in Figure 4-21. The velocities at motor A reach a high peak during the first half of the swing phase. This peak is moderate in positive coupling (about 250 °/s), large with no coupling (about 420 °/s) and very large in negative coupling configuration (600 °/s). The physiological torques produced by the motors are also significantly dependent upon the coupling configuration. In the cases of no coupling and negative coupling, both reach peak torques of about 75 Nm at the hip, while in positive coupling, the peak torque reaches up to 140 Nm. The effect of the actuator inertia is relatively important for the motor A (about 15 Nm), however the differences between the different coupling configurations are small. In conclusion, stair climbing is the most demanding activity since it requires simultaneously the greatest velocities and the greatest torques of the three activities. There is no clear advantage for any of the coupling configurations. Positive coupling better fulfills the requirement for the swing phase, while negative coupling performs better in the stance phase. The configuration without coupling would be the most adapted since it avoids both torque and velocity extremes.

4.2.3.2 Complete sagittal design

Remote actuation elements

The systems implemented for both the hip and knee flexion/extension actuation units are identical. It is composed of a motor EC-i 40, 100 W (Maxon motor AG, Sachseln, Switzerland), a planetary gearbox GP 42 HP (Maxon motor AG, Sachseln, Switzerland) with a transmission ratio of 1:74, and a custom pulley with helical groove for a 2mm-diameter cable. These elements are aligned with the motor axis and are illustrated in Figure 4-22

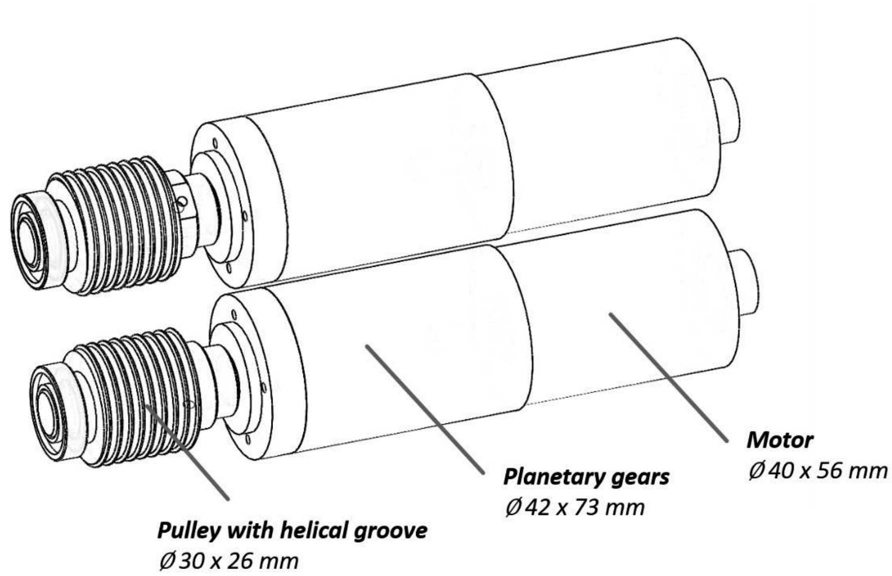

Figure 4-22 The remotely located elements of the hip and knee flexion/extension actuation units, including brushless motors, planetary gearbox and pulley

Transmission to the joints

The cable and pulley system chosen for the transmission of power from the remotely located actuation units to the joints has a superior compactness compared to belts for comparable torque transmission and is very rigid. Mechanical transmission through cables is subject to the main following challenges:

1. Transmission of efforts between cable and pulley (fastening of the cable)
2. Limit in the range of motion
3. Limit of pulley diameter as a function of cable diameter
4. Limit of cable angle and winding
5. Tensioning of the cable

Lowering the transmission ratio of the gearbox implies lowering the torque capacity of the gearbox and thereby lowering the size and weight of it. It also diminishes the losses that would otherwise increase with the number of gear stages. A ratio about 1:3 between the pulley at the motor and the pulley at the joint is a good compromise between the diameter and winding limitations. The pulleys at the joints are realized with a groove diameter of 84 mm; the transmission ratio between the pulley is 5:14. The total ratio from the motor to the joint is, then, about 1:207. In order to solve the challenge of the transmission of energy between the cable and pulley, the cables are built with swaged ends that are anchored on the larger joint pulleys. For the small motor pulleys with helical groove, the cables are wound about 3 turns and a half around them. Two screws press and lock the cables against the pulley. In order to pre-tension the cables, free-sliding pulleys are mounted on the structure and can be tightened with the help of screws.

The selection of the cable diameter is a compromise between the minimum bending radius, which mostly affects the lifespan of the cable and the maximal supported load. Other cable constructions are made out of different strand configurations, thin wires, or materials such as metals or polymers. The selected solution is a stainless steel wire rope of diameter 2.0 mm and configuration 6x19-WSC (Carlstahl Technocables, Germany), with terminations swaged with cylinders of 4.0 mm of diameter and 8.0 mm of length. The minimal breaking load of such a solution is 2.768 kN and has a minimum bending ratio of 25. A minimum pulley diameter of 50 mm would then be recommended. Because the small pulleys of the current design have a diameter of 30mm, they do not fit the recommendations. Tests of durability are required as future work to validate the current design. Risks are an early fatigue and the rupture of the most bended little wires which will reduce the total load capacity of the wire rope. Hence, it can lead to a higher risk of breakage of the wire ropes that would free the joint by cutting the transmission with the actuators.

Belt and pulleys or gears transmission systems could turn indefinitely (unlimited range of motion). However, particular attention is paid to the range of motion. Since the cables are anchored to the pulleys, the range of motion is limited by the position of anchorage. The targeted range of motion is about 160° (-20° to +140°) for the hip and about 140° for the knee (-10° to +130°). In the case of hip-knee coupling, the range of motion of motor B is unchanged, while the range of motion of motor A is a result of both hip and knee flexions and has a maximum rotation of 300°. Using a single groove per pulley provides range of motion to about 160°. The use of a helical groove is an option; however, it introduces lateral displacement. Ultimately, a design with two grooves is chosen; as a result two strands are necessary and are anchored separately and in opposition, see Figure 4-23.

The concept of the complete actuation of the hip and knee in the sagittal plane is illustrated in Figure 4-18. The transmission of motor B is linked to the hip through only one cable-and-pulley stage, from the motor to the hip joint. The transmission of motor A, however, needs two stages to reach the knee, as it first needs to pass through the hip. A pair of free pulleys transmits the energy from the motors and passes them to the knee joint. A key drawback of such a cable transmission is that, in the presented configuration, it is not possible to adjust the length of the segment along the thigh without changing the length of the cables. A mechanism to avoid this drawback is presented in section 4.2.5.2.

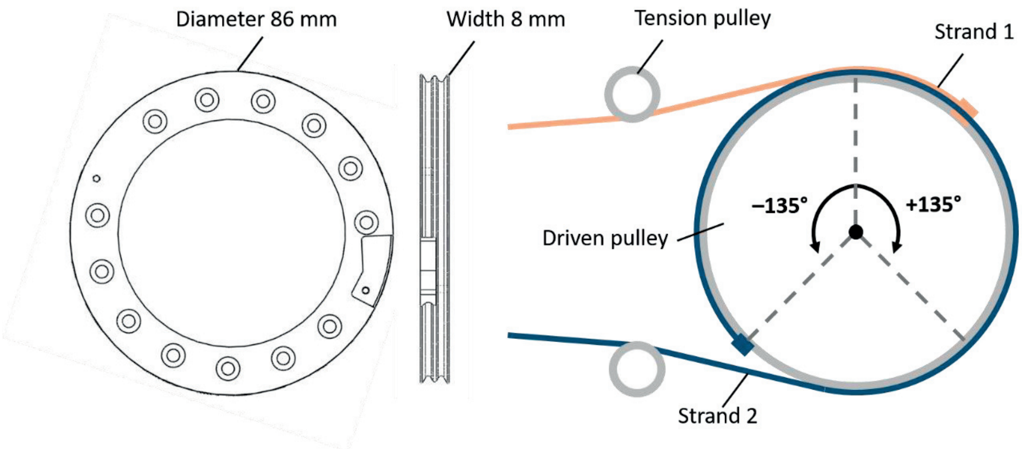

Figure 4-23 Illustration of the large pulley at the joint and its range of motion of approximately 270°

Ankle joint

The first iteration of the ankle joint design uses a passive approach. The solution should allow the three axes of rotation while constraining the motion with a visco-elastic behavior. A rubber system based on skateboard bushings are used. The mechanics is presented in Figure 4-24.

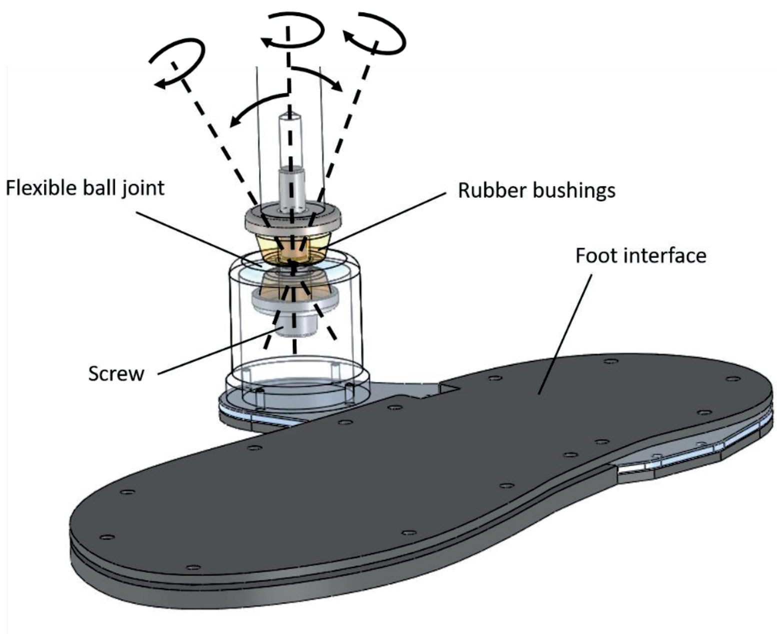

Figure 4-24 Illustration of the passive ankle joint, realized with rubber bushings

4.2.4 Design of the Hip Abduction/Adduction Actuation

Hip abduction/adduction is less frequently studied than hip, knee and ankle flexions/(extension). The kinematics and kinetics can be found in the literature for the walking activity; however, the same data for activities such as stairs climbing were not found. The RMS and peak torques during walking are reported to be slightly smaller than the same torques engaged in the hip flexion/extension. It is assumed that the amplitude of peak torques required in a stable gait are significantly less than the torques generated to recover from an unstable posture. Also, the efforts generated by a person without muscular weakness can be diminished by the use of the muscle about the torso, while people with neuromuscular diseases need to compensate for a general weakness through the residual muscle strength. Based on the curves reported in section 4.1.5, the power generated by the abductors during level walking is nominally about 10 W, with peaks about 25W. The range of motion about the hip abduction/adduction is quite small. Angles measured in a group of healthy persons during level walking range from an adduction of 5.4° to an abduction of 7.5°, hence, a total range of motion of 12.9° [131].

The constraints on the actuation and transmission unit of the hip abduction/adduction are: first, the mechanism should preferably be located at the back of the user, with the center of rotation aligned as much as possible with the natural hip joint. Second, it should be able to reach up to 100 Nm of peak torque and have a range of motion of ±20°. It should also be able to reach high dynamics and have a good backdrivability. Eventually, the solution should be lightweight and not greater than 60 mm of posterior depth so that the user can still sit on conventional chairs.

The design of the actuation and transmission mechanism is presented in Figure 4-25. A high density power motor EC-4pole, 200 W (Maxon motor AG, Sachseln, Switzerland) with a planetary gearbox (1 stage, transmission ratio of 1:14) GP 32 HP (Maxon motor AG, Sachseln, Switzerland).

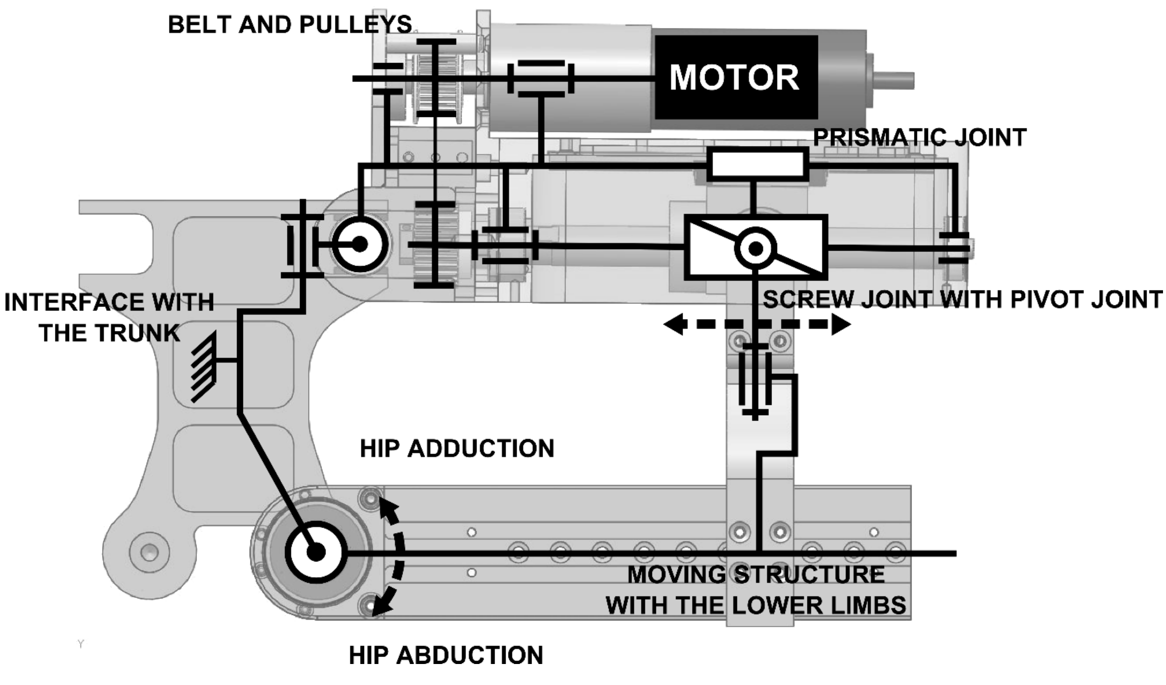

Figure 4-25 Illustration of the actuation and transmission unit of the hip abduction/adduction. © 2017, IEEE

The gearbox is coupled to a belt and pulley in order to transmit the effort on a ballscrew PSS 12 05 (FA compact series, NSK Ltd, Japan) with a pitch of 5 mm. The addition of a gearbox ahead of the screw reduces the effect of the inertia of the screw. The gearbox, however, adds some friction and reduces the backdrivability of the unit. Eventually, energy is transformed from by the translational motion of the nut back to a rotation via a four-bar linkage mechanism (see Figure 4-25). The system has a non-constant transmission ratio due to its geometry. However, over the predefined range of motion, the transmission ratio can be approximated by a constant with a mean deviation of 0.3°. The total transmission ratio is equal to 1:1’613.

4.2.5 Overview of the Complete Exoskeleton

4.2.5.1 Summary of the joint performances

The summary of the theoretical capacities of the three different joints of the exoskeleton are summarized in Table 4-5. Note that these values are the theoretical values obtained from the ideal case where the maximum efficiency possible is 100%.

Table 4-5 Theoretical capacities of the actuation units

Joint	Nominal Torque		Peak Torque	Nominal Velocity / Peak Velocity	
	At motor [mNm]	At joint [Nm]	At joint [Nm]	At motor [RPM]	At joint [°/s]
Hip abduction/abduction	92.9	150	-	16'500 / 25’000	49 / 60
Hip flexion/extension (motor B)	207	43	100	5’000 / 8’000	150 / 231
Knee flexion/extension (motor A)	207	43	100	5’000 / 8’000	150 / 231

4.2.5.2 Full exoskeleton design

The complete exoskeleton is illustrated in Figure 4-26. It includes six actuated degrees of freedom and three passive degrees of freedom. Physical interfaces are located at the feet, the shanks, the thighs (optional) and the trunk. Two sets of Lithium-Polymer batteries are in the back of the device with a total capacity of 768Wh and a total weight of 4.4 kg. The electronics are fully embedded in the device and can communicate with external computers or Android systems, as will be described in the next section. The structure of the exoskeleton is mostly made out of aluminium alloys because of of their low density properties, good mechanical properties, and ease of machining. The total weight of the device, including batteries, is about 22.5 kg, with two-thirds of the weight (about 15 kg) located around the lower back of the user.

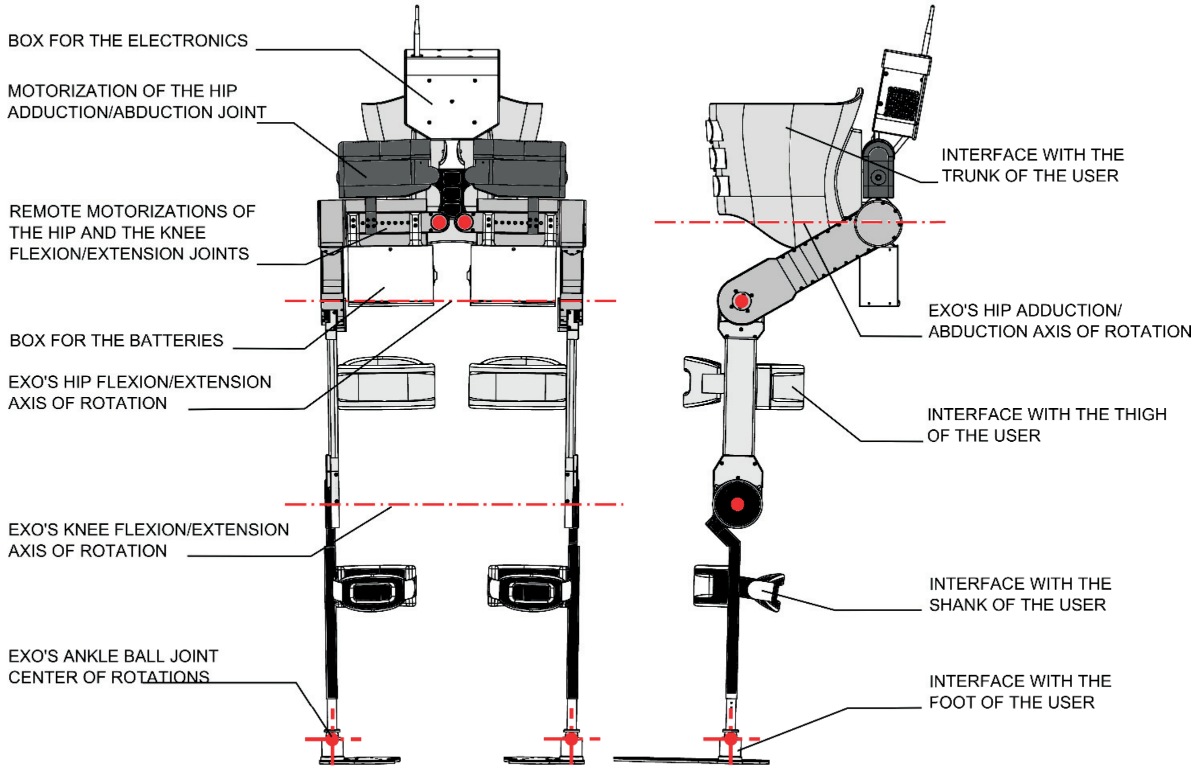

Figure 4-26 Illustration of the complete AUTONOMYO exoskeleton design. Copyright © 2017, IEEE

4.2.5.1 Electronics and Sensors

The electronics include one main board with an embedded computer and three motor drivers that can control two motors each.

Embedded computer

The embedded computer is based on a Beagle Bone Black computer (BeagleBoardd.org Foundation, Oakland USA), with a soft real-time Debian Linux operating system. The board is furtherly equipped with an IMU (inertial measurement unit) sensor that detects the orientation in space, and an Wi-Fi adapter for wireless communiation with external devices. The role of the main board is to manage the high level controller; this includes activities such as defining the position or torque trajectories and sending them to the motor boards, collecting the data from the sensors, and recording logs of the experiment onto an SD card. The main board is also programmed with a set of failure detection and can cut power to the motor drivers in case of emergency.

Motor drivers

The motor drivers are custom-designed printed circuit boards developed at the Laboratory of Robotic Systems (EPFL, Lausanne, Switzerland). Each unit can control up to two electric motors, brushed and brushless, and collect data from position sensors such as potentiometers or encoders. The motor drivers are also able to cut the power transmission to the motor in case failure is detected.

4.2.5.2 Physical interfaces and adjustment of the dimensions

Physical interfaces are a challenging aspect of exoskeleton design as their role is to transmit energy and motion to the body in a comfortable manner. These interfaces can either be tailor-made to best fit the user, or, adjustable. An adjustable design significantly augments design complexity, but allows quick interchange between users. The physical interfaces of each segment are described in the following sections:

Trunk interface

The trunk interface is composed of a rigid carbon fiber plate and a polymeric brace with two straps and buckles to support supporting high loading. The rigid plate of carbon fiber is molded from the part of the exoskeleton to which it is fastened while in use. This allows good mechanical coupling and the use of a single screw, which makes it easy to assemble/disassemble to or from the rest of the structure. Interfacing with the trunk is challenging since the trunk is a pluri-articulated segment. Thus, controlling the back in a predictive manner would result in constraining all motion from the pelvis to the neck. This would be very uncomfortable for the user.

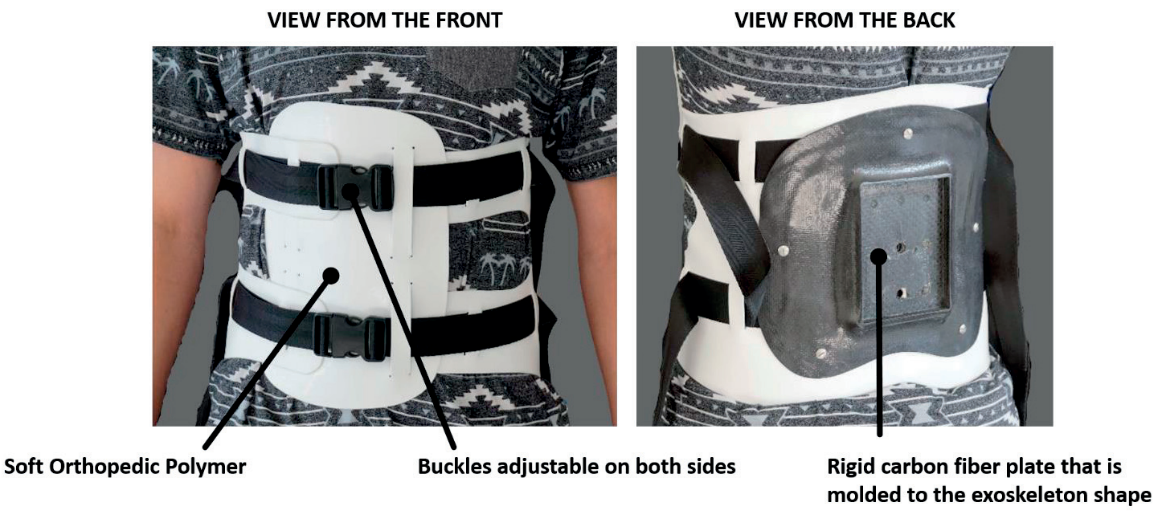

Figure 4-27 Pictures of the trunk interface from front and from behind

Thigh interface and segment adjustment

The necessity of a thigh interface for people with residual muscular capabilities is still under investigation. Tests of assisted walking have not demonstrated an absolute need for a thigh interface, but data need to be collected on patients' feedback and performance observations on other activities such as the sit-to-stand transition. The length of the segment going from the hip to the knee joint, however, does need to be adjusted in order to align the centers of rotation of the hips and knees of both the user and the exoskeleton.

As mentioned previously, the use of a remotely located actuator is challenging for the adjustment of the length of the segments as cable transmission design is dependent from the segment length. The optimal solutio would be a mechanical architecture that adjusts segment length without requiring a change in the cable length. A simple design is illustrated in Figure 4-28. In this mechanism, two pulleys, i.e. 702 and 803, are introduced, so that the cable makes an "S" shape. Pulleys 701 and 702 are mounted on the same structure and pulley 801, 802 and 803 on another one. When these two structures (the hip and the knee joints) are moved closer or away, the length of the three segments of the cable 900, 901 and 902 are modified. However, the sum of the length of the three segments is kept unchanged, because segment 900 and 901 move half the distance of that of segment 902. Once combined, the sum of the three segments is kept identical. The last pulley 802 pretenses the cable.

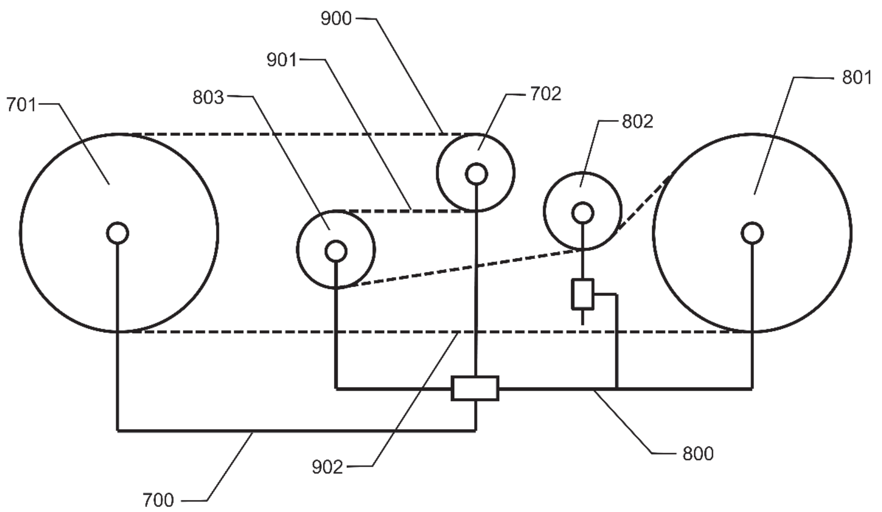

Figure 4-28 Schematic of an adjustable length mechanism for a cable transmission, where the length of the cable is independent from the distance between pulleys 701 and 801

This solution is, however, only applicable to a single-cable mechanism, while the segment of the exoskeleton includes preferably two cables to allow anchoring on both pulleys. A solution would then be to adjust the two cables, instead of just one; each cable follows the previously discussed path through the two additional pulleys, essentially combining segments 900 and 901. In this case, however, the displacement of the pulleys is too large by a factor of two. The chosen solution design keeps pulley 803 at an equal distance from both pulleys 701 and 801. Concretely, a double rack and pinion mechanism is used. Each rack is mounted on a separate structure and in opposition, so that the pinion can be placed in between them. The pulley 803 is freely mounted on the same axis as the pinion, so that when the structures are moved of a certain distance close or away from each other, the pulley moves only half the given distance. The final design is adjustable for inter hip-knee length from 352 mm to 500 mm as illustrated in Figure 4-29. To modify the dimension of the segment, 3 steps have to be performed: first, the tension pulley must be unscrewed until the cable is loose. Second, the two screws locking the two frames of the segment together must be unscrewed in order until dimensions can be adjusted; the frames should then be locked again. The tension pully must then be re-fastened until the cable is tight.

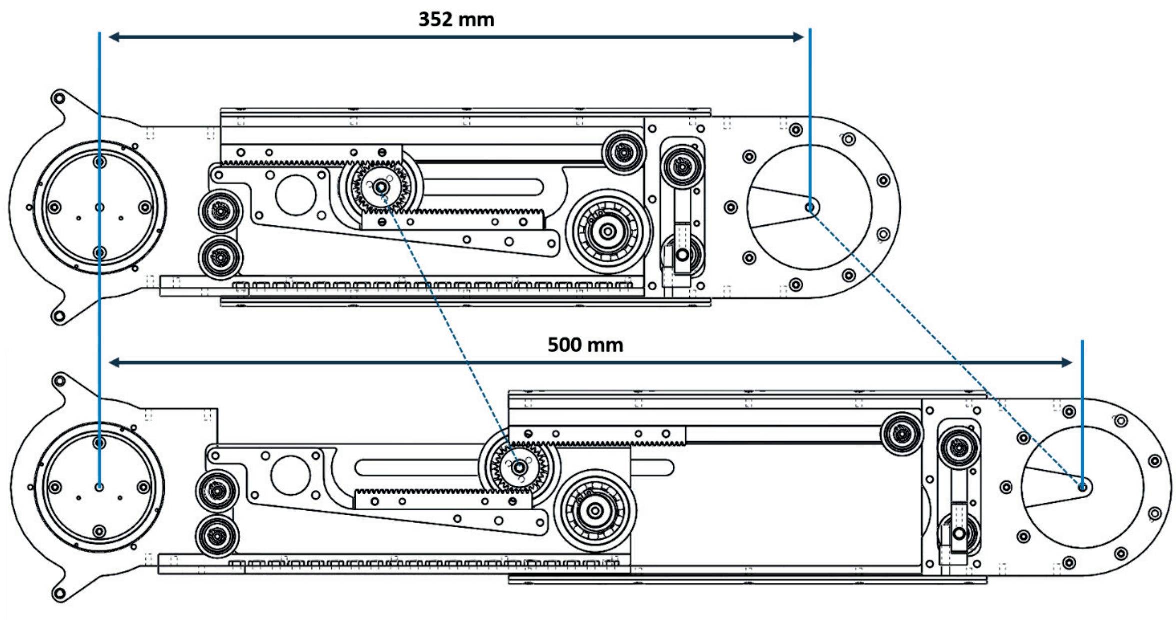

Figure 4-29 Design of the thigh segment with a rack and pinion mechanism to keep the same cable length while adjusting the segment length

Shank interface and segment adjustment

The shank interface is composed of a curved rigid carbon fiber structure padded with foam mounts on the front of the lower leg closely under the knee (see Figure 4-30). The part is fastened to other leg with a large band and a hook-and-loop locking system. The interface is mounted on the exoskeleton and held by a tube structure and locked by two manual fastening clamps (see Figure 4-30). When these clamps are opened, the interface can rotate freely and move vertically. This facilitates the donning and doffing of the device, as the interface can rotated 90° to let the user in, and rotate back to a close when the user is in position. The interface position can also be adjusted width-wise through an adjustable screw system. The tibia, or shank, segment of the exoskeleton is composed of two telescopic tubes that are locked by a double clamping fastener. This mechanism is very robust and allows rapid and precise adjustment of the segment length.

Foot interface

The foot interface is composed of a flexible sole to allow physiological rollover while the back part is rigid to allow a good coupling with the exoskeleton. Two straps, one at the back of the foot and one in the middle fasten the interface to the user. A ratchet system is used for all the straps; it is very convenient as it allows a secure fit without excessive effort.

Complete exoskeleton

The complete exoskeleton with all the elements discussed is shown in Figure 4-31. The trunk interface shown in the picture is an initial prototype, it has the advantage of being more rigid than the second versionbut is poorly adjustable. The segment along the femur in the picture is also the first version prototype that is not adjustable in length. The latest version of the exoskeleton can be seen in Chapter 5.

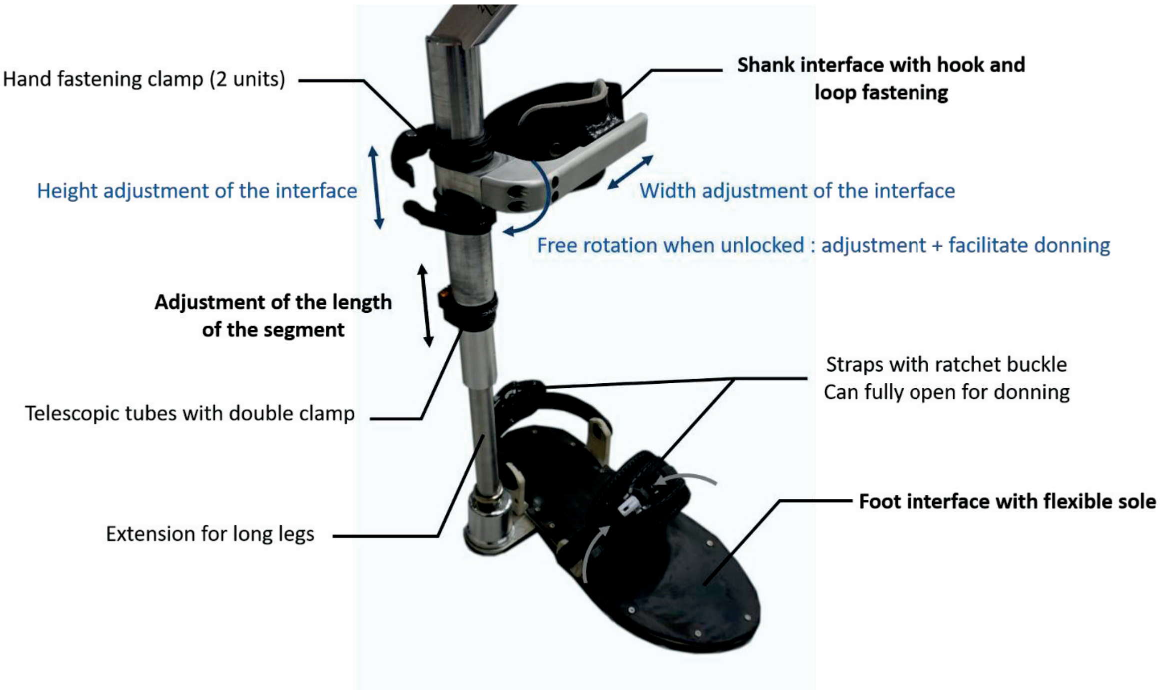

Figure 4-30 Shank and foot interface of the exoskeleton with adjustments

Figure 4-31 Picture of the AUTONOMYO exoskeleton being worn by a healthy user

4.3 Evaluation and Validation of the Performances

The exoskeleton is evaluated in two ways. The first evaluation characterizes the actuation units. This identification builds a model of the torque, which maps the torque applied at the joint with the current in the motor. It also investigates the real performances that motorization can achieve. The second evaluation focuses on assessing and comparing the performances given with different coupling configurations (e.g. positive and negative).

4.3.1 Actuators and transmission

The characterization of actuation and transmission is performed on two joints that each have a unique type of actuation unit: the hip flexion/extension joint is investigated and the hip abduction/adduction. For each joint, a data sampling is recorded. It includes the measurement of:

- the joint position and its derivatives (velocity and acceleration), as measured from the encoders located on the shaft of the motors.
- the current that passes through the motors, as collected from the motor drives. This current is proportional to the torque exerted by the motors.
- the external torque applied to the joint, as measured by an additional force sensor in the case of the isolated hip flexion/extension.

The force sensor used is a Strain Gauge – Micro Load Cell CZL635 (Phidgets Inc, Canada) with a range of 500N. The external force is applied by hand to the sensor. The data are generated possibly through three different methods:

- open loop current control, with a constant current trajectory and a modulated external force applied by the investigator
- current mode, but driven by sinusoidal current trajectories with variable frequencies and amplitudes
- closed loop position control, where the target is set as a cyclic trajectory that is modulated in frequency and amplitude.

After the acquisition of samples, a relationship must be defined between the current command at the motor and the kinetics observed at the joint. This is done through construction of a torque model, using a combination of linear regression andhand tuning. The linear regression approach is based on a linear parametric model with least square minimization of the error. The mathematical model of the regression is presented in Equation 4-4. An iterative approach is applied, where the number of terms in the model are added one by one and are selected based on an analysis of variance (ANOVA) that evaluates if the new model is significantly different from the previous iteration.

$$Y = X\beta + \varepsilon \quad \text{(a)}$$

$$Y = [\tau_{joint}(1), \tau_{joint}(2), \dots\ \tau_{joint}(n)]^T \quad \text{(b)}$$

$$\beta = [\beta_0, \beta_1, \dots\ \beta_m]^T \quad \text{(c)}$$

$$X = \begin{bmatrix} x_1(1) & x_2(1) & \cdots & x_m(1) \\ x_1(2) & & \ddots & \vdots \\ \vdots & & & \\ x_1(n) & & \cdots & x_m(n) \end{bmatrix} \quad \text{(d)}$$

$$\min(\epsilon): \quad \hat{\beta} = (X^T X)^{-1} X^T Y \quad \text{(e)}$$

Equation 4-4 Parametric linear regression method (a) definition of the problem, (b)-(d) construction of the different matrices and vectors, and (e) resolution of the problem with least square theorem. "*Y*" is the vector of external torques applied at the joint "τ_{joint}" at different time, "*X*" is the matrix of variables or function of variables that are recorded (variables of the model(s) as presented above, such as joint angular position, velocity, acceleration, external torque or power) at corresponding time, "β" is the vector of coefficients, "ε" is the vector of errors, and the symbol '^' refers to an estimation of the value.

4.3.1.1 Characterization of the hip flexion/extension actuation

The characterization of the hip flexion/extension gives best results with samples acquired based on method 1, where external torques are exerted on the device by hand while different constant currents are sent to the motor. Note that the actuation unit evaluated here is composed of a high torque density motor with a nominal torque of 207 mNm, which is coupled to a planetary gearhead of 3 stages with a transmission ratio of 1:74. A cable and pulley mechanism with a transmission ratio of 5:14 transmits the torque to the joint. The samples are recorded as the exoskeleton is fastened at the trunk level to a rigid structure while the legs can freely move in the air.

It was expected that the torque model would be most affected by gravity and inertia of the leg structure, the inertia of the motor, and the frictions of the gearbox and efficiency of the motor and of the cable transmission. Friction is usually the hardest effect to identify, as dry friction can present hysteresis, and both dry and viscous frictions can be dependent upon the instantaneous power and non-homogeneity in the mechanical parts. After the process of model refinement and different trials with friction models, a simple model expresses best the torques measured from the force sensor. This model is shown in Equation 4-5 (a). The goodness of fit is presented in a sample in Figure 4-32 where a constant torque from the motor is applied and the external torque is modulated as shown in the graphic.

The friction of the mechanism is identified as being mostly proportional to the torque from the motor and is expressed as a coefficient of efficiency. The efficiency largely depends on the direction of the power, because it is always opposed to the direction of the motion. The actuation system is generative when it produces greater torques than the load (including gravity and inertia), and dissipative when the external loads are greater. In dissipation, the actuation acts as a braking system, and the friction efforts working constructively with the those of the motor.

$$\tau_{joint} = -lmg \cdot \sin(\alpha) - I \cdot \ddot{\alpha} + \eta_{\pm} \cdot i \cdot \tau_{motor} \quad \text{(a)}$$

$$lmg = 11.5\ [Nm]$$
$$I = 1.43\ [Kg \cdot m^2]$$
$$\eta_{\pm} = \begin{cases} \eta_{+} = 0.55, if\ Power = (\tau_{motor} \cdot \dot{\alpha}) \geq 0 \\ \eta_{-} = 1.3, if\ Power = (\tau_{motor} \cdot \dot{\alpha}) < 0 \end{cases} \quad \text{(b)}$$

Equation 4-5 (a) Torque model of the hip flexion/extension actuation and (b), values of the identified parameters. "τ_{joint}" is the output torque at the joint measured by the force sensor, "τ_{motor}" is the input torque at the motor, "*i*" is the transmission ratio, "α" is the angular position at the joint and the dot and double dot symbols on top of a variable denote the first and second derivatives over time (joint velocity and acceleration respectively). "*lmg*", "*I*" and "η" are coefficients of the gravitational term, inertial term and torque ratio (efficiency of the transmission) respectively.

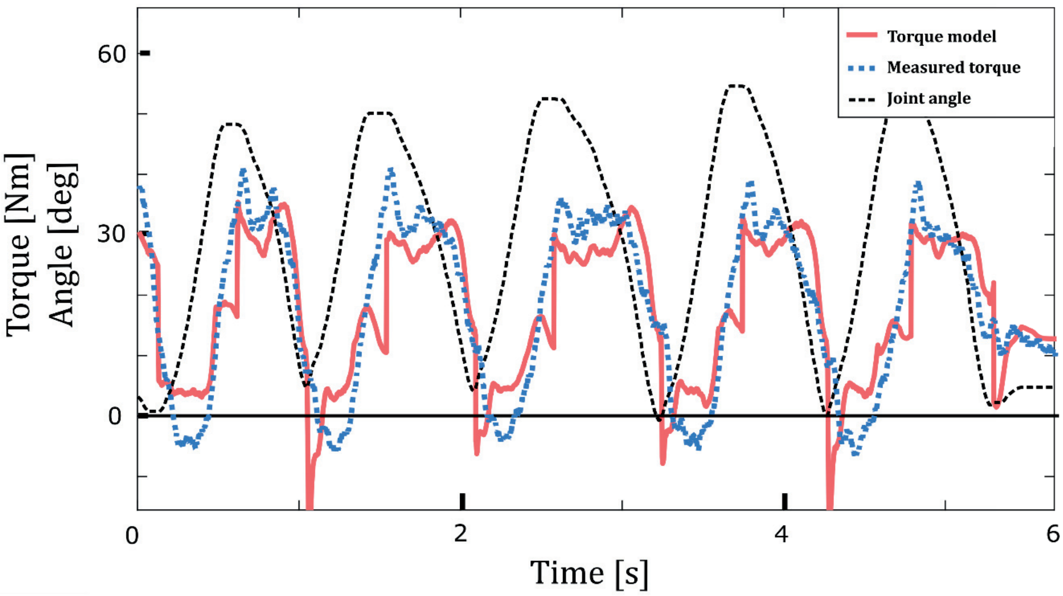

Figure 4-32 Sample of the identified model versus the measured torque at the hip flexion/extension joint.

The torque model and coefficients identified in Equation 4-5 (b) highlight the main components of the actuation mechanism. First, the gearbox introduces large friction with a high gap between the generative or dissipative power mode. This gap makes the system difficult to control and increases the risk of instability as the transmitted power switches from generative to dissipative. The poor efficiency in generative mode of the actuation means the motorization must be adjustable for higher power capabilities. Conversely, the large dissipative capabilities of the system can be seen as a benefit and a safety feature for activities such as sitting down from a standing position. There is, however, a large drawback from that friction on coupled actuation such as the one presented for the cable transmission through the hip and the knee. When the motors work in opposition, as it would often be the case at the hip joint with a coupled actuation, the leading motor needs to overcome three times the friction. For example, if motor A is producing an active torque of 10 Nm at the knee, it is producing at the same time a resistive torque of 23.6 Nm at the hip, so that motor B needs to generate a torque of 43 Nm for the sole purpose of counteracting motor A. Without friction, motor B would only need to generate 10 Nm. This is a serious drawback that must be considered in the design of coupled mechanisms.

The gravity and inertia follows both the approximate effect of a mass of 1 kg located at a distance of 1 m from the joint. The inertia of the actuation (motor + reductor) has a value of about $0.23 kgm^2$. Thus, it represents about 16% of the inertia perceived by the actuator. This contribution is quite low and means that larger motors with greater inertia could be used without significantly affecting performance.

In conclusion, the sagittal configuration has very good inertial properties with room to increase the motor size and capabilities. However, the efficiency of the gearbox is poor and has many drawbacks for the application, including that it is highly incompatible with a coupled configuration unless the motors are always generating a combined effort.

4.3.1.2 Characterization of the hip abduction/adduction actuation

The actuation unit of the hip abduction/adduction includes a high torque density with low inertia motor, a gearbox with a transmission ratio of 1:14, a belt and pulley that transfer the power to another axis, a ballscrew with a pitch of 5mm and a four-bar linkage to transmit the translational work of the screw to the final hip rotation. The total transmission ratio reaches a value of 1:1’613, while the motor has a nominal torque capacity of 92.9 mNm. The characterization is made based on samples of gait trajectories at frequencies ranging from 0.2 Hz to 1 Hz. This method was favored since the actuation system has poor backdrivability and is able to reach high torques compare to those generated through hand-operation. For the sampling acquisition, the exoskeleton is fastened on a structure at the trunk level, while the legs are free from constraints with the ground. The identified model is presented in Equation 4-6.

$$\tau_{\mathrm{joint}} = i \cdot \tau_{\mathrm{motor}} - lmg \cdot \cos(\alpha) - I \cdot \ddot{\alpha} - \lambda \cdot \dot{\alpha} - sf \qquad \text{(a)}$$

$$\begin{gathered} lmg = 55\ [Nm] \\ I = 15\ [Kg \cdot m^2] \\ \lambda = 6\ [Nm \cdot s/deg] \\ sf = \begin{cases} +20, if\ (\ddot{\alpha} \cdot \dot{\alpha}) \geq 0\ and\ if\ (0 > \dot{\alpha} > 3) \\ +20, if\ (\ddot{\alpha} \cdot \dot{\alpha}) < 0\ and\ if\ (-3 > \dot{\alpha} > 0) \\ -20, if\ (\ddot{\alpha} \cdot \dot{\alpha}) < 0\ and\ if\ (0 > \dot{\alpha} > 3) \\ -20, if\ (\ddot{\alpha} \cdot \dot{\alpha}) \geq 0\ and\ if\ (-3 > \dot{\alpha} > 0) \end{cases} \end{gathered} \qquad \text{(b)}$$

Equation 4-6 (a) Torque model of the hip abduction/adduction actuation and (b), values of the identified parameters. “τ_{joint}” is the output torque at the joint, “τ_{motor}” is the input torque at the motor, “*i*” is the transmission ratio, “α” is the angular position at the joint and the dot and double dot symbols on top of a variable denote the first and second derivatives over time (joint velocity and acceleration respectively). “*lmg*”, “*I*” and “λ” are coefficients of the gravitational term, inertial term and dry dynamic friction respectively. “*sf*” represents the static friction that appears at low velocity and depends if the system is accelerating or decelerating.

The results of the model are shown in Figure 4-33 with the torques reported at the level of the motor, while the angle position is at the joint. The trajectory taken as target in the graph is a physiological gait trajectory with a frequency of 0.33 Hz. The dominant terms are the dynamic friction that can be caused by the circulation of the balls between the nut and the screw. At this frequency, peak torques reach up half of the nominal torque. The second component is the effect of the gravity, and possibly some friction proportional to the torque that has not been identified. A constant torque of about 1/3 of the nominal torque (55 Nm at the joint level) is measured, while the load at the joint due to the gravity is only equal to 10 Nm. At this frequency, peak torques related to the inertia are measured at 20 Nm (reported to the joint), where half of the inertia is due to the motor and the other is due to the exoskeleton structure and other elements. The static friction is projected to be a constant 20 Nm at the joint level.

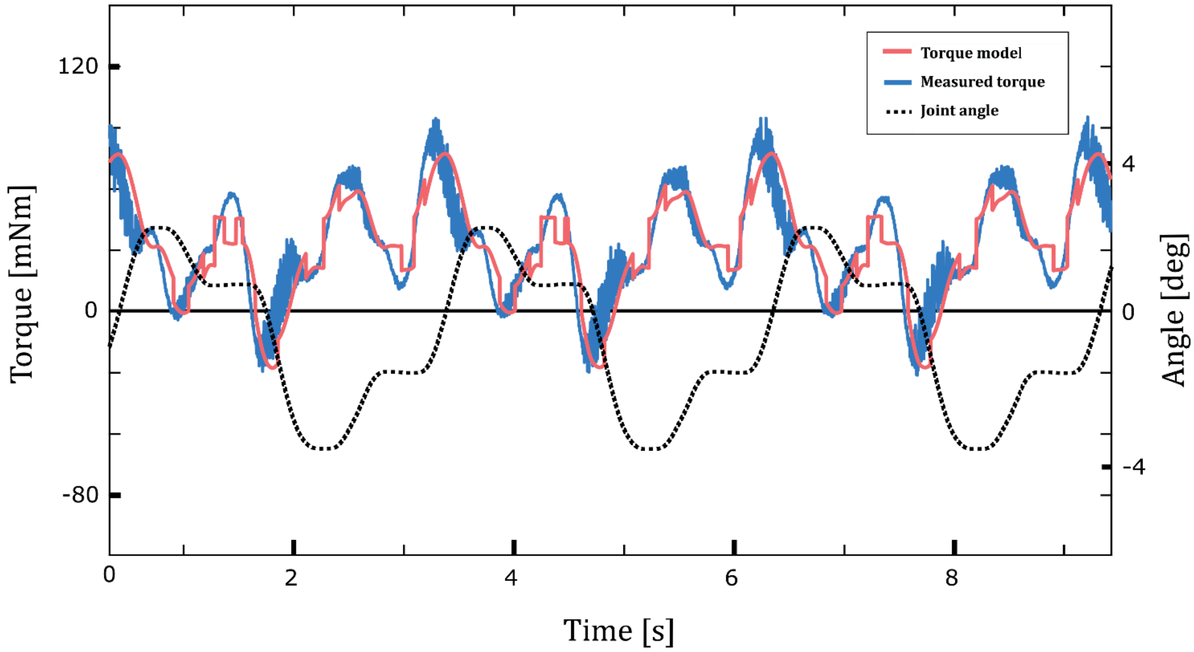

Figure 4-33 Sample of the identified torque model versus the measured torque (converted from current) at the hip abduction/adduction joint

In conclusion, the actuation unit of the hip abduction/adduction is adapted for position control with gait trajectories at frequencies going up to 1 Hz. It can handle high dynamics while also provided substantial torque to assist the user. The drawback of this design with a large transmission ratio, however, is that it has poor backdrivability, i.e. about 20 Nm of static friction and high resistance to velocity. The transmission ratio could possibly be reduced of a factor of two to benefit from better backdrivability and, potentially, without significantly diminishing the performances, as the dynamic friction would diminish by the same factor as that of the transmission ratio. The need of the user in terms of peak torques required must be clarified through more investigation.

4.3.2 Performances of the Different Configurations of Coupling

In the following of section 4.2.3 where a theoretical analysis of the performances of the different coupling configurations is addressed, the present section evaluates the performances of both positive and negative coupling directly on the exoskeleton. As previously discussed, one configuration (positive coupling) allows simultaneous and rapid motion of hip and knee flexion, but can exert only limited forces in that direction. Hence, positive coupling is best suited for swing phases. In opposition, the negative coupling configuration exerts large forces in a flexion-to-extension direction; however, motions of double flexion require motors to be able to deliver large velocities.

In order to perform the tests, each leg of the exoskeleton is assembled with a different configuration. The exoskeleton is fastened at the trunk level, while the legs are let free to move. Physiological gait trajectories are programmed and run on all the joints at the same time during the tests. The tests are performed with different walking frequencies from 0.33 Hz to 1 Hz so that the RMS current required to follow the trajectories and the velocity limitations can be recorded. Note that the actuation of the hip and knee flexions is limited by the maximal tension of the drivers to their nominal velocity of 5000 RPM or 175 °/s at the joints. The measured trajectories from the different joints for three walking frequencies are shown in Figure 4-34. The corresponding RMS currents are reported in Table 4-6.

Table 4-6 RMS current for the different joints during trajectory following at different gait frequencies.

	RMS current in <u>% of nominal capacity of the motor</u>					
	Negative coupling configuration			**Positive coupling configuration**		
Frequency	***0.33 Hz***	***0.5 Hz***	***1 Hz***	***0.33 Hz***	***0.5 Hz***	***1 Hz***
Hip abduction/adduction	41,6	51,9	88,3	39,7	51,9	88,0
Hip flexion/extension	15,1	36,0	72,4	11,7	14,2	25,5
Knee flexion/extension	11,3	-	-	9,6	17,6	-

All the actuation units are able to follow the gait trajectories at a frequency of 0.33 Hz, which represent a very slow velocity, see Figure 4-34. The trajectories at 0.5 Hz, which correspond to a moderately slow walking velocity, are achieved by all the joints but the knee flexion/extension in negative coupling, as the motor needs a higher tension to perform the targeted velocities. At 1 Hz, all the joints are at their limits, and the knee in positive coupling cannot follow the desired trajectory. The RMS current increases nonlinearly with the frequency. In positive coupling, only one quarter of the nominal torques are consumed for the trajectory tracking at the hip and the knee flexions. In negative coupling, a significant current is consumed for the hip flexion at 1 Hz (72.4 %), but the current consumed at lower frequencies and at the knee are acceptable. For the hip abduction, the amount of current required to follow the trajectories is significant but the remaining torque available is still large enough to provide an important support during gait.

These results support the observations made above after the characterization of the different actuation units. The velocity limitations of the actuation unit can be first improved by using motor drives with higher tension capacities or by using motors with a lower nominal voltage. However, even with higher velocity margins, the 1 Hz frequency will be hard to achieve in the configuration with negative coupling. Conversely, the positive coupling configuration seems well adapted to the walking activity as it can almost follow the trajectories at 1 Hz and can still dedicate 75% of its nominal torque to provide assistance to the user.

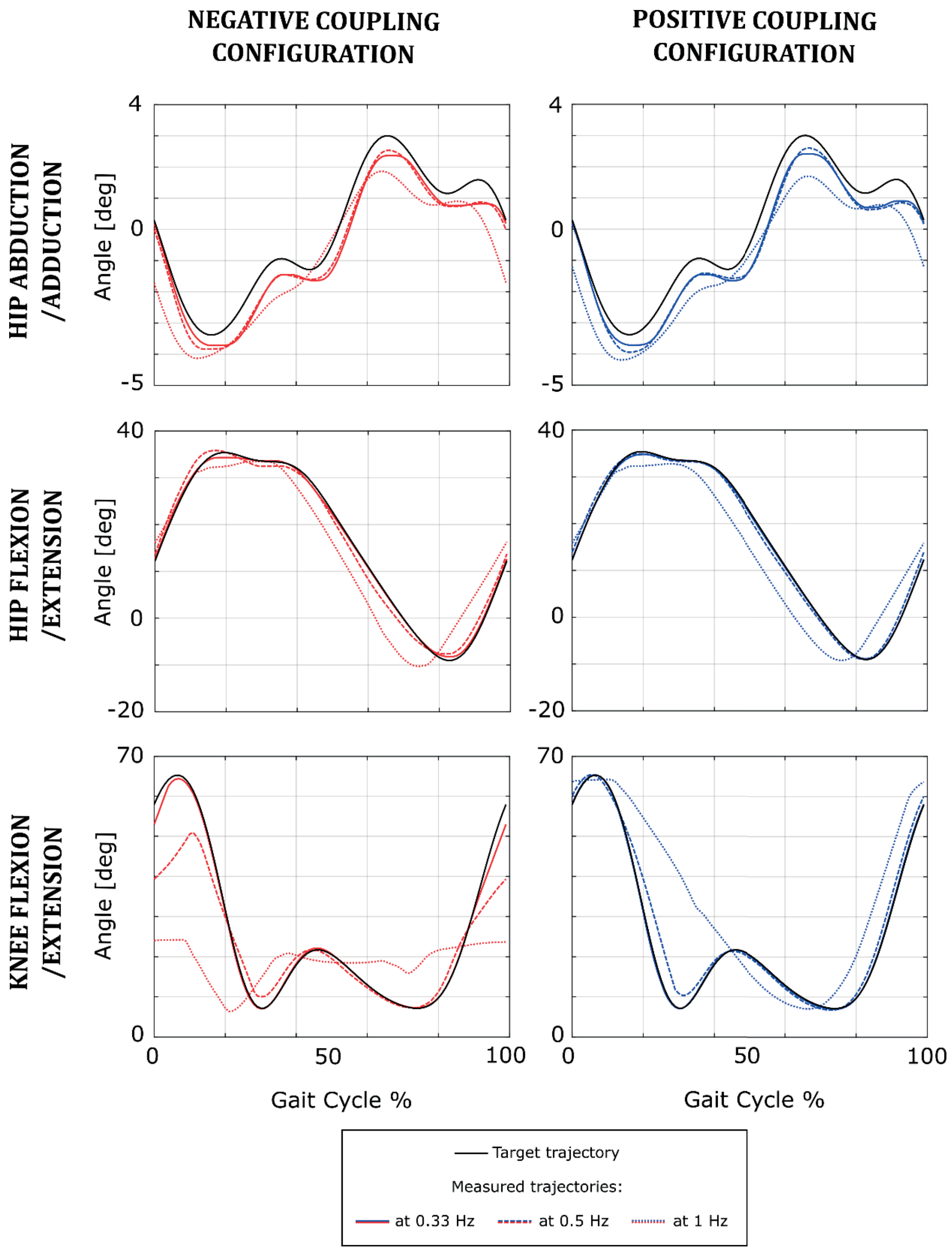

Figure 4-34 Measured trajectories at the different joints for walking frequencies of 0.33 Hz, 0.5 Hz and 1 Hz

4.4 Conclusion

Exoskeletons have been investigated mostly in terms of their use to people suffering from spinal cord injury. Such devices could in a similar manner compensate for the muscle weakness in people with neuromuscular diseases. Two key aspects need to be adapted in order to fit with such people: first, whereas exoskeletons SCI people follow a trajectory without intervention from the user, the human robot interaction must be collaborative so that both the user and the exoskeleton contribute to the motion. Second, SCI people use crutches or rollator to balance and also to perform some activities, including weight transition during level walking. Thus, due to the weak upper limbs of people with NMD, the use of crutches is compromised and therefore higher joint velocities and a short swing phase must be achievable.

A simulation of the leg segment with only the hip, knee and ankle flexion actuation was implemented to evaluate the dynamical performances and challenges. For each joint, a flat brushless motor with a harmonic drive gear located directly on the joints is simulated. Results show that for a nominal torque capacity of 50 Nm, peak torques due to the inertia go up to 125 Nm for both the hip and the knee, while both actuators follow a typical gait pattern at 0.84 Hz. These peak torques are due to both the inertia of the motor at the knee, and the added mass at the ankle of the actuator. This simulation highlights that the inertial effects induced by not only the inertia of the rotor of the motor but also the mass of the actuation unit must be optimized while designing.

An analysis of the contribution of each of the seven joint of the legs reveals that the most important joints are the hip abduction/adduction and the hip and knee flexion/extension. It is still an open question for future resaerch as to whether the ankle contribution can be replaced by a passive joint. It has been reported, even in a stair-climbing study, that wearing a rigid ankle foot orthosis reduces ambulation velocity.

The next step in the design was to optimize and reduce the effect of the inertia due to the actuation units. This was done by first selecting brushless motor technology, featuring a small diameter and high torque density with a planetary gearbox. Then an architecture with the motors remotely located from the joints and run with cable-driven transmission is proposed. This reduces the inertia induced by the mass of the actuators and keeps the flat segments aligned along the legs.

As a result of remotely locating the actuators from the joints, the transmission of the knee passes through the hip joint. This couples the two joints; two coupling configurations are possible, depending if the cables are crossed or not between the pulleys. The study of the coupling shows that one configuration cumulates the extension torques, which is beneficial during the stance phases of walking, stairs climbing or STS transitioning. However, this configuration also cumulates the flexion velocities required by the motors, such as those present in swing phase. The other configuration has an inverse performance; it allows rapid swing motions, but is limited in extension torque. The evaluation of both solutions on a test bench showed that one configuration can almost follow the walking trajectories at 1 Hz with a RMS current of one quarter of the nominal current while the other configuration could almost follow the trajectories at 2 Hz with the knee while consuming about 72 % of the nominal torque at 1 Hz. In conclusion, both configurations are very good in one application but underperform in the other. A compromise is to uncouple the two joints, or use a clutch to change of configuration as required.

The hip abduction/adduction actuation has been designed to deliver high peak torques. A motor with high power density and a small diameter was selected in combination with a small gearbox, a ballscrew and a four-bar linkage mechanism. The final transmission ratio is 1:1613 with a theoretical nominal torque of 150 Nm at the joint. The hip and knee flexions/extensions are performed with a three-stage gearbox, followed by a cable and pulley transmission. The total transmission ratio is equal to 1:207. A characterization of both type of actuation and transmission units was evaluated. The main contributions observed are: a friction proportional to the motor torque for the gearbox about the hip and knee flexion, which can be seen as an efficiency applied to the torque. For the actuation unit of the abduction, the most important factors of performance were determined to be the resistance to the velocity from the ballscrew and the dry static friction, which measured to approximately 20 Nm. Gait trajectory tests on the hip abduction/adduction show that the system could follow frequencies up to 1 Hz; however, about 88% of the nominal current is spent to reach this goal. The deep analysis of both actuation performances allow some room for a possible optimization of the actuation system.

Chapter 5 Control Strategies for People with Neuromuscular Diseases

This research investigates solutions for assisted ambulation targeting people with chronic muscle weaknesses. Previous work has been done to make people with complete spinal cord injury walk again, while other works have developed industrial solutions to enable healthy persons to excel in performing extremely physically intensive tasks. However, though one may not expect it, designing a device to assist a person who has a residual ability to walk is no easier than doing so for a person who has almost no ability to walk. In the case of a person with complete SCI wearing a LEE, the control of the body is split in two. The upper body and crutches (if any) provide the balance and are managed by the user, while the motion of the lower body is entirely executed by the exoskeleton upon request of the user. In the case of a healthy operator, the user has the capacity to modulate the forces applied to the environment, this is a reliable signal that can be used to control the exoskeleton. Another approach is to use a model of the load and compensate it through the exoskeleton with a sensor that can identify when the load is carried or not. Eventually, when the exoskeleton is used to assist a free motion, a common strategy is to implement negative damping [158], which applies a torque proportional to the velocity measured at the joint, and in the direction of the motion.

Developing a control strategy for a user with muscle weakness has two key aspects that must be addressed. First, it is often difficult for these users to move throughout the whole range of motion, not because of joint mechanical limitations but rather because of the force needed to lift the leg against the gravity, for example. Second, once an assistive procedure is launched, a poorly designed control strategy will make it difficult for the user to reverse the motion or provide a perceptible motion that could be detected as a voluntary action. In conclusion, strategies that can be used for healthy operators are not suitable for people with neuromuscular diseases.

People with NMD have also two main needs. First, mild exercise is recommended as it prevents muscles from wasting too rapidly; it also maintains the respiratory condition [7], [159]. Second, as presented in Chapter 2, the upper limbs of people with NMD are usually weakened. This means that the use of crutches is not recommended. Other auxiliary types of support can be considered, typically those allowing a fully vertical posture of the back. For these two reasons mainly, the control strategies for people with SCI are not suitable for people with NMD.

There are several specifications regarding an assistive strategy for people with NMD, or more generally, for people with debilitating muscle weakness:

1. The user should be physically involved in the ambulation process.

2. The amount of assistance should be tuanble to match the capacity of each user's muscle so that all muscles can be engaged without becoming overloaded.
3. The controller should be triggered by user intention, as naturally and as smoothly as possible.
4. The gait parameters should be regulated by user feedback metrics such as step length, step rate and walking velocity.
5. The initiation and termination of ambulation should be robust and intuitive to avoid accidents.
6. The controller should allow switching between activities (walking, stairs climbing or rising from a chair) in a very robust manner to avoid accidents.

In the following, a preliminary approach is implemented and tested. The control strategy is based on finite-state active impedance where the sensing is limited to the kinematics of the joints. The method and results presented in this chapter have been published in two different documents. First one is part of the *IEEE* International Conference on Biomedical Robotics and Biomechatronics, Enschede (NL), 2018 with the following authors: Amalric Ortlieb, Romain Baud, Tommaso Tracchia, Benoît Denkinger, Quentin Herzig, Hannes Bleuler and Mohamed Bouri, and under the title "An Active Impedance Controller to Assist Gait in People with Neuromuscular Diseases: Implementation to the Hip Joint of the AUTONOMYO Exoskeleton". Second one is part of Springer, "Wearable Robotics: Challenges and Trends, Proceedings of the 4th International Symposium on Wearable Robotics", from the conference WeRob, Pisa (IT), 2018, with the following authors: Amalric Ortlieb, Peter Lichard, Florin Dzeladini, Romain Baud, Hannes Bleuler, Auke Ijspeert and Mohamed Bouri, under the title "Investigation on Variable Impedance Control for Modulating Assistance in Walking Strategies with the AUTONOMYO exoskeleton".

5.1 Finite-State Active Impedance Control - Method

Impedance control has been widely used with various actuation-transmission units for both upper and lower limbs. Impedance can be used as a soft trajectory corrector where a force is provided by the exoskeleton to attract the end-effector along a defined path such as described in [160] and [154]. Such controllers are trajectory and time dependent and thus quite constraining for the user [161]. Another type of impedance based controller is called triggered assistance and has been mostly implemented for upper limbs [161]. The architecture of control proposed in the current section has been largely investigated in the domain of prosthetics for the lower limb (transfemoral and transtibial prosthesis) and is referred to as "finite-state controller". Such controllers are defined by a periodic sequence of states with state-constant impedance that typically simulates a spring and damper behavior [162]–[167]. The transition from one state to another is usually based on different events such as heel strike or toe off, which are identified using force sensors located in the prosthesis. Other events, such as a muscle activity or joint angle or velocity, are also frequently used [162]–[169]. Several activities, such as level walking, stairs or slope ascending / descending and sit-to-stand transition, have been studied in these papers. A few studies using foot orthosis [170], [171] or complete lower limb exoskeletons (three using the Indego® device [172]–[174] and two with the Hybrid Assistive Limb (HAL) device [175], [176]) implemented similar "finite-state" controllers. However, most of these strategies are constructed primarily on events related to ground reaction forces (e.g. detection of heel strike, displacement of the center of pressure), and also on events related to the motion of the joints.

In the current thesis, an active variable impedance controller using a finite-state approach designed for people with residual ability to ambulate is addressed. In order to involve the user in the ambulation process, the wearer must generate a motion to initiate the stepping. This section addresses the process of designing that signal input processing. First, the control scheme is described and its triggering properties are evaluated. Then, the controller's impedance is tuned for two pilots, one healthy and one with neuromuscular disease (limb girdle muscular dystrophy). Gait kinematics and dynamics are collected in order to evaluate the collaboration of the controller and the pilots. Third, the influence of the impedance parameters on gait is investigated.

The exoskeleton AUTONOMYO, presented in 1.1, is the investigation platform. The device has been designed to assist people with neuromuscular or neurological impairments, where a tradeoff between low impedance of the actuation (high backdrivability) and high power is key. AUTONOMYO counts three actuated degrees of freedom (DoFs) per leg, i.e. two at the hip and knee flexion/extension plus one at the hip adduction/abduction. Actuators, electronics and batteries are remotely located in the back of the user in order to optimize compactness and inertia along the limbs. More details can be found in 1.1 and in [177], [178].

5.1.1 Motivations towards Impedance Control

Human joints are controlled and stabilized by a set of muscles, tendons and ligaments. Muscles are unilateral actuators that are built in antagonist pairs such as the hamstring and quadriceps groups that generate the flexion/extension motion of the knee. The muscle-tendon pair can be seen as series elastic actuators due to the highly stretchable properties of their tissues [179]. Assembling a set of antagonistic muscles then results in a variable stiffness actuator. This is useful for dynamic activities due to its energy management characteristics, i.e. optimal storage and release of energy. The compensation of muscle weakness through the application of supplementary torques about a joint needs to be compatible with the physiological motor architecture in order to assist ambulation.

The torques applied to the body during walking demonstrates clear elastic behaviors that are quite constant during long defined states. As shown on Figure 5-1 for the hip flexion/extension, gait dynamics and kinematics from D. Winter [129] and S. Ounpuu [130] can be represented graphically to highlight this spring-like behavior. The natural gait seems to be generated with constant joint stiffness during two main intervals, similar to the stance and swing phases, both lasting about 40% of the cycle. These two phases are then connected by two short states of high impedance, each lasting about 10% of the cycle duration and corresponding to the double support phases.

Our work begins with an initial postulate that adding a supplementary power based on a spring-like behavior would allow to optimally combine both actions. In order to validate this intuition, one can draw the equations of two elastic elements in parallel, representing both the impedance of the muscle contraction and the action added by the actuator from the exoskeleton.

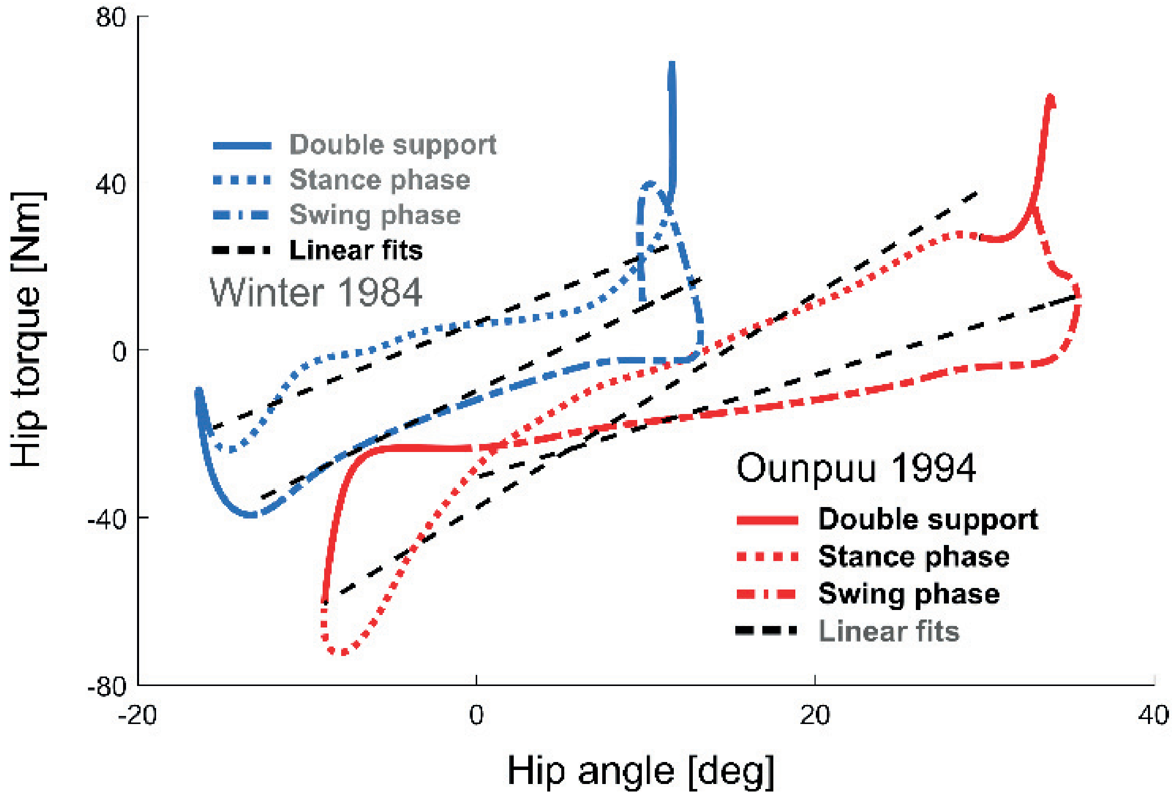

Figure 5-1 Hip flexion/extension torque during walking versus hip angle as reported in the literature by Winter and Ounpuu [129], [130]. Curves are split along the different gait phases, i.e. double support, stance and swing phases, to highlight the constant spring-like phase-related behavior. Copyright © 2018, IEEE

Equation 5-1 (a) expresses the natural torque at the joint where k_m is the muscle-tendon stiffness and α_0 is the "angle at equilibrium" or "attractive angle". Equation 5-1 (b) is the torque resulting from the addition of an impedance controller through the exoskeleton to the muscle activity, where k_{exo} and α_{0exo} are the simulated stiffness and angle at equilibrium, respectively, of the exoskeleton. The final impedance of the joint assisted by the exoskeleton is reported in Equation 5-1 (c) for the stiffness and Equation 5-1 (d) for the angle at equilibrium.

$$\tau_{joint} = k_m \cdot (\alpha - \alpha_0) \qquad \text{(a)}$$

$$\tau_{joint}{}' = k'_m \cdot (\alpha - \alpha_{0m}{}') + k_{exo} \cdot (\alpha - \alpha_{0exo}) \qquad \text{(b)}$$

$$k_{assisted} = k'_m + k_{exo} \qquad \text{(c)}$$

$$\alpha_{0assisted} = \frac{k'_m \cdot \alpha_{0m}{}' + k_{exo} \cdot \alpha_{0exo}}{k'_m + k_{exo}} \qquad \text{(d)}$$

Equation 5-1 (a) Hooke's law applied to a rotational spring, (b) Expression of two torques in parallel, (c) Equivalent stiffness of two spring in parallel and (d) Equivalent point of attraction of two springs in parallel

Equation 5-1 (a-d) show that the contributions of the muscles and the exoskeleton are linearly and proportionally combined. Simultaneously, the resulting angle at equilibrium is the weighted average between the individual angles at equilibrium over the individual stiffness ratios. Hence, the range of motion and level of assistance can easily be modulated following the controller's angle and stiffness parameters.

5.1.2 Generic Structure of the Controller

A finite-state active impedance controller is characterized by the following structure illustrated in Figure 5-2:

1. A low level controller, which regulates the torque applied by the exoskeleton.
2. A mid-level impedance controller, which generates a torque command based on the position and the orientation measured by the sensors, as well as their temporal derivatives.
3. A higher level controller, which detects the current state based on either sensors relative to the kinematics or their interactions with the environment. It then communicates the impedance parameters corresponding to that state to the impedance controller.

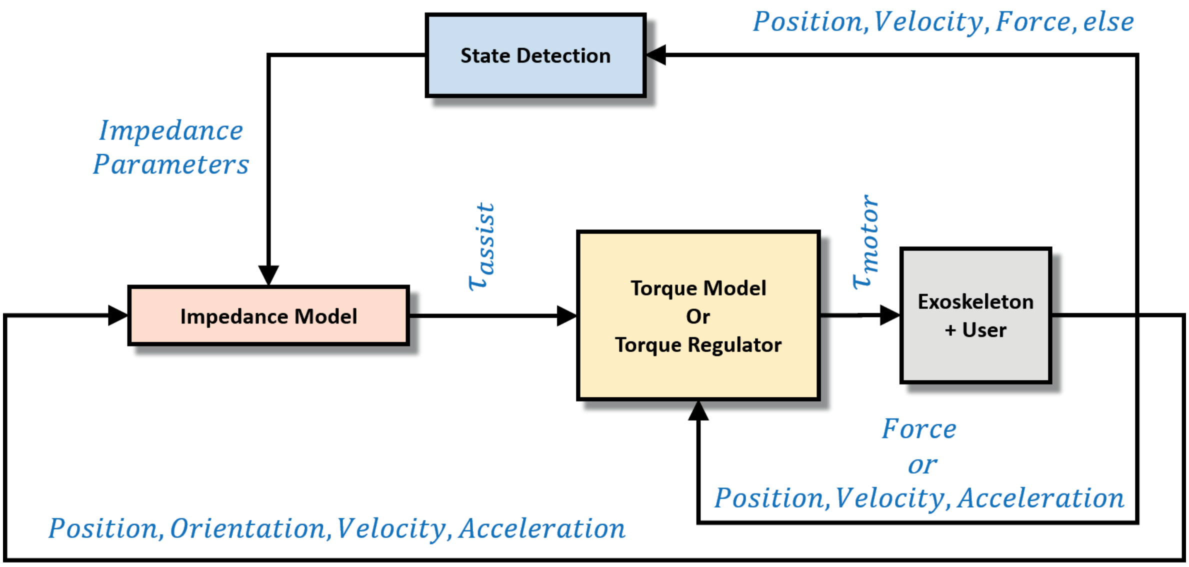

Figure 5-2 Generic structure of the finite-state active impedance controller

The key elements of a finite-state controller are, first, the definitions of the different states and the transition, based on the detection of particular events related to the kinematics or to ground reaction forces. Second, the parameters of the impedance for each state or phase must be tuned according to the application. One strength of the finite-state active impedance controller is that the impedance models can be very easily tuned and thus the level of assistance can be customized to the user.

5.1.3 Implementation in Level Walking

Based on the observation of the impedance during the gait presented in Figure 5-1, three states with different impedances are observed that have similar timing with the swing phase, the single stand phase (as only one foot is in contact with the ground) and the double stand phase. It is important to note that any activity should be composed of cyclic states which run continuously, while still states should pause and then re-start the activity. For example, if walking, the controller should allow the user to voluntarily stop, stand still and walk again as she/he intends to. In the current implementation, three phases are proposed: a “swing” phase, a “single stand” phase, and a “transition or double stance” phase. The “transition” phase is the “standing still” state. This is quite beneficial, as the controller does not have to differentiate between the walking and the standing mode. The schema of the three-phases controller is illustrated in Figure 5-3; the conditions for the transition from one state to the other are described in the next section. The continuous walking pattern is illustrated in red with each state duration in percentage of the cycle duration.

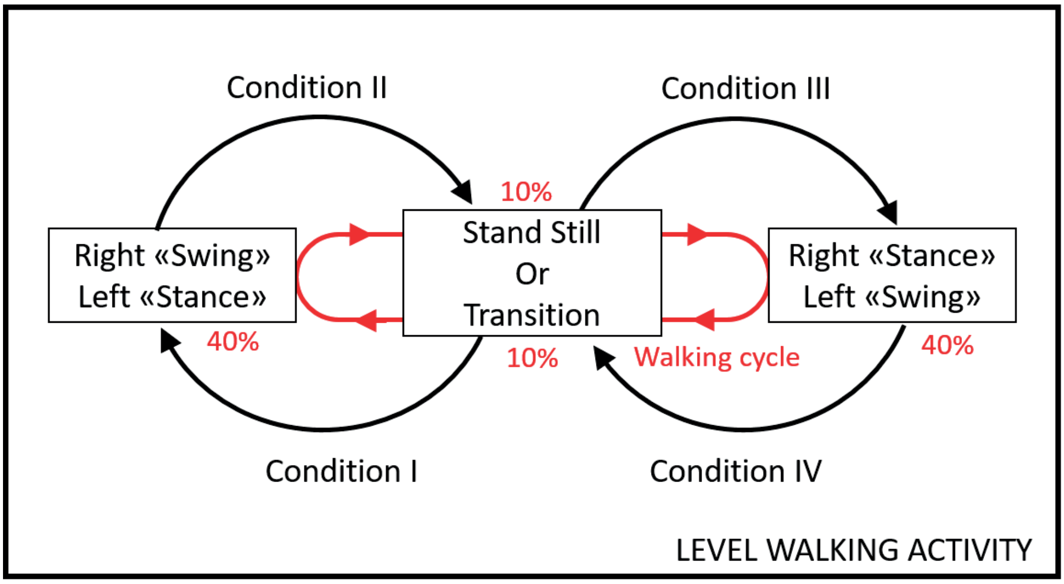

Figure 5-3 General schema of the three-phases finite-state controller

5.1.3.1 Phase detection

As discussed above, the controller consists of the simulation of impedance behaviors that evolves over the different phases of gait. A robust way to detect stance and swing phases is to use contact or force sensors under the feet. This approach has been widely explored both with prosthetics [180]–[182] and exoskeletons such as the EksoGT™ or HAL [183]. The approach explored here is based only on the kinematics and is able to predict motion intentions either while the foot is still in contact with or before it is in contact with the ground. Initial investigations indicate that the hip flexion velocity is a good predictor for the detection of the different impedance states. Three phases are proposed as candidates and are called “hip flexing”, “hip extending” and “static” phases. These phases are similar, respectively, to the “swing”, “stance” and “double support” standard phases. Equation 5-2 (a)-(c) express the conditions for such phase detection, where V_{hip} is the velocity measured at the hip joint on the reference side (e.g. left hip), V_{opp_hip} is the velocity measured at the opposite side (e.g. right hip), and V_{lim+} is an arbitrary threshold determining the detection of the phase transition. The latter threshold can be tailored to the user in order to adjust the sensitivity of the detection as will be presented in subsequent discussion.

$$
\begin{array}{lcc}
\text{Hip flexing phase condition:} & V_{hip} > V_{lim+} & \text{(a)} \\
\text{Hip extending phase condition:} & V_{opp\_hip} > V_{lim+} & \text{(b)} \\
\text{Static phase conditions:} & \begin{array}{c} V_{hip} \leq V_{lim+} \\ V_{opp\_hip} \leq V_{lim+} \end{array} & \text{(c)}
\end{array}
$$

Equation 5-2 Conditions defining the different control states : (a) condition for the flexing phase, (b) condition for the extending phase and (c) conditions for the static phase

Similarly, during the swing and (single) stance phases, the hip flexing and hip extending phases are intended to be synchronized in both the left and right legs. In order to ensure the symmetry of the controller, the same event is tested on both legs Equation 5-2 (a) and (b) to detect flexion. In case of a hip flexing phase on one leg, the opposite leg is automatically turned into hip extending mode. When neither leg is flexing, either the user is not walking or she/he is walking, but in a transition state. The different phases and impedances of the controller in the context of gait initiation, continuous walking, and gait termination are illustrated in Figure 5-4.

5.1.3.1 Gait initiation and termination

Initially, the user stands in an upright, still position which corresponds to the static phase of the controller (as none of the hips are flexing). In order to initiate gait, a flexion of one hip up to the velocity threshold V_{lim+} should be induced by the user such that the controller will turn into the hip flexing phase on that side, while the opposite leg turns into hip extending phase. Hence, the user must provide some critical force to move the leg and trigger the assistance by the exoskeleton. The amount of force to be exerted depends on both the passive (mechanical joints) and active (controller) impedance, which are mainly the dry friction and the torque in static phase. The force is also function of other parameters, i.e. the velocity threshold V_{lim+}.

Gait termination is defined as the sequence in which the controller switches to static phase and remains in that state. The transition from a flexing/extending phase to a static phase is usually natural. It can occur either as the swinging leg reaches a stable (maximum) angle of flexion, or as the wearer makes early contact with the ground. The static phase occurs at the end of each flexing phase, as the hip direction needs to revert to go forward. Gait can thus be terminated at the end of any step. This offers the full management of each step to the user. Time delay and triggering torques required to switch from a static to a hip flexing phase are investigated using the same setup as for the characterization of the actuation unit (Section 4.3) where the force is operated by hand through a force sensor. The experiment comports six values of V_{lim+} ranging from 10 to 100 [deg/s] and four values of stiffness in static phase from 0.5 to 3.0 [Nm/deg]. Results are presented in Figure 5-5 for the detection delay and torque required. Each data is averaged over a set of five measurements.

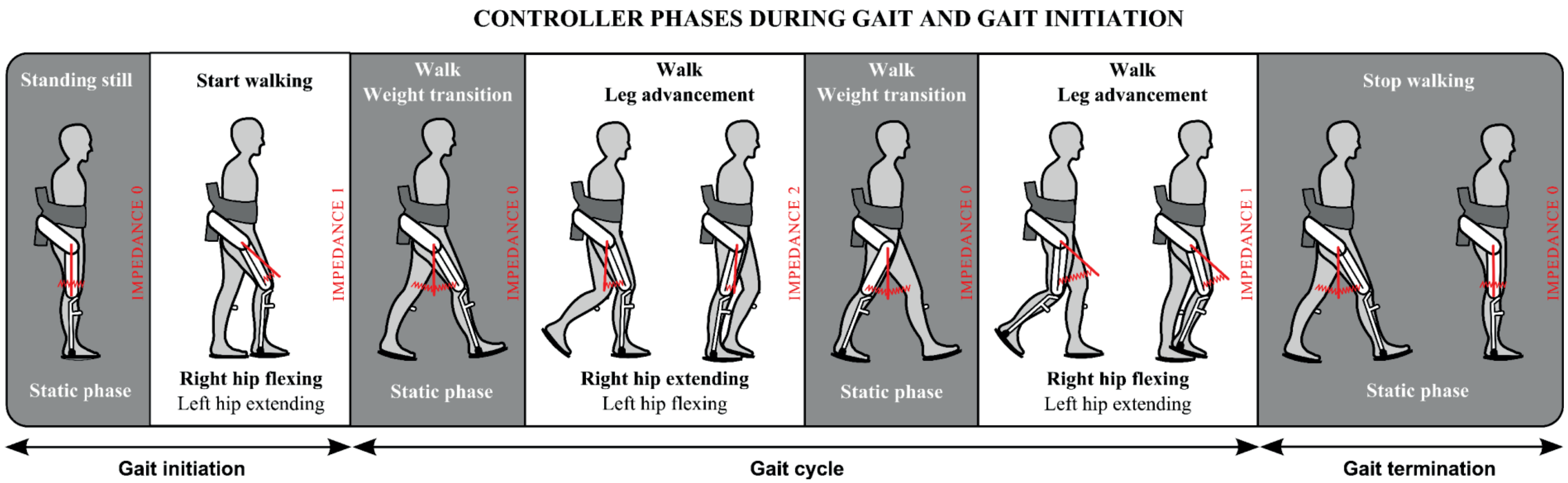

Figure 5-4 Illustration of the different phases of the controller, from gait initiation to termination through a full gait cycle. Impedance is represented by its theoretical mechanical equivalent, which is a fixed element linked to the femur segment by spring. The fixed element (i.e. large bar) reflects the simulated equilibrium angle. Copyright © 2018, IEEE.

Globally, the parameters of velocity and stiffness have opposite effects on the detection of initiation versus termination. The delay and torque necessary for initiating walking while in the static phase increase with the velocity threshold and the controller stiffness. Thus, a low velocity threshold is more adapted for people with muscle weakness. However, time delay and torque required to stop walking are lowered by increasing the velocity threshold and the static phase's stiffness parameter. In fact, when the velocity threshold is low, the controller can misinterpret small motions with intentions of motion, which can possibly induce unwanted oscillations. A good compromise between stability and low initiation torque can be found in a range of velocities between 30 and 60 [deg/s].

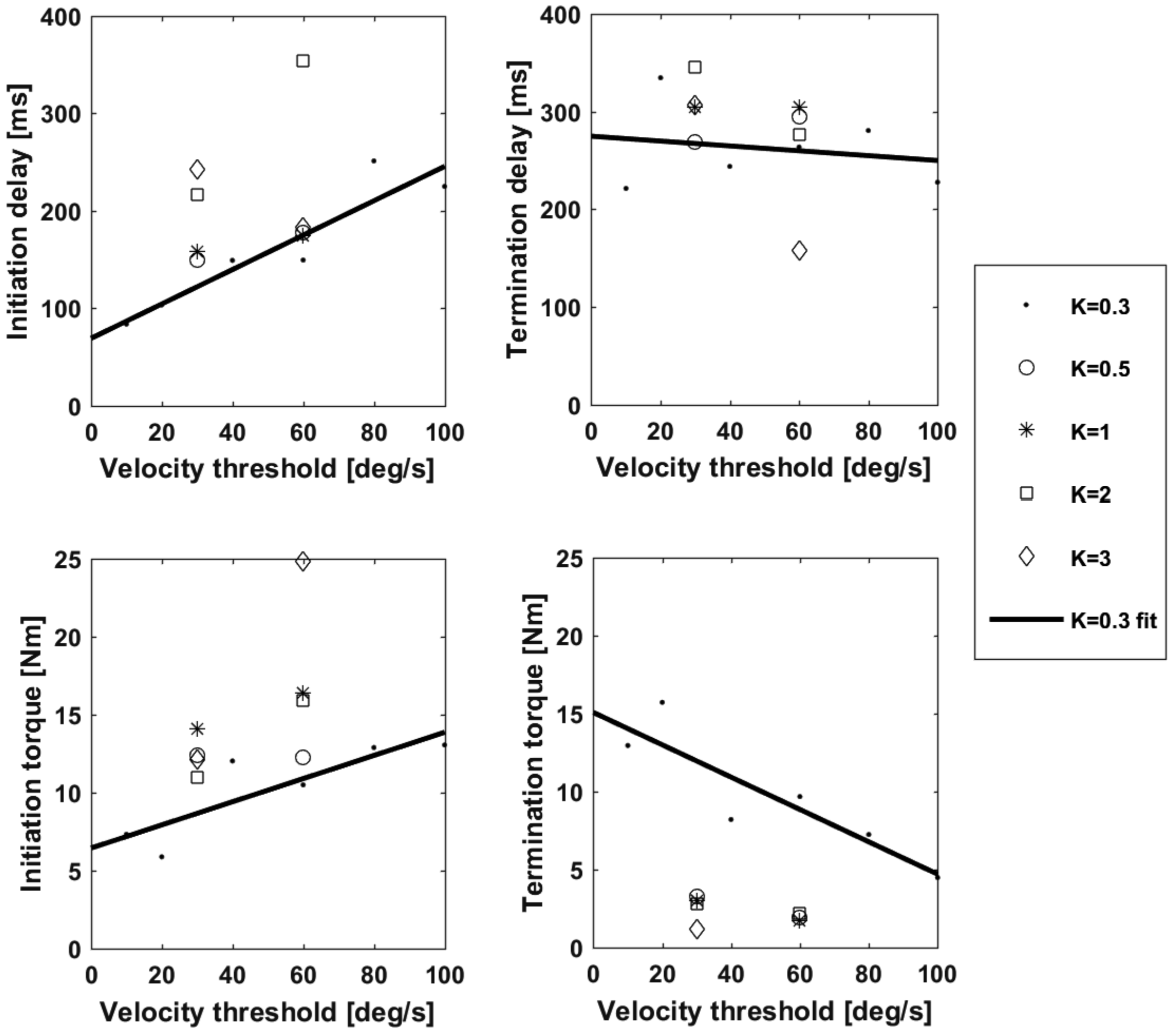

Figure 5-5 Effects of the velocity threshold V_{lim+} and stiffness parameter K in the static phase, (top) on the delays and (bottom) on the triggering torques

5.2 Finite-State Active Impedance Control – Evaluations

Two evaluations of the controller are conducted, the first one consists of a feasibility study performed on a pilot suffering from limb girdle muscular dystrophy as well as on a healthy user. The second evaluation is performed with a healthy user in different conditions to evaluate the impact of different impedances on the gait characteristics.

5.2.1 Feasibility Study on Healthy and Pilot with Limb Girdle Muscular Dystrophy

The three-phase variable impedance gait assistive strategy is used in a haptic context where the human-robot interaction is bi-directional. It is important for the evaluation to take place in the context defined originally, i.e. in overground walking with the exoskeleton in assistance mode.

5.2.1.1 Method

Two pilots, one healthy and one with a neuromuscular disease (NMD), walk on a pathway approximately twelve meters long using the AUTONOMYO exoskeleton. Both pilots are similar in height and weight (about 185cm and 70-80kg). The affected pilot has a limb girdle muscular dystrophy, with quasi-symmetrical strength in the lower limbs which implies the following joint characteristics: good about ankle dorsi- and plantar flexion, moderate about hip and knee extensions and poor about hip and knee flexions. The MRC manual muscle test on this pilot is reported in Table 5-1.

Table 5-1 Muscle strength of the pilot with limb girdle muscular dystrophy based on the MRC scale

Pilot with Limb Girdle Muscular Dystrophy		
Joint / direction	**Right side**	**Left side**
Hip abduction	1.5	1
Hip adduction	1.5	1.5
Hip flexion	1	0.5
Hip extension	1	1.5
Knee flexion	0.5	0.5
Knee extension	2	1.5
Dorsiflexion	2.5	2.5
Plantar flexion	2.5	2.5

*** 0 no force felt, 1 can see a contraction but no motion, 2 can move without gravity, 3 can move with gravity, 4 can exert a moderate force, 5 can exert a strong force**

The exoskeleton is controlled with the three-phase variable impedance strategy, where the impedance mimics a spring mechanism. A damping effect is also provided during the flexing and extending phases in order to avoid instability in the controller, particularly during transition between phases. The general form of the impedance is related in Equation 5-3, while the parameters depending on the phase and on the pilots are reported in Table 5-2.

$$\tau_{assist} = k \cdot (\alpha - \alpha_0) - \lambda \cdot \dot{\alpha} \qquad (15)$$

Equation 5-3 Controller impedance based on a visco-elastic behavior, where τ_{assist} is the torque provided to the pilot by the exoskeleton, *k* is the simulated spring stiffness, α_0 the simulated equilibrium angle and λ is the viscosity coefficient.

The impedance parameters have been tuned in accordance with the pilots' feedback and to match the target walking velocity. The evaluation of the controller is made considering its coherence with regards to the torque profiles from the literature. At this stage, the impact of the assistance on the energy expenditure or muscle activity has not been investigated.

Table 5-2 Parameters of impedance at the hip for the different phases and pilots

	Impedance parameters			
	Healthy pilot		Pilot with NMD	
Phases	*k [Nm/deg]*	α_0 *[deg]*	*k [Nm/deg]*	α_0 *[deg]*
Static phase "double support"	0,8	0	0,2	5
Flexing phase "swing"	1,5	30	0,6	30
Extending phase "stance"	1,4	0	0,4	-5
	Viscosity coefficient $\lambda = 0.11$ [Nm s/deg]			

5.2.1.2 Results

Both pilots were able to initiate and terminate walking at their convenience. The velocity threshold for the pilot with NMD is set to 20 deg/s, while for the healthy pilot a best value of 50 deg/s is found. The pilot with NMD requires a physical support in order to keep his balance while walking with the exoskeleton (can walk without the exoskeleton using a cane).

Figure 5-6 illustrates the hip angles and torques over one gait cycle (average over N>10 walking steps). The angles and torques from the literature are also reported in Figure 5-6. The reference walking kinematics and dynamics from the literature correspond to a greater walking velocity than that of the gait of the pilots wearing the exoskeleton.

1) Hip flexion/extension trajectories

Ranges of motion (RoM) at the hip are respectively 47° and 31° for the healthy and the NMD pilots, respectively. The NMD pilot reaches the full extension early at 35% of the gait cycle while the healthy pilot reaches at approximately 47%. Both perform very well when viewed through the literature; maximal extension has reached about 50-55% of the gait cycle. The assisted gait presents an overshoot of flexion about 6 degrees preceding heel strike. The healthy pilot has a short flexing phase with a high flexing velocity, compared to a long flexing phase with low velocity for the NMD pilot. However, the static phase following the flexion is especially long for the healthy pilot.

2) Hip flexion/extension torque

The assistance torques for both healthy and NMD-afflicted pilots are very similar during the extending phase, the following static phase and the beginning of the flexing phase. These torque patterns ranging from 10% to 85% of the gait cycle are similar, but smaller than torques presented in the literature. The event of heel strike, however, is documented in literature to have high extension torques whereas the controller provides very small torques during this static phase. This aspect is discussed in the following sections.

5.2.1.1 Discussion

Both the healthy pilot and the NMD pilot reported a synchronous and non-constraining motion of the exoskeleton while walking. In both cases, the action of the exoskeleton was reported as positive and impactful. Differences in kinematics and torque patterns from the use of the exoskeleton, compared to natural gait, from the literature have been documented in the previous sections. The most notable event is the long static phase experienced by a healthy user wearing the exoskeleton during the heel strike event. During natural walking, one tends to have a continuous forward motion of the center of mass (CoM) in order to lower the energy cost. In the case of wearing the exoskeleton, the transition phase (static phase during heel strike) is managed differently compared to non-assisted gait. First, the exoskeleton does not provide a push-off phase that comes originally from a strong flexion propulsion of the ankle. Secondly, it is carefully designed to ensure that the motion is quickly stopped during double support so that the pilot has the possibility to terminate gait without much effort.

The assistive torques provided reach about 70% of the peak torques reported by Stoquart et al. on treadmill for a bodyweight of 70kg [125] at a walking velocity of 2 km/h. Further comparisons have not been made since the dynamics are quite different between walking on a treadmill and walking over even or uneven ground.

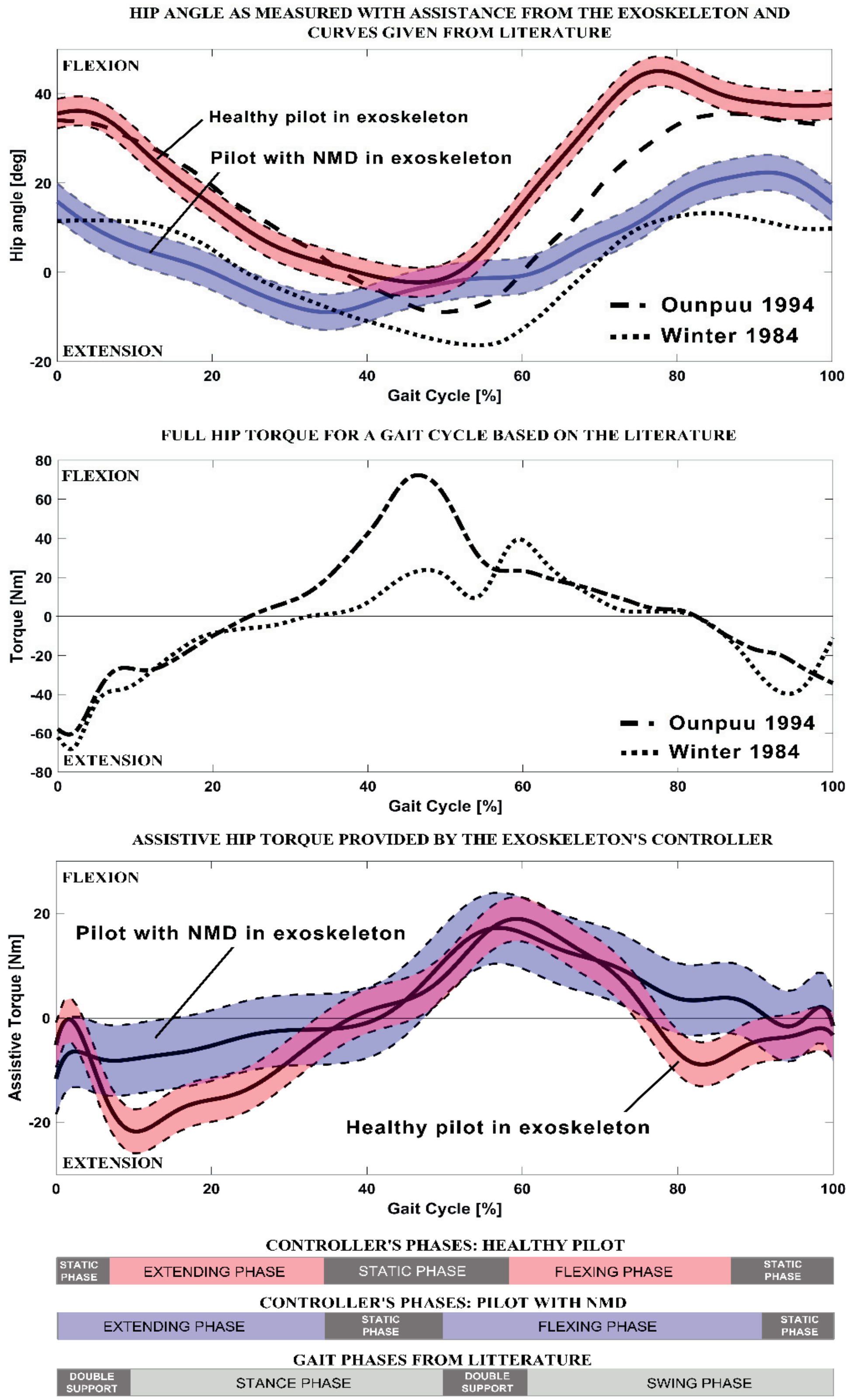

Figure 5-6 Kinematic and dynamic results of a healthy pilot and a pilot with a neuromuscular disease (NMD) assisted by the exoskeleton, and data from the literature with healthy adults.

5.2.2 Influence of Impedance Parameters on Gait

One of the strengths of the presented three-phase finite-state controller is that the parameters defining the simulated impedance can be tailored to the need of the user. The main objective is to be able to tune the impedance based on level of assistance provided each joint, the comfortable range of motion for the user, and the highest comfortable walking velocity. This section explores the effects of different impedance parameters upon gait characteristics. The level of user engagement is also varied to evaluate its impact on gait.

5.2.2.1 Material and Methods

The AUTONOMYO exoskeleton is used for this experiment as shown in Figure 5-7, with the three-phase finite-state active impedance controller. The impedance model, as described previously in Equation 5-3, is used. The stiffness k and the attractive angle α_0 can be adjusted to the need of the user. Note that the torque is limited, for this experiment, to a maximal value of 25 Nm (limitation to the nominal torque of the motors and with the transmission efficiency taken into account). The impedance varies depending on the walking phase, which may correspond to the swing-phase, stance-phase or double support-phase. Both gait initiation and phase detection are triggered through the hip flexion velocity as previously discussed in Section 5.1.3 and detailed further in [184]. Each step is triggered by a flexion motion of the hip that indicates the user's intent. The actuations about the hip adduction/abduction were locked to a 0° position to focus on the flexion/extension assistance. Due to this mobility constraint, a light physical support was needed.

Figure 5-7 The latest version of the AUTONOMYO haptic lower limb exoskeleton used to perform the tests

Trials have been performed over a ground distance of 18m with a healthy user (203cm, 95kg, 29 year-old) wearing the exoskeleton. Parameters explored are attractive angles (α_0) and stiffness (k) for the hip and knee during swing and stance phases. The level of exertion, which was self-described as low, comfortable or high, was modulated by the pilot to demonstrate the influence on the gait characteristics. The level of exertion is also referred to as the level of implication of the user, that is the amount of power that is intentionally exerted by the user. To evaluate gait characteristics, the following data were collected: time to travel the 18m, number of steps, cadence and range of motion at each joint. The parameters for each trial is shown in Table 5-3.

Table 5-3 Test conditions : impedance parameters and level of user exertion

Trial #	Hip				Knee				User exertion or implication
	Swing		Stance		Swing		Stance		
	k [Nm/deg]	α_0 [deg]	k [Nm/deg]	α_0 [deg]	k [Nm/deg]	α_0 [deg]	k [Nm/deg]	α_0 [deg]	
1	2	40	2	-10	0.5	50	0.5	5	Comfortable
2	2	60	2	-10	0.5	50	0.5	5	Low
3	2	60	2	-10	0.5	50	0.5	5	Comfortable
4	2	60	2	-10	0.5	50	0.5	5	High
5	3	60	3	-10	0.5	50	0.5	5	Low
6	3	60	3	-10	0.5	50	0.5	5	Comfortable
7	3	60	3	-10	0.5	50	0.5	5	High
8	0.5	40	0.5	-10	0.5	20	0.5	5	Comfortable
9	0.5	40	2	-20	0.5	20	1	5	Comfortable
10	2	40	0.5	-20	1	20	0.5	5	Comfortable
11	2	40	2	-20	1	20	1	5	Comfortable
12	2	40	2	-20	1	20	1	5	High

5.2.2.2 Results

The gait characteristics resulting from the different parameters of the controllers and the exertion of the user are summarized in Table 5-4. As depicted in Figure 5-8, the exertion of the user has a large effect on the walking speed and step length. The contribution of the stiffness coefficients is unclear, as only small modifications are observed in trials 8 to 11 while the stiffness is modulated during each phase of the gait. The range of motion of both hip and knee are correlated with the flexing phase attractive angles of both hip and knee (see Figure 5-8). However, the ranges of motion do not impact the step length. The cadence is inversely correlated with those hip and knee impedance parameters.

Table 5-4 Gait characteristics resulting from

Trial #	Walking speed [m/s] (km/h)	Hip range of motion [°]	Knee range of motion [°]	Cadence [steps/min]	Step length [m]
1	0.37 (1.32)	73	49	51	0.86
2	0.25 (0.9)	78	65	30	1
3	0.40 (1.44)	83	68	40	1.2
4	0.50 (1.8)	89	71	40	1.5
5	0.29 (1.05)	85	75	31	1.1
6	0.39 (1.41)	88	70	39	1.2
7	0.46 (1.66)	86	72	43	1.3
8	0.55 (1.99)	56	62	52	1.3
9	0.47 (1.71)	49	60	51	1.1
10	0.56 (2.01)	51	54	56	1.2
11	0.51 (1.85)	51	60	55	1.1
12	0.86 (3.09)	56	45	74	1.4

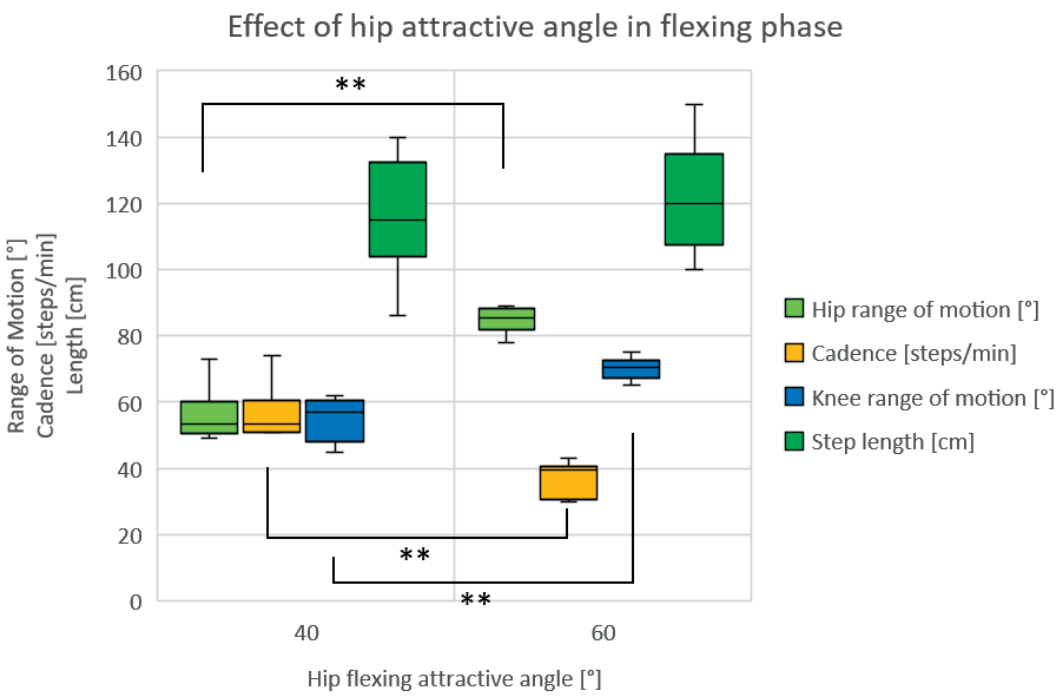

Figure 5-8 Correlation of the hip attractive angle in flexing phase with some gait characteristics ** indicates statistical significance (with p-value < 0.01)

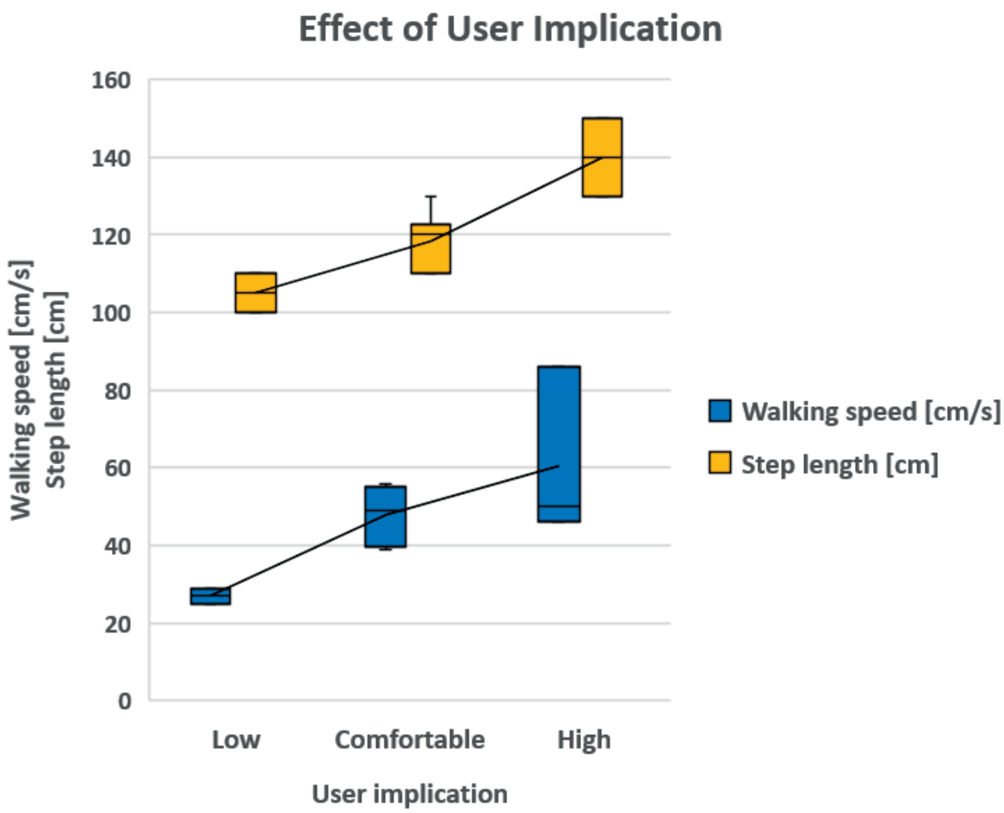

Figure 5-9 Correlation of the user implication with relevant gait characteristics

5.2.2.3 Discussion

This section has highlighted the flexibility of the controller. Three factors were preliminary evaluated: two impedance parameters (the attractive angle (α_0) and the stiffness (k)) and, the physical exertion of the user during ambulation. The user is primarily in charge of the walking performance, as demonstrated by the significant effect of the user effort on the walking speed and on the step length. This aspect is key, because it indicates that the motivation of the user and their subsequent contribution will heavily affect the performance of the device. In a rehabilitation setting, it can also provide feedback to therapists on the level of the engagement of the user.

The effect of the attractive angle is also shown to be important in tuning the range of motion of the joints. This is seen as a good variable for affecting the gait pattern of the user. However, it does not lead to greater walking speed, as it reduces the cadence but does not increase the step length. Neither did the variable stiffness correlate to the walking speed, as was expected. This observation can be explained by both a decrease of the user activity while receiving more assistance from the device and a difference in the level of assistance provided due to the programmed torque limit imposed upon the exoskeleton. These preliminary observations need further investigations, including more precise evaluation methods of the user exertion, i.e., oxygen intake or EMG (electromyography).

5.3 Conclusion

This chapter proposed and evaluated a collaborative strategy for determining the type and level of assistance an exoskeleton can provide. Using a rigid transmission over the hip joint of the AUTONOMYO exoskeleton, a full gait assistive strategy based on finite-state control is presented. Designed for people with muscle weakness or neurological disorders, particular attention is paid towards triggers to initiate or terminate assisted walking. A method actively involving the pilot in the gait through a detection of intention through the hip flexion motion is presented. Results show that torques under 8 Nm in flexion of the hip over a duration of 150 ms are sufficient to control the device. The control strategy, based on three states that can be compared to the stance, swing and double support phases of the gait, provides a powerful assistive controller free from spatial and temporal constraints. Moreover, impedance variation offers an easy and intuitive way for tuning the characteristics of the assistance, by for example, increasing the stiffness or augmenting the attractive angles.

An initial feasability study demonstrated that both a healthy user and a user with severe muscle weakness were able to collaborate with the device and walk. Further tests looking at metrics to quantify the impact of the exoskeleton on the user need to be performed. This could include the evaluation of the variation of metabolic expenditure with support from the exoskeleton as well as without. A study could evaluate muscular activity by observing the difference of timing and of amplitude in electromyography sensors. The impact of wearing the exoskeleton upon gait kinematics could also be observed to see if the user range of motion could be increased by using the exoskeleton.

This chapter also presents the evaluation of the impact of different parameters on the gait characteristics. The variables investigated are the user exertion and the different impedance parameters, such as the virtual stiffness or the attractive angle. Results show that user implication can affect step length and walking velocity. The attractive angle of the hip does not significantly impact the step length. However, it does have an important impact on the hip range of motion, the knee range of motion, and the cadence.

Further examinations need to be performed to investigate the potential impact of the AUTONOMYO exoskeleton, combined with a simple assistive controller, on a larger group of people with neuromuscular disorder. The preliminary results are promising. A further axis of research will be to combine a balance augmentation strategy with the current controller, so that the pilot can potentially walk independently.

Chapter 6 Discussion

Neuromuscular diseases are a large and heterogeneous set of diseases characterized by localized or general degenerative muscle wasting. Walking impairments are recurrent among these persons and are noted by characteristic gait with uncommon compensating patterns. At the time of this publication, most existing ambulation supporting devices are not adapted to the unique needs of people with neuromuscular diseases. Only ankle-foot orthoses have demonstrated a significant improvement in the gait in people with ankle weakness. This work investigates solutions for assisting people with muscle weakness in walking and performing other activities requiring ambulation. The concept is largely inspired by the work of pioneers in the development of exoskeleton devices for the mobilization of people with spinal cord injuries.

The challenges of designing assistive devices for people with neuromuscular diseases are numerous. One of the first challenges is also one of the most crucial: to build an exoskeleton that can walk on its own without the need of external support. This implies that the exoskeleton can either offer a stability zone that is so large that the risk of losing balance is very small, or, can dynamically recover from a dangerous situation as a healthy human body is able to. The difficulty in creating such an ability lies in the shared control between user and exoskeleton. In order to manage balance, there will be cases in which the exoskeleton will likely need to fully guide the user. Aside from these future perspectives, an infinite list of challenges can be cited, from the difficulty of fitting a device with different morphologies encountered in a large population to providing safety in a defined environment.

Despite the numerous challenges that exoskeleton designers are facing right now, academic and industrial communities have a significant interest in the development of new technologies for exoskeleton design. This is a driving force that will generate extremely useful resources in the near future. Although exoskeletons are still seen as a life changing device for many, the number of sales of such devices over the past few years in the limited market demonstrates the gap between the dream and the reality. Despite this projection, exoskeletons have nonetheless demonstrated their many health and lifestyle benefits for people who would otherwise be wheelchair-bound.

People with neuromuscular diseases are excellent candidates for exoskeleton design as they stand to benefit immensely from the technology. Exoskeletons can reduce the early fatigue that affects people with neuromuscular diseases and thereby promote a more active lifestyle. It is likely that, for safety reasons, the first devices will be released and used in controlled environment, before being available as a personal device at home.

6.1 Contributions

6.1.1 Evaluation of Gait in Persons with Neuromuscular Diseases

The first contribution consists of the first thorough literature survey on gait in neuromuscular diseases. The conclusions of this survey demonstrates the lack of comprehensive studies with a representative number of participants enrolled in the study. Only two types of NMD have been significantly studied, but rarely with a representive sample size. The other types of NMD can be found in, at most, 2 or 3 studies; however, a large number of them have not been investigated and, if so, the sample sizes are rarely representative. Despite the small number and limited quality of the studies, a description of most of the compensating patterns can be found in the literature.

In addition to the literature survey, an experimental study on a heterogeneous group of 14 persons with NMD was performed. The results consolidate the previous findings of gait patterns; such as knee hyperextension or foot drop. The study qualifies the need of participants, based on the observation of their compensating patterns. Thus, the contribution of this work is related not only to the observation of compensating patterns in people with neuromuscular diseases, but also to a greater understanding of the terms of assistance for people with neuromuscular diseases.

6.1.2 Development of a novel exoskeleton architecture

The main tangible contributions of this thesis is the realization of a full lower limb exoskeleton that is adjustable to the size of the user and includes six actuated degrees of freedom. A particular focus was placed on the optimization of the inertial effects of the actuators. This resulted in the use of small diameter and long electrical actuation remotely located from the joints. A first proof of concept was constructed in the form of a leg with three actuated degrees of freedom. The different contributions stemming from the mechanical design of the exoskeleton are described in the following sections.

6.1.2.1 Cable driven system with adjustable segment length

A pulley system connects the motor to the hip joint, as well as the hip with the knee. The second stage is particularly critical, as the segment (elaborate – “the segment” is very vague) must be adjusted to fit user dimensions. A novel solution of a rack and pinion system is designed which allows the length of the cable to be kept constant while the segment length is changed. The stainless steel cables are anchored on each pulley and have a range of motion of 270° in a very limited space.

6.1.2.1 Coupling configurations in locomotion

Another contribution is the kinematic analysis of different coupling configurations that are introduced by remotely locating the knee actuation unit in the upper back of the exoskeleton. The analysis is put in the perspective of the different activities such as level-walking, STS and stairs climbing. Both configurations have certain activities where they excel, but others where they perform badly in the others. Eventually, it is observed that the configuration without coupling is the most versatile one and has the highest potential for fitting the requirements.

6.1.2.2 Characterization of backdrivable mechanisms

Two backdrivable mechanisms were designed and then characterized. A ballscrew transmission with a four bar linkage was proposed for the actuation of the hip abduction/adduction. The transmission of the hip and knee flexion/extension was realized with a three-stage planetary gearbox before transmitting the efforts to a cable-pulley system described previously. Both systems present different types of friction that affects the backdrivability. An unconventional model with a variable efficiency in function of the sign of the power in the motor is proposed and validated for the actuation with the gearbox. A totally different model was identified for the ballscrew actuation unit, where the most important contribution comes from the friction that is proportional to the velocity.

6.1.3 Active impedance assistive controller

A novel architecture of finite-state controller based on active impedance was proposed and implemented on the exoskeleton. It is based on the study the relationship of gait between kinematics and kinetics, which reveals constant impedance behavior for different phases. The controller is implemented with a combined detection of state and detection of intention, which allows it to switch between adjustable preprogrammed constant-impedance behaviors.

6.1.3.1 Detection of intention

A novel method of phase detection was implemented that also includes detection of intention, i.e. the gait initiation and termination. The characteristics of the detection of intention were evaluated on a test bench and measured in terms of required torque and detection delay. The relationship between these characteristics and the velocity detection threshold were also measured.

6.1.3.2 Feasibility study with people with neuromuscular diseases

The controller was tested over five sessions with a pilot with limb girdle muscular dystrophy. After the first preliminary session, a set of parameters was determined to adapt to the pilot needs. In all four sessions, the pilot was able to initiate gait, and walk as he wanted while he was assisted in balancing with two people. The limitations of the pilot's capabilities in step length (hip range of motion) and sensitivity of detection of intention were addressed.

6.1.3.3 Preliminary evaluation of assistance tuning with impedance control

One of the key aims of the assistive strategy is to for any assistive device to be adaptable to different joints and level of assistance. The goal is to assist as needed so that the pilot can be independent whenever possible while functioning within his/her capabilities. A preliminary test investigating the influence of the user implication and different parameters from the simulated impedance (attractive angle or simulated stiffness during different phases) on gait characteristics (range of motion, step length, stride rate, walking velocity). Results show that step length and walking velocity are correlated with the user independence, while the attractive angle of the controller modulates the range of motion and the step length. The simulated stiffness was assumed to increase the level of assistance, as it increases the torque provided by the device; however, no significant effects upon gait parameters were observed.

6.2 Outlook

6.2.1 Actuation Architecture

The aim of the mechanical development was to design and validate powerful, lightweight and compact actuation units that can precisely allow force control and be as transparent (or backdrivable) as possible. Different architectures are used for the different joints. The characterization of the transmission units shows that ballscrew mechanisms have a significant resistance that is proportional to the velocity, while planetary gears provide important friction that is proportional to the torque. Some modifications can thus improve the backdrivability, for example, reducing the rotation velocity of the ballscrew by using a greater pitch (and reduce the transmission ratio) can decrease the resistance by a factor of two. For the friction induced by the planetary gears, it is important to reduce it as much as possible to reach 70-80% of efficiency. This could be attained by selecting more carefully the materials used, design technologies, and manufacturing precision.

One of the first limitations encountered was the velocity constraint due to the motor selection and the maximum voltage capacity of the electronics of the drive. For safety reasons, it is preferable to keep the initial electronics (with max. 50V), but to select equivalent motors with a different voltage over velocity ratio. The unique consequence is that it will consume more current, but will be able to reach twice the actual speed limit. The required velocity then depends on the coupling configuration for the hip and knee flexion/extension. Two configurations with a positive or negative coupling were tested, and the non-coupled configuration was simulated. The positive coupling shows velocity benefits, mostly in the swing phase, but also increases torques required by the actuation in stairs climbing or STS transition. The negative coupling helps the device benefit from more torque available during stance phase, but implies higher velocities at the motor. One of the main concerns with coupling is that, in the case of accumulated friction, a joint can be overly constrained and can become uncontrollable. A configuration without coupling will be more versatile but requires a decoupling mechanism that can be difficult to integrate. Another possibility, among others, would be to use both coupling and a clutching mechanism to allow switching from one configuration to the other. A thorough study of the different solutions in the future can address the feasibility of implementation and pros/cons of each solution.

6.2.2 Strategy of Assistance

A control strategy based on a limited state of impedance has been presented. The detection of intention and the state transitions are part of the controller, and are commanded by the hip velocity using only the encoder of the actuator. It performs well in terms of reactivity and controllability during level-walking, even with a pilot with large muscle weakness at the hip. However, in the case of uphill motion, steps were difficult to initiate due to the supplementary force required to flex the hip. Another negative aspect of this simple form of detection is that it cannot determine if the foot is in contact with the ground. This can particularly be an issue during stairs climbing, as an error of timing can lead to strong strike of the steps and bad foot positioning on the stair. Additional sensors such as instrumented soles to measure ground reaction forces are being developed in order to get more information on the load redistribution and contact with the ground. Inertial measurement units placed in each foot and mounted on the back of the exoskeleton help to provide information on the orientation of the adjacent limbs. The improvement of detection of intention and of some safety controllers will be investigated with a modified strategy based on these sensors. For example, ground reaction forces will help better trigger phase detection by better identifying the swing and the stance phase.

Impedance control in finite state is shown to be a good solution for adaptable and collaborative strategy in people with residual walking abilities. Stairs climbing and STS strategies have been implemented but not yet tested due to the mechanical limitations in the current configuration. Key variables to address are the number of finite states and the original impedance parameters that will be tuned afterwards. The pre-tuning should be done with a healthy pilot for each activity, until satisfactory supportive behavior of the exoskeleton is found. Once this step is complete, tests and tuning can be done with a pilot with muscle weakness.

Eventually, strategies for the augmentation of balance should be addressed. These strategies will be largely based on the ground reaction forces, which give an indication on the center of pressure and are one of the main indicators of balance stability. Static balance management strategies will be investigated and evaluated before exploring stepping methods for dynamic balance control. This step requires a tremendous work and is an active area of research.

6.2.3 Validation with Patients

In the framework of the current thesis, the level walking strategy has been tested on a few healthy subjects and one pilot with muscular dystrophy. The results are promising and a feasibility study is being set up with three groups of people: a small group of people with inclusion body myositis, a neuromuscular disease affecting mostly the knee muscles, a small group of people with multiple sclerosis, and a control group of healthy subjects. The feasibility study will consist of 3 to 5 sessions in which the participants will perform gait assessment exercises through 2- or 6-minutes walk test and undergo gait analysis with and without wearing the exoskeleton. This first clinical evaluation is planned for early 2019 and will lead to further assessment of rehabilitation perspective and/or safety in personal use. Due to its modular assistance capabilities, assistive full lower limb exoskeleton can offer support to a large range of neurological and neuromuscular disorders. Some of the candidates are people with incomplete spinal cord injury, multiple sclerosis, hip surgery, hemiplegia, etc. in addition to people with neuromuscular diseases and including elderly people. Further preliminary studies should investigate the compatibility and impact of wearing such an assistive device on the quality of life among these different populations.

Bibliography

[1] T. Schwanen, D. Banister, and A. Bowling, “Independence and mobility in later life,” *Geoforum*, vol. 43, no. 6, pp. 1313–1322, Nov. 2012.

[2] D. H. Metz, “Mobility of older people and their quality of life,” *Transport Policy*, vol. 7, no. 2, pp. 149–152, Apr. 2000.

[3] J. Shafrin, J. Sullivan, D. P. Goldman, and T. M. Gill, “The association between observed mobility and quality of life in the near elderly,” *PLOS ONE*, vol. 12, no. 8, p. e0182920, Aug. 2017.

[4] D. Blackwell, J. Lucas, and T. Clarke, “Summary health statistics for U.S. adults: National Health Interview Survey, 2012,” National Center for Health Statistics, 2014.

[5] H. L. Kamenetz, “A Brief History of the Wheelchair,” *Journal of the History of Medicine and Allied Sciences*, vol. XXIV, no. 2, pp. 205–210, 1969.

[6] E. H. Cup *et al.*, “Exercise Therapy and Other Types of Physical Therapy for Patients With Neuromuscular Diseases: A Systematic Review,” *Archives of Physical Medicine and Rehabilitation*, vol. 88, no. 11, pp. 1452–1464, Nov. 2007.

[7] R. T. Abresch, J. J. Han, and G. T. Carter, “Rehabilitation management of neuromuscular disease: the role of exercise training.,” *J Clin Neuromuscul Dis*, vol. 11, no. 1, pp. 7–21, Sep. 2009.

[8] R. T. Abresch, G. T. Carter, J. J. Han, and C. M. McDonald, “Exercise in Neuromuscular Diseases,” *Physical Medicine and Rehabilitation Clinics*, vol. 23, no. 3, pp. 653–673, Aug. 2012.

[9] A. Lo, “Lokomat training to improve gait in multiple sclerosis and freezing of gait in parkinson’s disease,” *Topics in Spinal Cord Injury Rehabilitation*, vol. 17, no. 1, pp. 66–69, 2011.

[10] J. Hidler *et al.*, “Multicenter Randomized Clinical Trial Evaluating the Effectiveness of the Lokomat in Subacute Stroke,” *Neurorehabilitation and Neural Repair*, vol. 23, no. 1, pp. 5–13, Jan. 2009.

[11] S. Jezernik, G. Colombo, T. Keller, H. Frueh, and M. Morari, “Robotic Orthosis Lokomat: A Rehabilitation and Research Tool,” *Neuromodulation: Technology at the Neural Interface*, vol. 6, no. 2, pp. 108–115, Apr. 2003.

[12] J. F. Veneman, R. Kruidhof, E. E. G. Hekman, R. Ekkelenkamp, E. H. F. V. Asseldonk, and H. van der Kooij, “Design and Evaluation of the LOPES Exoskeleton Robot for Interactive Gait Rehabilitation,” *IEEE Transactions on Neural Systems and Rehabilitation Engineering*, vol. 15, no. 3, pp. 379–386, Sep. 2007.

[13] L. E. Miller, A. K. Zimmermann, and W. G. Herbert, “Clinical effectiveness and safety of powered exoskeleton-assisted walking in patients with spinal cord injury: systematic review with meta-analysis,” *Med Devices (Auckl)*, vol. 9, pp. 455–466, Mar. 2016.

[14] A. Theadom *et al.*, “Prevalence of Muscular Dystrophies: A Systematic Literature Review,” *NED*, vol. 43, no. 3–4, pp. 259–268, 2014.

[15] M. Needham, A. Corbett, T. Day, F. Christiansen, V. Fabian, and F. L. Mastaglia, “Prevalence of sporadic inclusion body myositis and factors contributing to delayed diagnosis,” *Journal of Clinical Neuroscience*, vol. 15, no. 12, pp. 1350–1353, Dec. 2008.

[16] C. Dobloug *et al.*, “Prevalence and clinical characteristics of adult polymyositis and dermatomyositis; data from a large and unselected Norwegian cohort,” *Ann. Rheum. Dis.*, vol. 74, no. 8, pp. 1551–1556, Aug. 2015.

[17] A. Ohta, M. Nagai, M. Nishina, H. Tomimitsu, and H. Kohsaka, “Prevalence and incidence of polymyositis and dermatomyositis in Japan,” *Mod Rheumatol*, vol. 24, no. 3, pp. 477–480, May 2014.

[18] J. C. MacMillan and P. S. Harper, “The Charcot-Marie-Tooth syndrome: clinical aspects from a population study in South Wales, UK,” *Clinical Genetics*, vol. 45, no. 3, pp. 128–134, Mar. 1994.

[19] H. Skre, “Genetic and clinical aspects of Charcot-Marie-Tooth’s disease,” *Clinical Genetics*, vol. 6, no. 2, pp. 98–118, Aug. 1974.

[20] F. L. M. Norwood, C. Harling, P. F. Chinnery, M. Eagle, K. Bushby, and V. Straub, “Prevalence of genetic muscle disease in Northern England: in-depth analysis of a muscle clinic population,” *Brain*, vol. 132, no. 11, pp. 3175–3186, Nov. 2009.

[21] A. Chiò *et al.*, “Global Epidemiology of Amyotrophic Lateral Sclerosis: A Systematic Review of the Published Literature,” *NED*, vol. 41, no. 2, pp. 118–130, 2013.

[22] K. Bushby *et al.*, “Diagnosis and management of Duchenne muscular dystrophy, part 1: diagnosis, and pharmacological and psychosocial management,” *The Lancet Neurology*, vol. 9, no. 1, pp. 77–93, Jan. 2010.

[23] J. Jeppesen, A. Green, B. F. Steffensen, and J. Rahbek, “The Duchenne muscular dystrophy population in Denmark, 1977–2001: prevalence, incidence and survival in relation to the introduction of ventilator use,” *Neuromuscular Disorders*, vol. 13, no. 10, pp. 804–812, Dec. 2003.

[24] A. J. van Essen, H. F. Busch, G. J. te Meerman, and L. P. ten Kate, “Birth and population prevalence of Duchenne muscular dystrophy in The Netherlands,” *Hum. Genet.*, vol. 88, no. 3, pp. 258–266, Jan. 1992.

[25] A. E. Stark, “Determinants of the incidence of Duchenne muscular dystrophy,” *Ann Transl Med*, vol. 3, no. 19, Nov. 2015.

[26] K. M. D. Bushby, M. Thambyayah, and D. Gardner-Medwin, “Prevalence and incidence of Becker muscular dystrophy,” *The Lancet*, vol. 337, no. 8748, pp. 1022–1024, Apr. 1991.

[27] J. K. Mah, L. Korngut, J. Dykeman, L. Day, T. Pringsheim, and N. Jette, “A systematic review and meta-analysis on the epidemiology of Duchenne and Becker muscular dystrophy,” *Neuromuscular Disorders*, vol. 24, no. 6, pp. 482–491, Jun. 2014.

[28] T. D. Bird, “Myotonic Dystrophy Type 1,” in *GeneReviews®*, M. P. Adam, H. H. Ardinger, R. A. Pagon, S. E. Wallace, L. J. Bean, K. Stephens, and A. Amemiya, Eds. Seattle (WA): University of Washington, Seattle, 1993.

[29] C. Turner and D. Hilton-Jones, “The myotonic dystrophies: diagnosis and management,” *Journal of Neurology, Neurosurgery & Psychiatry*, vol. 81, no. 4, pp. 358–367, Apr. 2010.

[30] J. W. Day *et al.*, “Myotonic dystrophy type 2: molecular, diagnostic and clinical spectrum,” *Neurology*, vol. 60, no. 4, pp. 657–664, Feb. 2003.

[31] L. H. Wang and R. Tawil, “Facioscapulohumeral Dystrophy,” *Curr Neurol Neurosci Rep*, vol. 16, no. 7, p. 66, Jul. 2016.

[32] D. D. Kilmer *et al.*, “Profiles of neuromuscular diseases. Facioscapulohumeral muscular dystrophy,” *Am J Phys Med Rehabil*, vol. 74, no. 5 Suppl, pp. S131-139, Oct. 1995.

[33] R. Tawil, “Facioscapulohumeral muscular dystrophy,” vol. 5, no. 4, p. 6, 2008.

[34] K. D. Mathews and S. A. Moore, “Limb-girdle muscular dystrophy,” *Curr Neurol Neurosci Rep*, vol. 3, no. 1, pp. 78–85, Jan. 2003.

[35] M. Guglieri, V. Straub, K. Bushby, and H. Lochmüller, “Limb–girdle muscular dystrophies,” *Current Opinion in Neurology*, vol. 21, no. 5, p. 576, Oct. 2008.

[36] U. A. Badrising *et al.*, “Inclusion body myositis: Clinical features and clinical course of the disease in 64 patients,” *Journal of Neurology*, vol. 252, no. 12, pp. 1448–1454, Dec. 2005.

[37] K. M. Krajewski *et al.*, “Neurological dysfunction and axonal degeneration in Charcot–Marie–Tooth disease type 1A,” *Brain*, vol. 123, no. 7, pp. 1516–1527, Jul. 2000.

[38] “Switzerland’s population 2012 | Publication |,” Federal Statistical Office, Neuchâtel, 1155–1200, Nov. 2013.

[39] M. Zatz, M. R. Passos-Bueno, and M. Vainzof, “Neuromuscular disorders: genes, genetic counseling and therapeutic trials,” *Genet Mol Biol*, vol. 39, no. 3, pp. 339–348, 2016.

[40] R. Braun, Z. Wang, D. L. Mack, and M. K. Childers, “Gene therapy for inherited muscle diseases: Where genetics meets rehabilitation medicine,” *Am J Phys Med Rehabil*, vol. 93, no. 11 0 3, pp. S97–S107, Nov. 2014.

[41] M. Scoto, R. Finkel, E. Mercuri, and F. Muntoni, “Genetic therapies for inherited neuromuscular disorders,” *The Lancet Child & Adolescent Health*, vol. 2, no. 8, pp. 600–609, Aug. 2018.

[42] T. Niidome and L. Huang, “Gene Therapy Progress and Prospects: Nonviral vectors,” *Gene Therapy*, vol. 9, no. 24, pp. 1647–1652, Dec. 2002.

[43] G. Hollier-Hann, D. Cork, S. Ralston, and A. Curry, “PND52 - Health Technology Assessment of Gene Therapies for Inherited Genetic Disorders in the US and Europe,” *Value in Health*, vol. 21, p. S210, May 2018.

[44] A. Y. Manzur, T. Kuntzer, M. Pike, and A. Swan, “Glucocorticoid corticosteroids for Duchenne muscular dystrophy.,” *Cochrane Database Syst Rev*, no. 1, pp. CD003725–CD003725, 2008.

[45] S. Yusuf, P. Sleight, J. Pogue, J. Bosch, R. Davies, and G. Dagenais, “Effects of an angiotensin-converting-enzyme inhibitor, ramipril, on cardiovascular events in high-risk patients.,” *N Engl J Med*, vol. 342, no. 3, pp. 145–153, Jan. 2000.

[46] F. W. Booth, “Effect of limb immobilization on skeletal muscle,” *Journal of Applied Physiology*, vol. 52, no. 5, pp. 1113–1118, May 1982.

[47] Y. Kawakami *et al.*, “Changes in muscle size, architecture, and neural activation after 20 days of bed rest with and without resistance exercise,” *Eur J Appl Physiol*, vol. 84, no. 1–2, pp. 7–12, Feb. 2001.

[48] M. Toigo and U. Boutellier, “New fundamental resistance exercise determinants of molecular and cellular muscle adaptations,” *Eur J Appl Physiol*, vol. 97, no. 6, pp. 643–663, Aug. 2006.

[49] G. Goldspink, “Malleability of the motor system: a comparative approach,” *Journal of Experimental Biology*, vol. 115, no. 1, pp. 375–391, Mar. 1985.

[50] P. M. Clarkson and I. Tremblay, “Exercise-induced muscle damage, repair, and adaptation in humans,” *Journal of Applied Physiology*, vol. 65, no. 1, pp. 1–6, Jul. 1988.

[51] H. Alexanderson, C. H. Stenström, G. Jenner, and I. Lundberg, “The safety of a resistive home exercise program in patients with recent onset active polymyositis or dermatomyositis,” *Scand. J. Rheumatol.*, vol. 29, no. 5, pp. 295–301, 2000.

[52] A. S. Aldehag, H. Jonsson, and T. Ansved, “Effects of a hand training programme in five patients with myotonic dystrophy type 1,” *Occup Ther Int*, vol. 12, no. 1, pp. 14–27, 2005.

[53] T. Taivassalo, N. De Stefano, J. Chen, G. Karpati, D. L. Arnold, and Z. Argov, “Short-term aerobic training response in chronic myopathies,” *Muscle Nerve*, vol. 22, no. 9, pp. 1239–1243, Sep. 1999.

[54] T. Taivassalo *et al.*, “Effects of aerobic training in patients with mitochondrial myopathies,” *Neurology*, vol. 50, no. 4, pp. 1055–1060, Apr. 1998.

[55] T. Taivassalo *et al.*, “Aerobic conditioning in patients with mitochondrial myopathies: physiological, biochemical, and genetic effects,” *Ann. Neurol.*, vol. 50, no. 2, pp. 133–141, Aug. 2001.

[56] M. I. Trenell, C. M. Sue, G. J. Kemp, T. Sachinwalla, and C. H. Thompson, “Aerobic exercise and muscle metabolism in patients with mitochondrial myopathy,” *Muscle Nerve*, vol. 33, no. 4, pp. 524–531, Apr. 2006.

[57] R. G. Haller, P. Wyrick, T. Taivassalo, and J. Vissing, “Aerobic conditioning: an effective therapy in McArdle’s disease,” *Ann. Neurol.*, vol. 59, no. 6, pp. 922–928, Jun. 2006.

[58] D. B. Olsen, M. C. Ørngreen, and J. Vissing, “Aerobic training improves exercise performance in facioscapulohumeral muscular dystrophy,” *Neurology*, vol. 64, no. 6, pp. 1064–1066, Mar. 2005.

[59] P. Cejudo *et al.*, “Exercise training in mitochondrial myopathy: a randomized controlled trial,” *Muscle Nerve*, vol. 32, no. 3, pp. 342–350, Sep. 2005.

[60] G. F. Wiesinger *et al.*, “Improvement of physical fitness and muscle strength in polymyositis/dermatomyositis patients by a training programme,” *Br. J. Rheumatol.*, vol. 37, no. 2, pp. 196–200, Feb. 1998.

[61] G. F. Wiesinger *et al.*, “Benefit of 6 months long-term physical training in polymyositis/dermatomyositis patients,” *Br. J. Rheumatol.*, vol. 37, no. 12, pp. 1338–1342, Dec. 1998.

[62] S. G. Aitkens, M. A. McCrory, D. D. Kilmer, and E. M. Bernauer, “Moderate resistance exercise program: its effect in slowly progressive neuromuscular disease,” *Arch Phys Med Rehabil*, vol. 74, no. 7, pp. 711–715, Jul. 1993.

[63] J. M. Florence and J. M. Hagberg, “Effect of training on the exercise responses of neuromuscular disease patients,” *Med Sci Sports Exerc*, vol. 16, no. 5, pp. 460–465, Oct. 1984.

[64] H. Dawes *et al.*, “A pilot randomised controlled trial of a home-based exercise programme aimed at improving endurance and function in adults with neuromuscular disorders,” *J. Neurol. Neurosurg. Psychiatry*, vol. 77, no. 8, pp. 959–962, Aug. 2006.

[65] Y. P. Demir, “Neuromuscular Diseases and Rehabilitation,” *Neurological Physical Therapy*, 2017.

[66] T. Ansved, “Muscle training in muscular dystrophies,” *Acta Physiol. Scand.*, vol. 171, no. 3, pp. 359–366, Mar. 2001.

[67] S. Armand, E. Watelain, M. Mercier, G. Lensel, and F.-X. Lepoutre, “Identification and classification of toe-walkers based on ankle kinematics, using a data-mining method,” *Gait & Posture*, vol. 23, no. 2, pp. 240–248, Feb. 2006.

[68] I. Moreno, I. Mendioroz, A. Poza, M. Martí, and D. M. López, “Analysis of gait and movement of upper limbs in muscular dystrophies,” *Neurologia*, vol. 20, no. 7, pp. 341–348, 2005.

[69] A. Ortlieb, J. Olivier, M. Bouri, H. Bleuler, and T. Kuntzer, “From gait measurements to design of assistive orthoses for people with neuromuscular diseases,” in *2015 IEEE International Conference on Rehabilitation Robotics (ICORR)*, 2015, pp. 368–373.

[70] S. Armand, M. Mercier, E. Watelain, K. Patte, J. Pelissier, and F. Rivier, “A comparison of gait in spinal muscular atrophy, type II and Duchenne muscular dystrophy,” *Gait & Posture*, vol. 21, no. 4, pp. 369–378, Jun. 2005.

[71] E. Wojciechowski *et al.*, “Gait patterns of children and adolescents with Charcot-Marie-Tooth disease,” *Gait & Posture*, vol. 56, pp. 89–94, Jul. 2017.

[72] S. Bozgeyik, İ. Alemdaroğlu, N. Bulut, Ö. Yılmaz, and A. Karaduman, “Neck flexor muscle strength and its relation with functional performance in Duchenne muscular dystrophy,” *European Journal of Paediatric Neurology*, vol. 21, no. 3, pp. 494–499, May 2017.

[73] H. Awano *et al.*, “Ambulatory capacity in Japanese patients with Duchenne muscular dystrophy,” *Brain and Development*, vol. 40, no. 6, pp. 465–472, Jun. 2018.

[74] L. N. Alfano *et al.*, “Modeling functional decline over time in sporadic inclusion body myositis,” *Muscle & Nerve*, vol. 55, no. 4, pp. 526–531, Apr. 2017.

[75] D. Bachasson *et al.*, “Relationship between muscle impairments, postural stability, and gait parameters assessed with lower-trunk accelerometry in myotonic dystrophy type 1,” *Neuromuscular Disorders*, vol. 26, no. 7, pp. 428–435, Jul. 2016.

[76] A. Barp *et al.*, “Muscle MRI and functional outcome measures in Becker muscular dystrophy,” *Scientific Reports*, vol. 7, no. 1, Dec. 2017.

[77] T. E. Davenport *et al.*, “Lower Extremity Peak Force and Gait Kinematics in Individuals With Inclusion Body Myositis,” *Arthritis Care & Research*, vol. 67, no. 1, pp. 94–101, 2014.

[78] D. Park and J.-S. Park, “Quantitative Assessment of Trunk Muscles Involvement in Patients with Myotonic Dystrophy Type 1 Using a Whole Body Muscle Magnetic Resonance Imaging,” *ENE*, vol. 77, no. 5–6, pp. 238–245, 2017.

[79] D. Park, S.-H. Lee, J.-H. Shin, and J.-S. Park, “Lower limb muscle magnetic resonance imaging in myotonic dystrophy type 1 correlates with the six-minute walk test and CTG repeats,” *Neuromuscular Disorders*, vol. 28, no. 1, pp. 29–37, Jan. 2018.

[80] N. H. M. Rijken, B. G. M. van Engelen, J. W. J. de Rooy, V. Weerdesteyn, and A. C. H. Geurts, “Gait propulsion in patients with facioscapulohumeral muscular dystrophy and ankle plantarflexor weakness,” *Gait & Posture*, vol. 41, no. 2, pp. 476–481, Feb. 2015.

[81] I. APRILE *et al.*, “Balance and walking in facioscapulohumeral muscular dystrophy: multiperspective assessment,” *EUROPEAN JOURNAL OF PHYSICAL AND REHABILITATION MEDICINE*, vol. 48, no. 3, p. 10, 2012.

[82] Z. Matjačić, A. Olenšek, J. Krajnik, B. Eymard, A. Zupan, and A. Pražnikar, “Compensatory mechanisms during walking in response to muscle weakness in spinal muscular atrophy, type III,” *Gait & Posture*, vol. 27, no. 4, pp. 661–668, May 2008.

[83] K. A. Bernhardt, T. H. Oh, and K. R. Kaufman, “Gait patterns of patients with inclusion body myositis,” *Gait & Posture*, vol. 33, no. 3, pp. 442–446, Mar. 2011.

[84] S. Boccardi, C. Gabardi, A. Negrini, and G. C. Santambrogio, “Locomotor and posture strategies in patients with Duchenne Muscular Dystrophy (DMD): Part I. Gait analysis,” *Europa Medicophysica*, vol. 33, no. 1, pp. 13–22, 1997.

[85] N. Chen *et al.*, “Gait characteristics of Duchenne muscular dystrophy children at normal speeds,” *Chinese Journal of Tissue Engineering Research*, vol. 17, no. 20, pp. 3770–3776, 2013.

[86] M. G. D'Angelo *et al.*, "Gait pattern in Duchenne muscular dystrophy," *Gait & Posture*, vol. 29, no. 1, pp. 36–41, Jan. 2009.

[87] L. Doglio, E. Pavan, I. Pernigotti, P. Petralia, C. Frigo, and C. Minetti, "Early signs of gait deviation in Duchenne muscular dystrophy," *Eur J Phys Rehabil Med*, vol. 47, no. 4, pp. 587–594, Dec. 2011.

[88] R. Don *et al.*, "Foot drop and plantar flexion failure determine different gait strategies in Charcot-Marie-Tooth patients," *Clinical Biomechanics*, vol. 22, no. 8, pp. 905–916, Oct. 2007.

[89] M. Ferrarin *et al.*, "Gait pattern classification in children with Charcot–Marie–Tooth disease type 1A," *Gait & Posture*, vol. 35, no. 1, pp. 131–137, Jan. 2012.

[90] M. Galli *et al.*, "Gait pattern in myotonic dystrophy (Steinert disease): A kinematic, kinetic and EMG evaluation using 3D gait analysis," *Journal of the Neurological Sciences*, vol. 314, no. 1, pp. 83–87, Mar. 2012.

[91] N. Gaudreault, D. Gravel, and S. Nadeau, "Evaluation of plantar flexion contracture contribution during the gait of children with Duchenne muscular dystrophy," *Journal of Electromyography and Kinesiology*, vol. 19, no. 3, pp. e180–e186, Jun. 2009.

[92] N. Gaudreault, D. Gravel, S. Nadeau, S. Houde, and D. Gagnon, "Gait patterns comparison of children with Duchenne muscular dystrophy to those of control subjects considering the effect of gait velocity," *Gait & Posture*, vol. 32, no. 3, pp. 342–347, Jul. 2010.

[93] M. Goudriaan *et al.*, "Gait deviations in Duchenne muscular dystrophy—Part 1. A systematic review," *Gait & Posture*, vol. 62, pp. 247–261, May 2018.

[94] M. Goudriaan *et al.*, "Gait deviations in Duchenne muscular dystrophy—Part 2. Statistical non-parametric mapping to analyze gait deviations in children with Duchenne muscular dystrophy," *Gait & Posture*, vol. 63, pp. 159–164, Jun. 2018.

[95] B. Guillebastre, P. Calmels, and P. Rougier, "Effects of muscular deficiency on postural and gait capacities in patients with Charcot-Marie-Tooth disease," *J Rehabil Med*, vol. 45, no. 3, pp. 314–317, Mar. 2013.

[96] M. Iosa *et al.*, "Mobility assessment of patients with facioscapulohumeral dystrophy," *Clinical Biomechanics*, vol. 22, no. 10, pp. 1074–1082, Dec. 2007.

[97] R. A. Kennedy, K. Carroll, and J. L. McGinley, "Gait in children and adolescents with Charcot-Marie-Tooth disease: a systematic review," *Journal of the Peripheral Nervous System*, vol. 21, no. 4, pp. 317–328.

[98] A. Kuruvilla, J. L. Costa, R. B. Wright, D. M. Yoder, and T. P. Andriacchi, "Characterization of gait parameters in patients with Charcot-Marie-Tooth disease," *Neurol India*, vol. 48, no. 1, pp. 49–55, Mar. 2000.

[99] T. Lencioni *et al.*, "Electromyographic and biomechanical analysis of step negotiation in Charcot Marie Tooth subjects whose level walk is not impaired," *Gait & Posture*, vol. 62, pp. 497–504, May 2018.

[100] C. Marchesi *et al.*, "Gait patterns and clinical correlation in adults with Charcot-Marie-Tooth disease," *J. Neurol.*, vol. 258, pp. 110–110, May 2011.

[101] C. J. Newman *et al.*, "The characteristics of gait in Charcot-Marie-Tooth disease types I and II," *Gait & Posture*, vol. 26, no. 1, pp. 120–127, Jun. 2007.

[102] S. Õunpuu *et al.*, "A comprehensive evaluation of the variation in ankle function during gait in children and youth with Charcot–Marie–Tooth disease," *Gait & Posture*, vol. 38, no. 4, pp. 900–906, Sep. 2013.

[103] J. Ropars *et al.*, “Muscle Activation during Gait in Children with Duchenne Muscular Dystrophy,” *PLOS ONE*, vol. 11, no. 9, p. e0161938, Sep. 2016.

[104] K. L. Siegel, T. M. Kepple, and S. J. Stanhope, “A case study of gait compensations for hip muscle weakness in idiopathic inflammatory myopathy,” *Clinical Biomechanics*, vol. 22, no. 3, pp. 319–326, Mar. 2007.

[105] V. Tiffreau, C. Detrembleur, P. V. D. Bergh, A. Renders, V. Kinet, and T. Lejeune, “Gait abnormalities in type 1 myotonic muscular dystrophy: 3D motion analysis, energy cost and surface EMG,” *Computer Methods in Biomechanics and Biomedical Engineering*, vol. 15, no. sup1, pp. 171–172, Sep. 2012.

[106] D. Trias, M. Gioux, M. Cid, and C. Bensch, “Gait analysis of myopathic children in relation to impairment level and energy cost,” *Journal of Electromyography and Kinesiology*, vol. 4, no. 2, pp. 67–81, Jan. 1994.

[107] R. B. Wright, D. M. Yoder, J. L. Costa, and T. P. Andriacchi, “Characterization of gait parameters in adult-onset myotonic dystrophy: Abnormal hip motion,” *Archives of Physical Medicine and Rehabilitation*, vol. 76, no. 1, pp. 33–38, Jan. 1995.

[108] R. Ganea *et al.*, “Gait Assessment in Children With Duchenne Muscular Dystrophy During Long-Distance Walking:,” *Journal of Child Neurology*, Jul. 2011.

[109] B. J. Goldfarb and S. R. Simon, “Gait patterns in patients with amyotrophic lateral sclerosis,” *Arch Phys Med Rehabil*, vol. 65, no. 2, pp. 61–65, Feb. 1984.

[110] K. Heberer *et al.*, “Hip kinetics during gait are clinically meaningful outcomes in young boys with Duchenne muscular dystrophy,” *Gait & Posture*, vol. 48, pp. 159–164, Jul. 2016.

[111] B. Killen, Z. Robertson, and M. Phillips, “G.P.11.15 Differences in gait kinematics in people with Charcot-Marie-Tooth disease using different types of AFO,” *Neuromuscular Disorders*, vol. 17, no. 9, p. 827, Oct. 2007.

[112] S. Radovanović *et al.*, “Comparison of temporal and stride characteristics in myotonic dystrophies type 1 and 2 during dual-task walking,” *Gait & Posture*, vol. 44, pp. 194–199, Feb. 2016.

[113] S. Radovanovic, M. Milicev, S. Peric, I. Basta, V. Kostic, and Z. Stevic, “Gait in amyotrophic lateral sclerosis: Is gait pattern differently affected in spinal and bulbar onset of the disease during dual task walking?,” *Amyotroph. Lateral Scher. Frontotemp. Degenerat.*, vol. 15, no. 7–8, pp. 488–493, Dec. 2014.

[114] J. P. J. Bakker, I. J. M. De Groot, A. Beelen, and G. J. Lankhorst, “Predictive factors of cessation of ambulation in patients with Duchenne muscular dystrophy,” *Am J Phys Med Rehabil*, vol. 81, no. 12, pp. 906–912, Dec. 2002.

[115] F. Menotti, F. Felici, A. Damiani, F. Mangiola, R. Vannicelli, and A. Macaluso, “Charcot-Marie-Tooth 1A patients with low level of impairment have a higher energy cost of walking than healthy individuals,” *Neuromuscular Disorders*, vol. 21, no. 1, pp. 52–57, Jan. 2011.

[116] M. Razeghi, M. Rostami, N. Jamshidi, and H. Ghomashchi, “Ground reaction force analysis for assessing the differences between normal and waddling gait patterns,” *Biomedical Engineering - Applications, Basis and Communications*, vol. 25, no. 2, 2013.

[117] N. Gaudreault, D. Gravel, S. Nadeau, P. Desjardins, and A. Brière, “A method to evaluate contractures effects during the gait of children with Duchenne dystrophy,” *Clin. Orthop. Relat. Res.*, vol. 456, pp. 51–57, Mar. 2007.

[118] M. Iosa *et al.*, “Mobility assessment of patients with facioscapulohumeral dystrophy,” *Clinical Biomechanics*, vol. 22, no. 10, pp. 1074–1082, Dec. 2007.

[119] M. Iosa, C. Mazza, F. Pecoraro, I. Aprile, E. Ricci, and A. Cappozzo, “Control of the upper body movements during level walking in patients with facioscapulohumeral dystrophy,” *Gait Posture*, vol. 31, no. 1, pp. 68–72, Jan. 2010.

[120] S. Ounpuu *et al.*, “A comprehensive evaluation of the variation in ankle function during gait in children and youth with Charcot-Marie-Tooth disease,” *Gait Posture*, vol. 38, no. 4, pp. 900–906, Sep. 2013.

[121] N. Ciesla, V. Dinglas, E. Fan, M. Kho, J. Kuramoto, and D. Needham, “Manual Muscle Testing: A Method of Measuring Extremity Muscle Strength Applied to Critically Ill Patients,” *J Vis Exp*, no. 50, Apr. 2011.

[122] A. Ortlieb, J. Olivier, M. Bouri, and H. Bleuler, “Evaluation of an active optical system for lower limb motion tracking,” presented at the 3-D Analysis of Human Movement, Lausanne, Switzerland, 2014.

[123] A. Ortlieb, J. Olivier, M. Bouri, and H. Bleuler, “A robotic platform for lower limb optical motion tracking in open space,” presented at the MESROB, Lausanne, Switzerland, 2014.

[124] R. W. Bohannon, “Comfortable and maximum walking speed of adults aged 20—79 years: reference values and determinants,” *Age Ageing*, vol. 26, no. 1, pp. 15–19, Jan. 1997.

[125] G. Stoquart, C. Detrembleur, and T. Lejeune, “Effect of speed on kinematic, kinetic, electromyographic and energetic reference values during treadmill walking,” *Neurophysiologie Clinique/Clinical Neurophysiology*, vol. 38, no. 2, pp. 105–116, Apr. 2008.

[126] J. Olivier, A. Ortlieb, P. Bertusi, T. Vouga, M. Bouri, and H. Bleuler, “Impact of ankle locking on gait implications for the design of hip and knee exoskeletons,” in *2015 IEEE International Conference on Rehabilitation Robotics (ICORR)*, 2015, pp. 618–622.

[127] J. L. Lelas, G. J. Merriman, P. O. Riley, and D. C. Kerrigan, “Predicting peak kinematic and kinetic parameters from gait speed,” *Gait & Posture*, vol. 17, no. 2, pp. 106–112, Apr. 2003.

[128] H. J. Ralston, “Energy-speed relation and optimal speed during level walking,” *Internationale Zeitschrift für Angewandte Physiologie Einschliesslich Arbeitsphysiologie*, vol. 17, no. 4, pp. 277–283, Oct. 1958.

[129] D. A. Winter, “Kinematic and kinetic patterns in human gait: Variability and compensating effects,” *Human Movement Science*, vol. 3, no. 1–2, pp. 51–76, Mar. 1984.

[130] S. Ounpuu, “The biomechanics of walking and running,” *Clin Sports Med*, vol. 13, no. 4, pp. 843–863, Oct. 1994.

[131] A. G. Schache and R. Baker, “On the expression of joint moments during gait,” *Gait & Posture*, vol. 25, no. 3, pp. 440–452, Mar. 2007.

[132] M. K. Y. Mak, O. Levin, J. Mizrahi, and C. W. Y. Hui-Chan, “Joint torques during sit-to-stand in healthy subjects and people with Parkinson’s disease,” *Clinical Biomechanics*, vol. 18, no. 3, pp. 197–206, Mar. 2003.

[133] A. Protopapadaki, W. I. Drechsler, M. C. Cramp, F. J. Coutts, and O. M. Scott, “Hip, knee, ankle kinematics and kinetics during stair ascent and descent in healthy young individuals,” *Clinical Biomechanics*, vol. 22, no. 2, pp. 203–210, Feb. 2007.

[134] N. Yagn, “Apparatus for facilitating walking,” US Patent 420179A, 28-Jan-1890.

[135] M. Vukobratovic, D. Hristic, and Z. Stojiljkovic, “Development of active anthropomorphic exoskeletons,” *Med. & biol. Engng.*, vol. 12, no. 1, pp. 66–80, Jan. 1974.

[136] M. K. Vukobratovic, “When were active exoskeletons actually born?,” *Int. J. Human. Robot.*, vol. 04, no. 03, pp. 459–486, Sep. 2007.

[137] M. Vukobratovic and D. Juricic, “Contribution to the Synthesis of Biped Gait,” *IEEE Transactions on Biomedical Engineering*, vol. BME-16, no. 1, pp. 1–6, Jan. 1969.

[138] A. B. Zoss, H. Kazerooni, and A. Chu, “Biomechanical design of the Berkeley lower extremity exoskeleton (BLEEX),” *IEEE/ASME Transactions on Mechatronics*, vol. 11, no. 2, pp. 128–138, Apr. 2006.

[139] H. Kawamoto and Y. Sankai, “Power Assist System HAL-3 for Gait Disorder Person,” in *Computers Helping People with Special Needs*, K. Miesenberger, J. Klaus, and W. Zagler, Eds. Springer Berlin Heidelberg, 2002, pp. 196–203.

[140] C. Vaney *et al.*, “Robotic-Assisted Step Training (Lokomat) Not Superior to Equal Intensity of Over-Ground Rehabilitation in Patients With Multiple Sclerosis,” *Neurorehabilitation and Neural Repair*, vol. 26, no. 3, pp. 212–221, Mar. 2012.

[141] A. Mayr, M. Kofler, E. Quirbach, H. Matzak, K. Fröhlich, and L. Saltuari, “Prospective, Blinded, Randomized Crossover Study of Gait Rehabilitation in Stroke Patients Using the Lokomat Gait Orthosis,” *Neurorehabilitation and Neural Repair*, vol. 21, no. 4, pp. 307–314, Jul. 2007.

[142] H. Ali, “Bionic Exoskeleton: History, Development and the Future,” *IOSR Journal of Mechanical and Civil Engineering*, p. 5.

[143] A. M. Dollar and H. Herr, “Lower Extremity Exoskeletons and Active Orthoses: Challenges and State-of-the-Art,” *IEEE Transactions on Robotics*, vol. 24, no. 1, pp. 144–158, Feb. 2008.

[144] C. J. Walsh, K. Endo, and H. Herr, “A quasi-passive leg exoskeleton for load-carrying augmentation,” *Int. J. Human. Robot.*, vol. 04, no. 03, pp. 487–506, Sep. 2007.

[145] M. A. McDowell, C. D. Fryar, C. L. Ogden, and K. M. Flegal, “Anthropometric Reference Data for Children and Adults: United States, 2003-2006: (623932009-001).” American Psychological Association, 2008.

[146] “Percentage distribution of waist circumference, by body mass index category (BMI), household population aged 20 to 69 years, Canada, 1981 and 2007-2009,” 2009 2007.

[147] E. Churchill and J. T. McConville, “Sampling and Data Gathering Strategies for Future USAF Anthropometry,” Air Force Aerospace Medical Research Lab Wright-Patterson Afb Oh, Feb. 1976.

[148] R. Contini, “Body Segment Parameters, Part II,” vol. 16, no. 1, pp. 1–19, Spring 1972.

[149] G. Barbareschi, R. Richards, M. Thornton, T. Carlson, and C. Holloway, “Statically vs dynamically balanced gait: Analysis of a robotic exoskeleton compared with a human,” in *2015 37th Annual International Conference of the IEEE Engineering in Medicine and Biology Society (EMBC)*, Milan, 2015, pp. 6728–6731.

[150] W. G. Janssen, H. B. Bussmann, and H. J. Stam, “Determinants of the Sit-to-Stand Movement: A Review,” *Phys Ther*, vol. 82, no. 9, pp. 866–879, Sep. 2002.

[151] R. G. Burdett, R. Habasevich, J. Pisciotta, and S. R. Simon, “Biomechanical Comparison of Rising from Two Types of Chairs,” *Physical Therapy*, vol. 65, no. 8, pp. 1177–1183, Aug. 1985.

[152] S. A. Radtka, G. B. Oliveira, K. E. Lindstrom, and M. D. Borders, “The kinematic and kinetic effects of solid, hinged, and no ankle–foot orthoses on stair locomotion in healthy adults,” *Gait & Posture*, vol. 24, no. 2, pp. 211–218, Oct. 2006.

[153] J. M. Porto *et al.*, “Contribution of hip abductor–adductor muscles on static and dynamic balance of community-dwelling older adults,” *Aging Clin Exp Res*, Sep. 2018.

[154] C.-A. Lahiff, T. Ramakrishnan, S. H. Kim, and K. Reed, “Knee orthosis with variable stiffness and damping that simulates hemiparetic gait,” in *2016 38th Annual International Conference of the IEEE Engineering in Medicine and Biology Society (EMBC)*, Orlando, FL, USA, 2016, pp. 2218–2221.

[155] A. Ortlieb, J. Olivier, M. Bouri, and H. Bleuler, “Series Elastic Actuation for Assistive Orthotic Devices: Case Study of Pneumatic Actuator,” in *New Trends in Medical and Service Robots*, P. Wenger, C. Chevallereau, D. Pisla, H. Bleuler, and A. Rodić, Eds. Springer International Publishing, 2016, pp. 113–125.

[156] J. Olivier, A. Ortlieb, M. Bouri, H. Bleuler, and R. Clavel, “A Ball-Screw Driven Motorized Hip Orthosis,” *Transaction on Control and Mechanical Systems*, vol. 3, no. 2, pp. 100–108, 2014.

[157] J. Olivier, A. Ortlieb, M. Bouri, and H. Bleuler, “Mechanisms for actuated assistive hip orthoses,” *Robotics and Autonomous Systems*, vol. 73, pp. 59–67, Nov. 2015.

[158] G. Aguirre-Ollinger, J. E. Colgate, M. A. Peshkin, and A. Goswami, “A 1-DOF assistive exoskeleton with virtual negative damping: effects on the kinematic response of the lower limbs,” in *2007 IEEE/RSJ International Conference on Intelligent Robots and Systems*, 2007, pp. 1938–1944.

[159] E. H. Cup *et al.*, “Exercise Therapy and Other Types of Physical Therapy for Patients With Neuromuscular Diseases: A Systematic Review,” *Archives of Physical Medicine and Rehabilitation*, vol. 88, no. 11, pp. 1452–1464, Nov. 2007.

[160] R. Riener, L. Lunenburger, S. Jezernik, M. Anderschitz, G. Colombo, and V. Dietz, “Patient-cooperative strategies for robot-aided treadmill training: first experimental results,” *IEEE Transactions on Neural Systems and Rehabilitation Engineering*, vol. 13, no. 3, pp. 380–394, Sep. 2005.

[161] L. Marchal-Crespo and D. J. Reinkensmeyer, “Review of control strategies for robotic movement training after neurologic injury,” *Journal of NeuroEngineering and Rehabilitation*, vol. 6, p. 20, Jun. 2009.

[162] S. K. Au, J. Weber, and H. Herr, “Powered Ankle–Foot Prosthesis Improves Walking Metabolic Economy,” *IEEE Transactions on Robotics*, vol. 25, no. 1, pp. 51–66, Feb. 2009.

[163] S. Au, M. Berniker, and H. Herr, “Powered ankle-foot prosthesis to assist level-ground and stair-descent gaits,” *Neural Networks*, vol. 21, no. 4, pp. 654–666, May 2008.

[164] K. Fite, J. Mitchell, F. Sup, and M. Goldfarb, “Design and Control of an Electrically Powered Knee Prosthesis,” in *2007 IEEE 10th International Conference on Rehabilitation Robotics*, 2007, pp. 902–905.

[165] B. E. Lawson, A. H. Shultz, and M. Goldfarb, “Evaluation of a coordinated control system for a pair of powered transfemoral prostheses,” in *2013 IEEE International Conference on Robotics and Automation*, 2013, pp. 3888–3893.

[166] M. Liu, F. Zhang, P. Datseris, and H. (Helen) Huang, “Improving Finite State Impedance Control of Active-Transfemoral Prosthesis Using Dempster-Shafer Based State Transition Rules,” *J Intell Robot Syst*, vol. 76, no. 3–4, pp. 461–474, Dec. 2014.

[167] D. Zlatnik, B. Steiner, and G. Schweitzer, “Finite-state control of a trans-femoral (TF) prosthesis,” *IEEE Transactions on Control Systems Technology*, vol. 10, no. 3, pp. 408–420, May 2002.

[168] C. D. Hoover, G. D. Fulk, and K. B. Fite, “Stair Ascent With a Powered Transfemoral Prosthesis Under Direct Myoelectric Control,” *IEEE/ASME Transactions on Mechatronics*, vol. 18, no. 3, pp. 1191–1200, Jun. 2013.

[169] D. L. Grimes, “An active multi-mode above knee prosthesis controller,” Thesis, Massachusetts Institute of Technology, 1979.

[170] A. W. Boehler, K. W. Hollander, T. G. Sugar, and D. Shin, “Design, implementation and test results of a robust control method for a powered ankle foot orthosis (AFO),” in *2008 IEEE International Conference on Robotics and Automation*, 2008, pp. 2025–2030.

[171] Y. D. Li and E. T. Hsiao-Wecksler, “Gait mode recognition and control for a portable-powered ankle-foot orthosis,” in *2013 IEEE 13th International Conference on Rehabilitation Robotics (ICORR)*, 2013, pp. 1–8.

[172] R. J. Farris, H. A. Quintero, and M. Goldfarb, “Performance Evaluation of a Lower Limb Exoskeleton for Stair Ascent and Descent with Paraplegia,” *Conf Proc IEEE Eng Med Biol Soc*, vol. 2012, pp. 1908–1911, 2012.

[173] S. Murray and M. Goldfarb, “Towards the use of a lower limb exoskeleton for locomotion assistance in individuals with neuromuscular locomotor deficits,” in *2012 Annual International Conference of the IEEE Engineering in Medicine and Biology Society*, 2012, pp. 1912–1915.

[174] H. A. Quintero, R. J. Farris, C. Hartigan, I. Clesson, and M. Goldfarb, “A Powered Lower Limb Orthosis for Providing Legged Mobility in Paraplegic Individuals,” *Top Spinal Cord Inj Rehabil*, vol. 17, no. 1, pp. 25–33, 2011.

[175] H. Kawamoto, S. Kanbe, and Y. Sankai, “Power assist method for HAL-3 estimating operator’s intention based on motion information,” in *The 12th IEEE International Workshop on Robot and Human Interactive Communication, 2003. Proceedings. ROMAN 2003.*, 2003, pp. 67–72.

[176] Y. Sankai, “HAL: Hybrid Assistive Limb Based on Cybernics,” in *Robotics Research*, Springer, Berlin, Heidelberg, 2010, pp. 25–34.

[177] A. Ortlieb, M. Bouri, R. Baud, and H. Bleuler, “An assistive lower limb exoskeleton for people with neurological gait disorders,” in *2017 International Conference on Rehabilitation Robotics (ICORR)*, 2017, pp. 441–446.

[178] A. Ortlieb, J. Olivier, M. Bouri, H. Bleuler, and T. Kuntzer, “From gait measurements to design of assistive orthoses for people with neuromuscular diseases,” in *2015 IEEE International Conference on Rehabilitation Robotics (ICORR)*, 2015, pp. 368–373.

[179] M. R. Shorten, “Muscle Elasticity and Human Performance,” *Current Research in Sports Biomechanics*, vol. 25, pp. 1–18, 1987.

[180] J. Sun and P. A. Voglewede, “Powered Transtibial Prosthetic Device Control System Design, Implementation, and Bench Testing,” *J. Med. Devices*, vol. 8, no. 1, pp. 011004-011004–8, Dec. 2013.

[181] Q. Wang, K. Yuan, J. Zhu, and L. Wang, “Finite-state control of a robotic transtibial prosthesis with motor-driven nonlinear damping behaviors for level ground walking,” in *2014 IEEE 13th International Workshop on Advanced Motion Control (AMC)*, Yokohama, Japan, 2014, pp. 155–160.

[182] D. Zlatnik, B. Steiner, and G. Schweitzer, “Finite-state control of a trans-femoral (TF) prosthesis,” *IEEE Transactions on Control Systems Technology*, vol. 10, no. 3, pp. 408–420, May 2002.

[183] H. Kawamoto, Suwoong Lee, S. Kanbe, and Y. Sankai, “Power assist method for HAL-3 using EMG-based feedback controller,” in *SMC’03 Conference Proceedings. 2003 IEEE International Conference on Systems, Man and Cybernetics. Conference Theme - System Security and Assurance (Cat. No.03CH37483)*, Washington, DC, USA, 2003, vol. 2, pp. 1648–1653.

[184] A. Ortlieb *et al.*, “An Active Impedance Controller to Assist Gait in People with Neuromuscular Diseases: Implementation to the Hip Joint of the AUTONOMYO Exoskeleton,” presented at the BioRob, Enschede, Netherlands, 2018.

Curriculum Vitae

AMALRIC ORTLIEB

Chemin de Planeyse 2
2013 Colombier
Switzerland

Cell phone: 076 / 822.45.57
Email: amalric.ortlieb@autonomyo.com

Date of birth: December 24th 1988
Place of origin: Cortaillod (NE)
Citizenship: Swiss
Marital status: Single

• Education

2019	**Ph.D. in Robotics, Control and Intelligent Systems program** *Swiss Federal Institute of Technology (EPFL), Switzerland* **Thesis:** Wearable exoskeletons to support ambulation in people with neuromuscular diseases, design rules and control
2013	**Master of Science in Control and Mechatronics (Major) and Biomedical Technologies (Minor),** *Swiss Federal Institute of Technology (EPFL), Switzerland* **Thesis:** Characterization and Control of an Assistive Hip Orthosis for the Elderly
2011	**Bachelor of Science in Mechanical Engineering,** *Swiss Federal Institute of Technology (EPFL), Switzerland*
2007	**Baccalaureate, Bilingual English-French in Philosophy**, *Lycée Denis-de-Rougemont, Switzerland*

• Professional Experience

2014 - 2019	**Doctoral assistant**, Laboratory of Robotic Systems (LSRO) – EPFL, Lausanne, Switzerland Teaching and supervision of master and semester projects Teaching of practical works in haptics and human-robot interfaces
2013	**Research assistant (60%-80%)**, Laboratory of Robotic Systems (LSRO) – EPFL, Lausanne, Switzerland Simulation of gait dynamics Pre-study on assistance for the ambulation of people with neuromuscular diseases

2011 - 2012	**Research and development assistant (25%)**, Komax Medtech, La Chaux-de-Fonds, Switzerland Mechanical design and CAD parts management
2010	**Study assistant (30%)**, Cohort Lc65+, CHUV, Lausanne, Switzerland Data entry and verification
2009 - 2010	**Student-assistant,** Section of mechanical engineering – EPFL, Lausanne, Switzerland Control I for BA3 Mechanical design project for BA2 CAD for BA1
2009 (1 month)	**Internship in mechanical workshop**, Manufacture horlogère Cartier, La Chaux-de-Fonds, Switzerland
2008 (1 month)	**Internship in precious metallurgy**, Precinox SA, La Chaux-de-Fonds, Switzerland

• Research interests

- Mechanical design and control of mobile robots
- Dynamics of human and robots
- Human motion analysis
- Rehabilitation and design of clinical experiments

• Languages

- French (Native)
- English (Fluent)
- German (B2)
- Spanish (B1)
- Dutch (A1)
- Mandarin (A0)

• Publications

Book Chapters

1. **A. Ortlieb**, J. Olivier, M. Bouri, and H. Bleuler, "A Robotic Platform for Lower Limb Optical Motion Tracking in Open Space," in New Trends in Medical and Service Robots, H. Bleuler, M.

Bouri, F. Mondada, D. Pisla, A. Rodic, and P. Helmer, Eds. Springer International Publishing, 2016, pp. 93–105.

2. **A. Ortlieb**, J. Olivier, M. Bouri, and H. Bleuler, "Series Elastic Actuation for Assistive Orthotic Devices: Case Study of Pneumatic Actuator," in *New Trends in Medical and Service Robots*, P. Wenger, C. Chevallereau, D. Pisla, H. Bleuler, and A. Rodić, Eds. Springer International Publishing, 2016, pp. 113–125.
3. R. Baud, **A. Ortlieb**, J. Olivier, M. Bouri, and H. Bleuler, "HiBSO Hip Exoskeleton: Toward a Wearable and Autonomous Design," in *New Trends in Medical and Service Robots*, 2016, pp. 185–195.
4. **A. Ortlieb**, M. Bouri, and H. Bleuler, "AUTONOMYO: Design Challenges of Lower Limb Assistive Device for Elderly People, Multiple Sclerosis and Neuromuscular Diseases," in *Wearable Robotics: Challenges and Trends*, Springer, Cham, 2017, pp. 439–443.
5. **A. Ortlieb** *et al.*, "Investigation on Variable Impedance Control for Modulating Assistance in Walking Strategies with the AUTONOMYO Exoskeleton," in *Wearable Robotics: Challenges and Trends*, Springer, Cham, 2018

Journal Papers

1. J. Olivier, **A. Ortlieb**, M. Bouri, H. Bleuler, and R. Clavel, "A Ball-Screw Driven Motorized Hip Orthosis," *Transaction on Control and Mechanical Systems*, vol. 3, no. 2, pp. 100–108, 2014.
2. J. Olivier, **A. Ortlieb**, M. Bouri, and H. Bleuler, "Mechanisms for actuated assistive hip orthoses," *Robotics and Autonomous Systems*, 2014.

Conference Proceedings and Posters

1. **A. Ortlieb**, J. Olivier, M. Bouri, and H. Bleuler, "Evaluation of an active optical system for lower limb motion tracking," presented at the 3-D Analysis of Human Movement, Lausanne, Switzerland, 2014.
2. J. Olivier, **A. Ortlieb**, P. Bertusi, T. Vouga, M. Bouri, and H. Bleuler, "Impact of ankle locking on gait implications for the design of hip and knee exoskeletons," in *2015 IEEE International Conference on Rehabilitation Robotics (ICORR)*, 2015, pp. 618–622.
3. **A. Ortlieb**, J. Olivier, M. Bouri, H. Bleuler, and T. Kuntzer, "From gait measurements to design of assistive orthoses for people with neuromuscular diseases," in *2015 IEEE International Conference on Rehabilitation Robotics (ICORR)*, 2015, pp. 368–373.
4. J. Olivier, **A. Ortlieb**, M. Bouri, and H. Bleuler, "Investigations on the Influence of an Assistive Hip Orthosis on Gait," presented at the RAAD, Belgrade, Serbia, 2016
5. **A. Ortlieb**, M. Bouri, R. Baud, and H. Bleuler, "An assistive lower limb exoskeleton for people with neurological gait disorders," in *2017 International Conference on Rehabilitation Robotics (ICORR)*, 2017, pp. 441–446.
6. **A. Ortlieb** *et al.*, "An Active Impedance Controller to Assist Gait in People with Neuromuscular Diseases: Implementation to the Hip Joint of the AUTONOMYO Exoskeleton," presented at the BioRob, Enschede, Netherlands, 2018.

Patents

1. **A. Ortlieb** and M. Bouri, "Modular and Minimally Constraining Lower Limb Exoskeleton for Enhanced Mobility and Balance Augmentation," WO/2018/065913, 13-Apr-2018.

Ce document a été imprimé au Centre d’impression EPFL,
imprimerie climatiquement neutre, certifiée myClimate.